

---

# THE BRADLEY DEPARTMENT OF ELECTRICAL ENGINEERING

---

## VIRGINIA TECH

---

An Intermediate Report of Research

**RADIO CHANNEL MODELING  
IN MANUFACTURING ENVIRONMENTS  
(Parts II and III)**

Work Performed for:

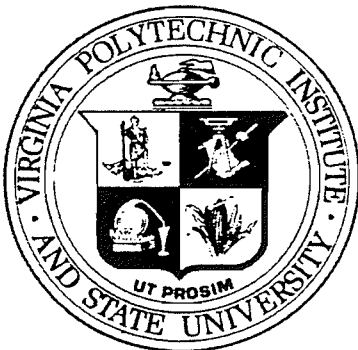
Dr. James J. Solberg  
Computer Integrated Design,  
Manufacturing and Automation Center  
Purdue University  
West Lafayette, IN 47907

In partial fulfillment of  
CIDMAC Subcontract 0440670A

by

Scott Y. Seidel  
Koichiro Takamizawa  
Dr. Theodore S. Rappaport

Bradley Department of Electrical Engineering  
Virginia Polytechnic Institute and State University  
Blacksburg, VA 24061



February 28, 1989

---

VIRGINIA POLYTECHNIC INSTITUTE AND STATE UNIVERSITY  
Blacksburg, Virginia 24061 (703)961-6646

---



## Table of Contents

I. Introduction	1
II. Power Distribution	2
III. Autocorrelation Coefficient Function	13
3.1 General Autocorrelation	13
3.2 Application of Autocorrelation Coefficient Function to Normal Distribution	16
3.3 Spatial Correlation	17
3.4. Temporal Correlation	28
IV. Joint Probability of Path Occupancy	32
V. Conclusion	41
VI. References	43
Appendix A. CDF of Received Signal Power	44
Appendix B. Scatter Plots of Path Attenuation	49
Appendix C. Power Law Exponent and Standard Deviation	72
Appendix D. CDF of Received Power over Local Areas	79
Appendix E. Temporal Autocorrelation Coefficient Functions	84
Appendix F. Conditional Probability of Path Occupancy	97

## I. Introduction

Stochastic processes are completely described in terms of n-th order statistics [1,10,12]. To more accurately model the radio channel in manufacturing environments, it is desirable to determine second order statistics for the channel impulse response. The primary statistics previously determined [2,15] have shown the average number of multipath components in factories as well as the large scale signal amplitude distribution at various excess delays. These statistics are an important part of the channel model as they provide a method for predicting signal strengths and delay spreads for random locations. However, they are not enough to describe the relationship between signals over time and space within a local (small scale) area.

In this report, we investigate the secondary statistics of indoor radio channels in the factory environment for small scale areas. Once secondary statistics are known, it is important to know how they may be incorporated into a statistical model. Under the assumption that multipath signal amplitudes are jointly log-normally distributed over space and time, application of correlation into a statistical model is presented. In addition, the distributions of received power within a particular excess delay interval are examined for both global and local areas. Conditional probabilities of path occupancy are presented which show the effect power control will have on indoor radio systems. In this report, the term *multipath signal* or *multipath component* refers to the power or voltage received over a 7.8 ns time interval. The models developed in this report are based upon empirical measurements made with a probing pulse [2,3,4].

This interim report presents analysis towards the development of channel models for indoor factory radio communication channels. The work is being conducted on the campus of Virginia Polytechnic Institute and State University as research grant number 88-1861-06, which was awarded by Purdue University as CIDMAC subcontract number 0440670A in August 1988.

This report constitutes deliverables 3 and 4 of the subcontract. This grant is supporting two Electrical Engineering graduate students, Scott Seidel and Koichiro Takamizawa.

## II. Power Distribution

The total power contained in a received multipath profile with a particular transmitter-receiver (T-R) separation of  $d$  meters is well described by the log-normal distribution about a mean power law of  $d^n$ . Free-space path loss is assumed for the first 2.3 meters ( $10\lambda$ ) and values of  $n$  are given in [3,13,14]. It is shown here that not only is the total signal power log-normally distributed, but the received multipath power within a particular excess delay interval is also log-normally distributed about some mean  $d^n$  power law. Thus, for a given excess time delay for a receiver located at a particular T-R separation, the received power is log-normal. This is similar to the simulation of urban radio propagation (SURP) channel model [5,6,7,8]. At first glance, this appears to contradict the results presented in [2,15] that individual multipath amplitudes are Rayleigh distributed. However, it is important to remember that the results in [2,15] assumed no information about T-R separation. The multipath amplitudes have been shown to be Rayleigh distributed if the transmitter and receiver are placed at a random separation. It is shown here that a log-normal distribution is a good model for amplitudes when the T-R separation is known. Figures 1 and 2 show the cumulative distribution function of the received signal power relative to the local mean within a particular excess delay interval. The figures, which are based on the entire ensemble of measurements in [4], also show the CDF of the log-normal distribution with the least mean-square error fit to a mean  $d^n$  power law and standard deviation about the mean for measured data in LOS and obstructed topographies, respectively. These figures demonstrate that for a particular T-R separation and topography, the log-normal distribution for received signal power within a particular excess delay interval

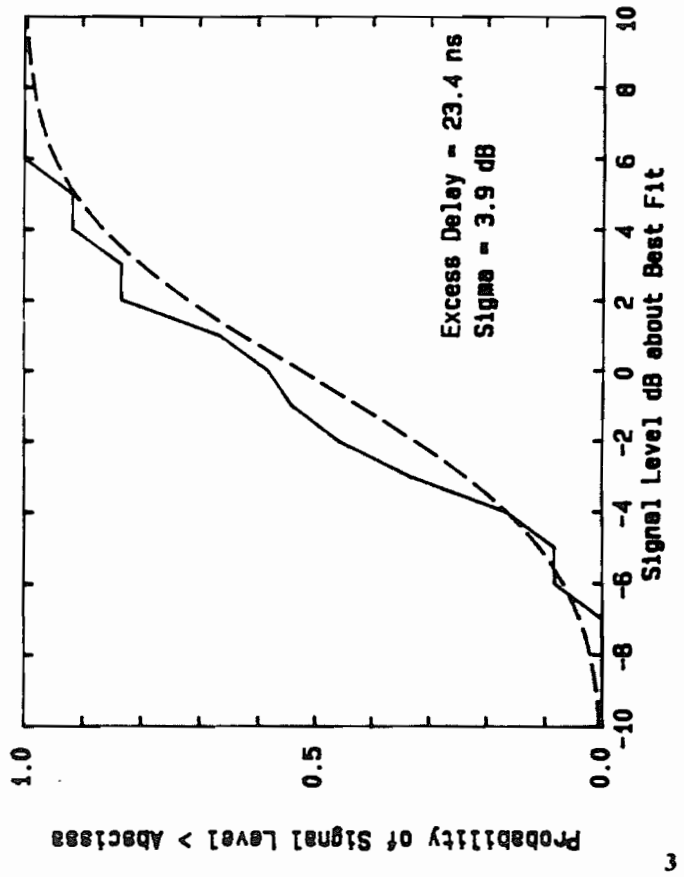
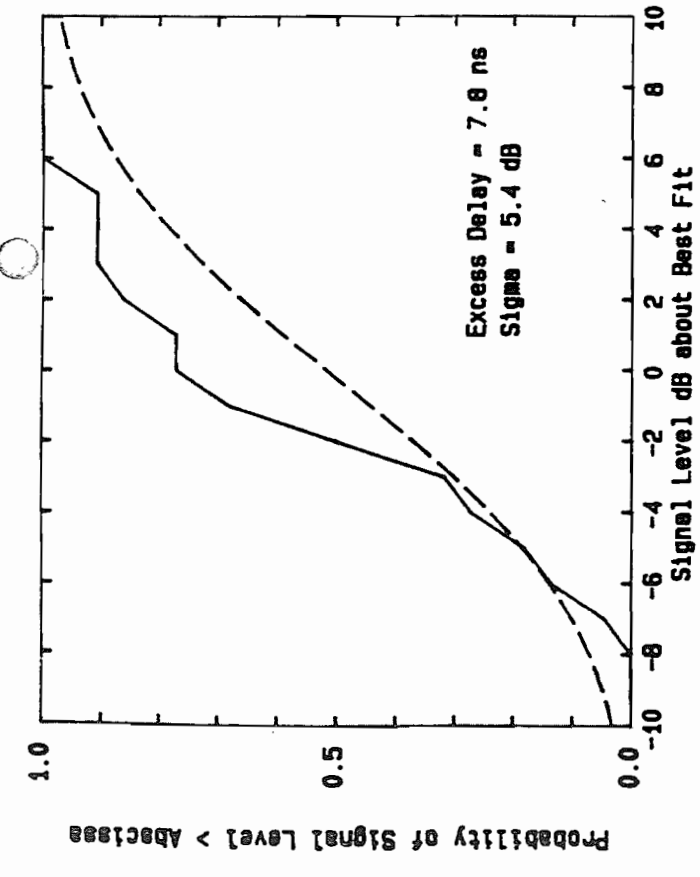
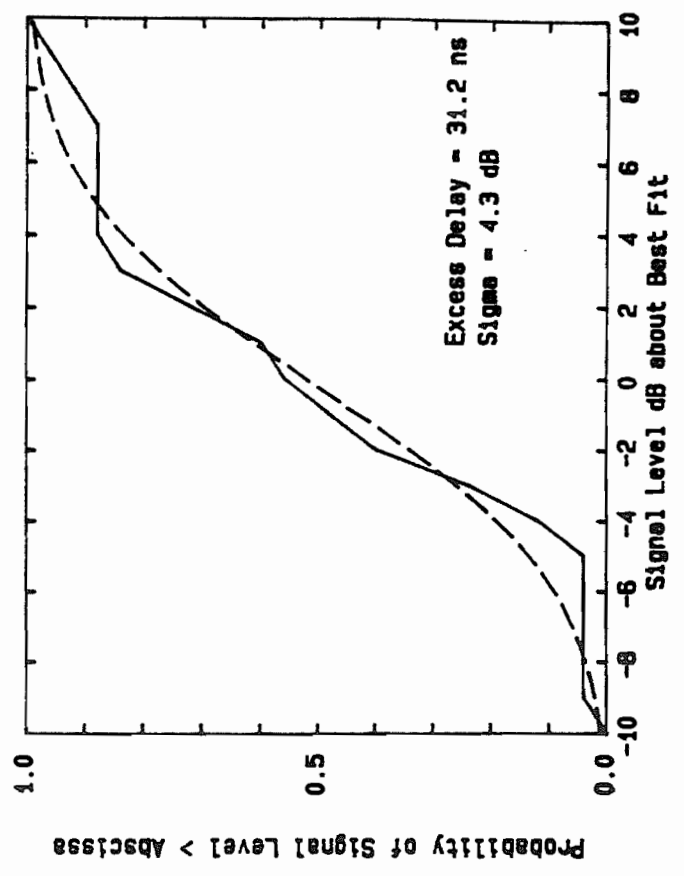
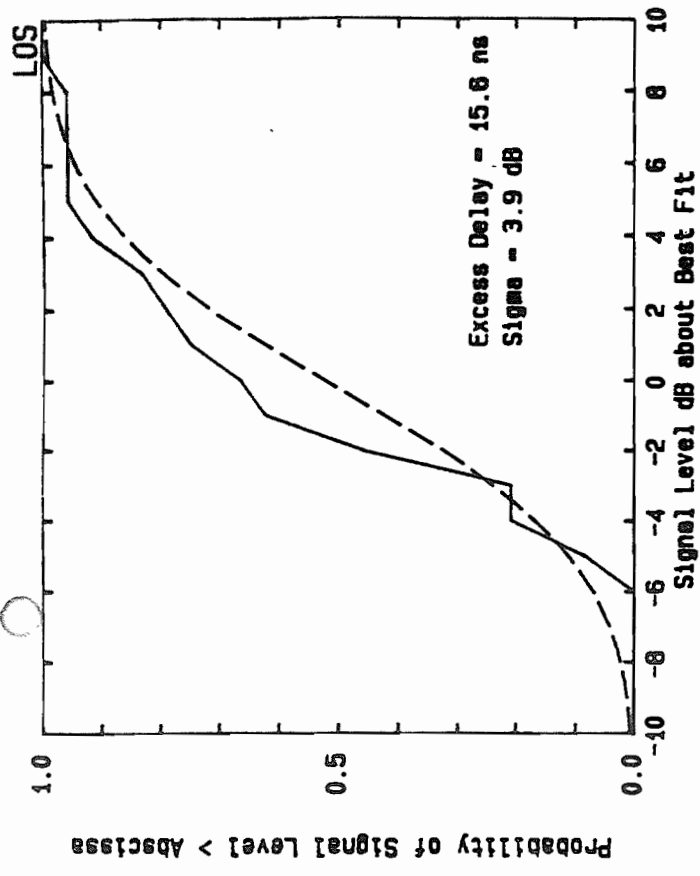


Figure 1. CDF of received signal power and CDF of log-normal distribution fit to the experimental mean and variance for LOS topographic

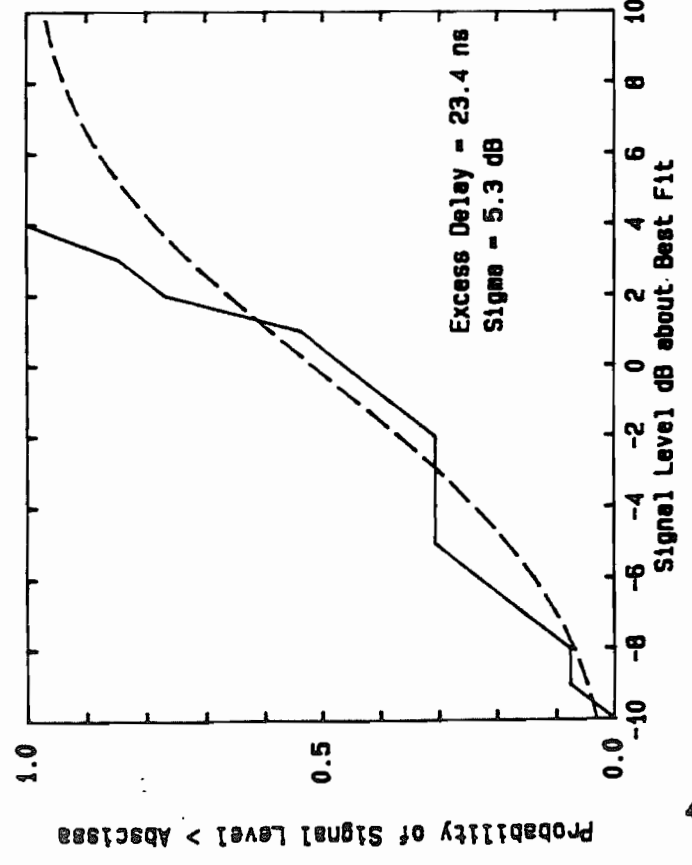
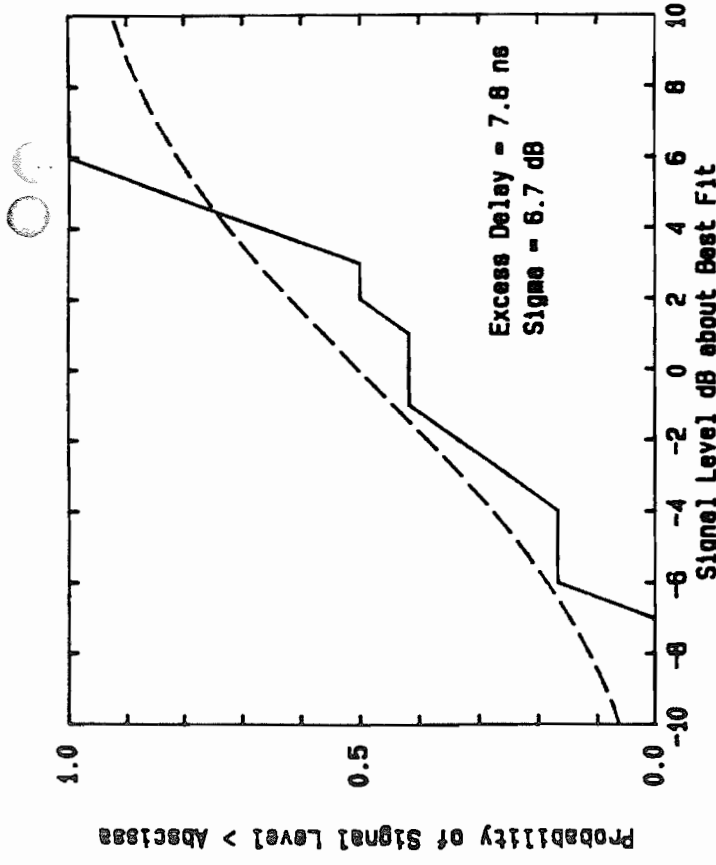
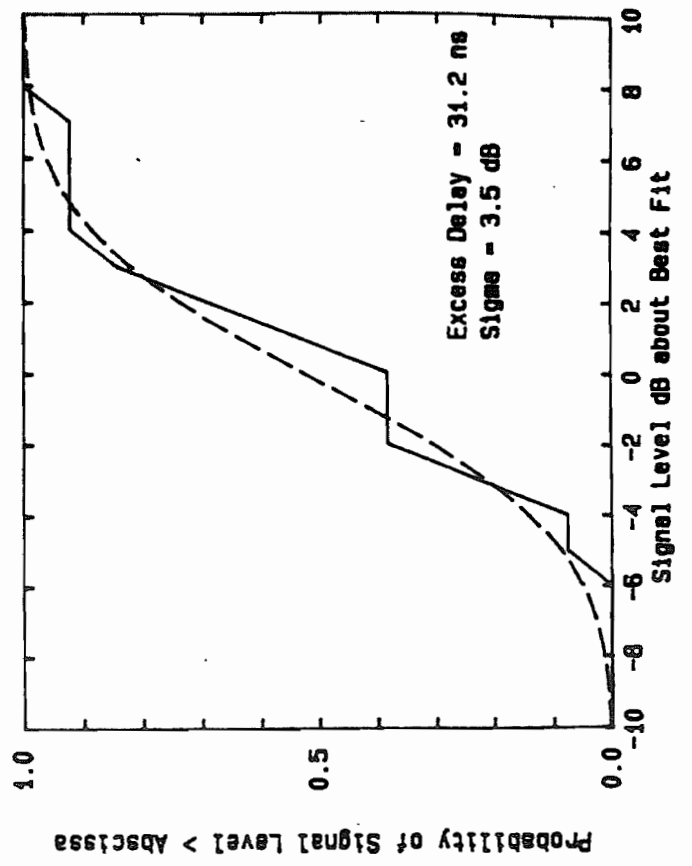
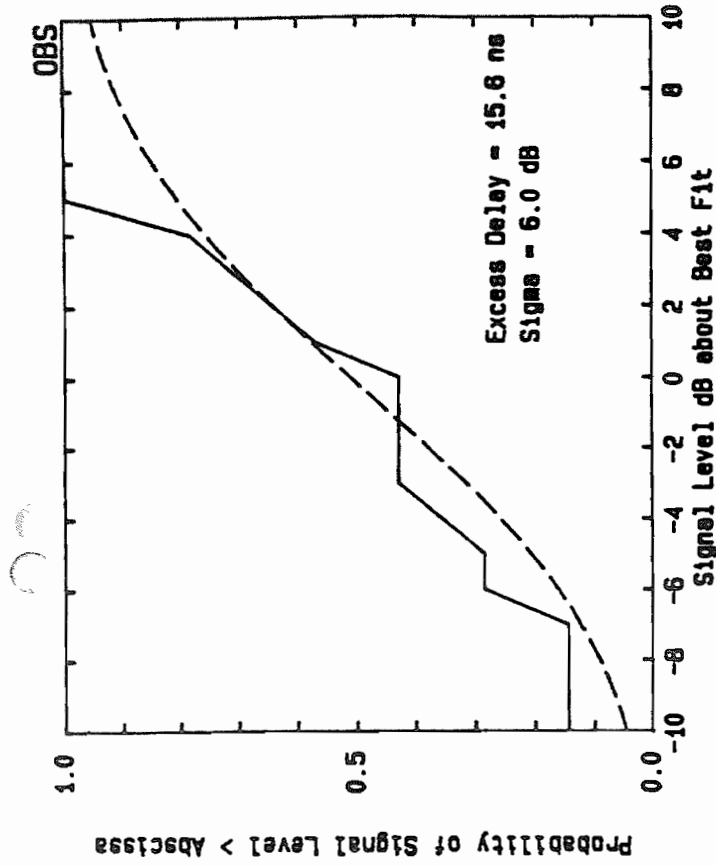


Figure 2. CDF of received signal power and CDF of log-normal distribution fit to the experimental mean and variance for OBS tonographics.

models the measured data reasonably well. The mean power law exponent  $n$  and standard deviation  $\sigma$  have been found for each excess delay interval by minimizing the mean square error fit to a log-normal distribution. Figure 3 is a scatter plot of path attenuation with respect to distance for different excess delay intervals. Each point on a scatter plot represents the local average of received power over a 1 meter measurement track [2,3,4]. The best mean square fit to a  $d^n$  power law, and  $\pm$  one standard deviation about the mean are shown. The exponential decay of the power contained in components with small excess delay is shown to obey nearly the same power law as the total received power shown in [3]. This indicates that most of the received power arrives early in the profile and shows that power contained in components with large excess delay decreases more rapidly than that of components with small excess delay. Figures 4 and 5 show how the power law exponent  $n$  changes with excess delay for LOS and obstructed topographies, respectively. Note that in these figures, the exponent increases (attenuation increases) down the vertical axis. In obstructed topographies, the power of multipath components with small excess delay obeys a power law in which the signal attenuates ( $n$  increases) more rapidly than in line-of-sight topographies. This is expected since shadowing due to obstructions causes attenuation to be greater than in unobstructed topographies.

Figures 6 and 7 show that the standard deviation about the mean power law is nearly constant with respect to excess delay and can be modeled by a constant of about 4 dB for LOS topographies and 5 dB for obstructed topographies. Variations in the standard deviation are to be expected due to the small amount of measured data. The standard deviation in obstructed topographies is slightly larger than in LOS topographies since the effects of shadowing cause greater variation in path attenuation.

Figures 8 and 9 show the CDF of multipath signal amplitudes over a local area and the CDF of a log-normal distribution fit to the mean and standard deviation of the measured data over a local area for measurement locations PB1BC (LOS) and PC5AC (OBS), respectively (Figs. 5 and 6 in [3]). The log-normal distribution over small scale distances appears to well



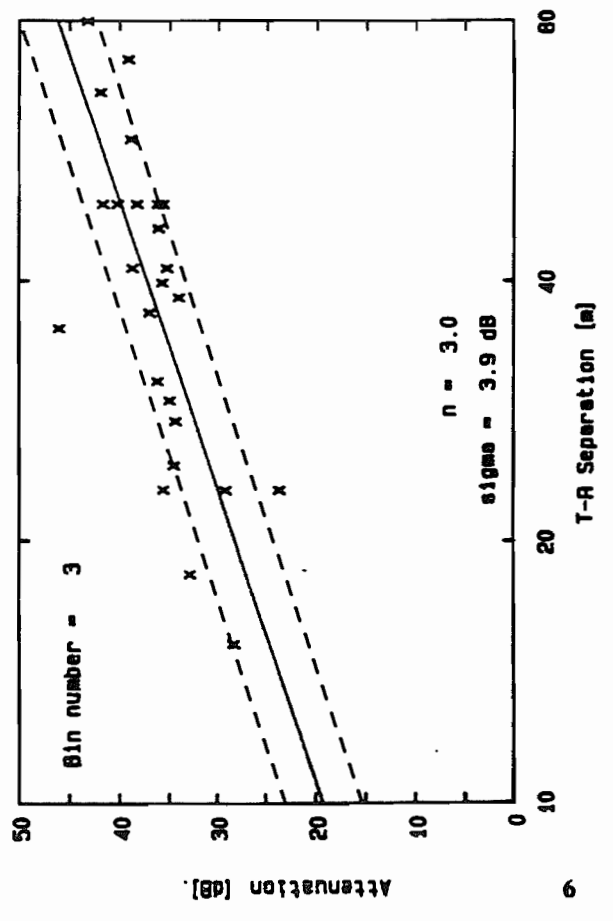
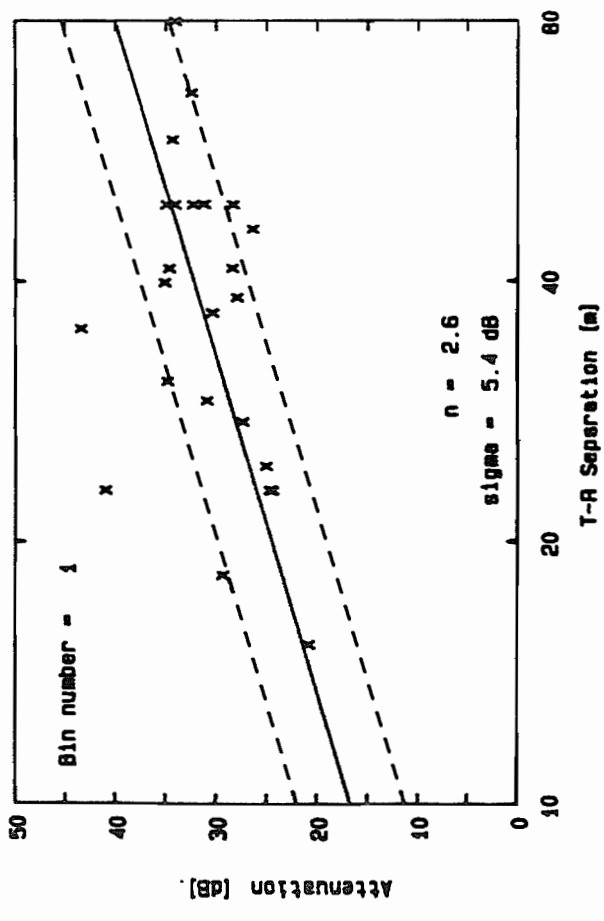
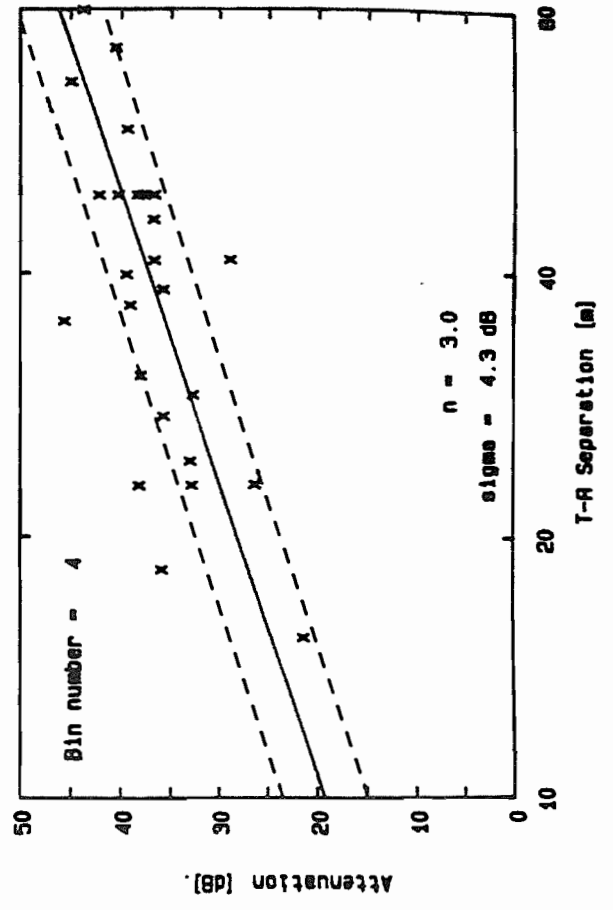
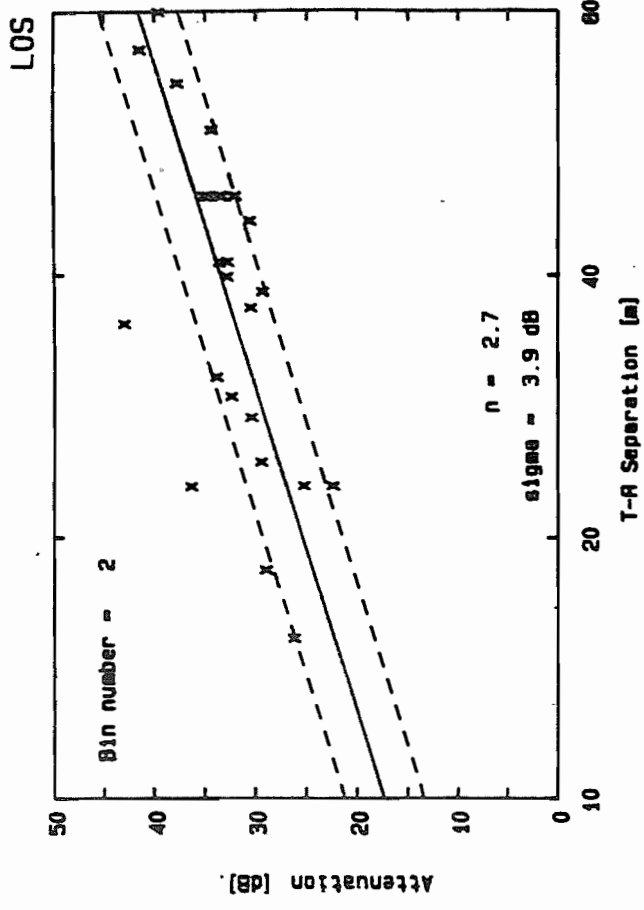


Figure 3. Scatter plot of path attenuation with respect to T-R separation.

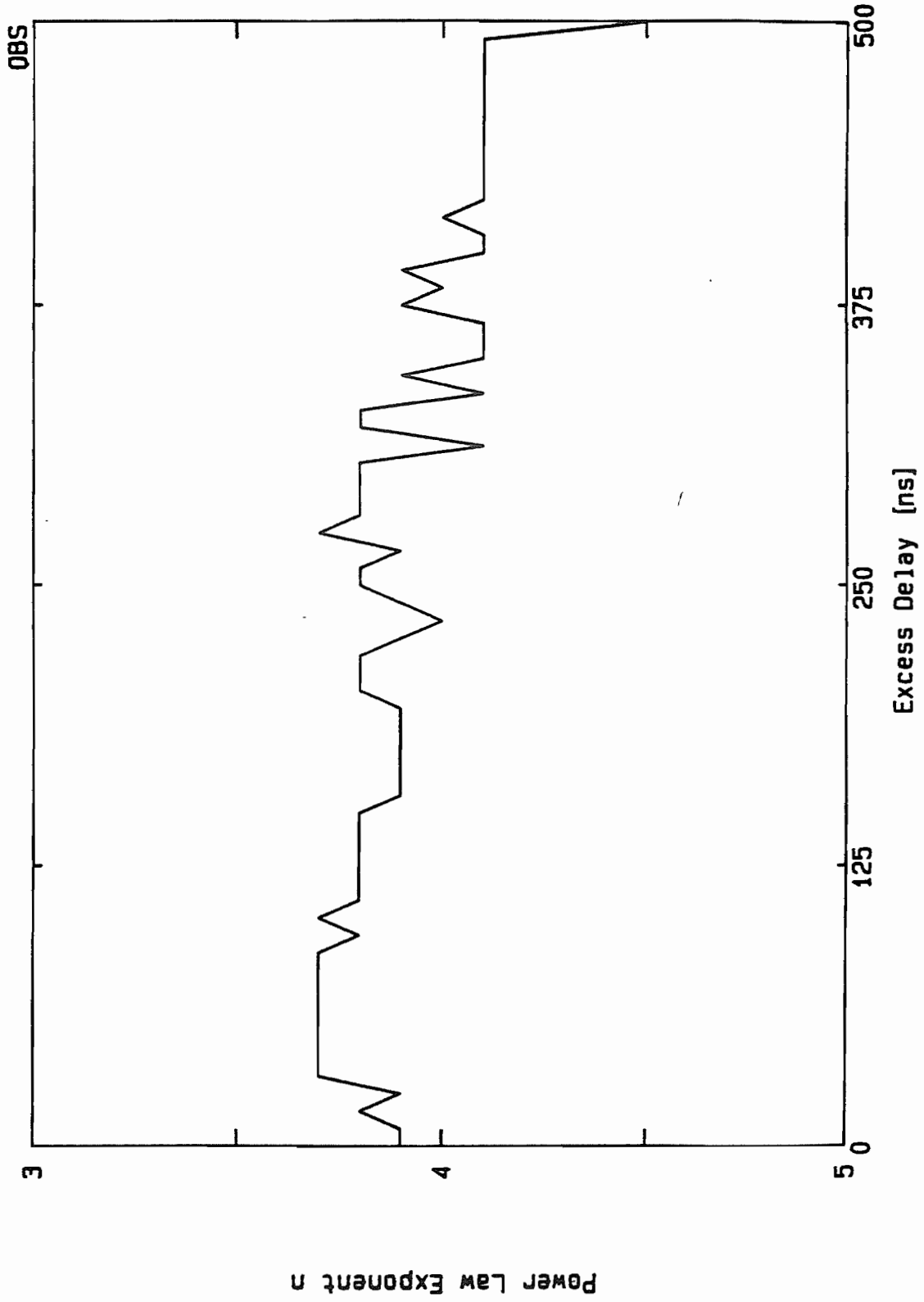


Figure 5. Variation of power law exponent  $n$  with respect to excess delay for OBS topographics

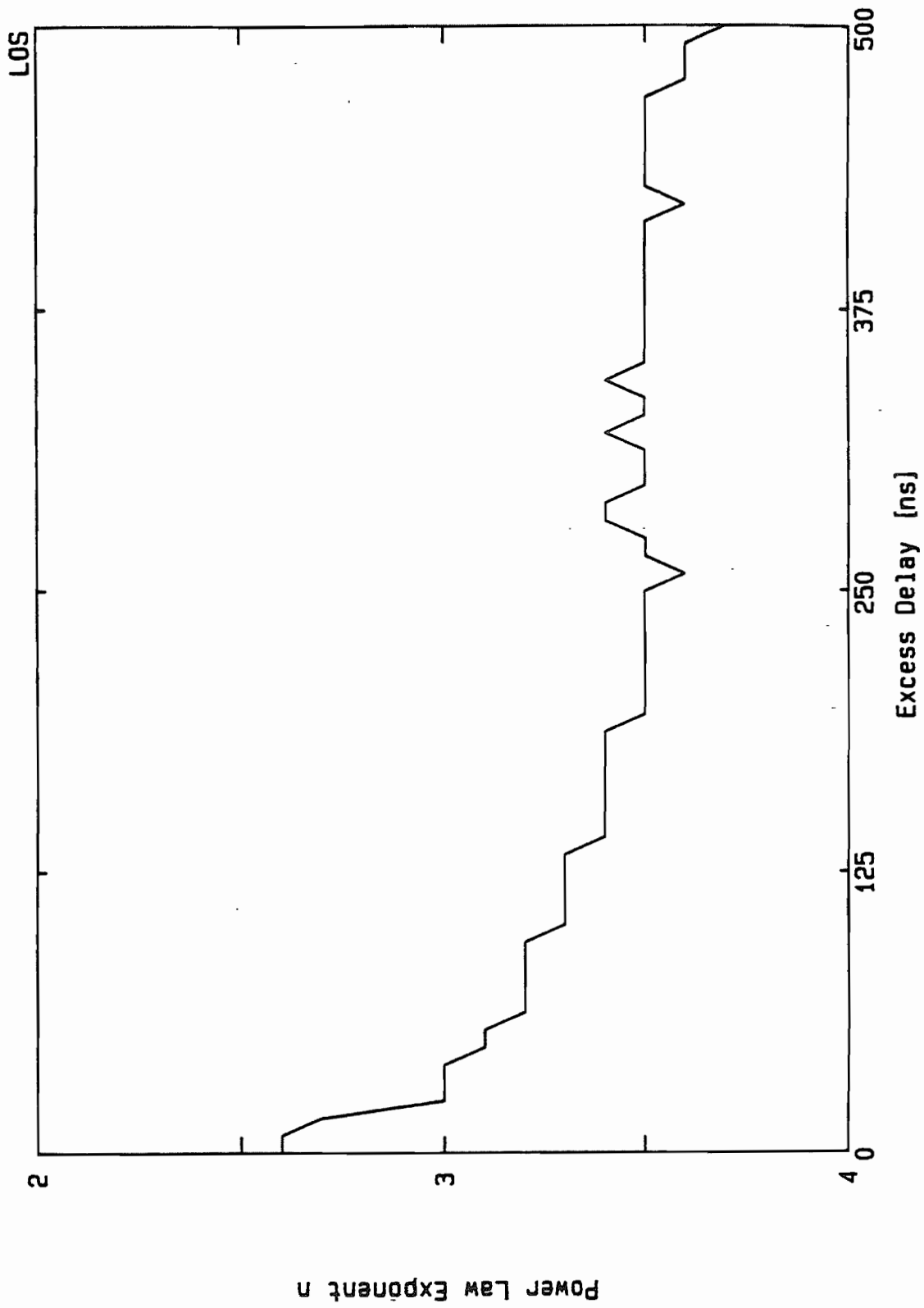


Figure 4. Variation of power law exponent  $n$  with respect to excess delay for LOS topographies

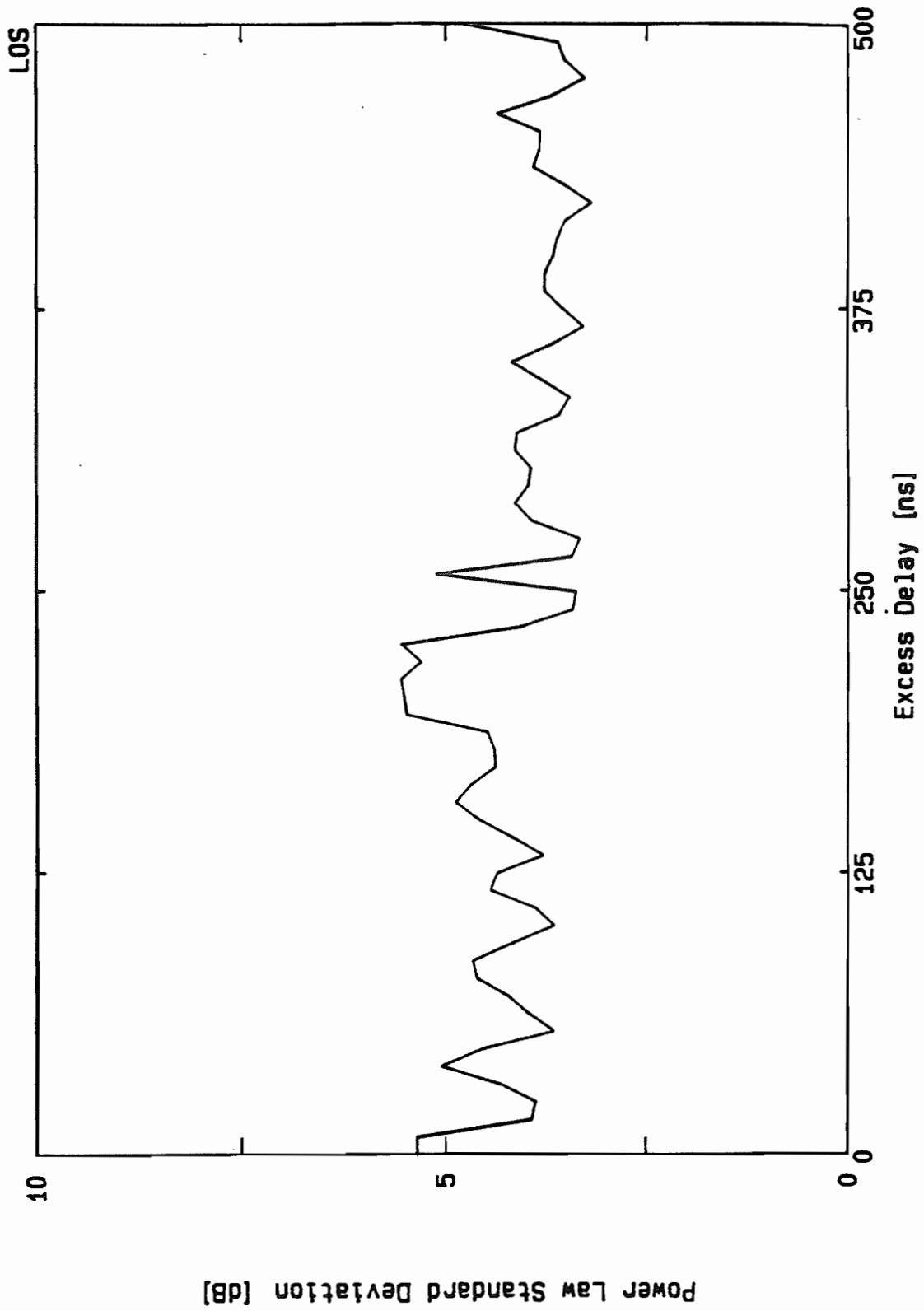


Figure 6. Variation of standard deviation about mean  $d^n$  power law with respect to excess delay for LOS topographies.

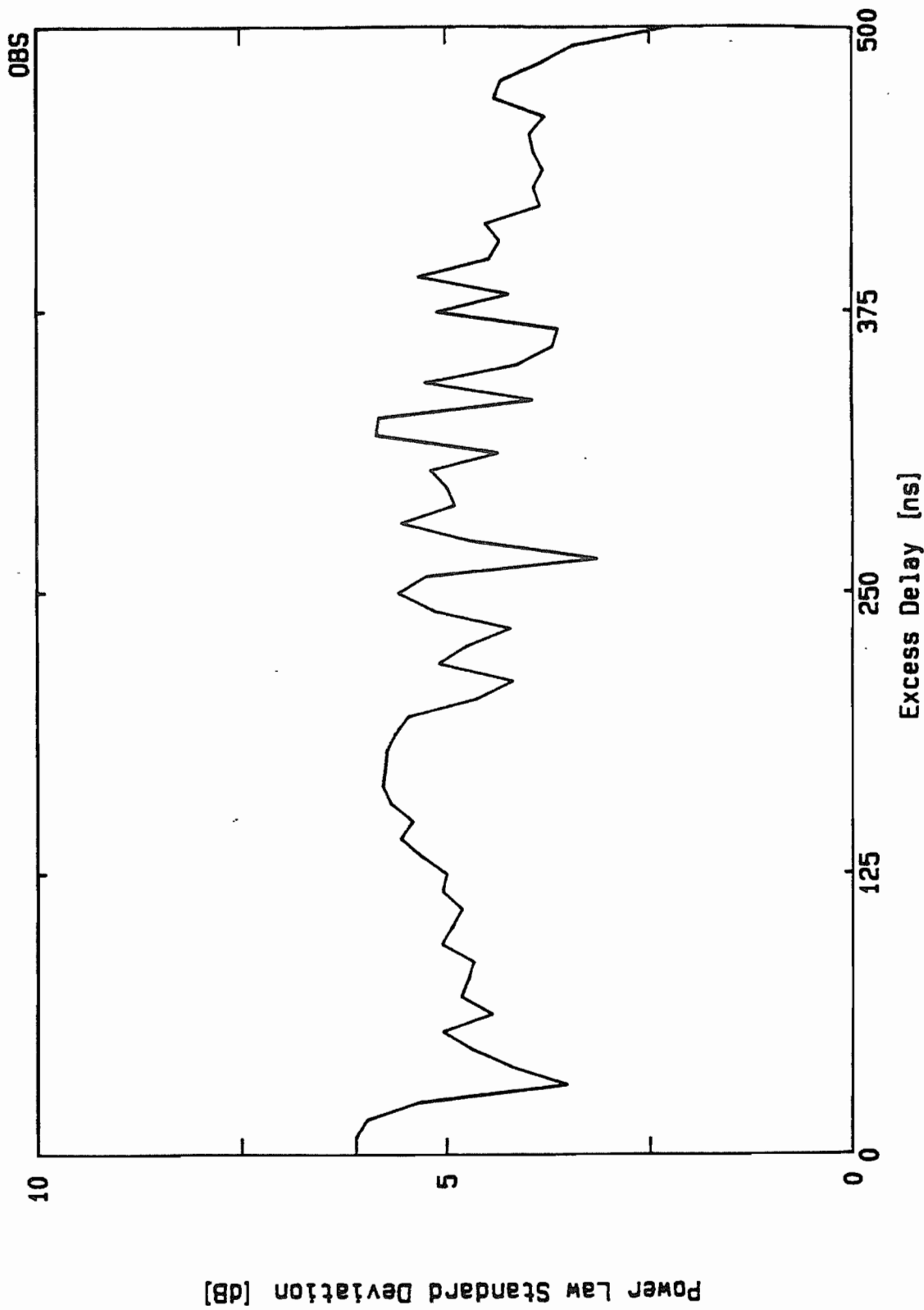


Figure 7. Variation of standard deviation about mean  $d^n$  power law with respect to excess delay for OBS topographies.

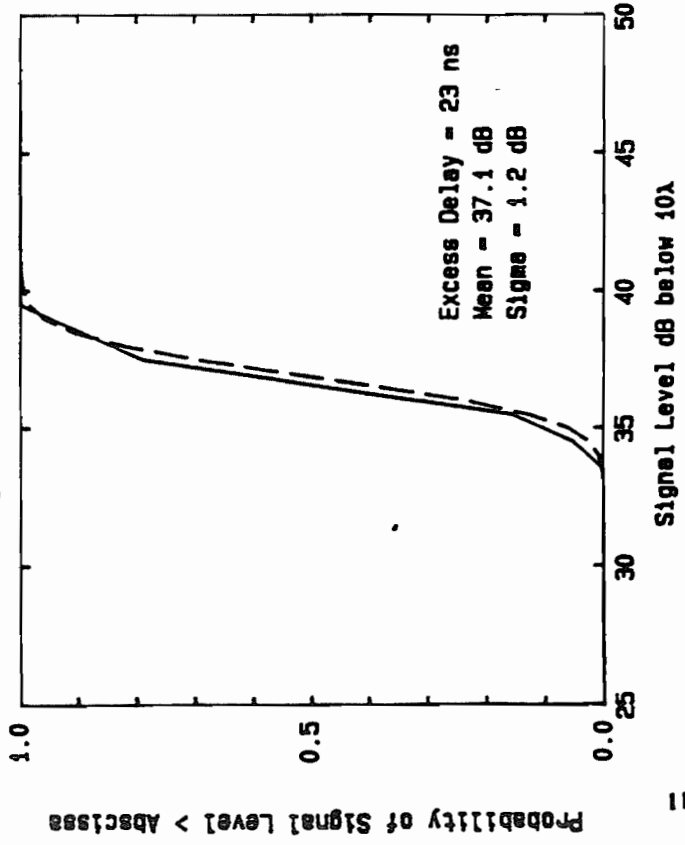
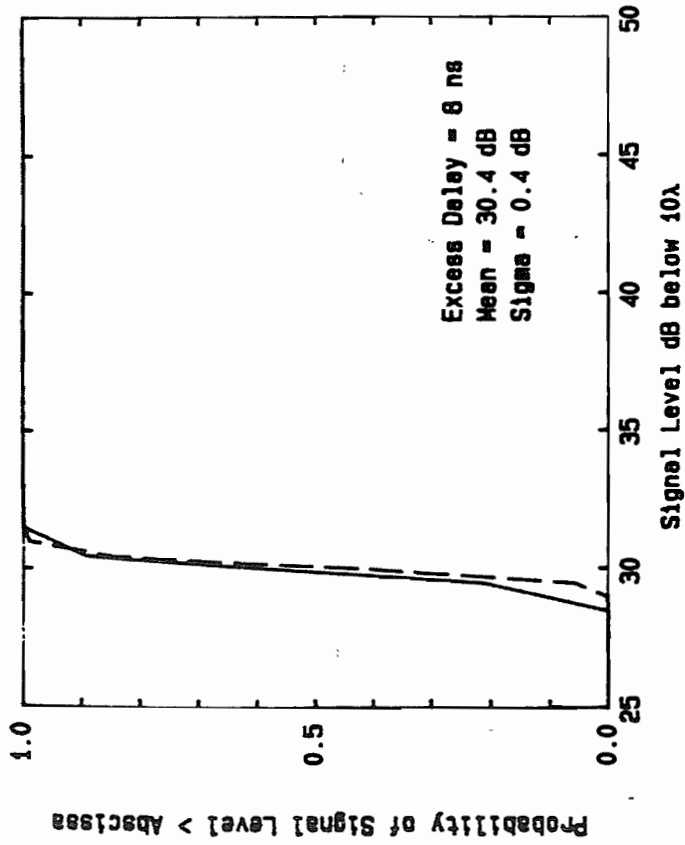
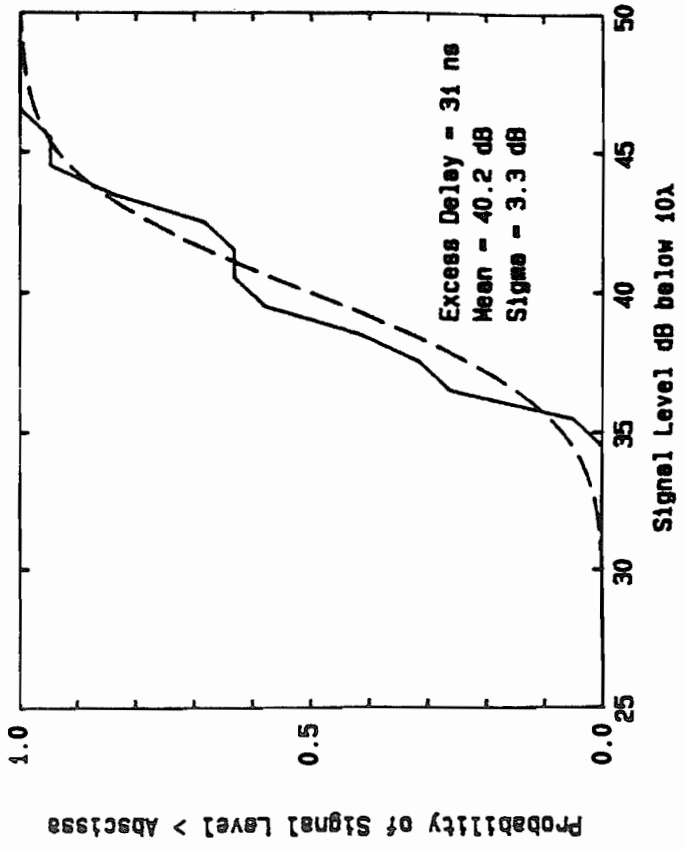
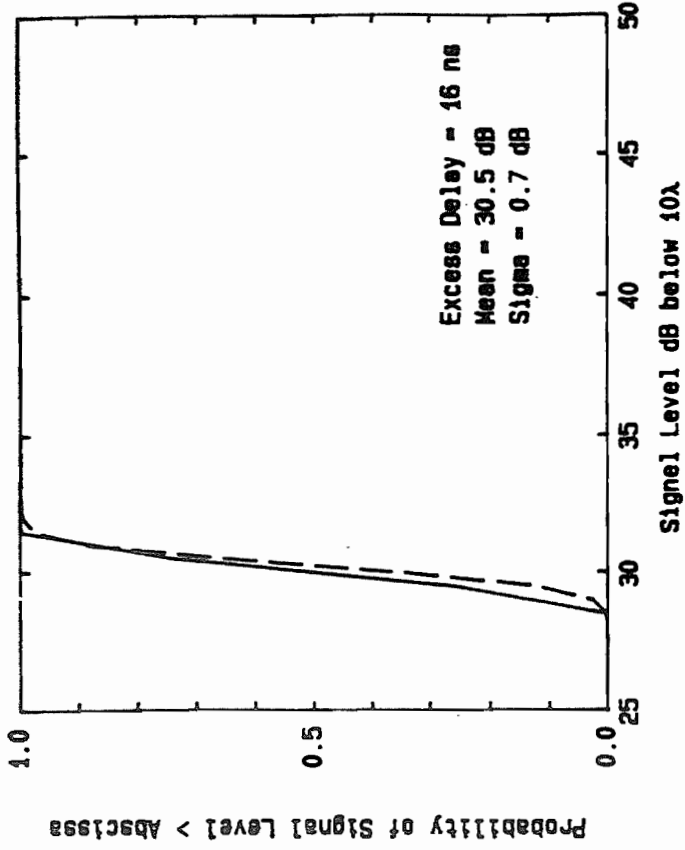


Figure 8. CDF of multipath signal amplitude over a local area and CDF of a log-normal distribution fit to the experimental mean and variance. PB18C (LOS)

PC5AC

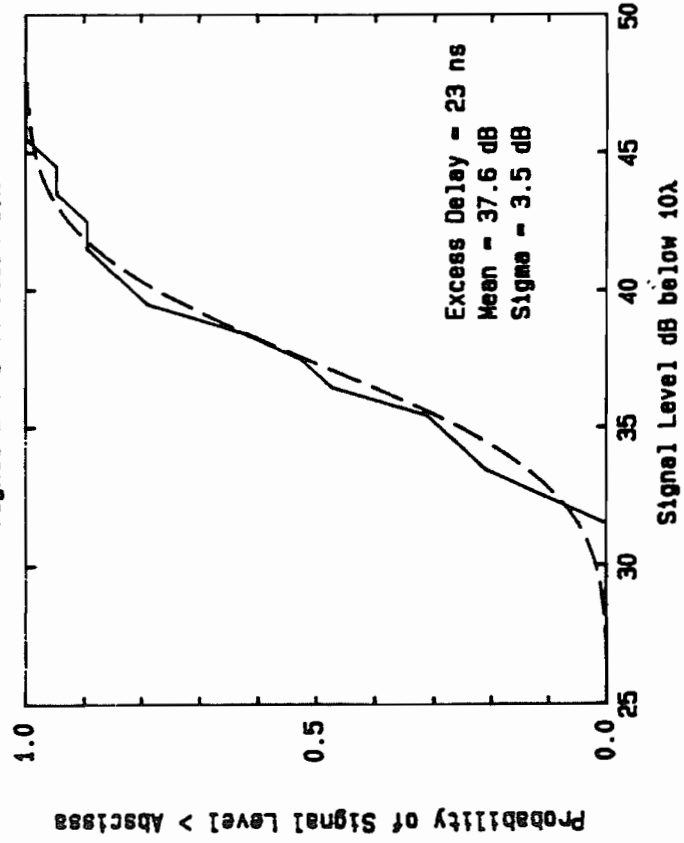
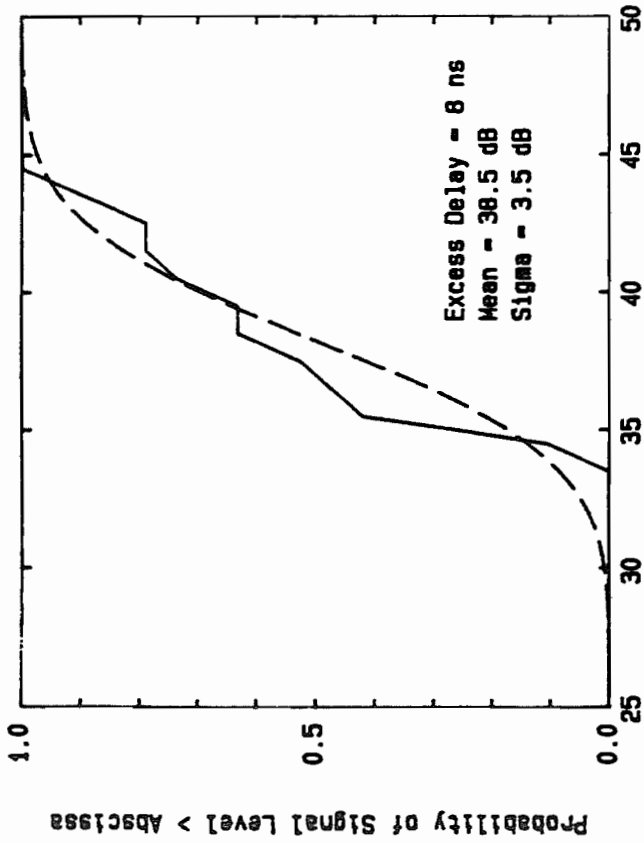
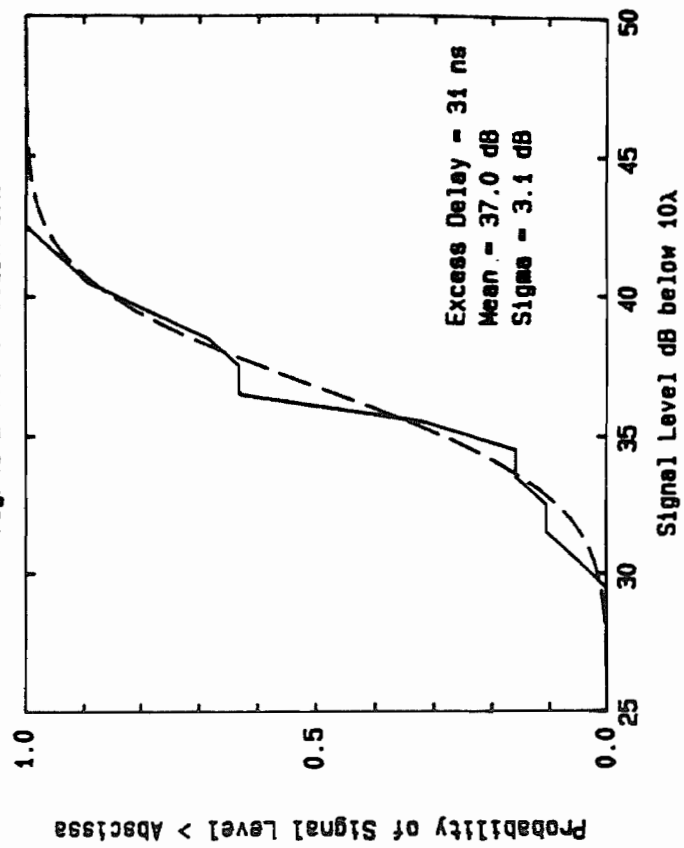
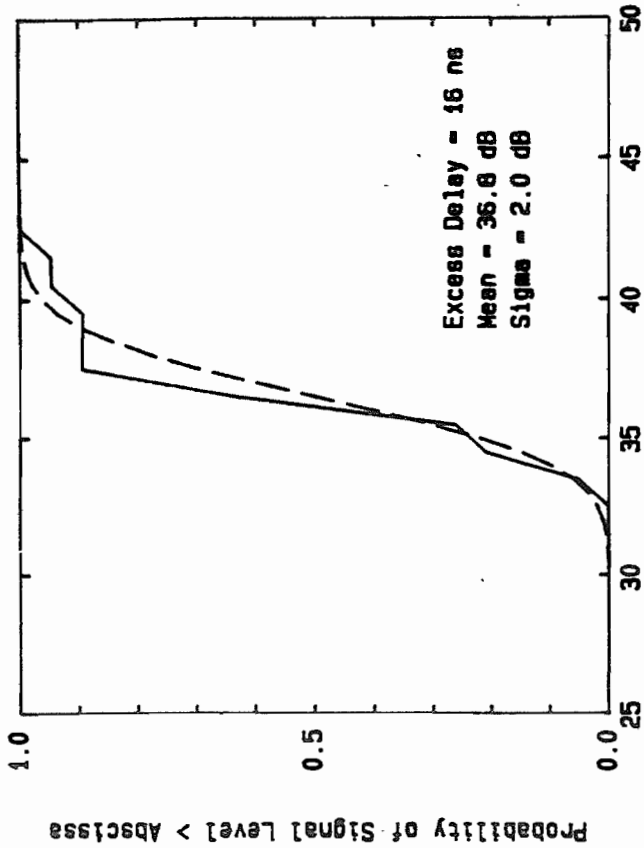


Figure 9. CDF of multipath signal amplitude over a local area and CDF of a log-normal distribution fit to the experimental mean and variance. PC5AC (OBS)





model the amplitude of individual multipath components. Note that the small variance of multipath signals which arrive early in the LOS profile indicates that virtually no fading occurs on these signals.

Histograms of the standard deviation for local areas and excess delay time are shown in Figs. 10 and 11. Due to the small amount of data, it is difficult to empirically determine the distribution. However, it appears that the local standard deviation may be uniformly distributed over 0 dB to 5 dB for multipath components with small excess delays, and over 0 dB to 2.5 dB (0 dB to 3.5 dB) for components with large excess delays in obstructed (line-of-sight) topography. The range of standard deviation of signal strength about the local mean appears to decrease linearly with excess delay.

As will now be shown, the tractability of the joint log-normal distribution makes it easy to incorporate correlation statistics into a channel model since the log-normal distribution is just the normal distribution with data values in dB [9].

### **III. Autocorrelation Coefficient Function**

#### **3.1 General Autocorrelation**

Intuition leads us to believe that amplitudes of multipath components which exist at various locations and time delays are correlated. This has been found to be the case for urban mobile radio channels [5,6,7,8]. The general correlation coefficient is assumed to be a function of both space and time. Computation of the correlation of multipath amplitudes for all locations and time delays, although desirable, is not possible due to the limited amount of measured data and the difficulty of identifying the location and orientation of scatterers in an

# HISTOGRAM OF LOCAL STANDARD DEVIATION LINE-OF-SIGHT TOPOGRAPHY

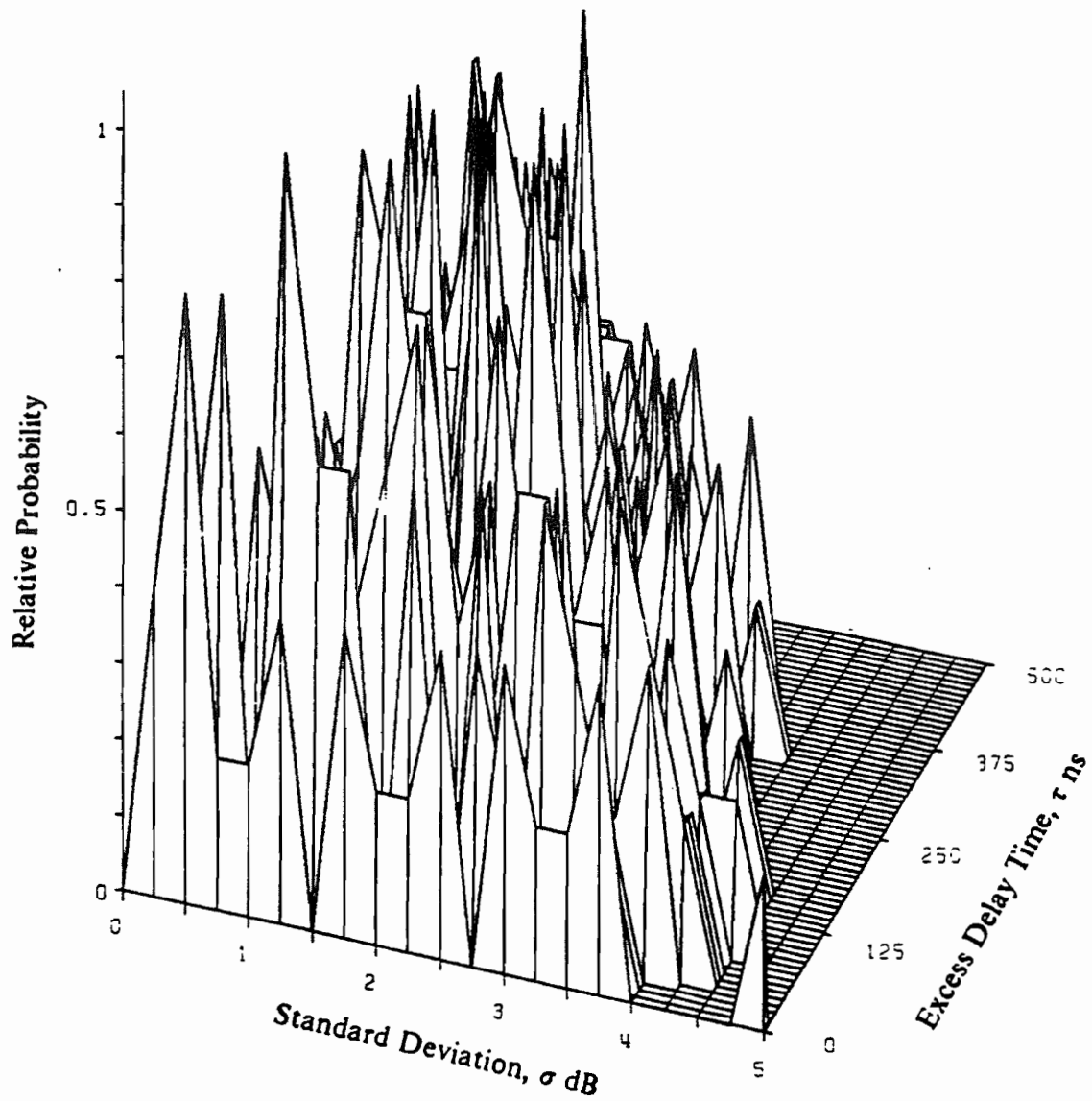


Figure 10. Histogram of local standard deviation for LOS topographies.

# HISTOGRAM OF LOCAL STANDARD DEVIATION OBSTRUCTED TOPOGRAPHY

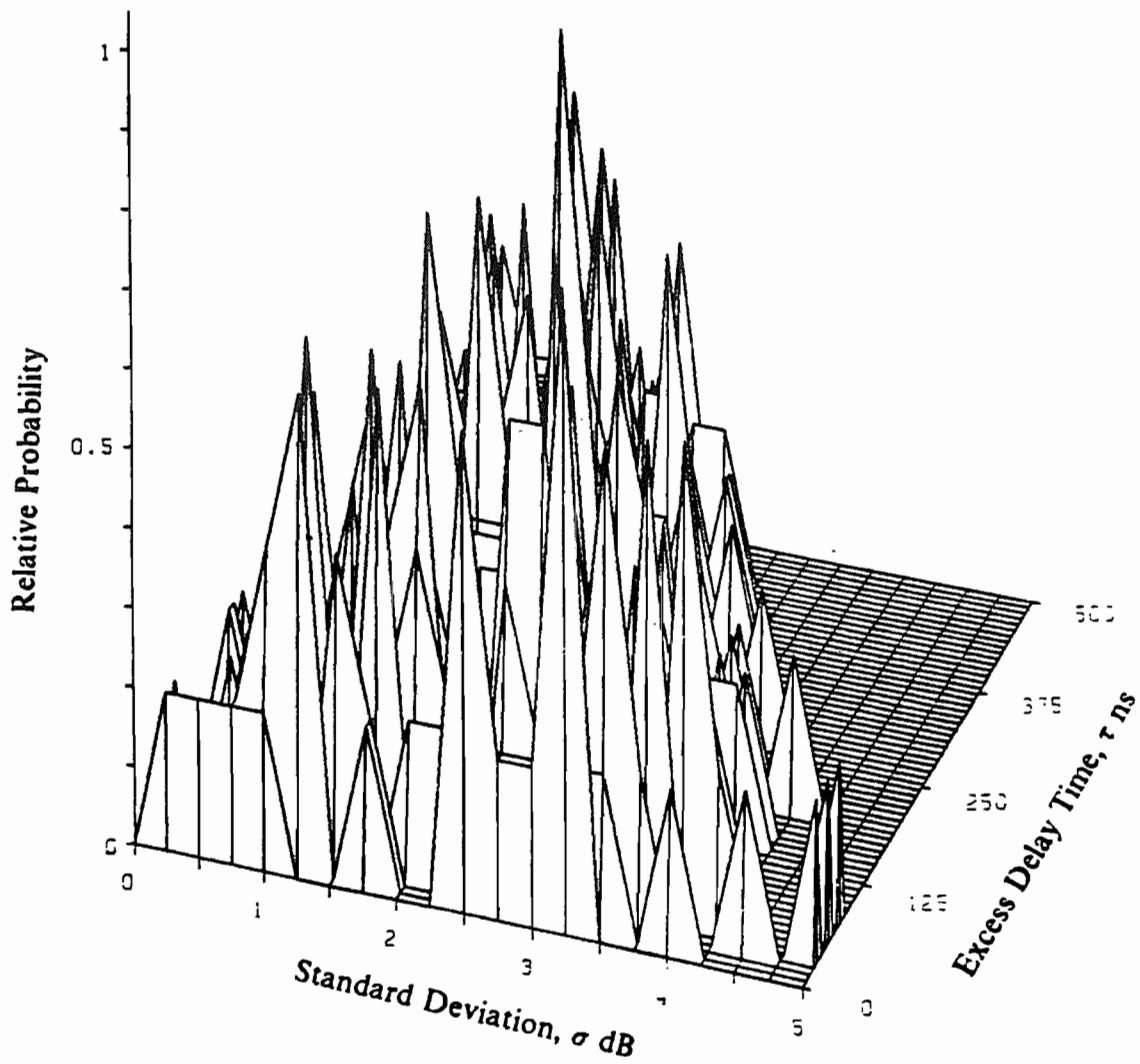


Figure 11. Histogram of local standard deviation for OBS topographies

indoor radio channel. Therefore, it is necessary to assume that temporal and spatial correlations are independent. The space and time correlation function can be written as

$$r_{aa}(A(x_1, \tau_1), A(x_2, \tau_2)) = K \hat{r}_{aa}(A(x_1), A(x_2); \tau) \tilde{r}_{aa}(A(\tau_1), A(\tau_2); x) \quad (1)$$

where  $A$  is a multipath amplitude for a particular spatial location  $x$  and excess delay  $\tau$ ,  $r_{aa}$  is the space and time correlation,  $\hat{r}_{aa}$  is the spatial correlation, and  $\tilde{r}_{aa}$  is the temporal correlation. Assuming independence, autocorrelation coefficients (ACC) for received signal levels are estimated individually over space and time.

### 3.2 Application of Autocorrelation Coefficient Function to Normal Distribution

The jointly normal probability density function of random variables  $A(\xi_1)$  and  $A(\xi_2)$  is defined as [6,10,12]

$$f_{X,Y}(x,y) = \frac{1}{2\pi\sigma_x\sigma_y(1-r^2)^{1/2}} \exp \left[ -\frac{\frac{(x-\bar{x})^2}{\sigma_x^2} - \frac{2r(x,y)(x-\bar{x})(y-\bar{y})}{\sigma_x\sigma_y} + \frac{(y-\bar{y})^2}{\sigma_y^2}}{2(1-r^2)} \right] \quad (2)$$

where

$$x = \Lambda(\xi_1)$$

$$y = \Lambda(\xi_2)$$

$$\bar{x} = \text{average of } \Lambda(\xi_1)$$

$$\bar{y} = \text{average of } \Lambda(\xi_2)$$

$$\sigma_x^2 = \text{variance of } \Lambda(\xi_1)$$

$$\sigma_y^2 = \text{variance of } \Lambda(\xi_2)$$

$$r = r_{aa}(\Lambda(\xi_1), \Lambda(\xi_2)), \quad -1 \leq r_{aa}(\Lambda(\xi_1), \Lambda(\xi_2)) \leq 1$$

The conditional probability density function of  $y$  given the value of  $x$  is [6,10]

$$f_y(y|x) = \frac{1}{\sqrt{2\pi(1-r^2)}} \exp \left[ -\frac{\left( y - \bar{y} - r(x - \bar{x}) \frac{\sigma_y}{\sigma_x} \right)^2}{2(1-r^2)\sigma_y^2} \right] \quad (3)$$

Thus, the conditional distribution of  $A(\xi_2)$  given the value of  $A(\xi_1)$  can be calculated by assuming a log-normal distribution with a conditional mean

$$\overline{\Lambda(\xi_2)} | \Lambda(\xi_1) = \overline{\Lambda(\xi_2)} - r_{aa}(A(\xi_1), A(\xi_2)) (A(\xi_1) - \overline{\Lambda(\xi_1)}) \frac{\sigma_{\Lambda(\xi_2)}}{\sigma_{\Lambda(\xi_1)}} \quad (4a)$$

and a conditional variance

$$\sigma_{\Lambda(\xi_2) | \Lambda(\xi_1)}^2 = (1 - r_{aa}^2(A(\xi_1), A(\xi_2))) \sigma_{\Lambda(\xi_2)}^2 \quad (4b)$$

When random variables  $x$  and  $y$  are in dB, then the density functions in equations (2) and (3) describe a log-normal distribution. The autocorrelation coefficients are computed with data values in dB since a joint log-normal distribution is assumed.

### 3.3 Spatial Correlation

Inspection of the profiles and intuition about the physical causes of multipath propagation lead us to believe that multipath component amplitudes are correlated over small distances. Over large distances, it is reasonable to assume signal strengths are uncorrelated. This has been shown for urban mobile radio channels [5,7,8,11]. A valid model must be able to generate profiles which produce the same correlation statistics as measured data. Also, the distance at which multipath signal amplitudes become uncorrelated is important in the analysis of antenna diversity.

We assume that multipath amplitudes are jointly log-normally distributed over local areas. The log-normal distribution was shown to be a good model for individual multipath signal levels over local areas in Section II. If the amplitude of a multipath signal which occurs at a particular excess delay at one location is known, then the conditional amplitude of the multipath signal amplitude at a distance  $\Delta x$  away with the same excess delay is log-normally distributed with mean and variance as derived from (4a) and (4b), where

$$\overline{A(x + \Delta x; \tau)} | A(x; \tau) = \overline{A(x; \tau)} + \hat{r}_{aa}(\Delta x; \tau) (A(x; \tau) - \overline{A(x; \tau)}) \quad (5a)$$

$$\sigma_{A(x+\Delta x; \tau) | A(x; \tau)}^2 = (1 - \hat{r}_{aa}(\Delta x; \tau)^2) \sigma_{A(x; \tau)}^2 \quad (5b)$$

and

$A(x; \tau)$  = multipath signal amplitude at location  $x$  and excess delay  $\tau$

$\overline{A(x; \tau)}$  = local spatial average of multipath signal amplitude at location  $x$   
and excess delay  $\tau$

$\overline{A(x + \Delta x; \tau)} | A(x; \tau)$  = conditional spatial average of multipath signal amplitude  
at location  $x + \Delta x$  and excess delay  $\tau$

$\hat{r}_{aa}(\Delta x; \tau)$  = spatial autocorrelation coefficient at separation  $\Delta x$  and excess delay  $\tau$

$\sigma_{A(x; \tau)}^2$  = spatial variance of multipath signal amplitude at location  $x$   
and excess delay  $\tau$

$\sigma_{A(x+\Delta x; \tau) | A(x; \tau)}^2$  = conditional spatial variance of multipath signal amplitude at  
location  $x$  and excess delay  $\tau$

The estimate of  $\hat{r}_{aa}(\Delta x; \tau)$  for each local area is obtained from [1,10,12]

$$\hat{r}_{aa}(x_1, x_2; \tau) = \frac{E[(A(x_1; \tau) - \overline{A(x_1; \tau)}) (A(x_2; \tau) - \overline{A(x_2; \tau)})]}{\sqrt{E[(A(x_1; \tau) - \overline{A(x_1; \tau)})^2] E[(A(x_2; \tau) - \overline{A(x_2; \tau)})^2]}} \quad (6)$$

Assuming spatial wide-sense stationarity over small distances and particular excess delay times,

$$\overline{A(x_1; \tau)} = \overline{A(x_2; \tau)} = \overline{A(x; \tau)} \quad (7a)$$

and

$$\hat{r}_{aa}(x_1, x_2; \tau) = \hat{r}_{aa}(|x_1 - x_2|; \tau) = \hat{r}_{aa}(\Delta x; \tau). \quad (7b)$$

The autocorrelation coefficient reduces to

$$\hat{r}_{aa}(\Delta x; \tau) = \frac{E[(A(x; \tau) - \overline{A(x; \tau)}) (A(x + \Delta x; \tau) - \overline{A(x; \tau)})]}{E[(A(x; \tau) - \overline{A(x; \tau)})^2]} \quad (8)$$

This is defined as the autocorrelation coefficient with respect to distance for a constant excess delay within a local area. Since data exist only at discrete points and autocorrelation coefficient functions (ACCF) are estimated for particular excess delay times, this reduces to

$$r_{aa}(j; \tau) = \frac{E[(A_i - \bar{A}) (A_{i+j} - \bar{A})]}{E[(A_i - \bar{A})^2]} \quad (9)$$

where

$i$  = profile number (1 to 19)

$j$  = integer number of  $\lambda/4$  separations between profiles (based on measurements in [2,3,4])

$A_i$  = multipath signal amplitude in profile number  $i$

$A_{i+j}$  = multipath signal amplitude in profile number  $i+j$

$\bar{A}$  = spatial average of multipath signal amplitude for a given excess delay and local area.

The expected values are computed as follows:

$$\bar{A} = \frac{1}{N} \sum_{i=1}^N A_i \quad (10a)$$

$$E[(A_i - \bar{A})^2] = \frac{1}{N} \sum_{i=1}^N (A_i - \bar{A})^2 \quad (10b)$$

= Local spatial variance of multipath signal amplitude

where  $N$  is the number of profiles where multipath component  $A_i$  exists ( $N$  has a maximum value of 19, based on measurements in [3,4,14], and thresholding as described in [2]).

$$E[(A_i - \bar{A})(A_{i+j} - \bar{A})] = \frac{1}{N} \sum_{i=1}^N (A_i - \bar{A})(A_{i+j} - \bar{A}) \quad (10c)$$

= Local spatial covariance of multipath signal amplitudes

where  $N$  is the number of profiles where multipath components  $A_i$  and  $A_j$  simultaneously exist within the same local area for a constant excess delay. Typical second order statistics are computed by averaging the local area statistics over the measurement ensemble.

Only locations where multipath components exist are used in the autocorrelation coefficient estimate computation. This means that the correlation of multipath amplitudes is conditioned upon simultaneous path existence. Empirical data show that over small scale distances of 1 meter, multipath components at particular excess delays exist over the local area, although they may undergo fading [3]. In cases where no multipath components exist at a particular excess delay, the autocorrelation coefficient function is undefined. In these cases, the autocorrelation coefficient estimate for the particular excess delay interval is not included in the estimate of the average local ACCF. With only nineteen profiles, the maximum number of data pairs to average into the autocorrelation coefficient is  $19-j$  for an integer separation of  $j$  profiles ( $\Delta x = j\lambda/4$ ). The question then becomes: how many data pairs are necessary to obtain an accurate estimate of the true autocorrelation coefficient function? Data are presented for



separations of up to ten profiles ( $2.5 \lambda$ ), but it must be kept in mind that our estimate of the ACCF is more accurate at small separations than larger ones. In addition to the fewer number of data pairs to average, the assumption of wide sense stationarity over distance becomes inaccurate. We will show for local areas in different factories and different T-R separations, the autocorrelation coefficient function can vary widely.

Figures 12 and 13 show the ACCF for the particular measurement locations PB1BC (LOS) and PC5AC (OBS), respectively. Notice the wide variation of our estimate of the autocorrelation coefficient (ACC) for various separations and excess delays. This is partially due to the small amount of data we have to compute the second order statistics over local areas. It also suggests that the spatial ACCF may be a random process for small changes in receiver location, in which case the channel is not wide sense stationary, even over small distances. Based on our data, autocorrelation coefficient functions at different measurement locations appear very different. This indicates that over large distances, the channel is not wide-sense stationary. Figures 14 and 15 show the average ACCF as a function of separation distance for various excess delays. The dashed lines represent  $\pm$  one standard deviation of the autocorrelation coefficient about the mean. Such a large standard deviation indicates that the spatial autocorrelation may assume almost any value. However, to incorporate correlation into a statistical model, it is necessary to assume wide-sense stationarity over local areas and statistically determine a particular autocorrelation coefficient function for any local area based on the average of the autocorrelation coefficient compiled from each local area.

Figures 16 and 17 show the average ACCF for various separation distances and excess delays for line-of-sight and obstructed topographies, respectively. On the average, multipath signal amplitudes become decorrelated over small distances ( $\lambda/2$ ) and even become slightly anti-correlated about the local mean value for distances of about  $\lambda/2$  to  $2\lambda$ . For small excess delays, the amplitudes are noticeably more correlated over small distances than are multipath amplitudes of signals which arrive later in the profile. We believe this occurs because the first

# AUTOCORRELATION COEFFICIENT FUNCTION

PB1BC

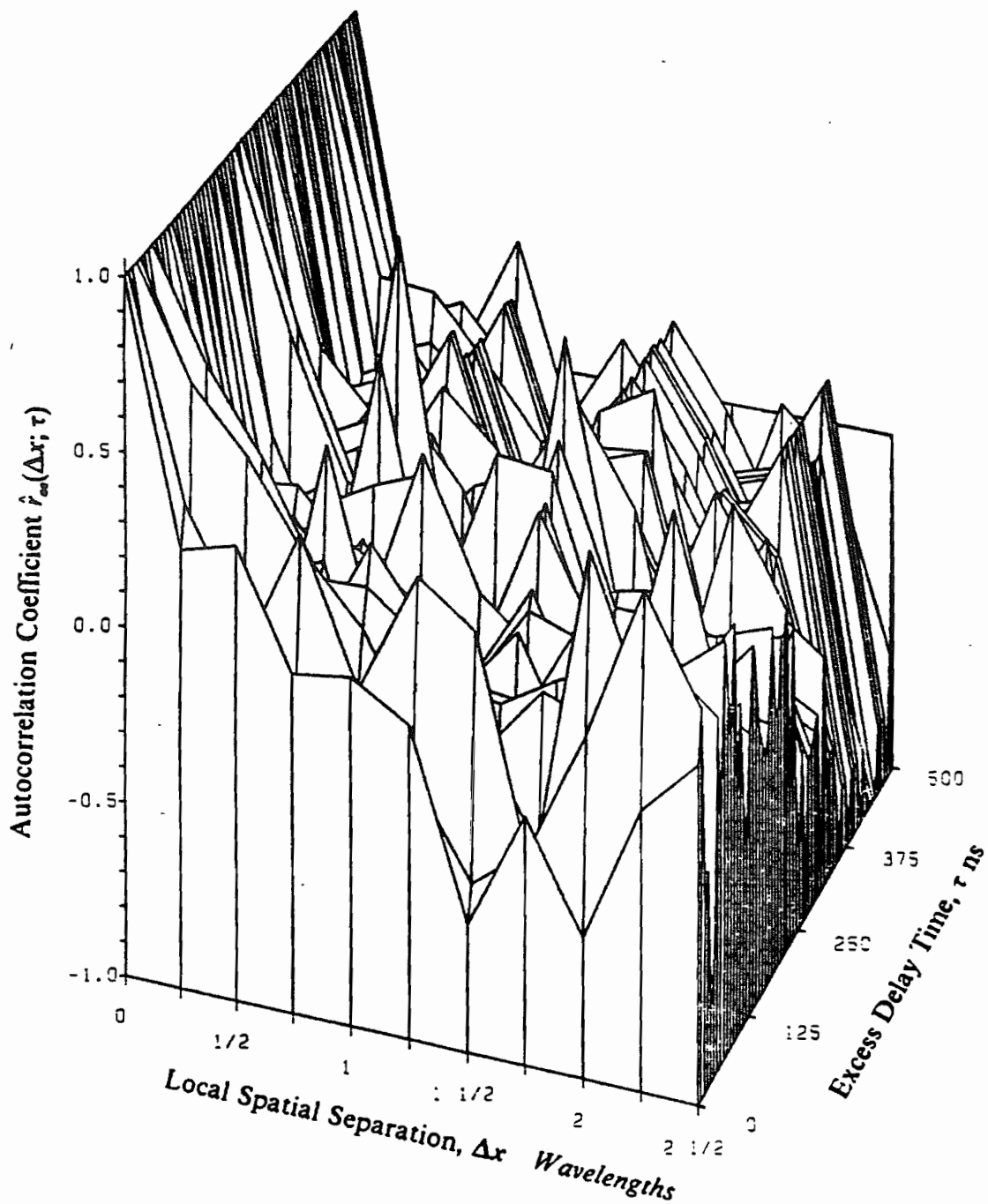


Figure 12. Spatial autocorrelation coefficient function for PB1BC (LOS).

# AUTOCORRELATION COEFFICIENT FUNCTION PCSAC

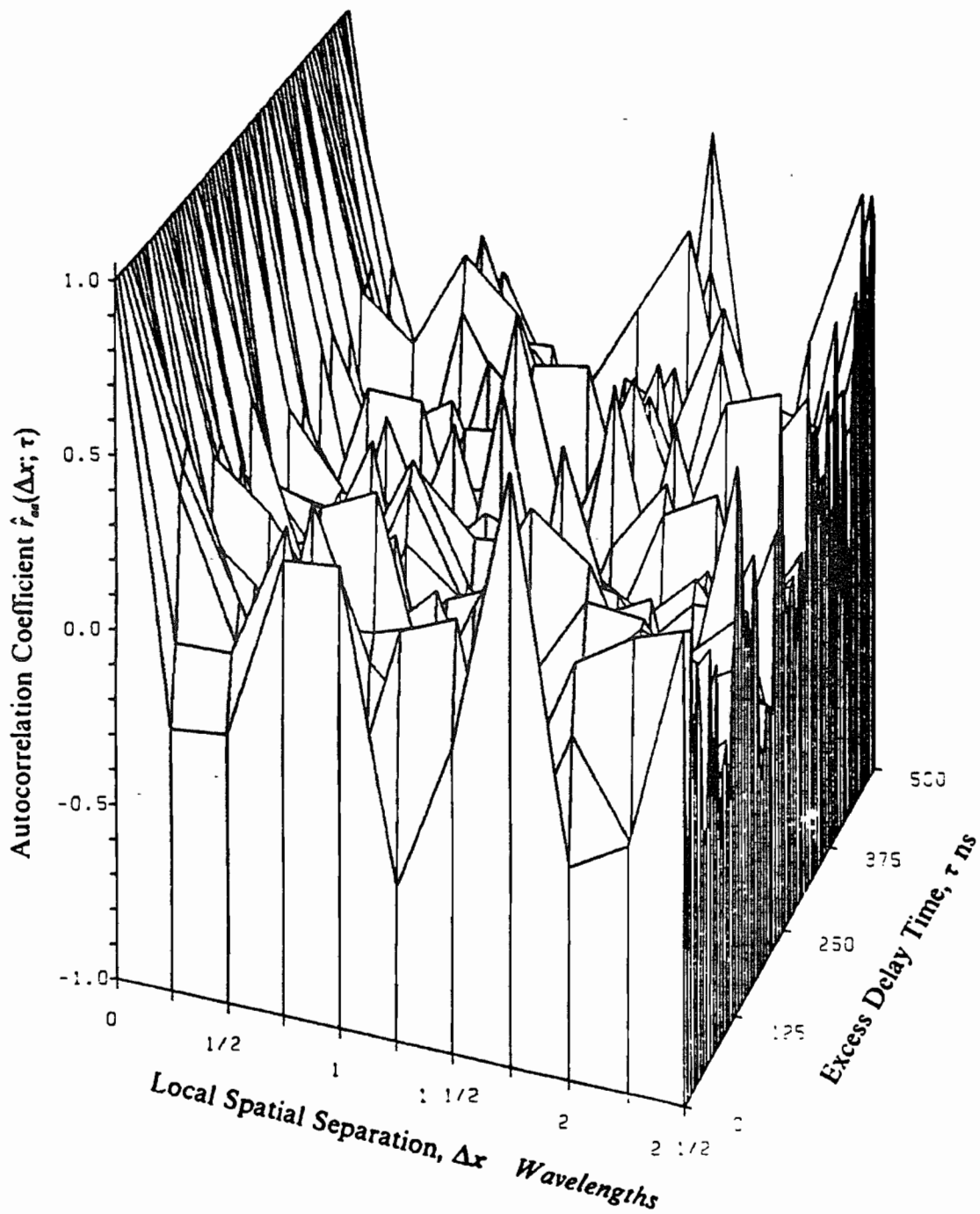


Figure 13. Spatial autocorrelation coefficient function for PCSAC (OBS).

b: LOS.LST

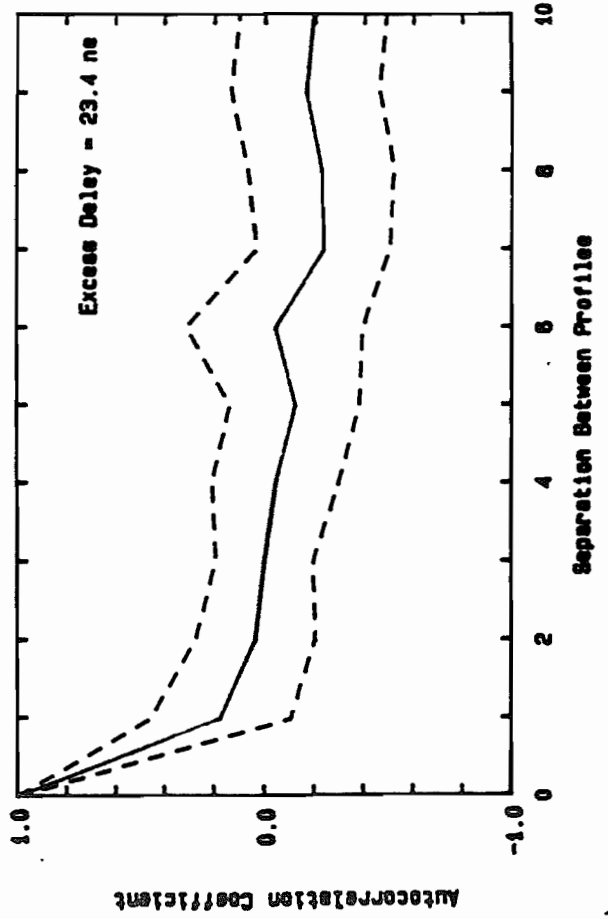
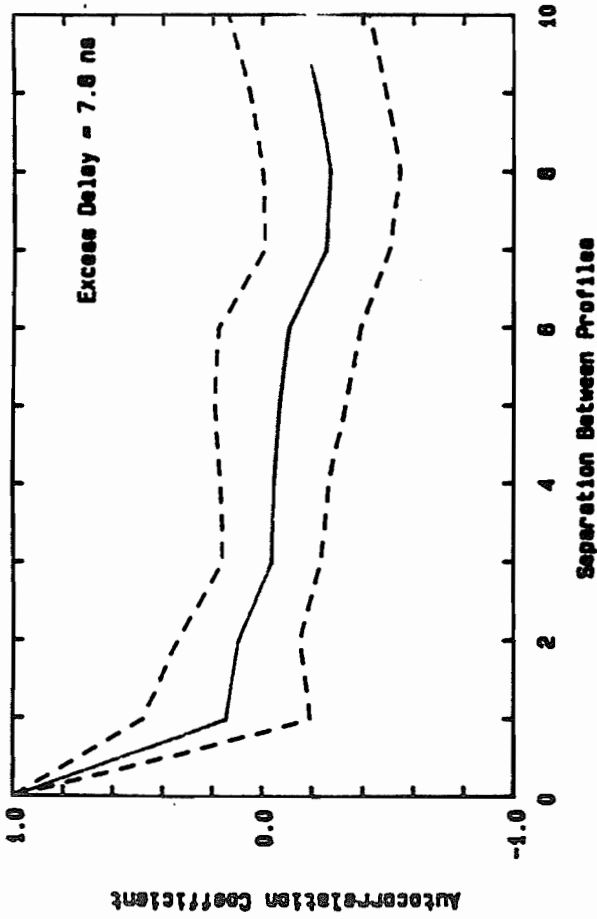
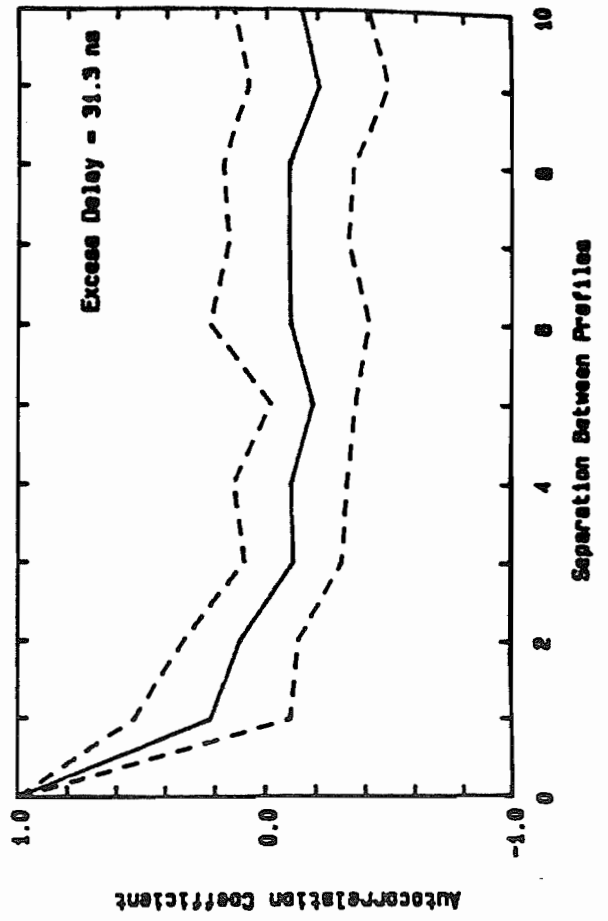
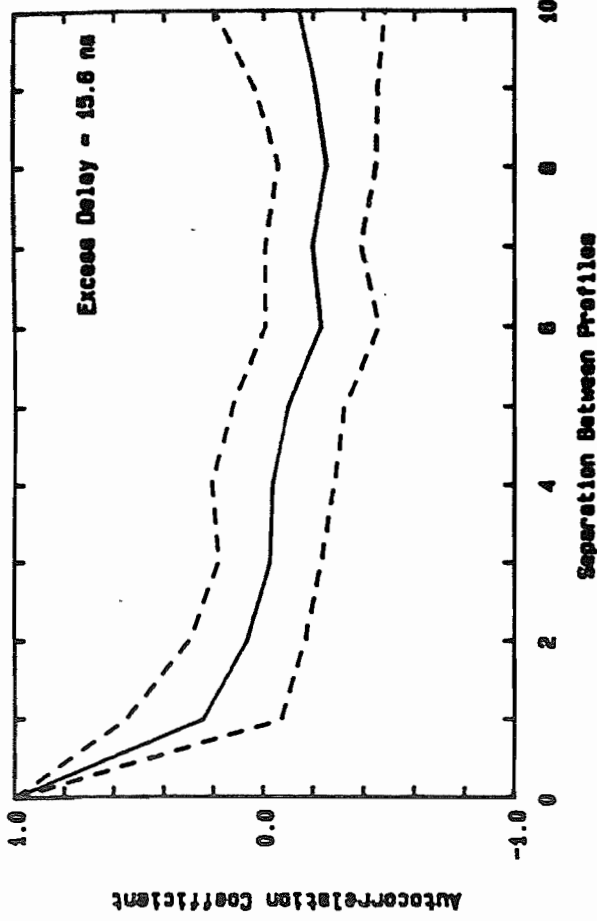


Figure 14. Average and standard deviation of spatial autocorrelation coefficient function

b: OBS. LST

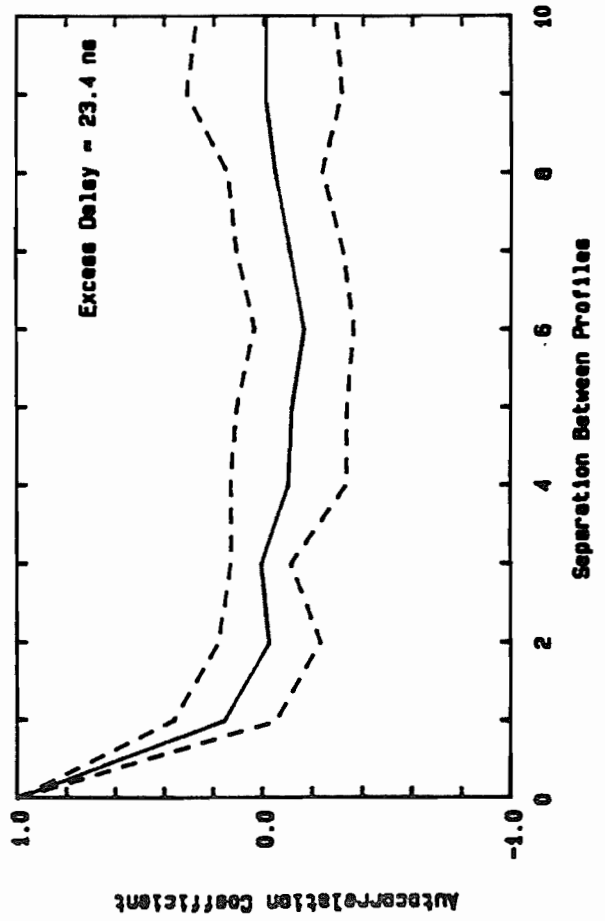
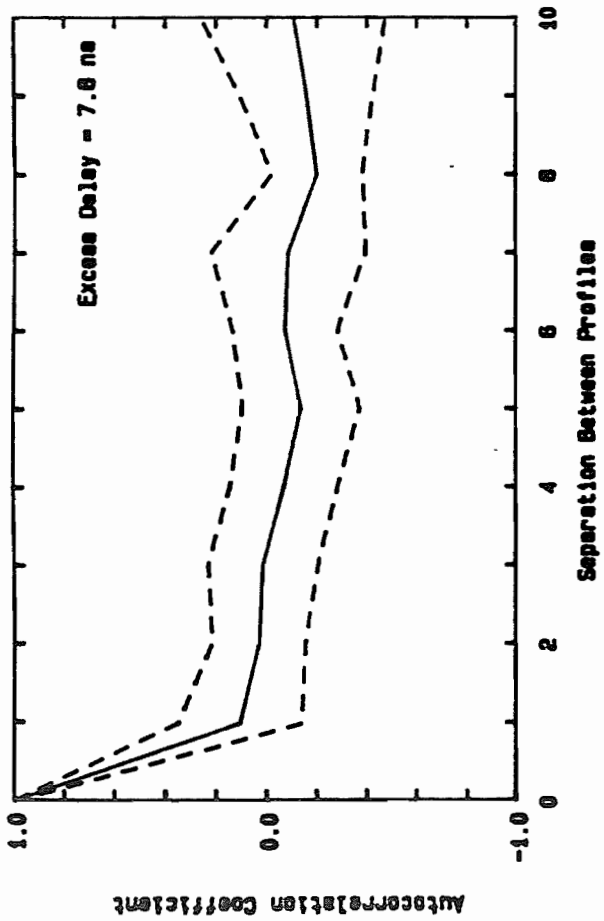
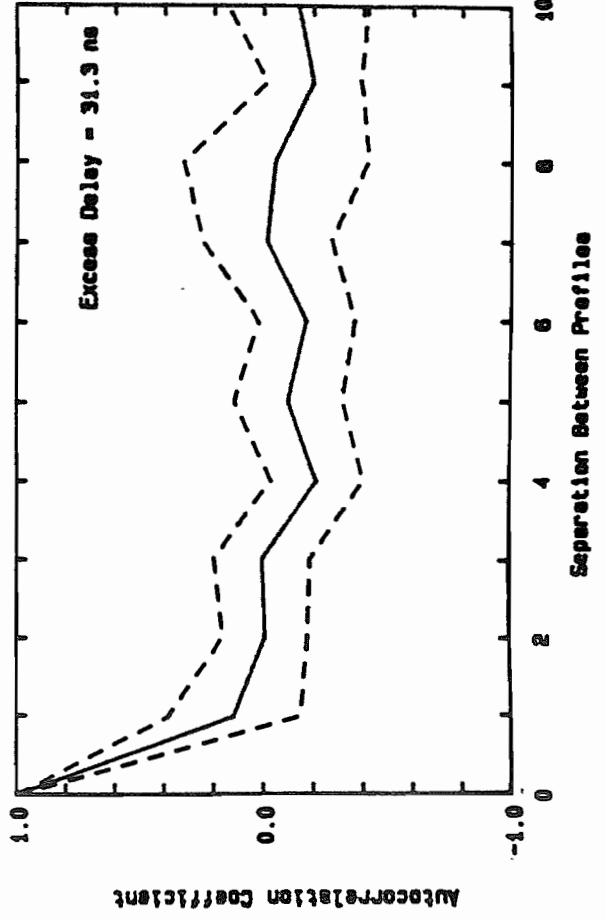
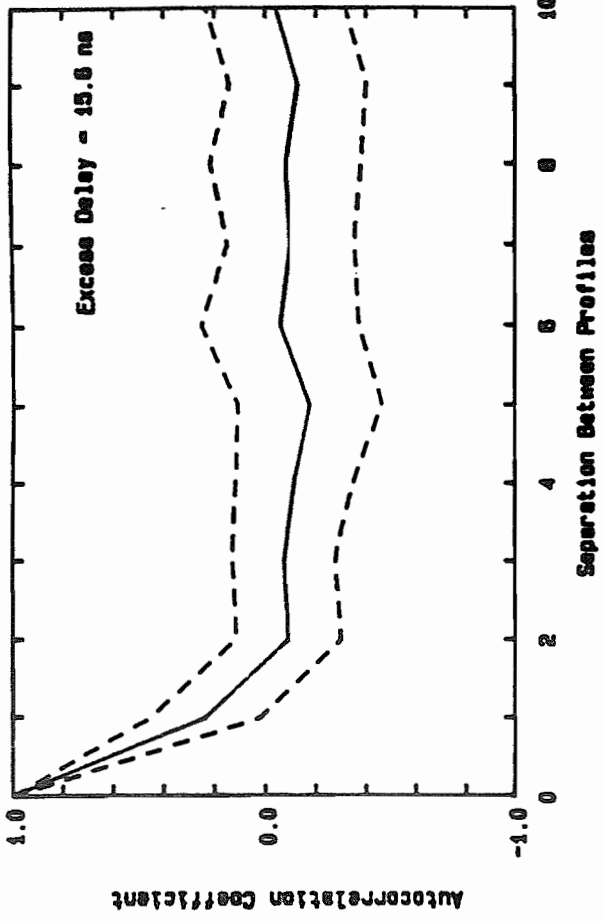


Figure 15. Average and standard deviation of spatial autocorrelation coefficient function for OBS tomography

# AVERAGE AUTOCORRELATION COEFFICIENT FUNCTION LINE-OF-SIGHT TOPOGRAPHY

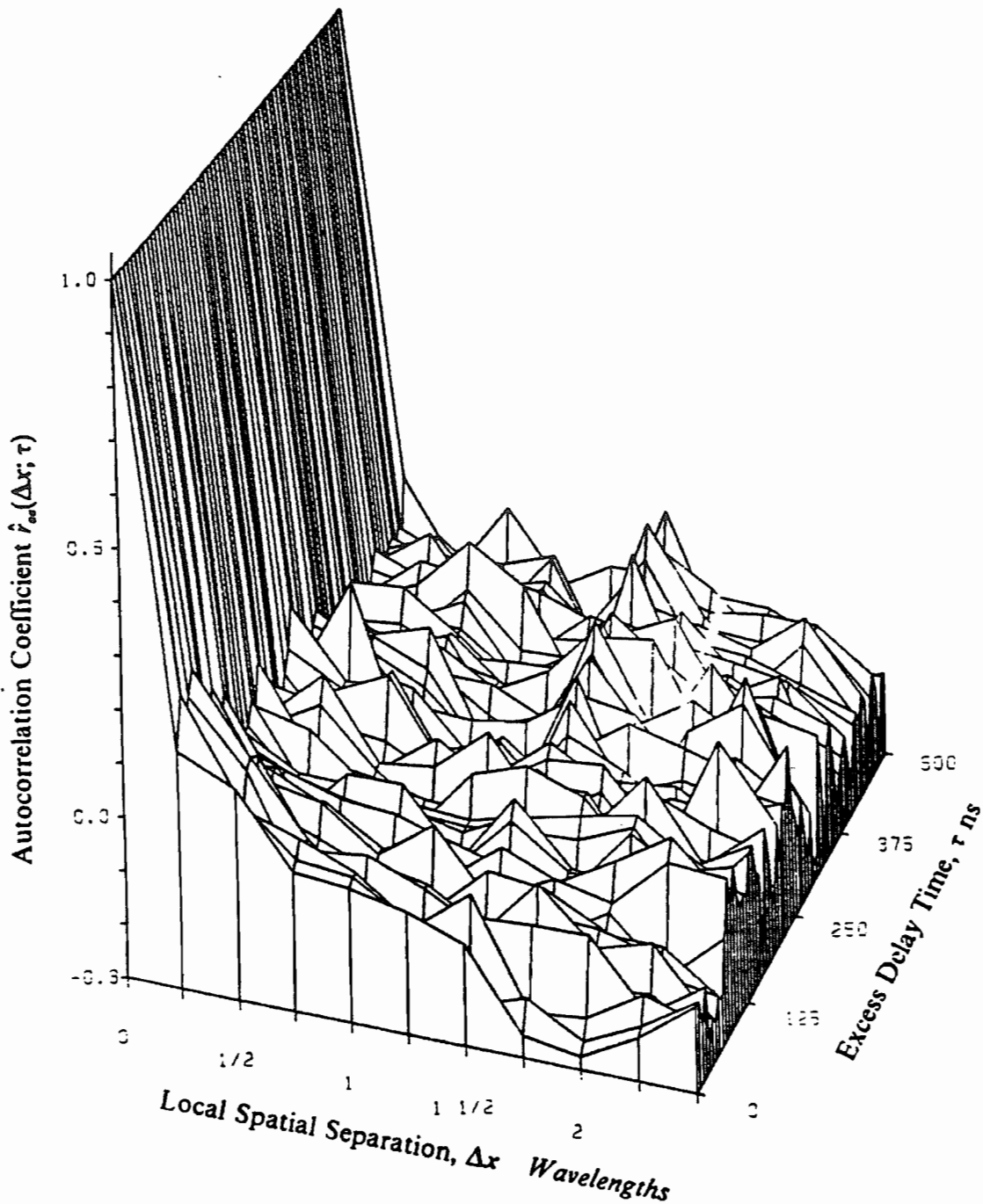


Figure 16. Average spatial autocorrelation coefficient function for LOS topographies.

# AVERAGE AUTOCORRELATION COEFFICIENT FUNCTION OBSTRUCTED TOPOGRAPHY

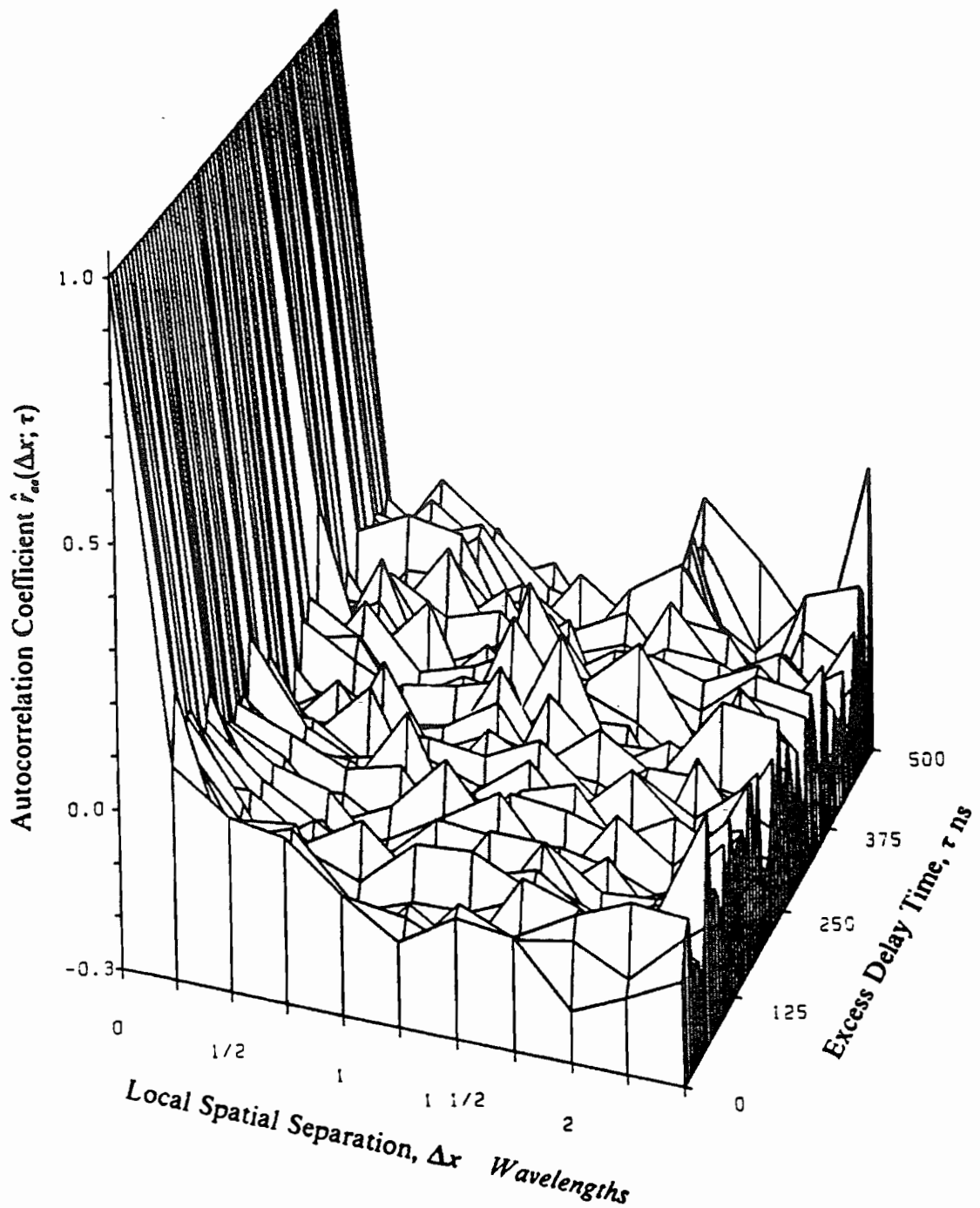


Figure 17. Average spatial autocorrelation coefficient function for OBS topographies.

arriving multipath signals are either direct LOS or are due to reflection from a single scatterer whereas later arriving multipath signals are likely due to multiple reflections from many random scatterers which exist throughout the factory. The phase angle of the later arriving multipath components are likely to change more over short distances than will the phase angles of the first few direct or nearly direct paths. Since it is likely that several multipath components occupy later excess delay intervals (sub-paths exist within the measurement resolution), one would expect the fading to be uncorrelated. Average correlation over short distances of the first few multipath amplitudes is greater in LOS topographies than in obstructed topographies because the first few arriving paths are more likely to be caused by direct wall, ceiling, and floor reflections.

### 3.4. Temporal Correlation

We assume that multipath signal amplitudes are jointly log-normally distributed over small excess delay time differences. Under this assumption, the amplitude of a multipath component at excess delay time  $\tau_2$  given that a component exists at time  $\tau_1$  can be estimated by a log-normal distribution with mean and variance which are derived from (4a) and (4b).

$$\overline{\Lambda(\tau_2)} | \Lambda(\tau_1) = \overline{\Lambda(\tau_2)} + \tilde{r}_{aa}(\tau_1, \tau_2)(\Lambda(\tau_1) - \overline{\Lambda(\tau_1)}) \frac{\sigma_{\Lambda(\tau_2)}}{\sigma_{\Lambda(\tau_1)}} \quad (11a)$$

$$\sigma_{\Lambda(\tau_2) | \Lambda(\tau_1)}^2 = (1 - \tilde{r}_{aa}(\tau_1, \tau_2)^2) \sigma_{\Lambda(\tau_2)}^2 \quad (11b)$$

where for a given local area,

$\Lambda(\tau_i)$  = multipath signal amplitude at excess delay time  $\tau_i$

$\overline{\Lambda(\tau_i)}$  = spatial average of multipath signal amplitude at excess delay time  $\tau_i$

$\tilde{r}_{aa}(\tau_1, \tau_2)$  = temporal autocorrelation coefficient between time  $\tau_1$  and  $\tau_2$

$\sigma_{\Lambda(\tau_i)}^2$  = variance of multipath signal amplitude at excess delay time  $\tau_i$



$\sigma_{A(\tau_2) | A(\tau_1)}^2$  = variance of multipath signal amplitude at excess delay time  $\tau_2$  given  $A(\tau_1)$

The estimate of temporal autocorrelation coefficient  $\tilde{r}_{aa}(\tau_1, \tau_2)$  given that multipath components exist at both  $\tau_1$  and  $\tau_2$  for each local area is given by

$$\tilde{r}_{aa}(\tau_1, \tau_2) = \frac{E[(A(\tau_1) - \overline{A(\tau_1)}) (A(\tau_2) - \overline{A(\tau_2)})]}{\sqrt{E[(A_k(\tau_1) - \overline{A_k(\tau_1)})^2] E[(A_k(\tau_2) - \overline{A_k(\tau_2)})^2]}} \quad (12)$$

where

$A(\tau_i)$  = multipath signal amplitude in profile  $k$  at time  $\tau_i$

$\overline{A(\tau_i)}$  = spatial average of multipath amplitude at time  $\tau_i$

Once again, wide-sense stationarity of multipath signal amplitudes between profiles at each local area must be assumed to calculate the temporal ACCF. Then, the average path amplitude at  $\tau_i$  is

$$\overline{A(\tau_i)} = \frac{1}{N} \sum_{k=1}^N A_k(\tau_i) \quad (13)$$

where  $k$  ( $k < N$ ) is profile number where multipath components exist at both  $\tau_1$  and  $\tau_2$ .  $N$  is the number of profiles (19) where multipath components exist at both time  $\tau_1$  and  $\tau_2$ . Since data only exist at discrete time intervals, the ACCF reduces to

$$\tilde{r}_{aa}(i,j) = \frac{E[(A_{k,i} - \overline{A}_i) (A_{k,j} - \overline{A}_j)]}{\sqrt{E[(A_{k,i} - \overline{A}_i)^2] E[(A_{k,j} - \overline{A}_j)^2]}} \quad (14)$$

where

$A_{k,i}$  = multipath signal amplitude in profile  $k$  at excess delay  $i$

$\overline{A}_i$  = local spatial average of multipath signal amplitude at excess delay  $i$

# AUTOCORRELATION COEFFICIENT FUNCTION PB1BC

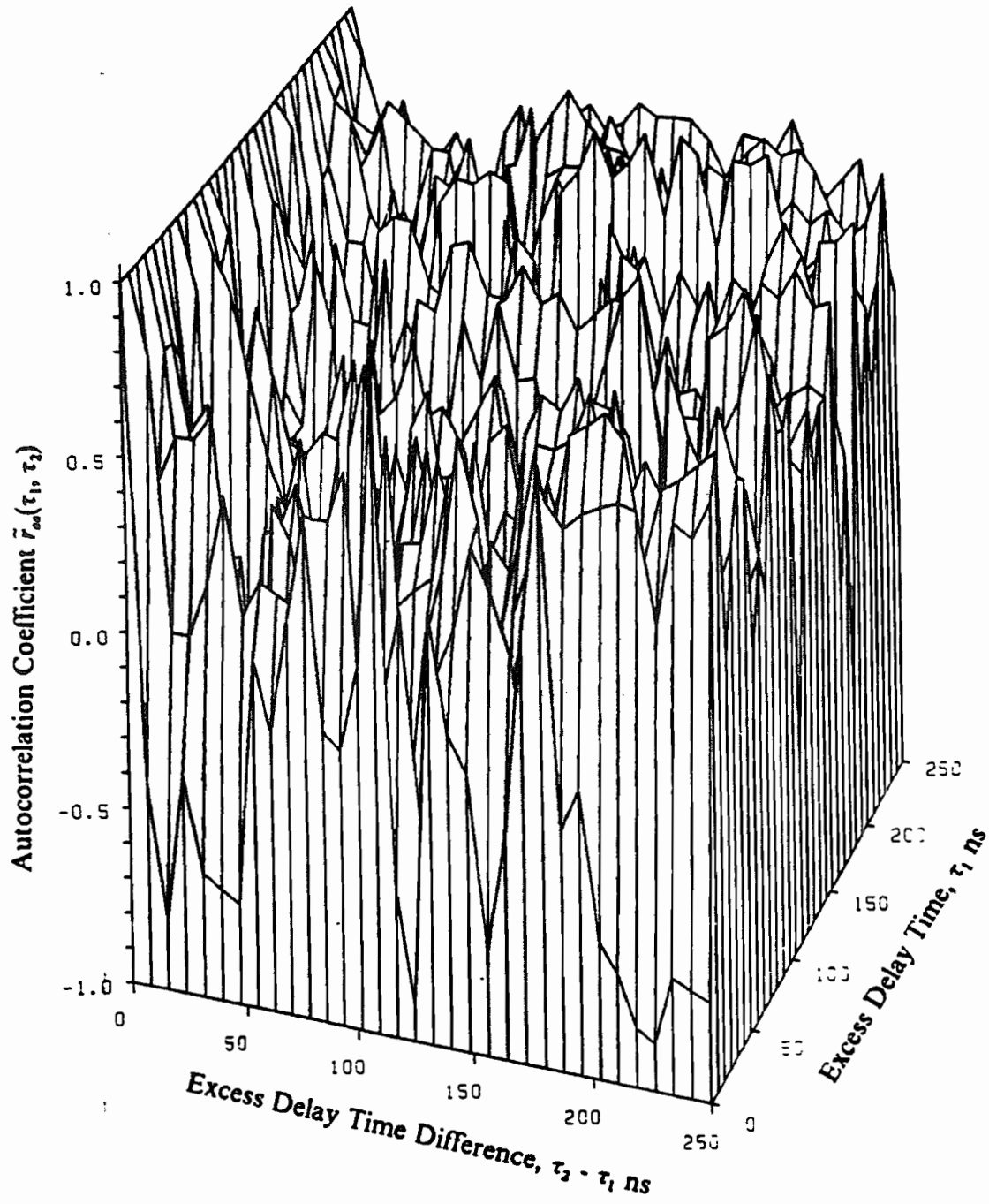


Figure 18. Average temporal autocorrelation coefficient function for PB1BC (LOS).

# AUTOCORRELATION COEFFICIENT FUNCTION

PC5AC

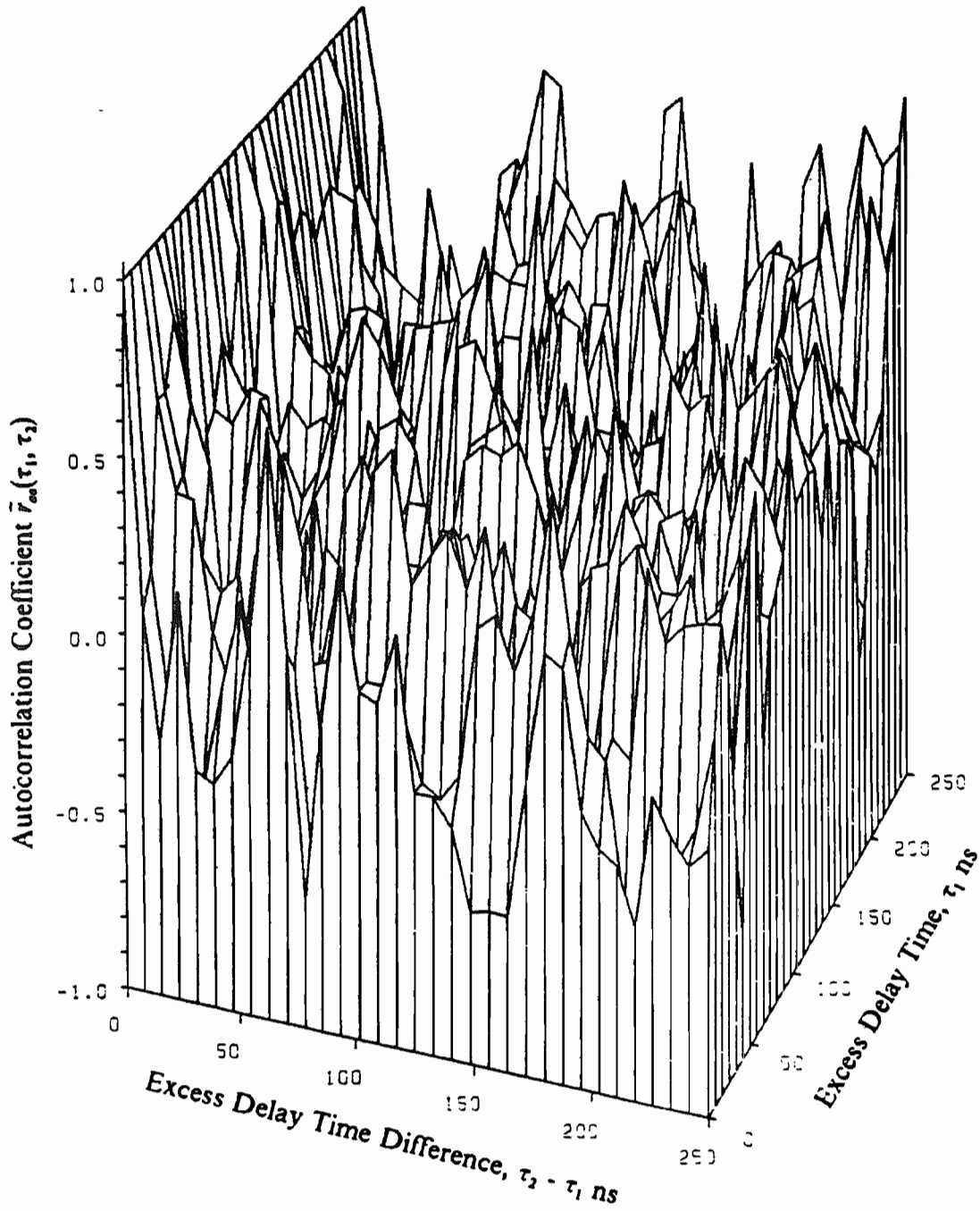


Figure 19. Average temporal autocorrelation coefficient function for PC5AC (OBS).



The temporal autocorrelation coefficient function for the particular measurement locations PB1BC (LOS) and PC5AC (OBS) are shown in Figs. 18 and 19, respectively. Similar to the spatial autocorrelation coefficient function, the temporal ACCF also varies widely over excess delay time  $\tau_1$ . These plots suggest that temporal autocorrelation is also a random process which is a function of excess delay. Figures 20 and 21 show the average of our estimate of the temporal autocorrelation coefficient for various excess delays for LOS and obstructed topographies. In addition, Figures 22 and 23 show the average and  $\pm$  one standard deviation of the temporal ACCF at  $\tau_1 = 0, 8$  and  $47$  nanoseconds for the same topographies.

In the case of LOS topography with  $\tau_1 = 0$  ns, the signal amplitudes decorrelate very rapidly. In particular, the signal amplitudes decorrelate at  $\tau_2 = 8$  ns, anti-correlate at  $\tau_2 = 16$  ns, and then stay uncorrelated for  $\tau_2 > 16$  ns. As excess delay  $\tau_1$  increases, the correlation within 20-50 nanoseconds of maximum correlation increases as compared to small excess delays. On the other hand, in the case of obstructed topographies, the path amplitudes have very similar ACCF for  $\tau_1 = 0$  to  $100$  ns. For  $\tau_1 > 100$  ns, the obstructed topographies also show the increase in correlation coefficient similar to LOS.

#### IV. Joint Probability of Path Occupancy

The temporal autocorrelation coefficient function described in section 3.4 is defined under the assumption that multipath components exist for both excess delay times  $\tau_1$  and  $\tau_2$ . Application of the autocorrelation coefficient in the channel model requires knowledge of the conditional probability of path occupancy, where the existence of a multipath signal at excess delay  $\tau_2$  is conditioned upon the existence of a signal at  $\tau_1$  ( $\tau_1 < \tau_2$ ).

Figure 24 shows the probability of path occupancy at time  $\tau_2$  given that path exists at time  $\tau_1$  for LOS topographies. The probability is calculated by counting the number of profiles over

# AVERAGE AUTOCORRELATION COEFFICIENT FUNCTION

LINE-OF-SIGHT TOPOGRAPHY

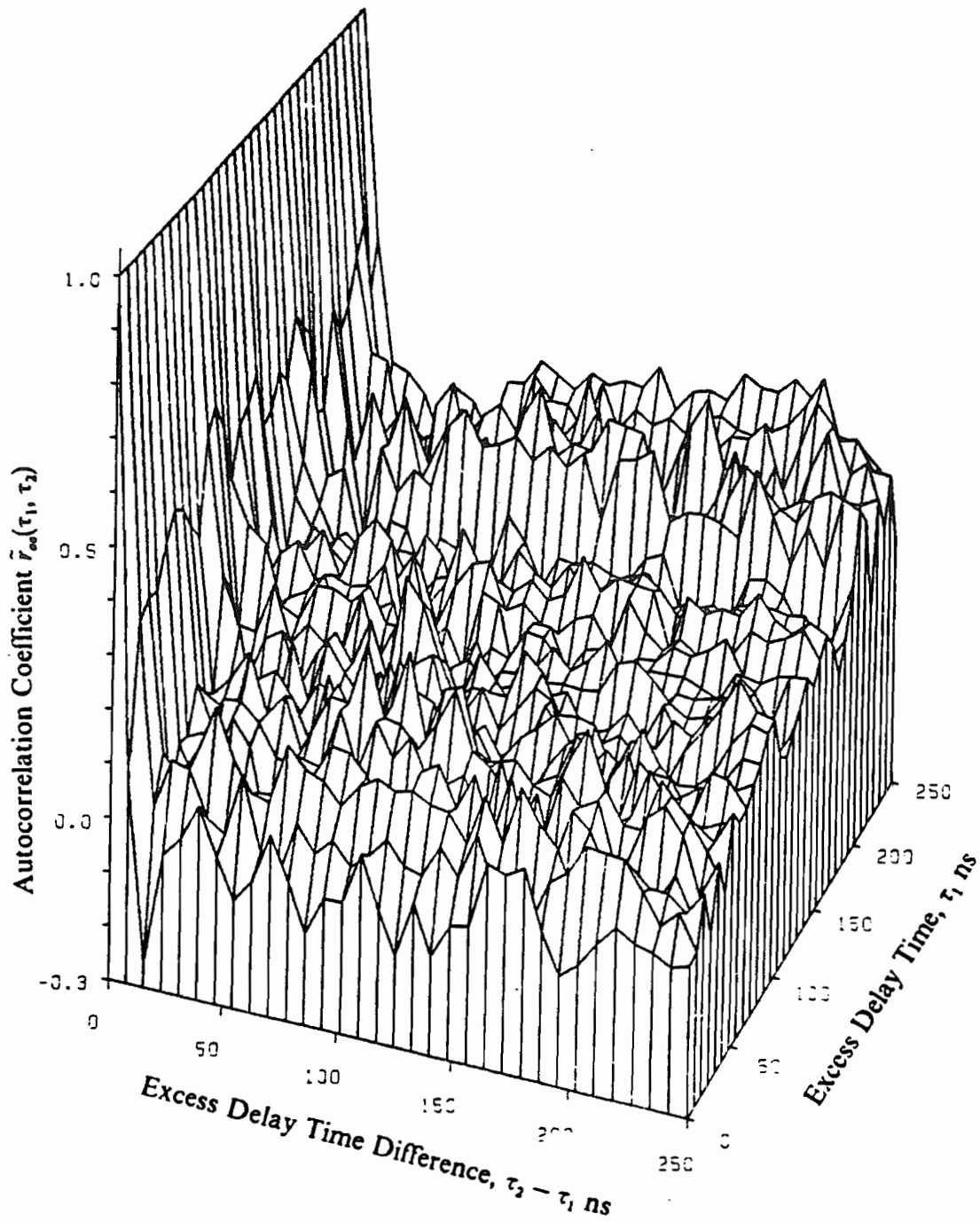


Figure 20. Average temporal autocorrelation coefficient function for LOS topographies.

# AVERAGE AUTOCORRELATION COEFFICIENT FUNCTION OBSTRUCTED TOPOGRAPHY

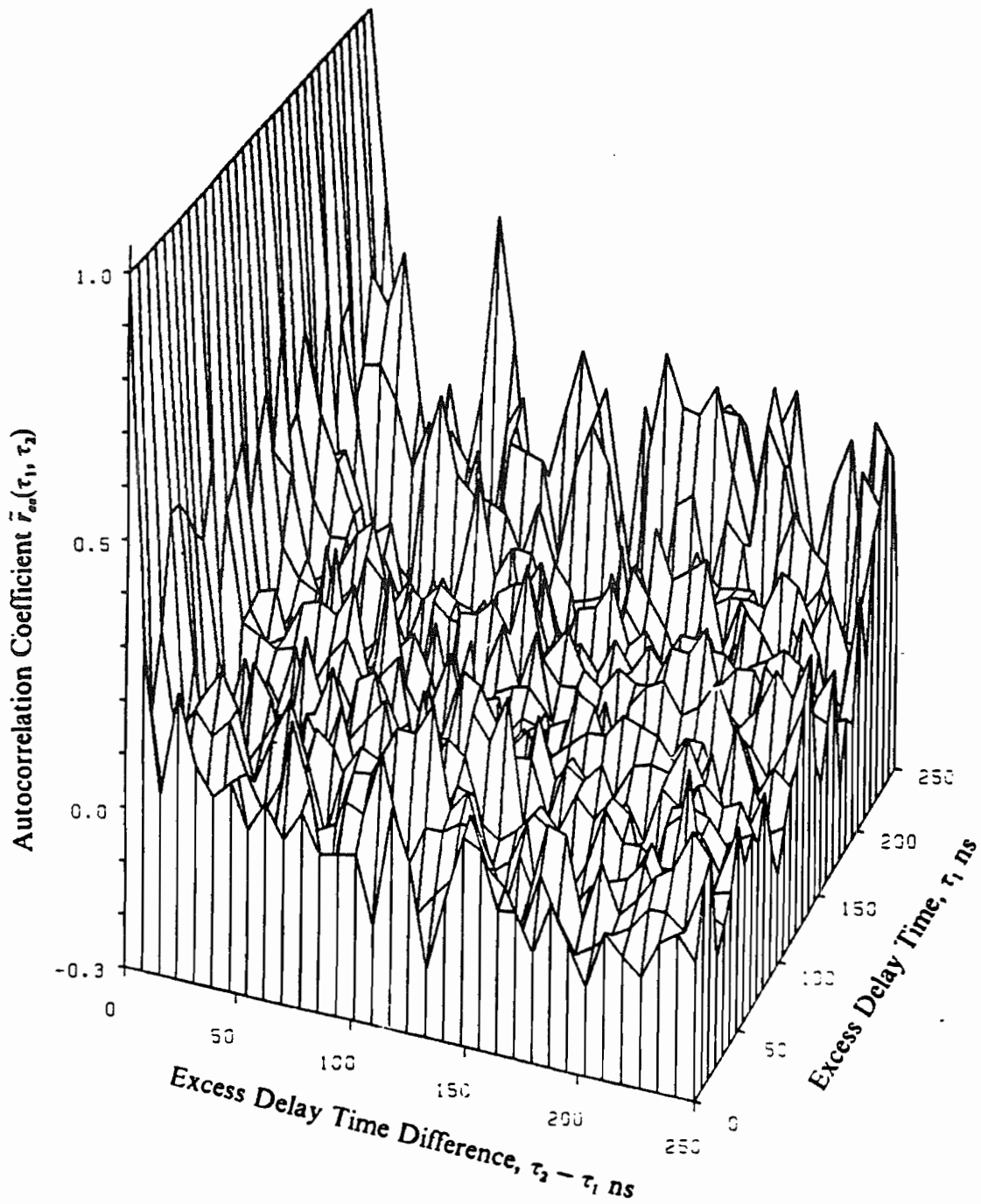


Figure 21. Average temporal autocorrelation coefficient function for OBS topographies.

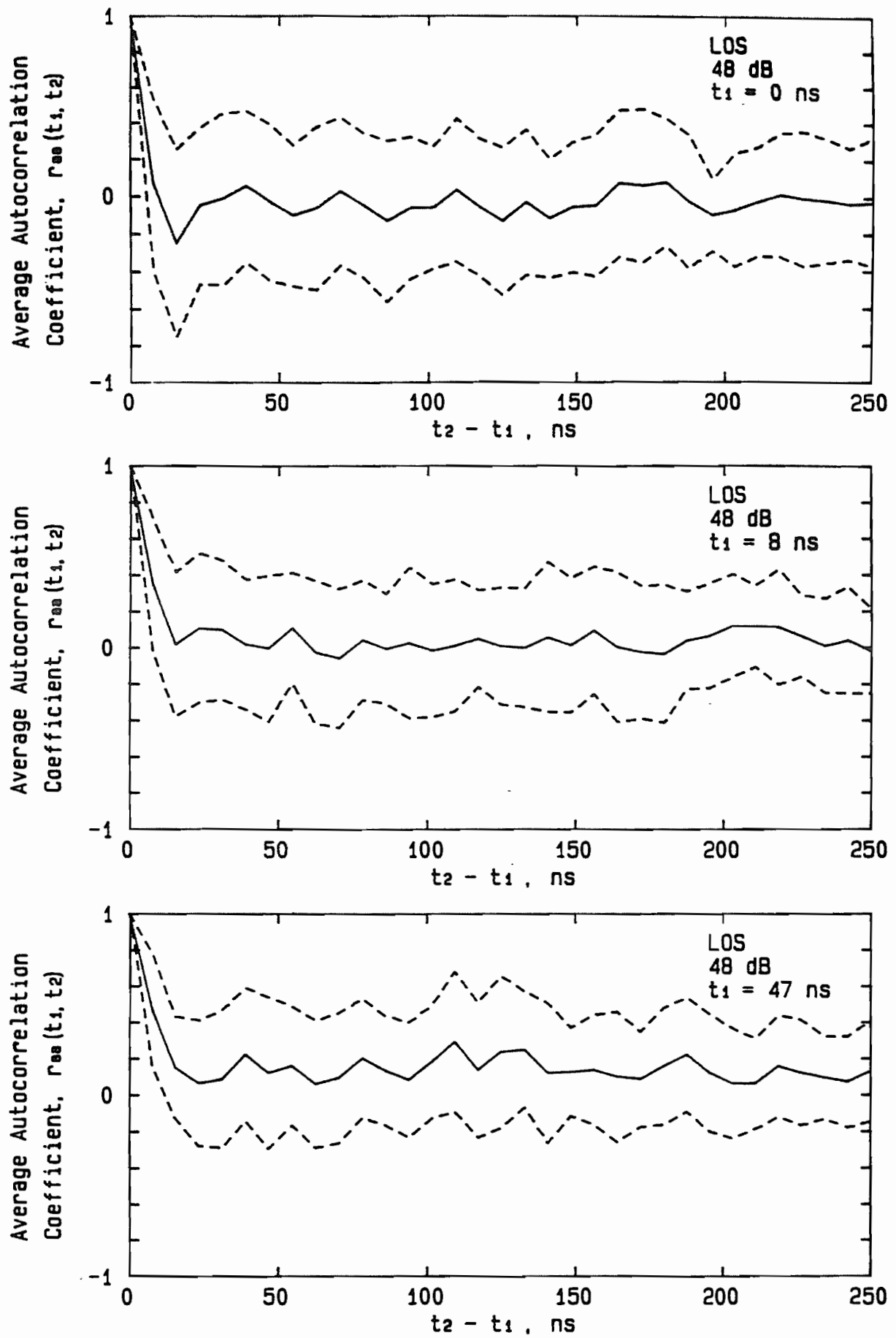


Figure 22. Average and standard deviation of temporal autocorrelation coefficient function for LOS topographies.



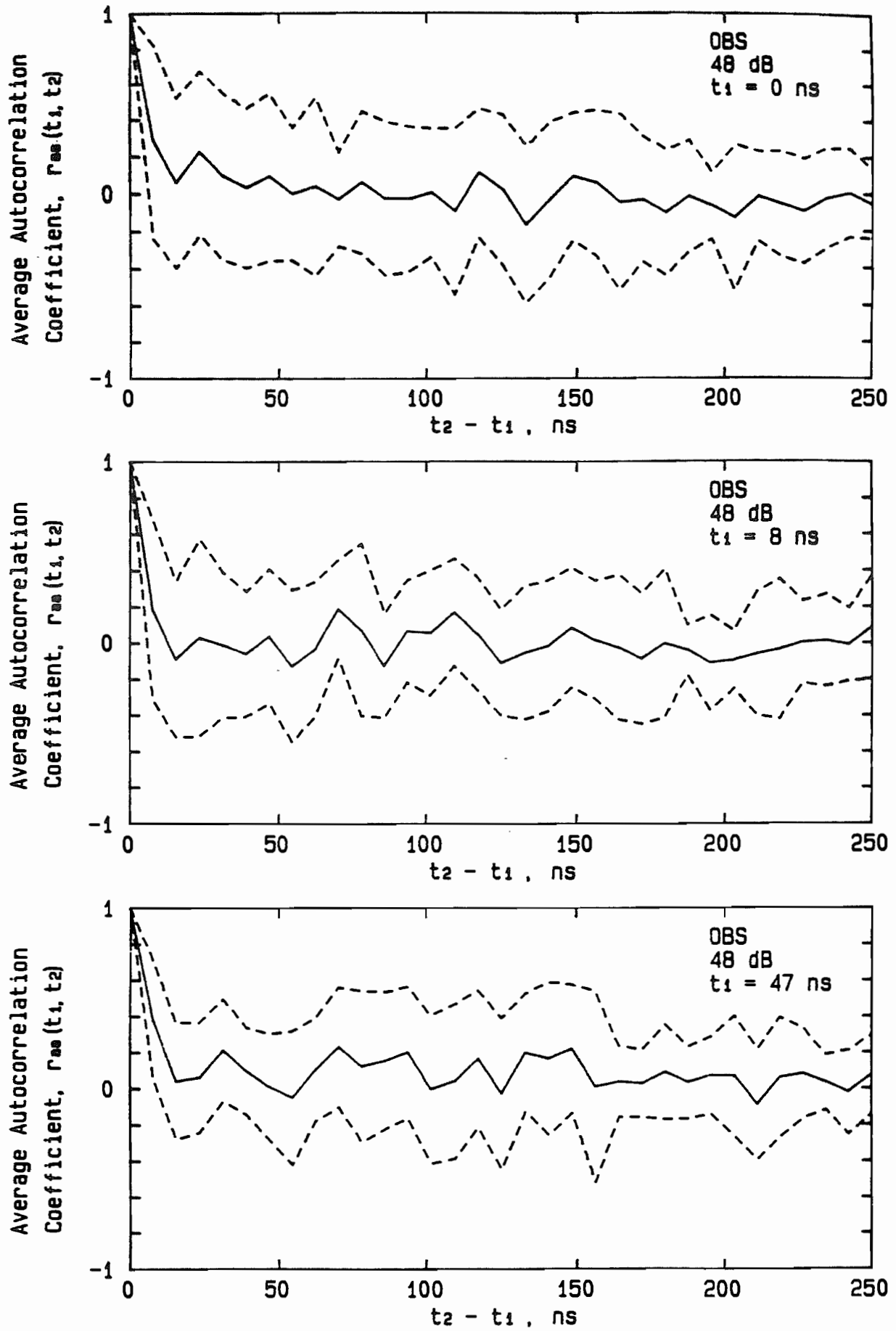


Figure 23. Average and standard deviation of temporal autocorrelation coefficient function for OBS topographies.

the ensemble of data which have signal amplitudes at  $\tau_1$  and  $\tau_2$  which are both greater than a specified received power threshold. It is apparent from the figure that for a low threshold (48 dB below level received at  $10\lambda$  T-R separation) and  $\tau_1$  less than 50 nanoseconds, the probability can be modeled as a linear function of time difference  $\tau_2 - \tau_1$ . As time  $\tau_1$  increases, the probability approaches an exponential decay. This implies that power delay profiles are not wide sense stationary for  $\tau_1$  less than 100 nanoseconds, since the conditional probability distribution of multipath existence is a function of excess delay. The figure also shows that the decay constants are very similar for  $\tau_1$  greater than 100 ns which suggest that power delay profiles may be temporally wide sense stationary for  $\tau_1$  greater than 100 ns.

Note in Fig. 24 where  $\tau_1 = 203$  nanoseconds, there is zero probability that multipath components exist at 30 dB threshold for the entire range of time differences. This is due to the fact that none of the measured profiles had signal amplitudes above the receiver threshold at 203 ns excess time delay.

Observations similar to LOS topographies are made for the obstructed topographies which are shown in Appendix F. As in LOS topographies, the conditional probability of path occupancy decreases rapidly as the received power threshold is increased. This suggests that adaptive power control at the receiver or transmitter is desirable to reduce the likelihood of receiving multipath components, as long as sufficient SNR can be maintained for the direct (LOS) signal. In obstructed topographies, the probability of path occupancy decreases even more than in LOS topographies for increasing time difference. This agrees with the observation [2,15] that a greater number of multipath components exist in LOS topographies. By using antenna diversity and or equalization to improve the instantaneous SNR of the desired signal component, in conjunction with power control to reduce intersymbol interference (ISI) due to multipath, it is likely that several hundred kilobit per second data transmission can be supported inside factories.

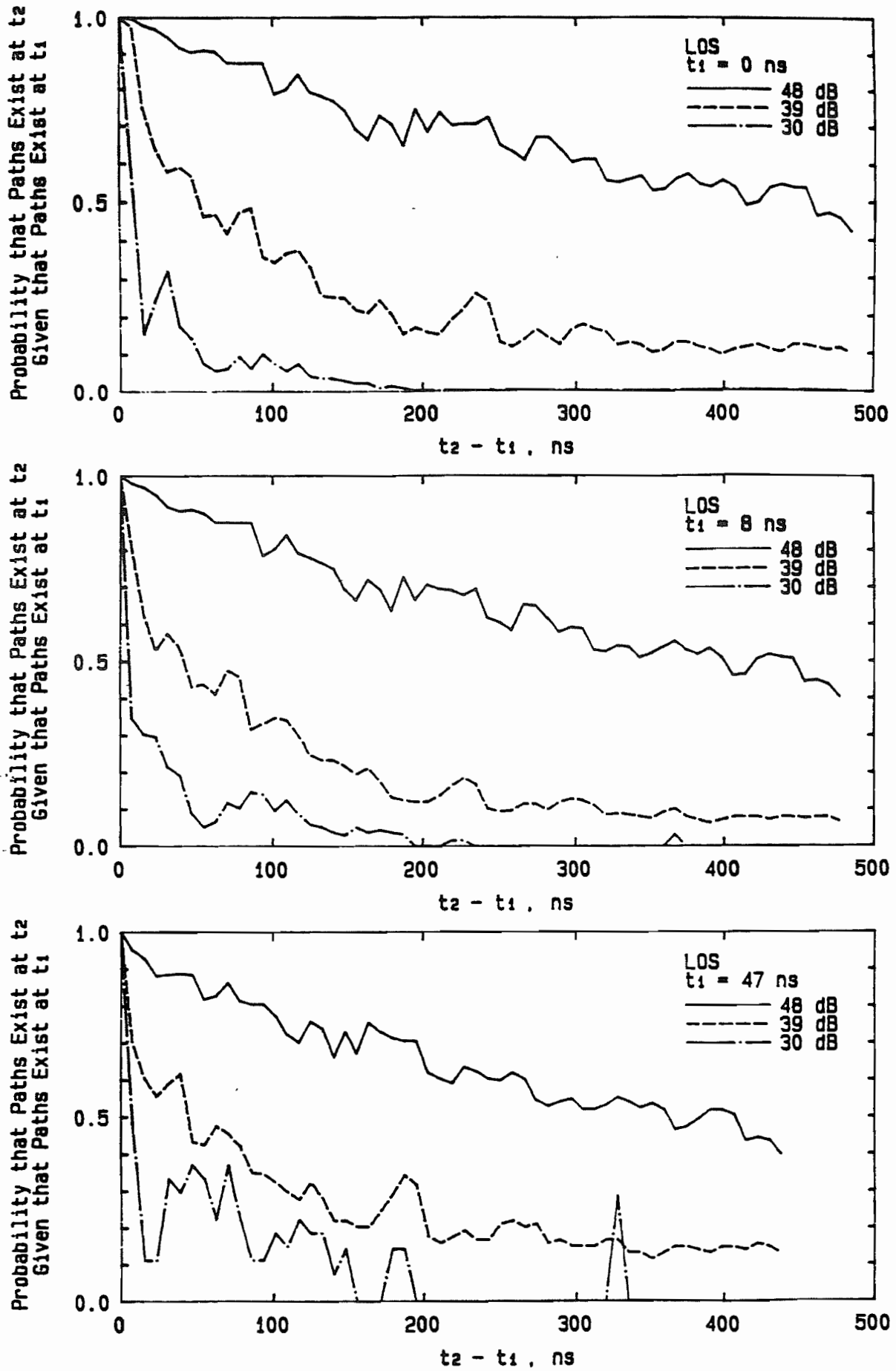


Figure 24. Conditional probability of path occupancy for LOS topographies.

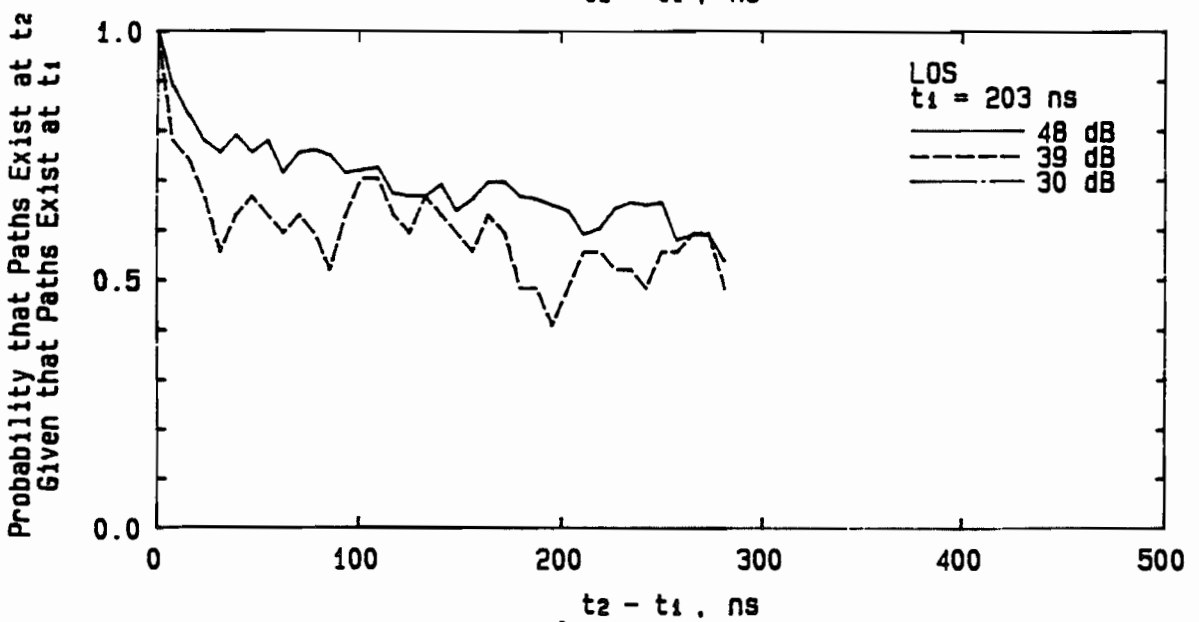
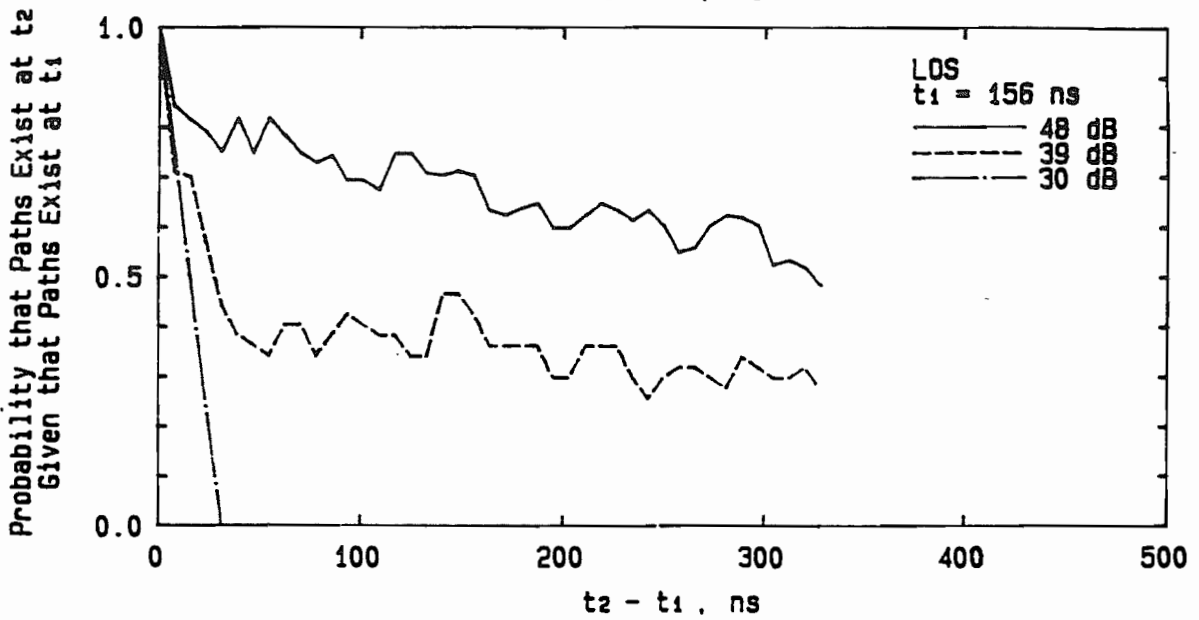
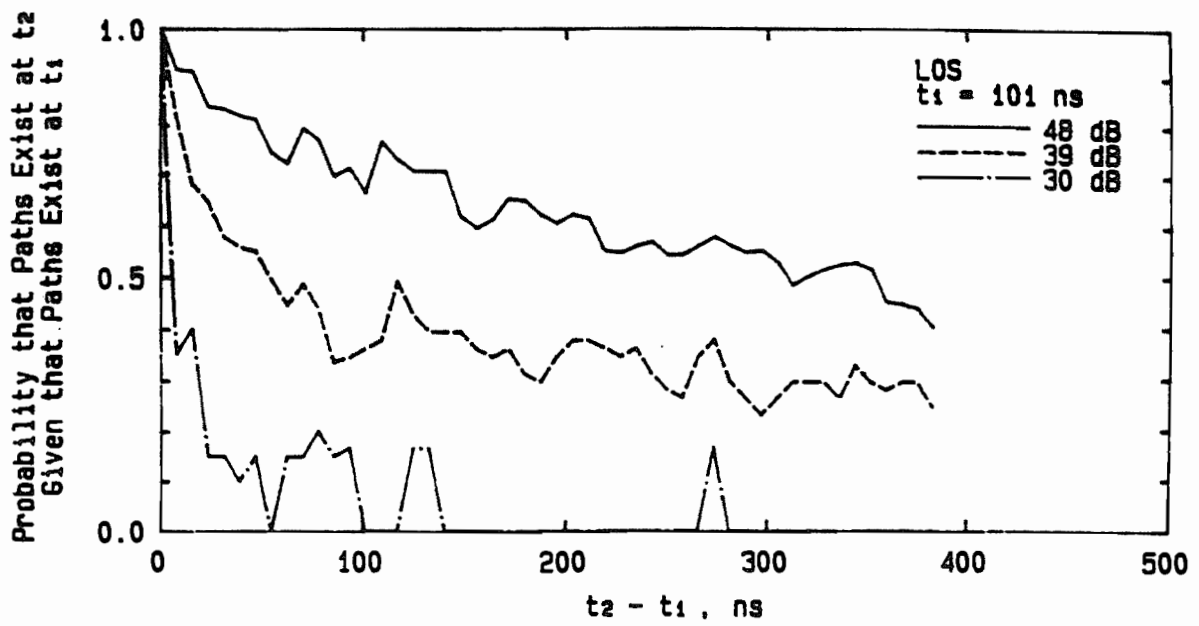


Figure 24. Continued.

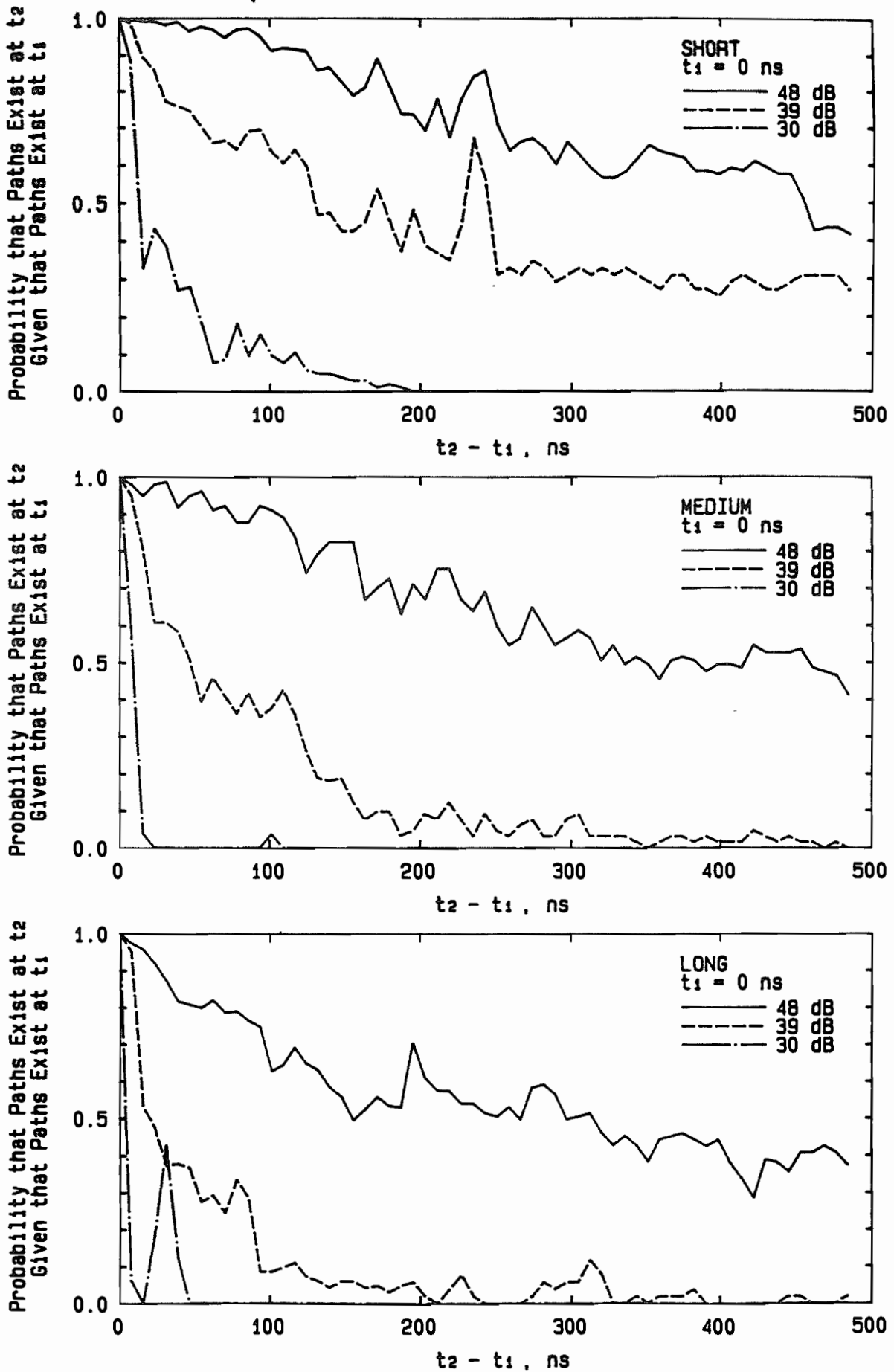


Figure 25. Conditional probability of path occupancy. a) short (10-25 m), b) medium (25-40 m), and c) long (40-80 m) T-R separations.

The conditional probabilities of path occupancy as a function of T-R separation, which is computed by partitioning the ensemble of data into three T-R separations (10-25 m, 25-40 m, and 40-80 m), are shown in Fig. 25. For small T-R separations, the probability exceeds 0.9 out to  $\tau_2 = 100$  nanoseconds. As the T-R separation is increased, the probability decreases more rapidly. This is an indication that for the short T-R separations, the multipath components arrive at the receiver in many adjacent excess delay intervals. In Appendix F, it can be seen that if a multipath component exists, say between 40 ns and 100 ns, there is a significant probability ( $> 0.25$ ) that strong components will exist at excess delays of several hundred nanoseconds beyond  $\tau_1$ . This shows that although power control will ameliorate multipath delay spread in a probabilistic sense, there will be times when multipath components occur at large excess delays in spite of reduced power. It can be shown that the conditional probabilities given in Appendix F confirm the path occupancy probabilities given in [2,15].

## V. Conclusion

Although the indoor radio channel cannot be completely characterized by only first and second-order statistics, they provide a more complete model of multipath propagation inside buildings than has been previously proposed [13]. We have shown that multipath components which arrive at particular excess delays have amplitudes which attenuate according to some mean  $d^n$  power law and have signals which are log-normally distributed about the mean. Also, we showed that a log-normal distribution is a good model for multipath signal amplitudes over local areas for particular excess delay times. This is fortunate, since log-normal distributions are completely characterized by first and second moments, and they are simple to use in a statistical channel impulse response model.

It appears that both spatial and temporal correlation may be a random process over local areas. This means that the indoor radio channel is not wide-sense stationary over distance or time. However, it is useful to assume that the channel is wide-sense stationary over local areas in order to compute the second-order (correlation) statistics, and apply them to a statistical model. On the average, multipath amplitudes are correlated over short distances ( $\lambda/2$ ) and for small excess delay time differences ( $< 50$  ns), but one must remember that the autocorrelation coefficient function of multipath signal amplitudes may assume almost any value. Application of the correlation coefficient to a statistical model channel simulator has been described, using the assumptions that the distribution of path amplitudes is jointly log-normal over space and excess delay, and that multipath components at particular excess delays exist at those delays over a space of 1 meter.

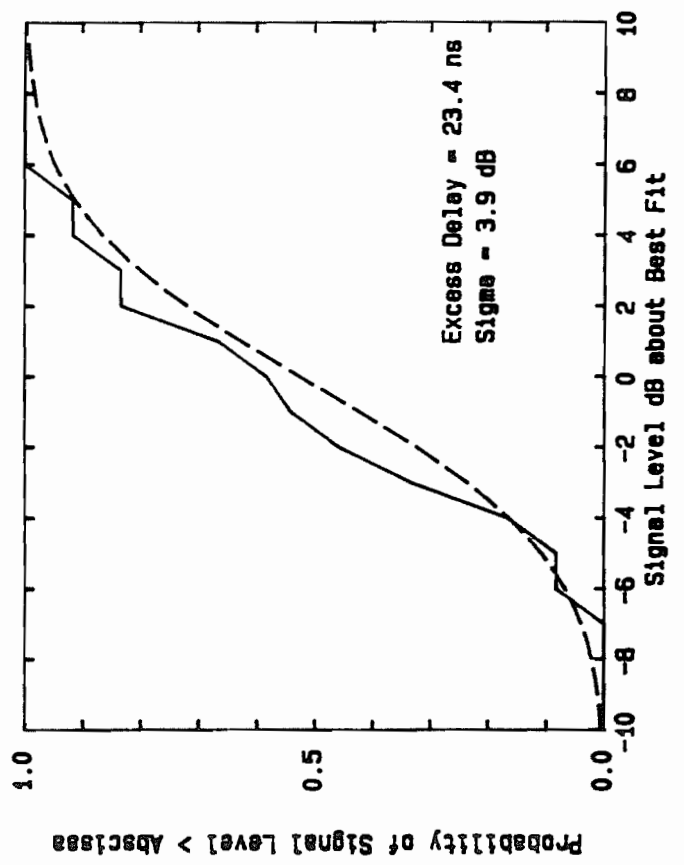
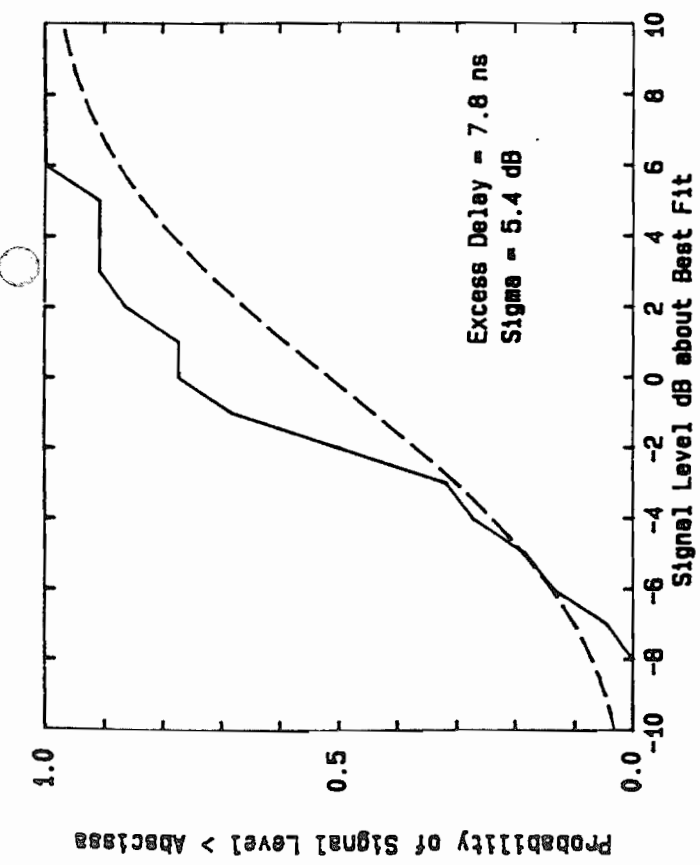
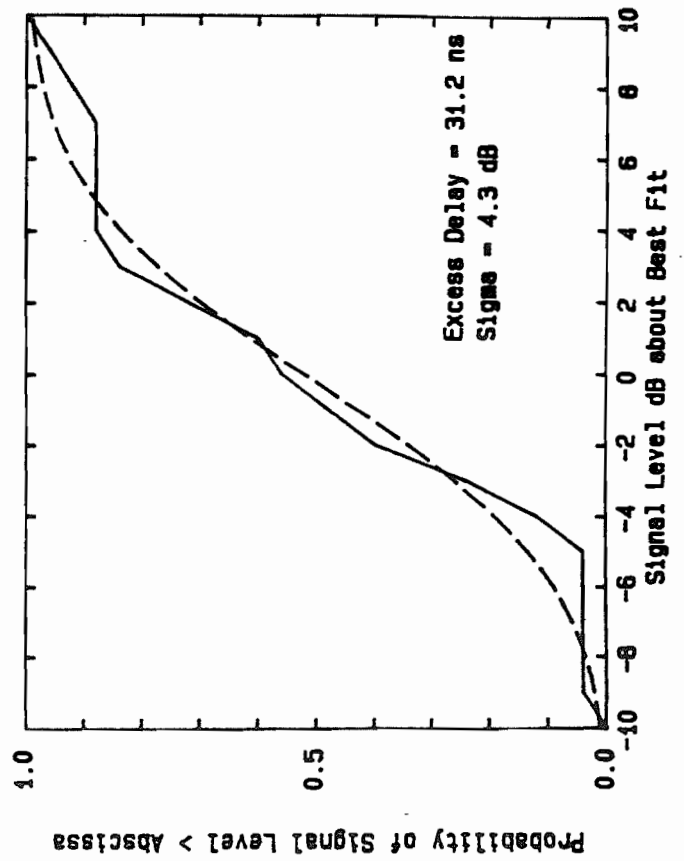
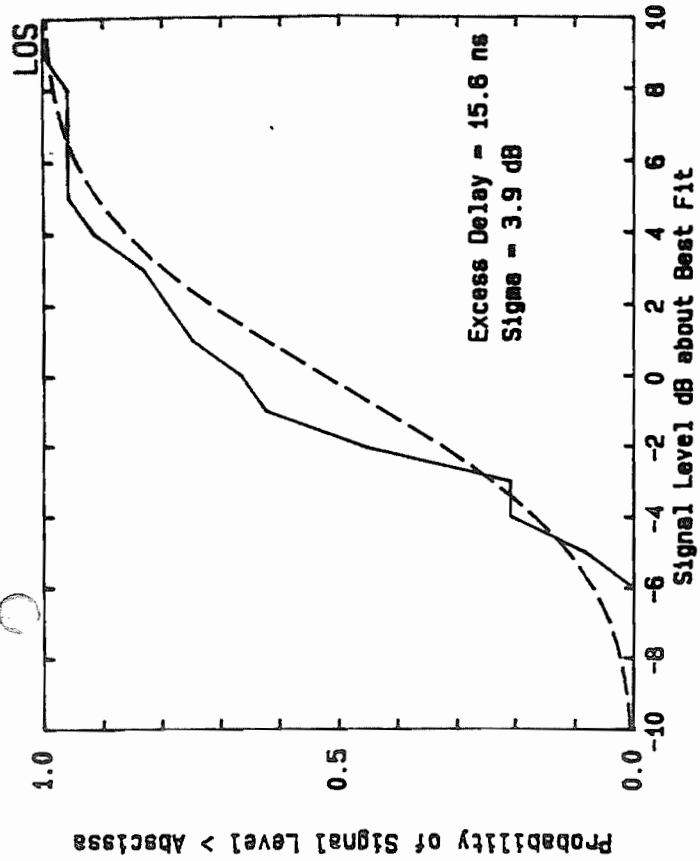
The curves which show conditional probability of path occupancy indicate that adaptive power control in conjunction with antenna diversity and equalization might solve multipath propagation problems in indoor radio channels. Solving the multipath problem would make possible wideband data communications and RF navigation systems inside buildings.

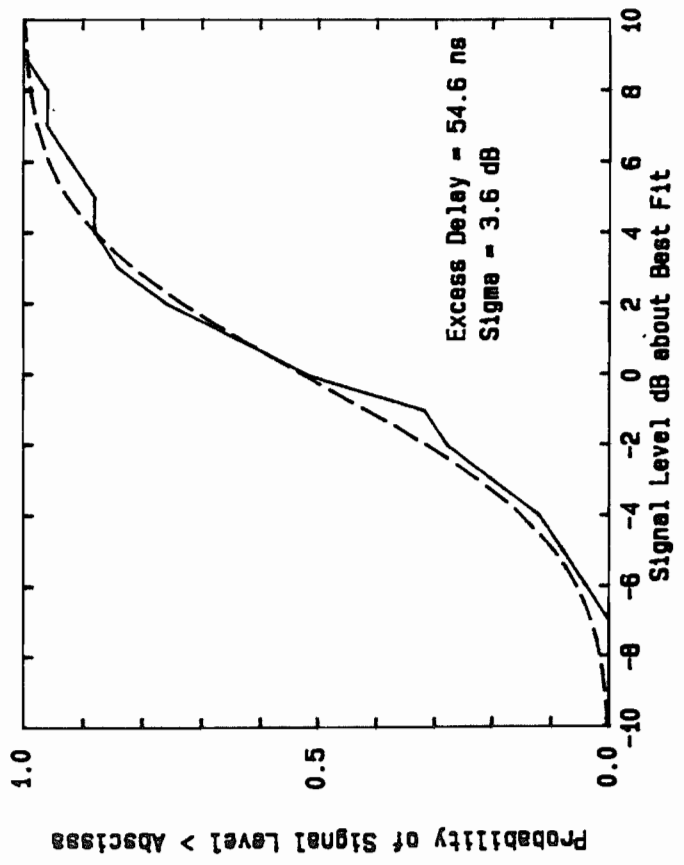
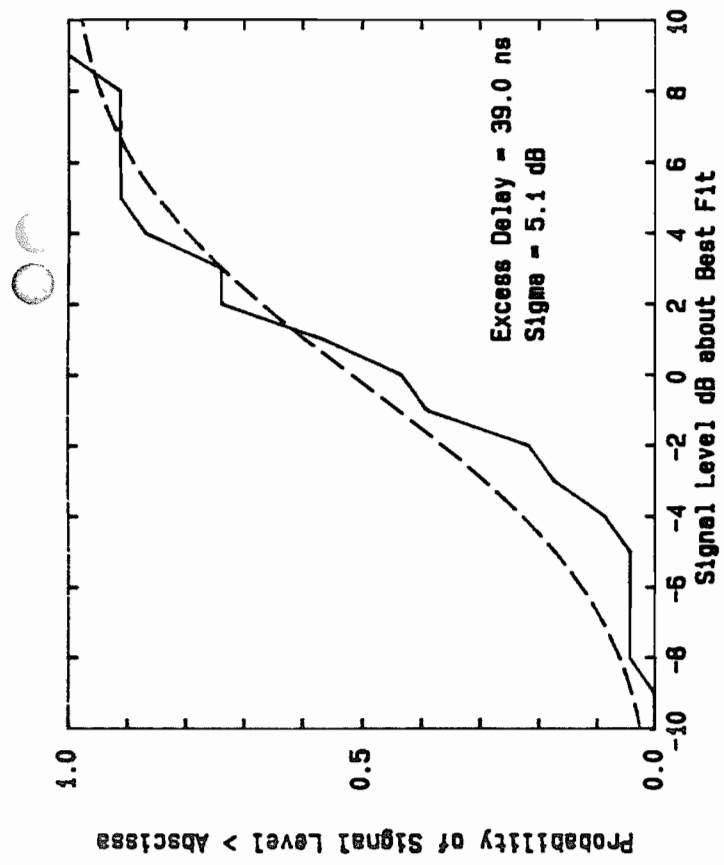
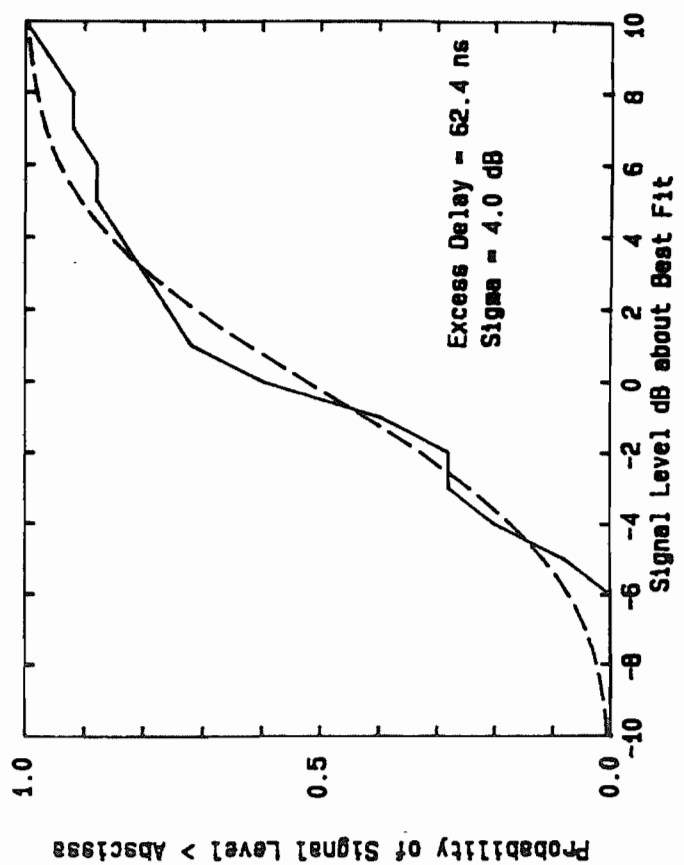
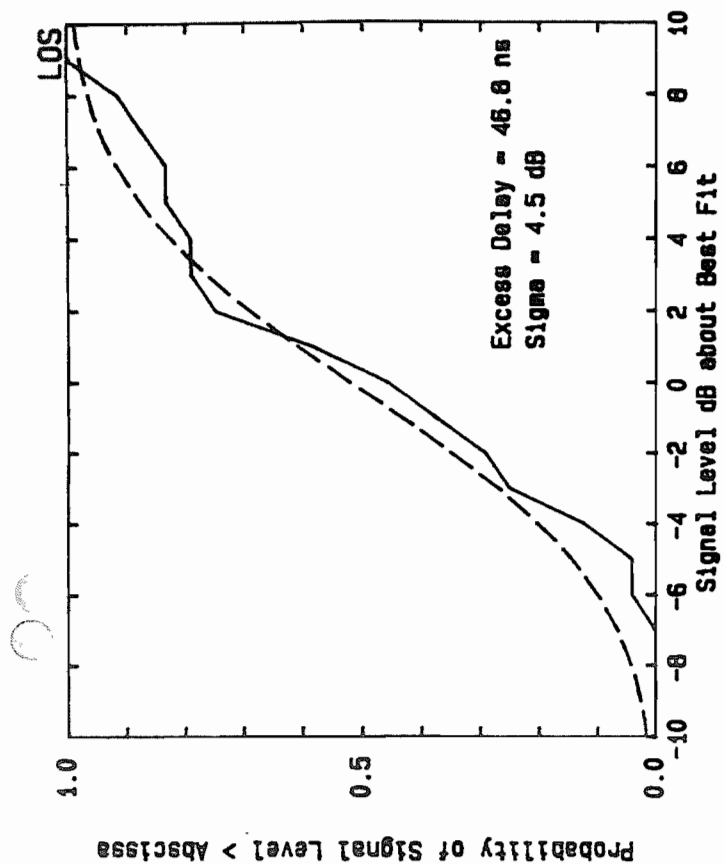
## VI. References

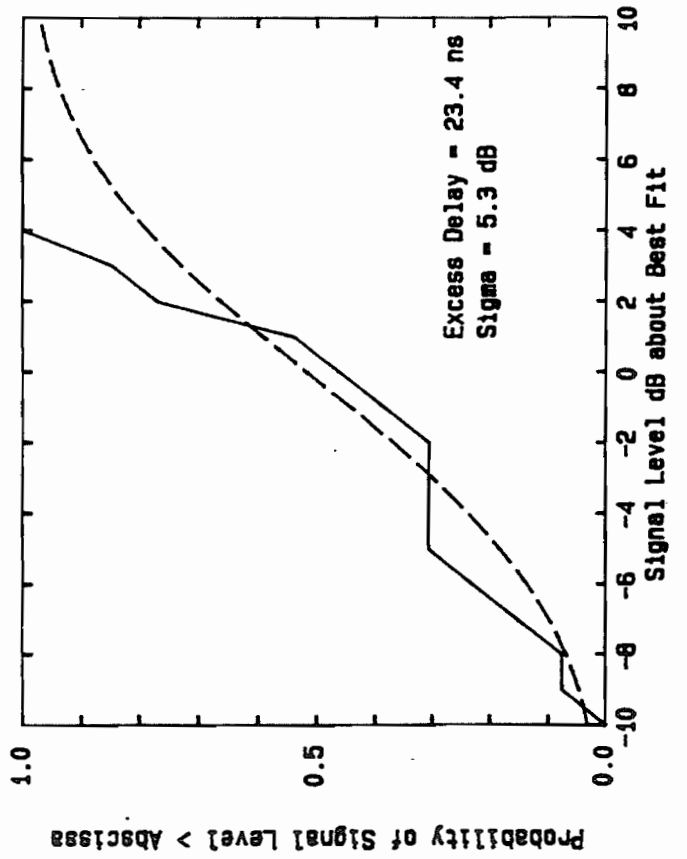
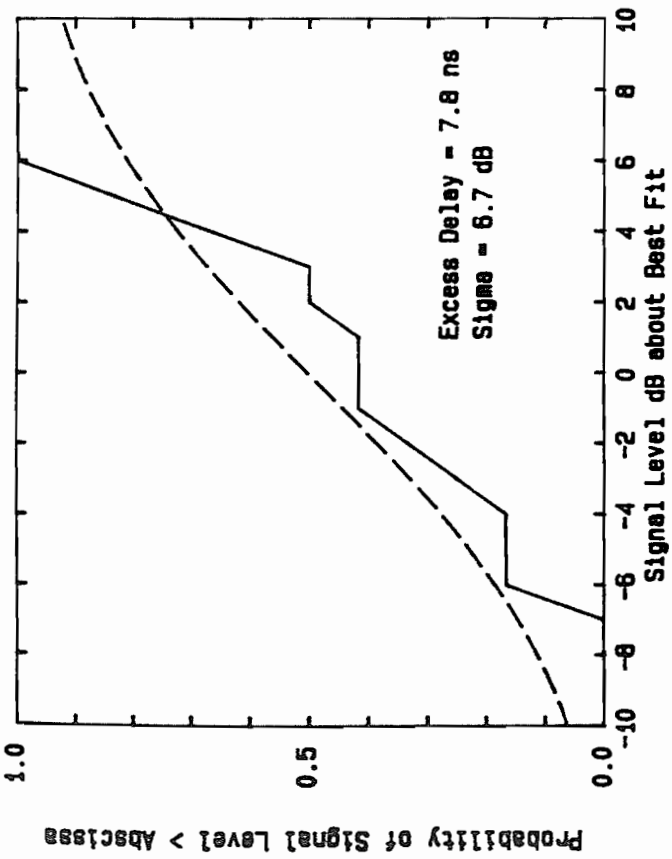
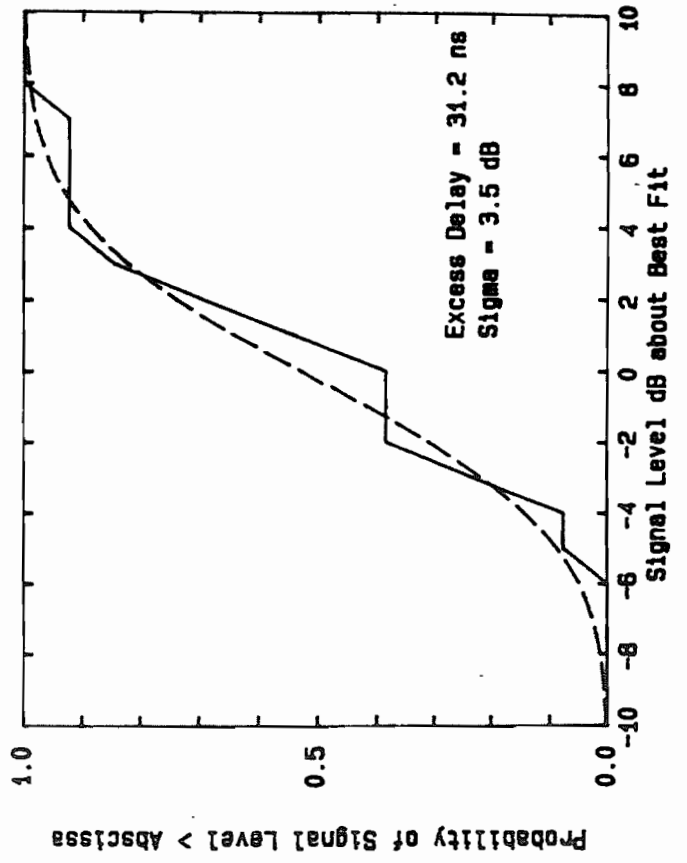
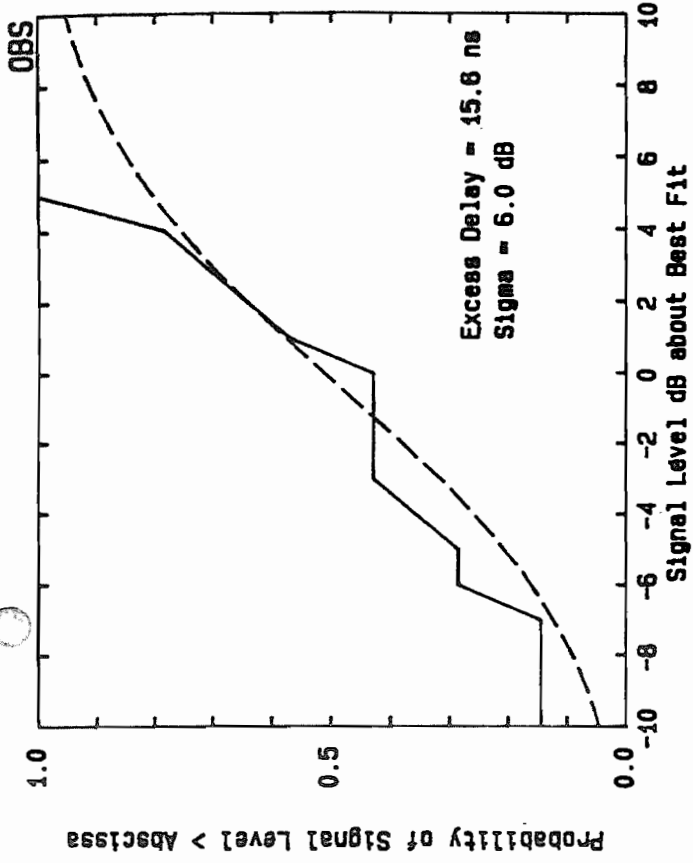
- [1]. Athanasios Papoulis, *Probability, Random Variables, and Stochastic Process*, McGraw-Hill Book Company, New York, 1984.
- [2]. Theodore S. Rappaport, *Radio Channel Modeling in Manufacturing Environments*, An intermediate report prepared for Purdue University's Computer Integrated Design, Manufacturing and Automation Center, Virginia Polytechnic Institute and State University, Blacksburg, Virginia, December 15, 1988.
- [3]. Theodore S. Rappaport, "Characterization of UHF multipath radio channels in factory buildings," *IEEE Trans. on Ant. and Prop.*, to be published July 1989.
- [4]. Theodore S. Rappaport, "Characterizing the UHF factory multipath channel," *Ph. D. Thesis*, Purdue University, West Lafayette, IN, December 1987.
- [5]. George L. Turin, Fred D. Clapp, Tom L. Johnson, Stephen B. Fine and Dan Lavry, "A statistical model of urban multipath propagation," *IEEE Trans. on Veh. Technol.*, vol. VT-21, pp. 1-9, Feb. 1972.
- [6]. H. Suzuki, "A statistical model for urban radio propagation," *Ph. D. Thesis*, University of California, Berkeley, June 1975.
- [7]. H. Suzuki, "A statistical model for urban radio propagation," *IEEE Trans. Comm.*, vol. COM-25, pp. 673-680, July 1977.
- [8]. Homayoun Hashemi, "Simulation of the urban radio propagation," *IEEE Trans. on Veh. Technol.*, vol. VT-28, pp. 213-225, August 1979.
- [9]. John Griffiths, *Radio Wave Propagation and Antennas*, Prentice-Hall, New Jersey, Ch. 7, 1987.
- [10]. Carl W. Helstrom, *Probability and Stochastic Processes for Engineers*, Macmillan Publishing Company, New York, 1984.
- [11]. D.C. Cox, "910 MHz urban mobile radio propagation: multipath characteristics in New York City," *IEEE Trans. Comm.*, vol. COM-21, pp. 1187-1194, Nov. 1973.
- [12]. K. Sam Shanmugan and Arthur M. Breipohl, *Random Signals: Detection, Estimation and Data Analysis*, John Wiley & Sons, New York, 1988.
- [13]. A.A.M. Saleh and R.A. Valenzuela, "A statistical model for indoor multipath propagation," *IEEE Journal on Sel. Areas in Comm.*, vol. SAC-5, pp. 128-137, Feb. 1987.
- [14]. T. Rappaport, C. McGillem, "UHF Fading in Factories," *IEEE Journal on Sel. Areas in Comm.*, vol. SAC-7, pp.40-48, Feb. 1989.
- [15]. K. Takamizawa, S. Seidel, T. Rappaport, "Indoor Radio Channel Models for Manufacturing Environments," *IEEE Southeastcon 1989 Proceedings*, April 10, 1989, Columbia, SC.

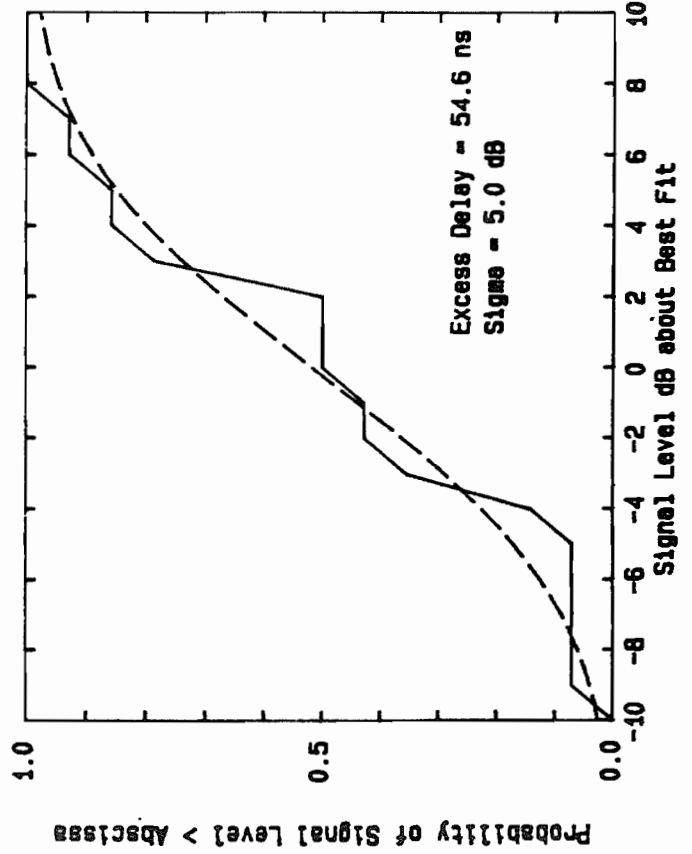
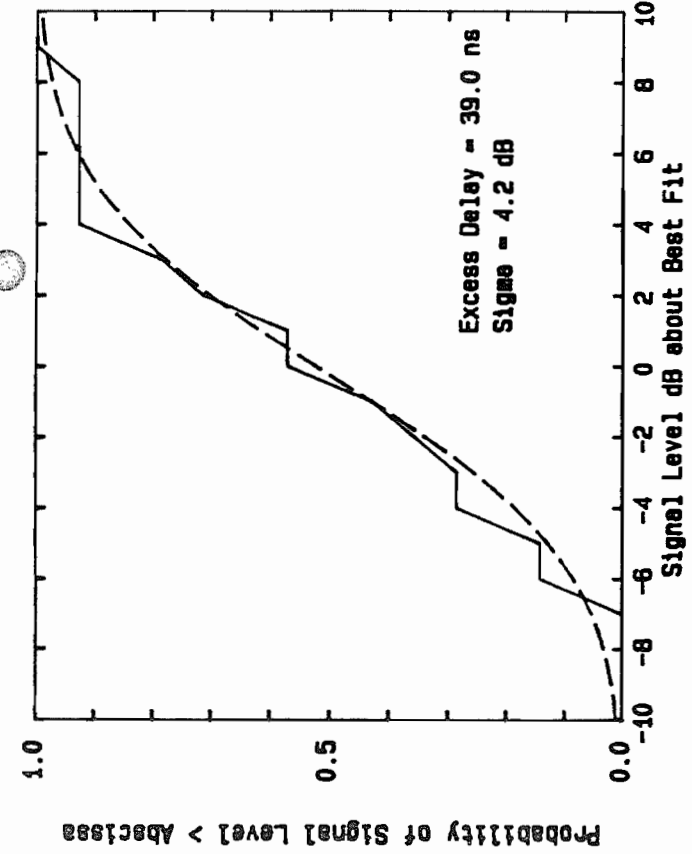
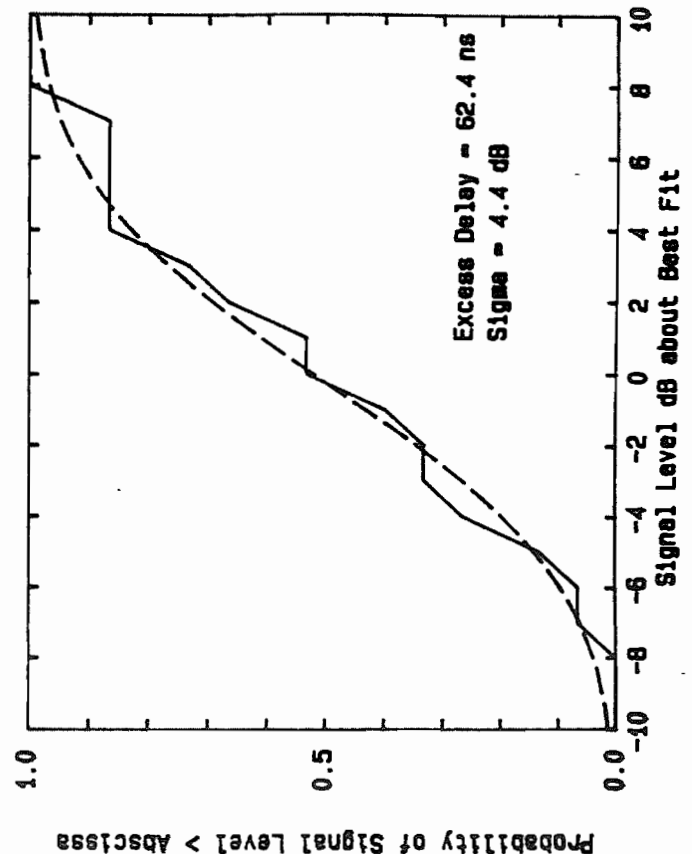
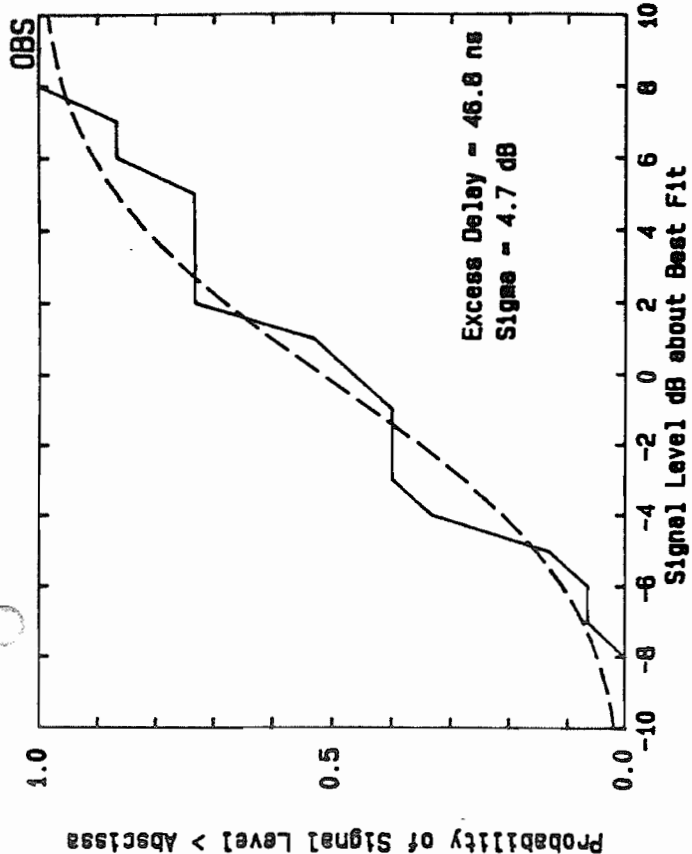


## Appendix A. CDF of Received Signal Power

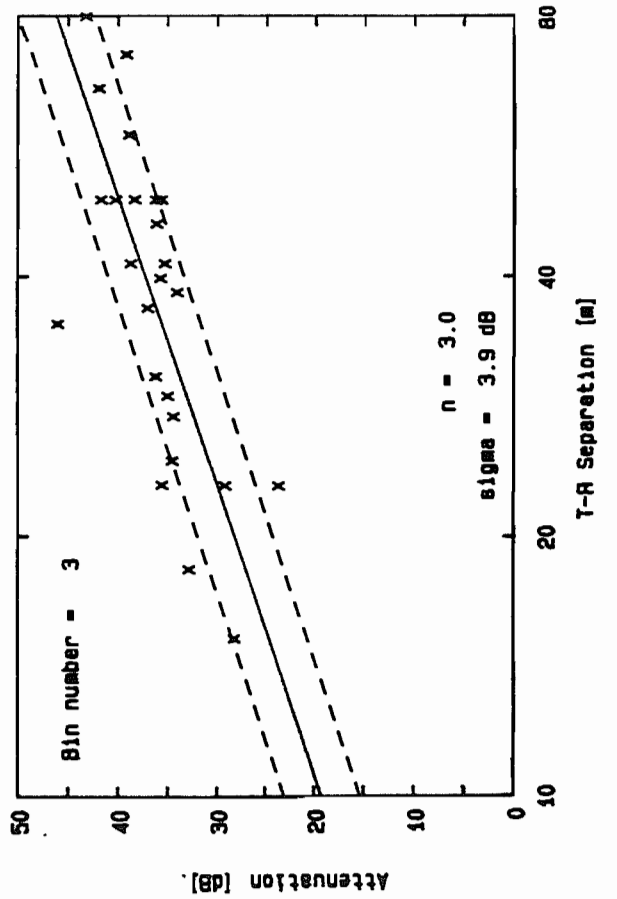
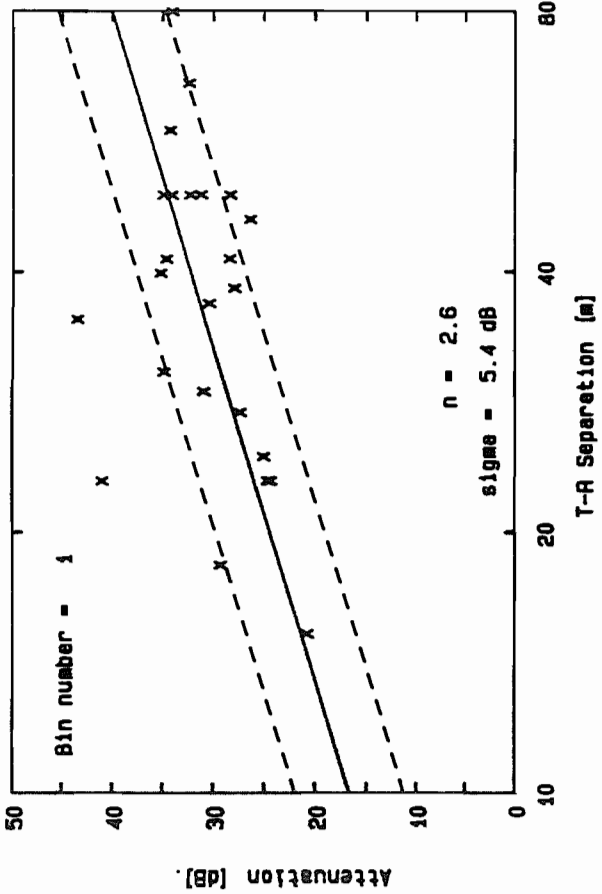
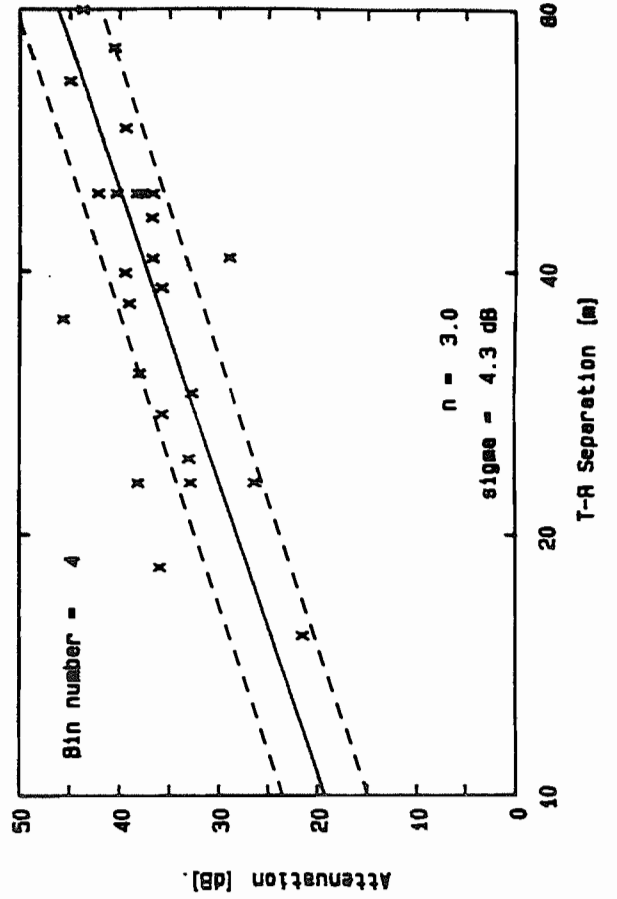
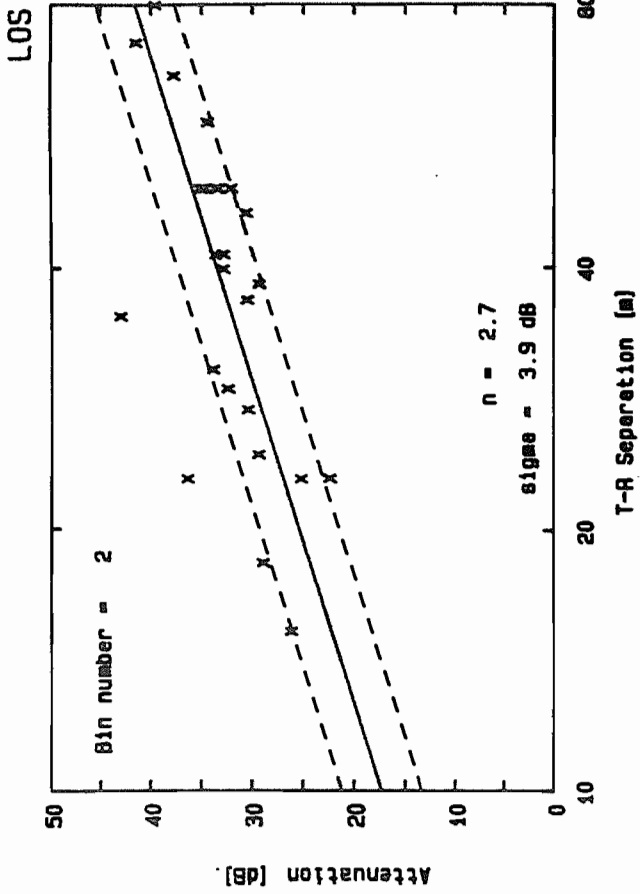


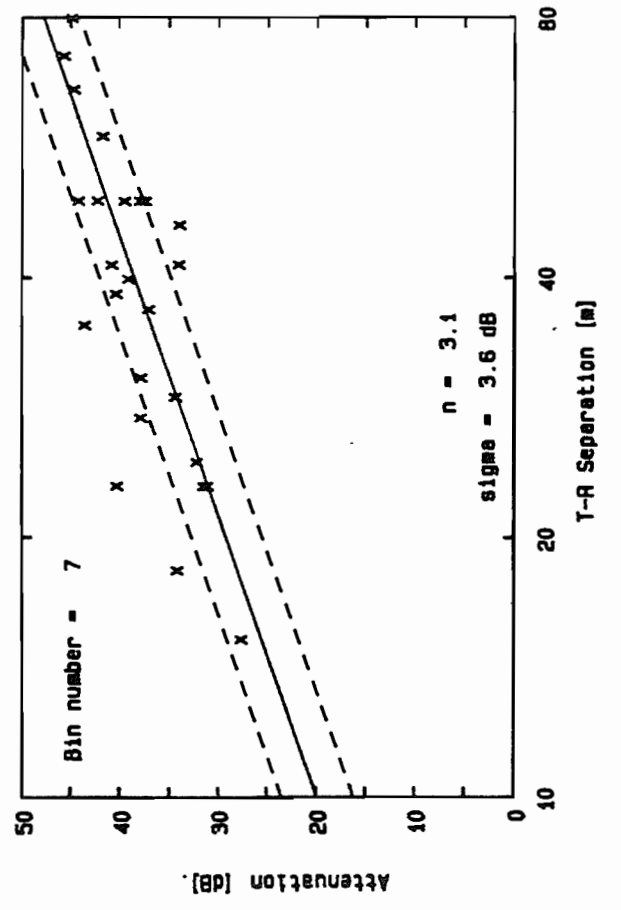
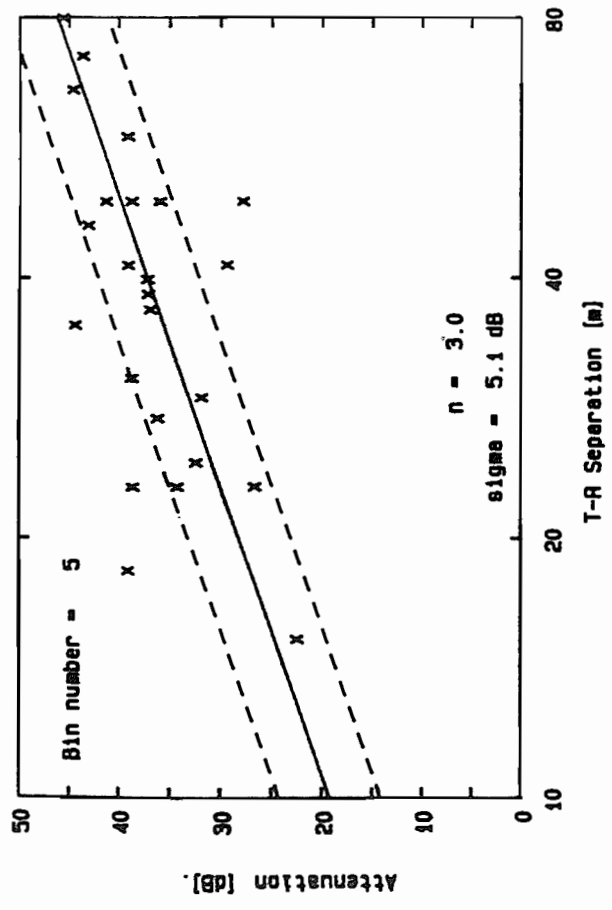
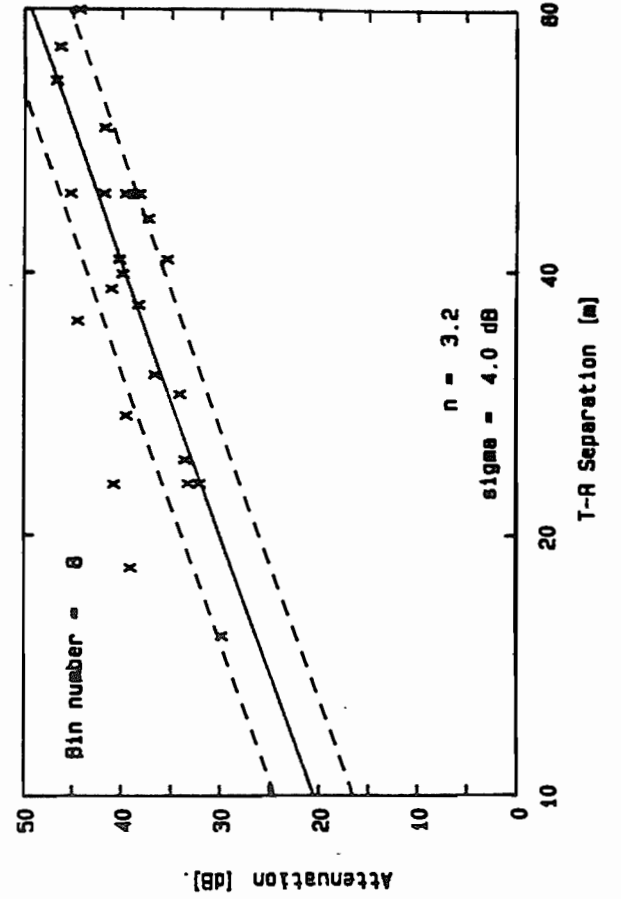
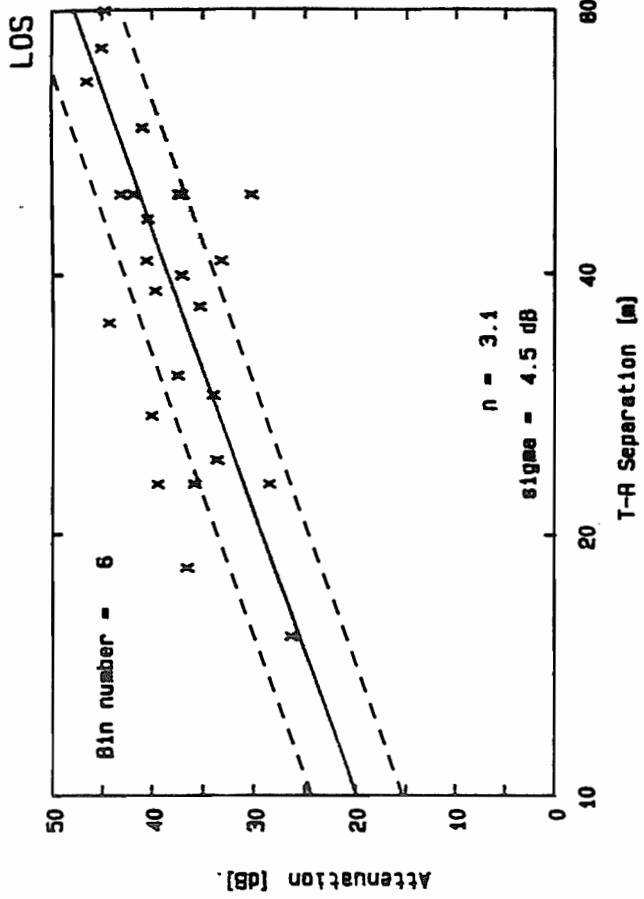




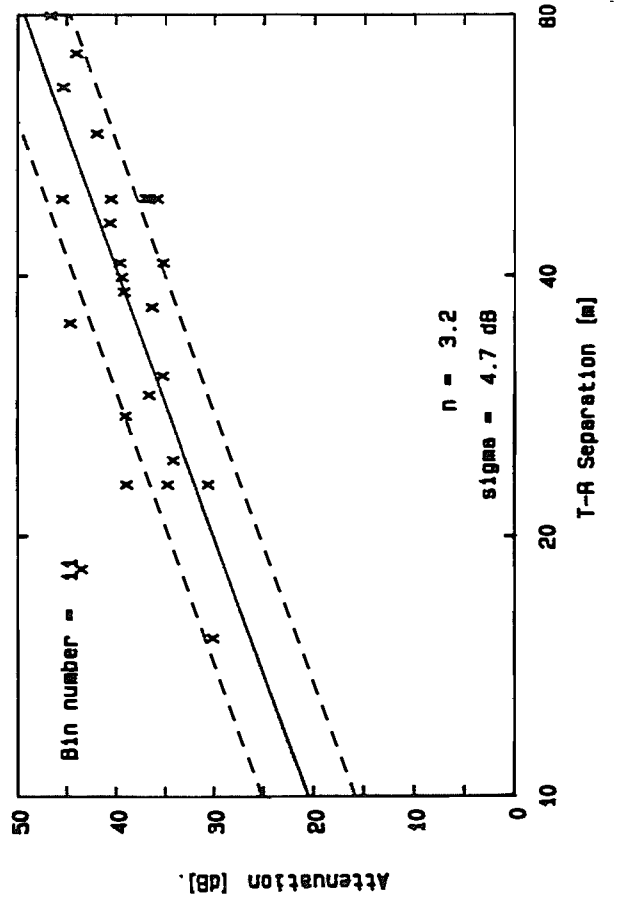
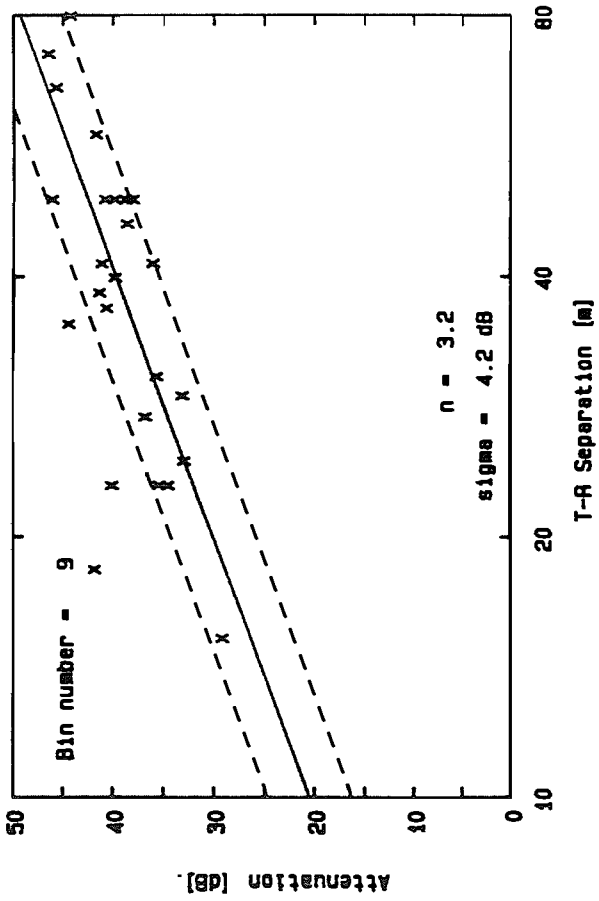
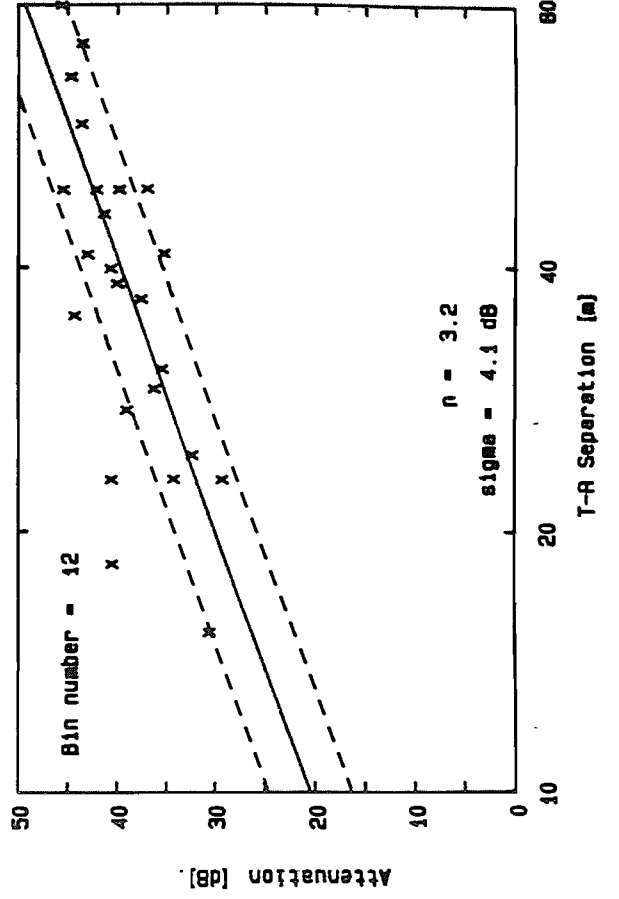
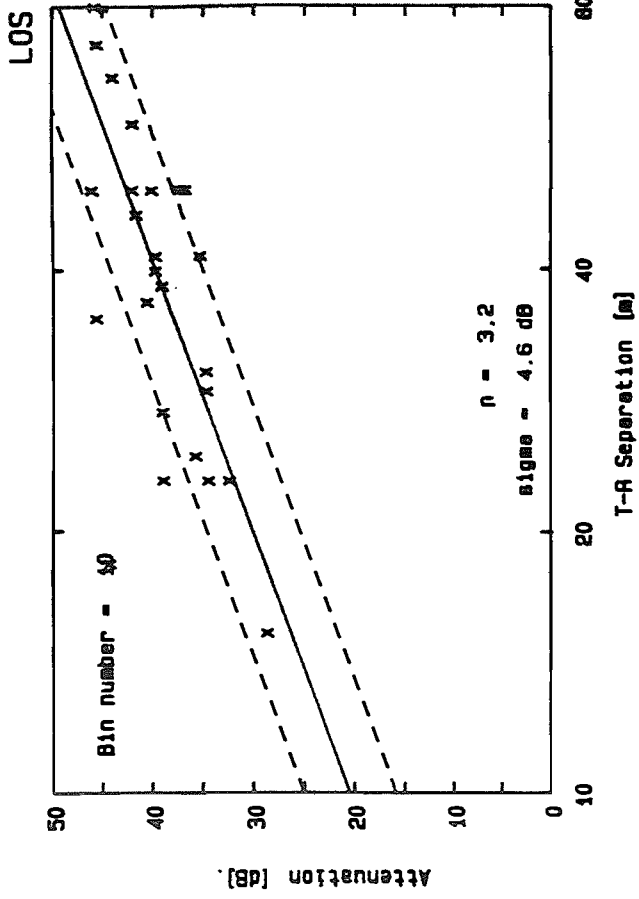


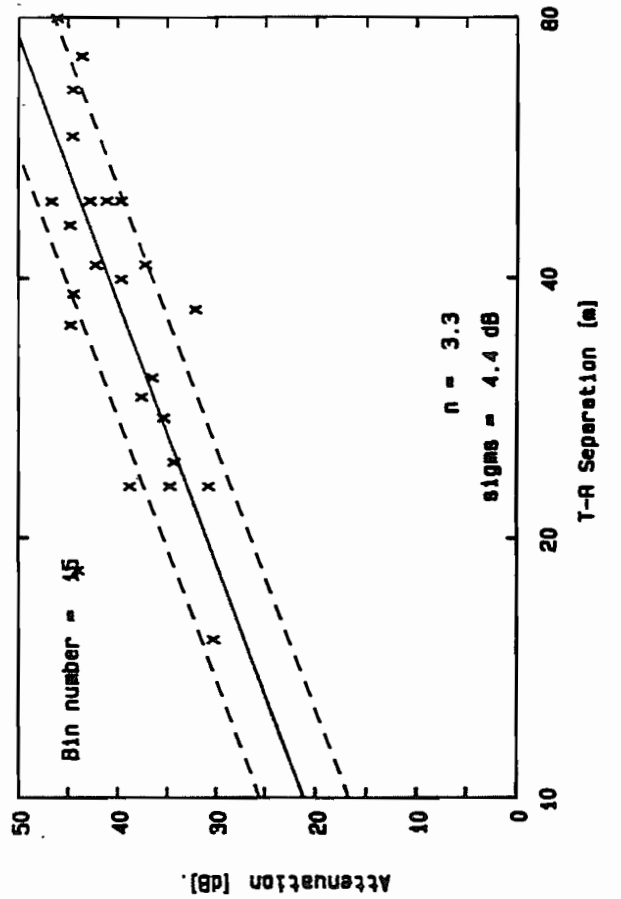
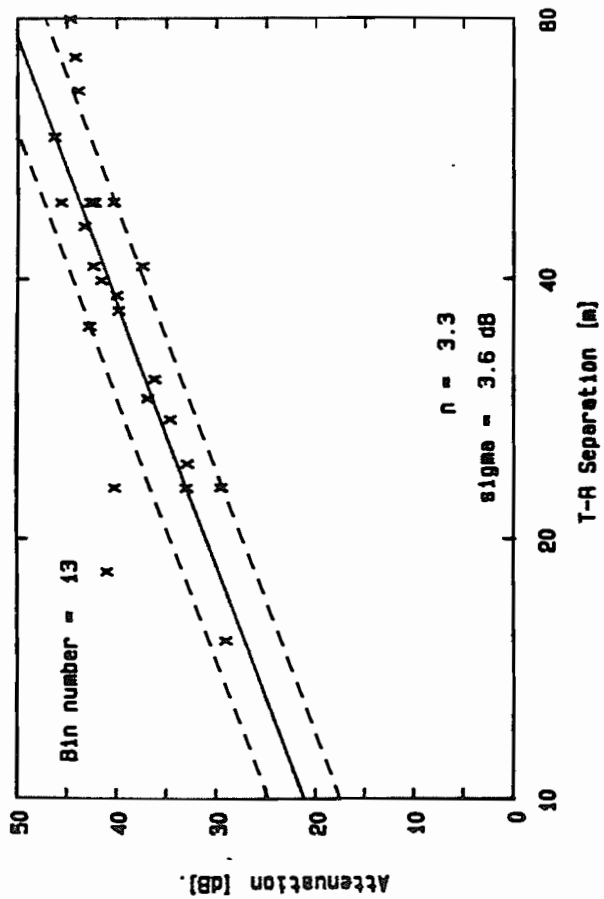
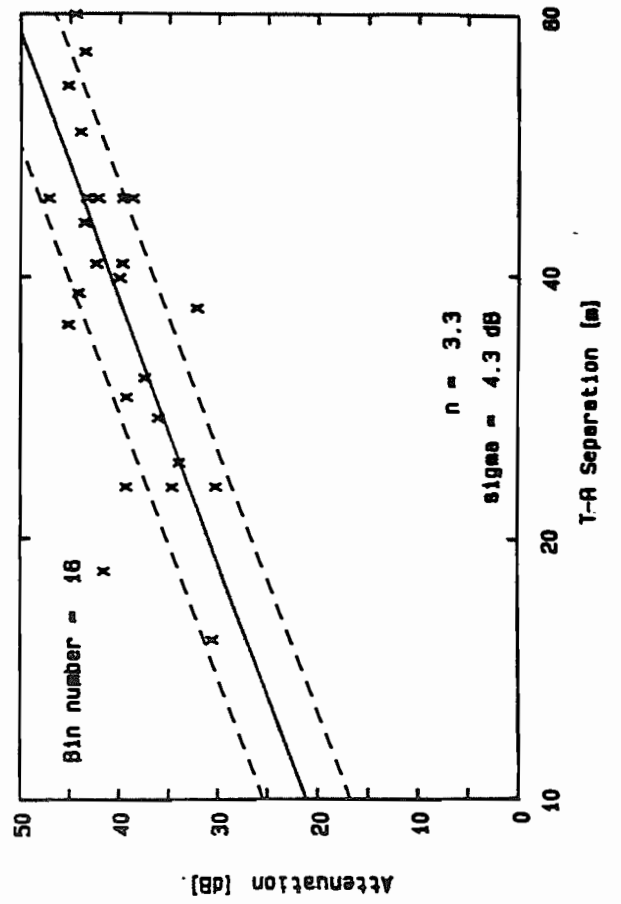
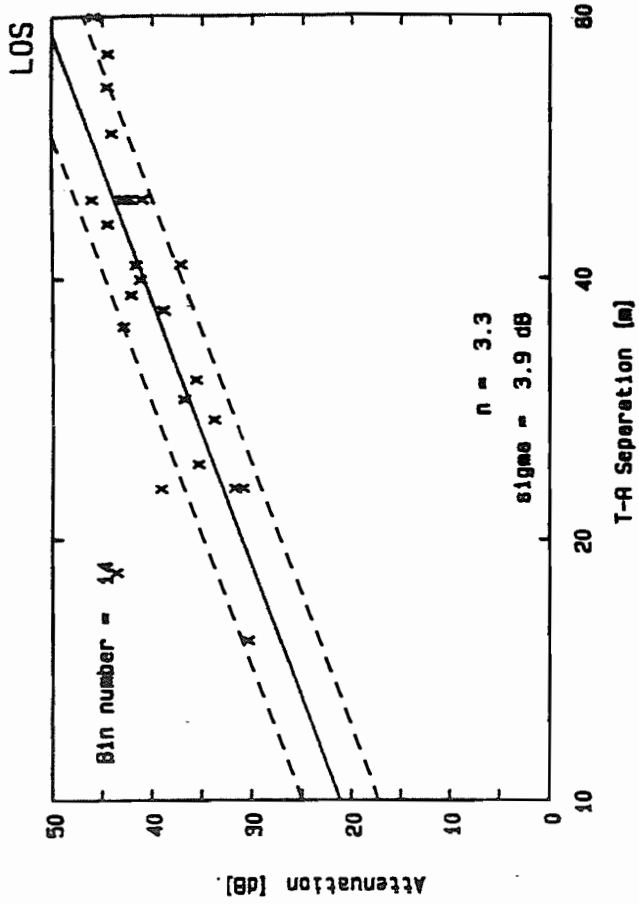
## **Appendix B. Scatter Plots of Path Attenuation**

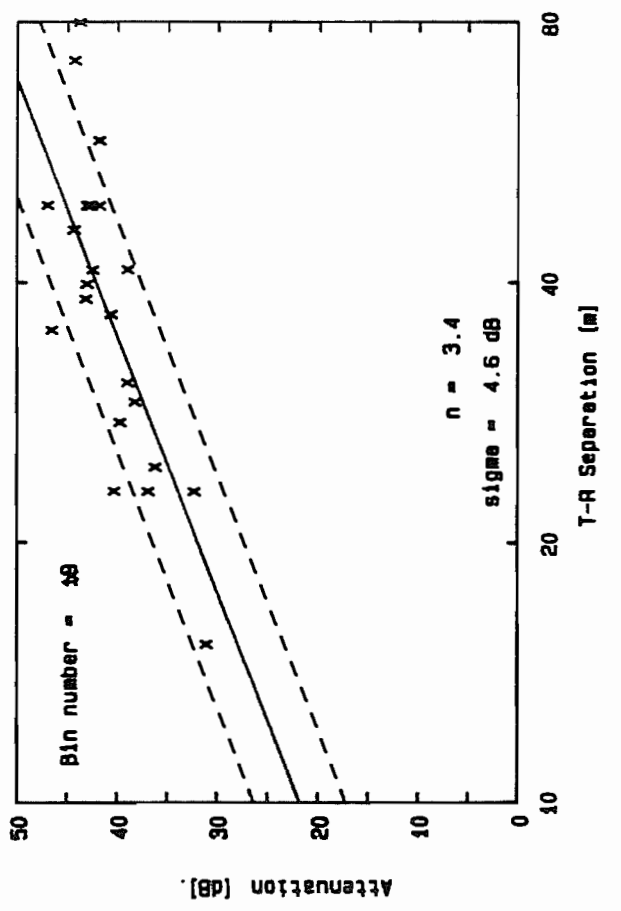
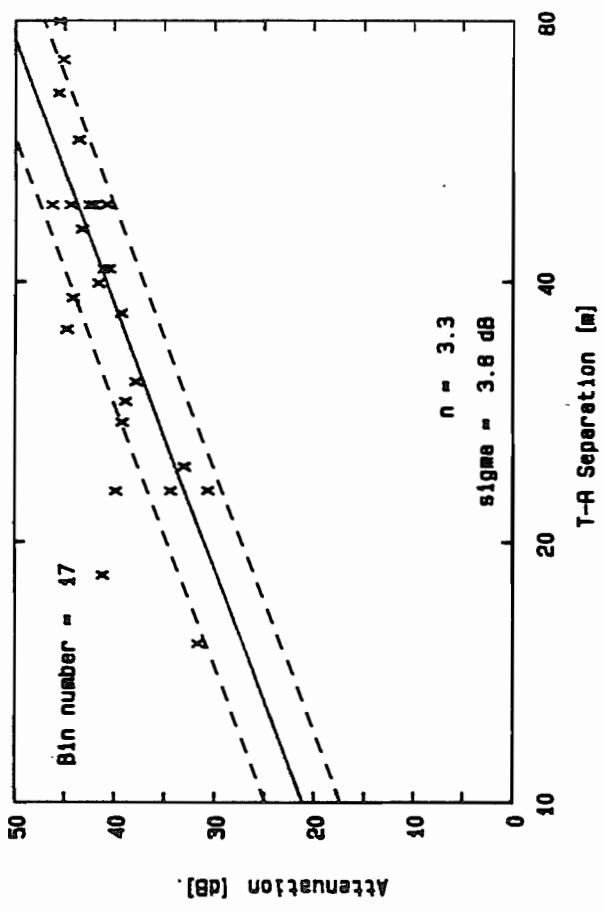
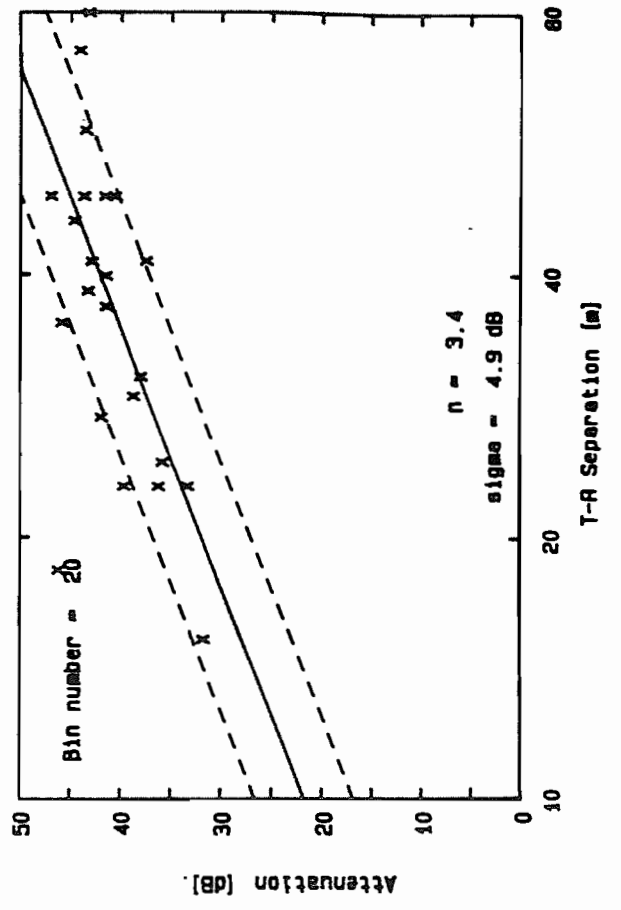
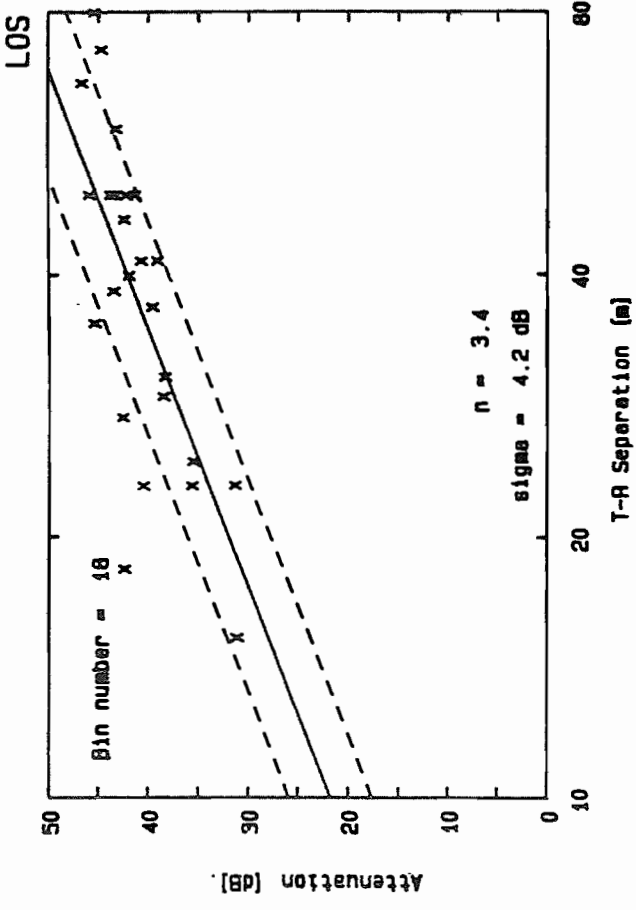


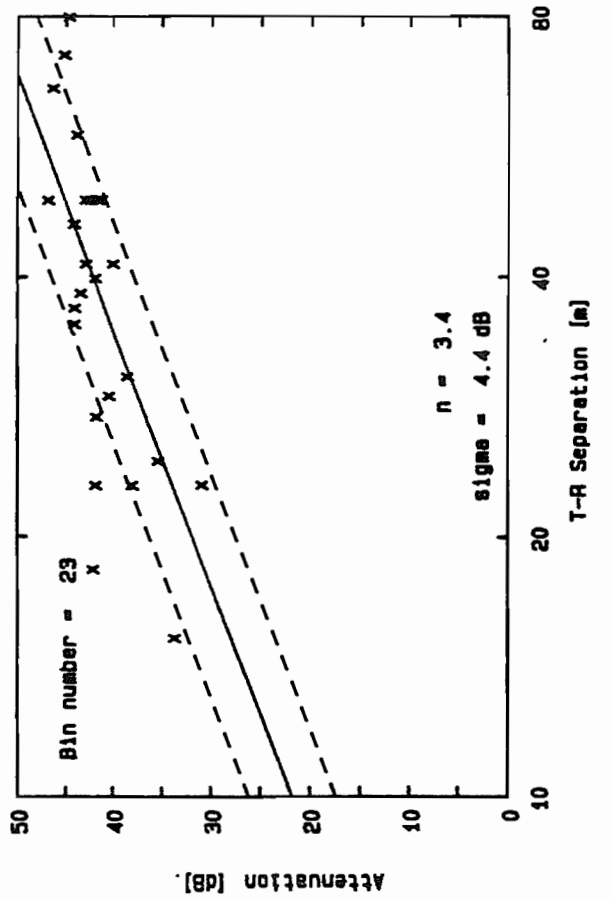
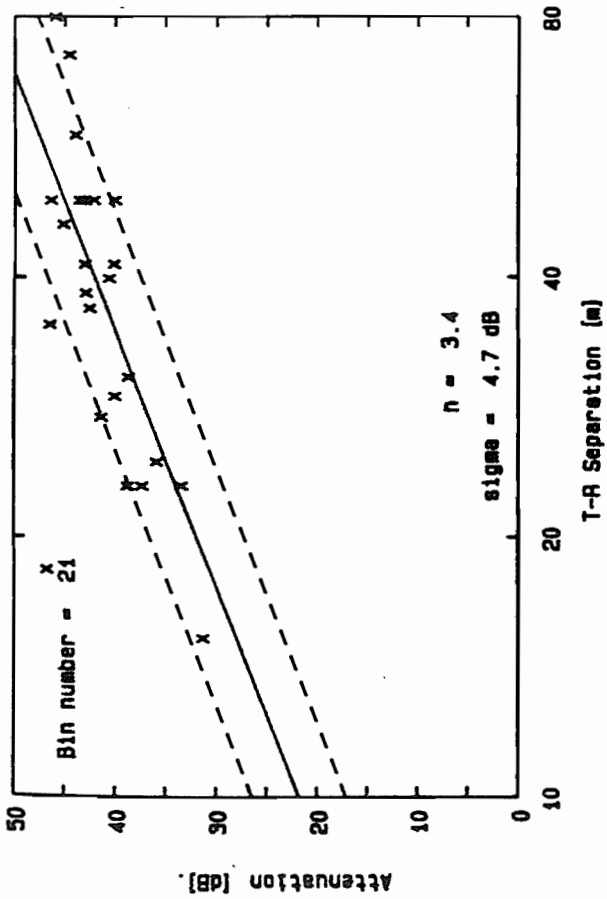
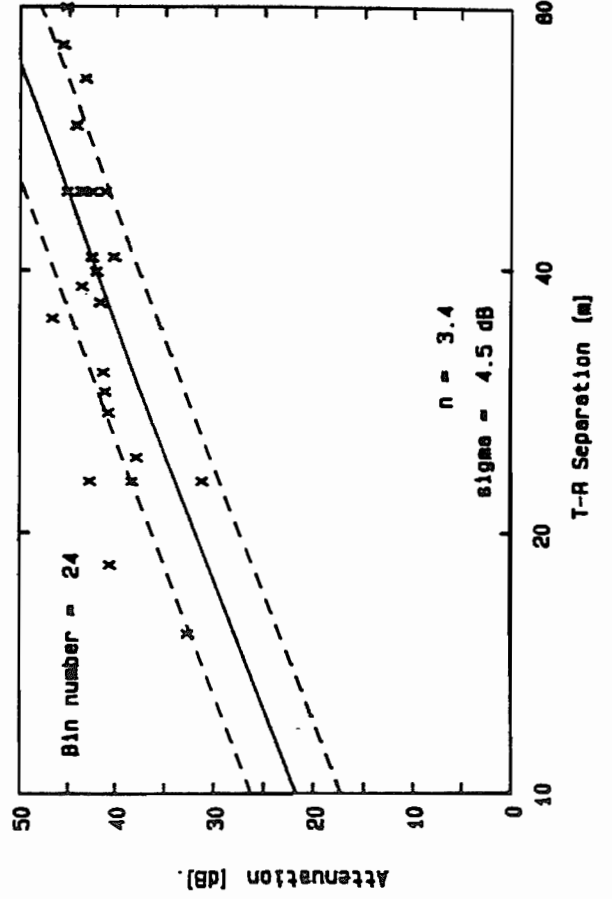
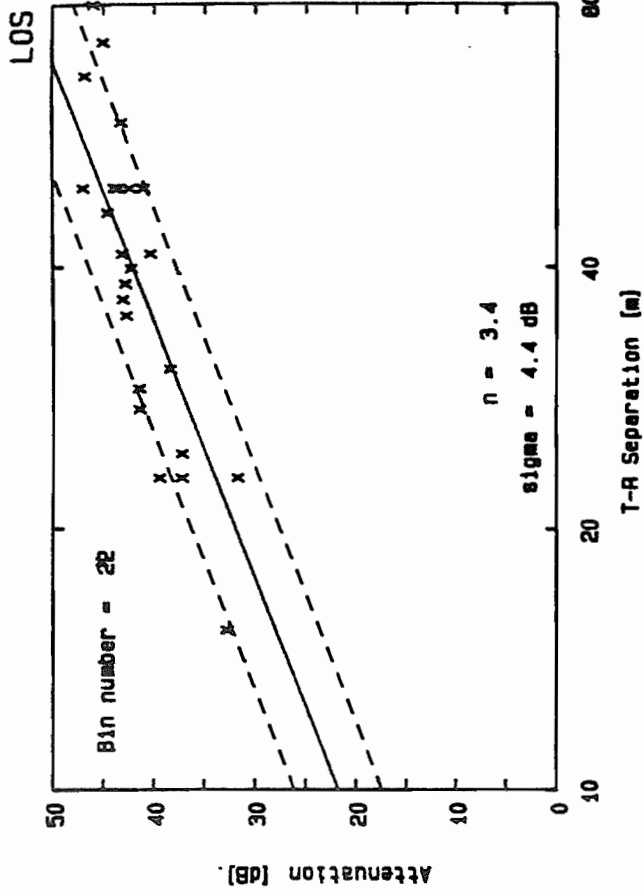


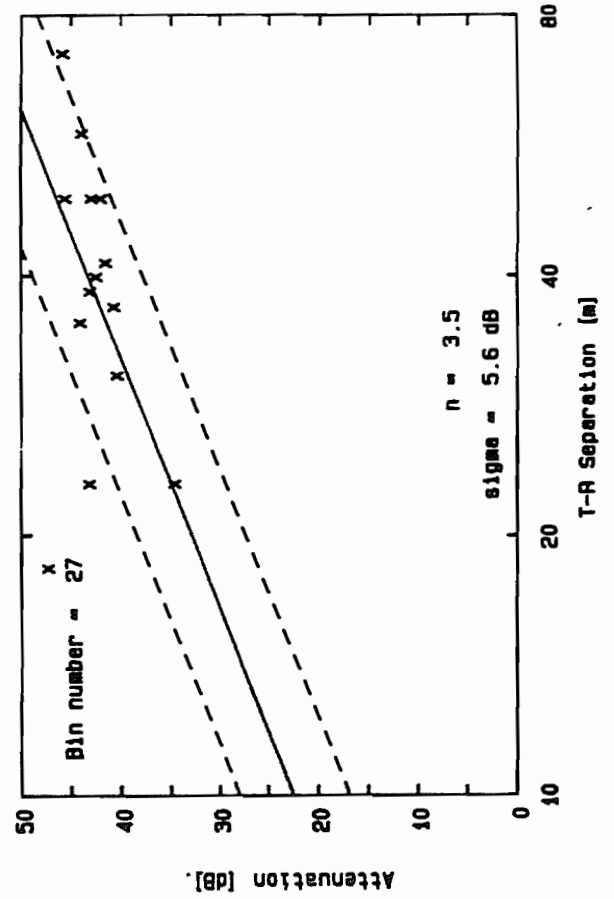
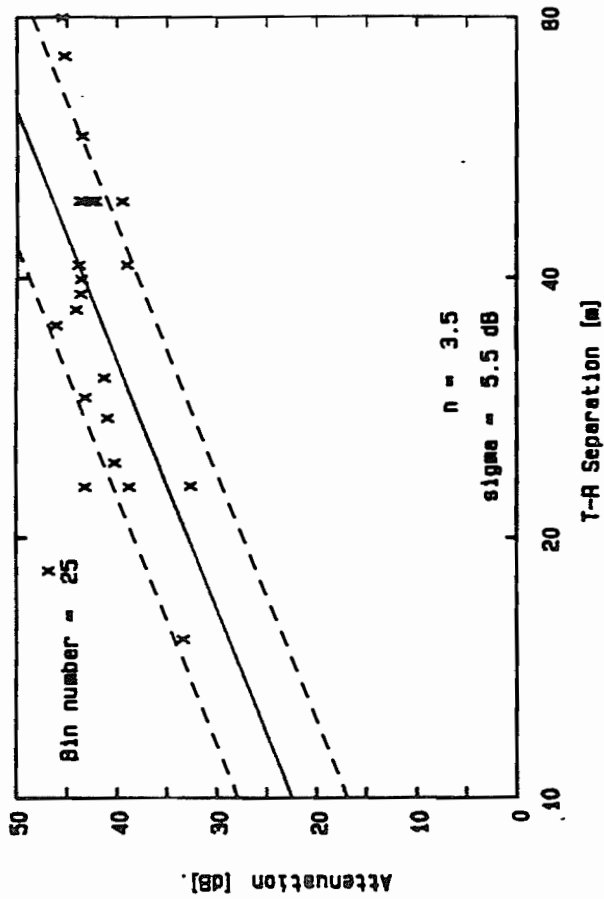
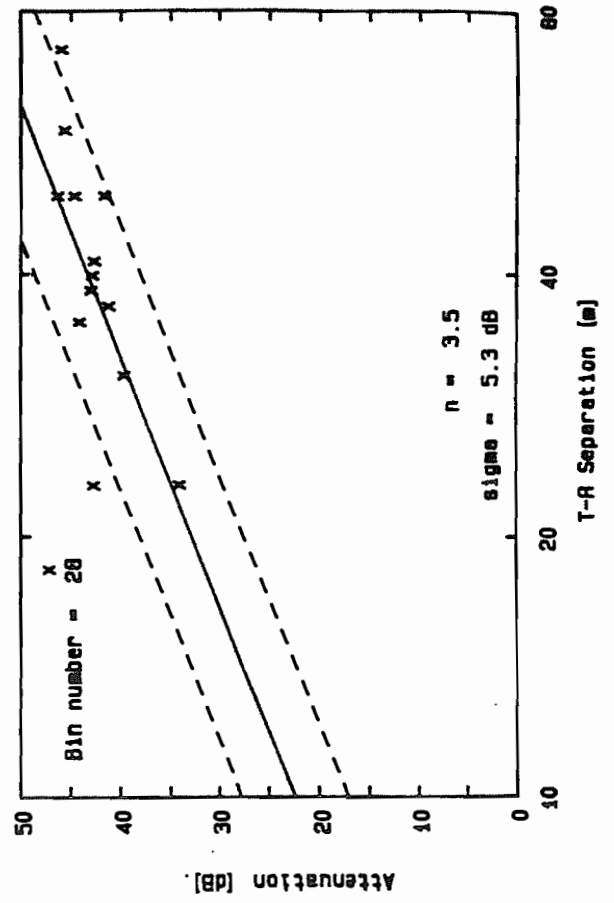
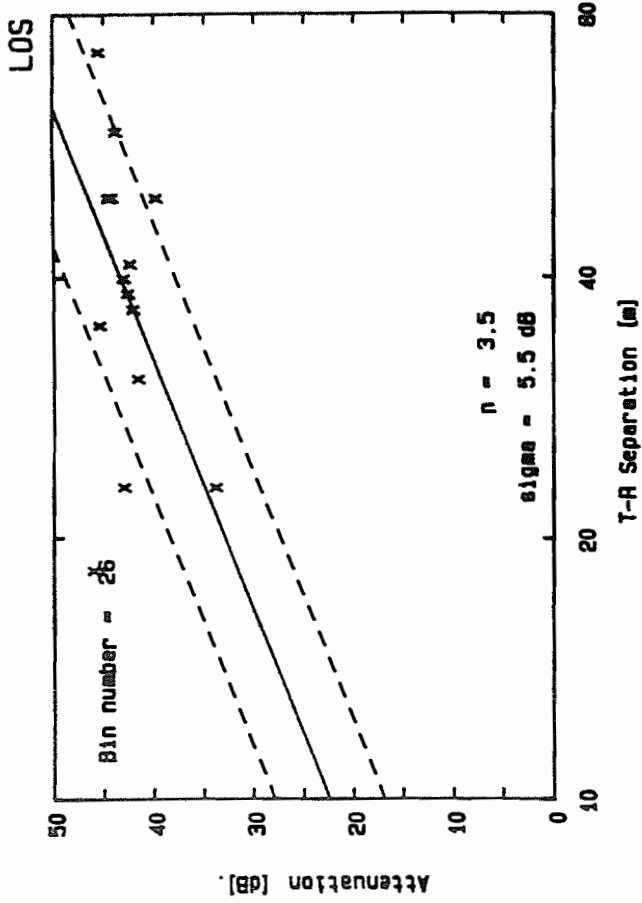




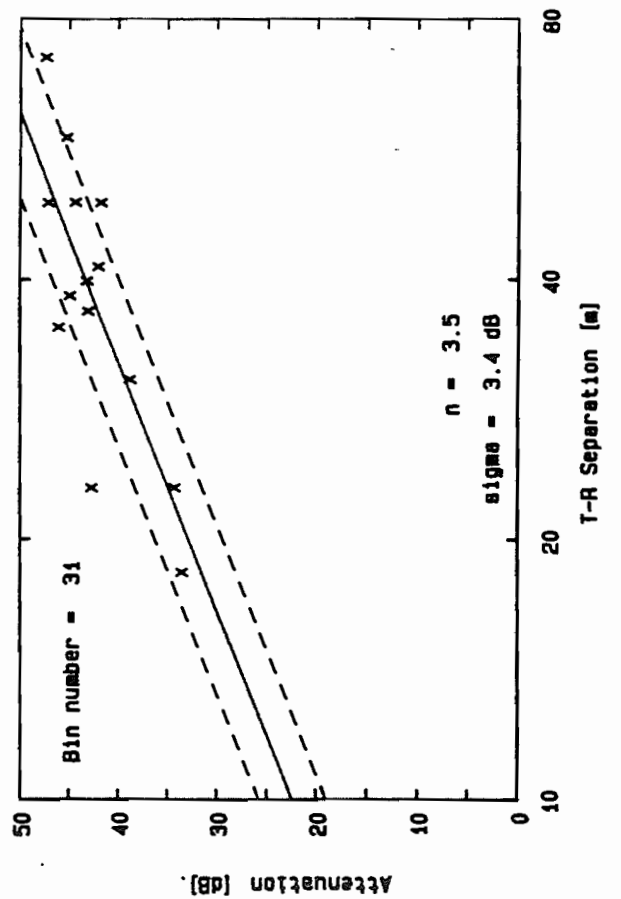
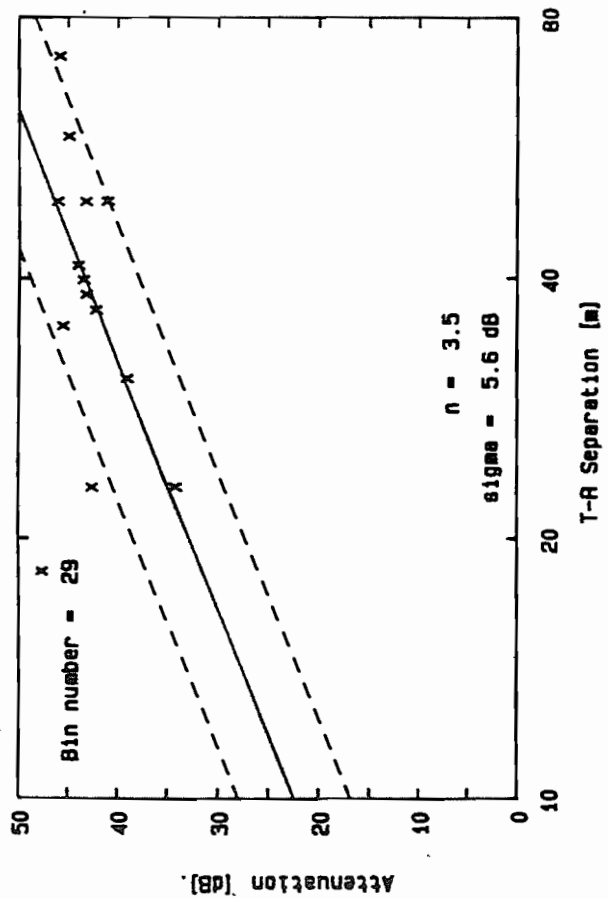
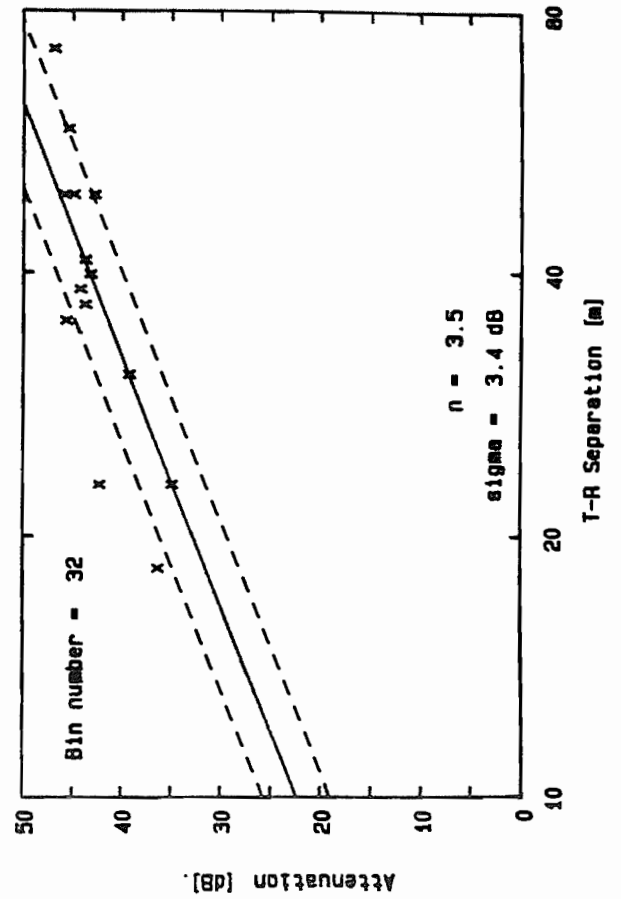
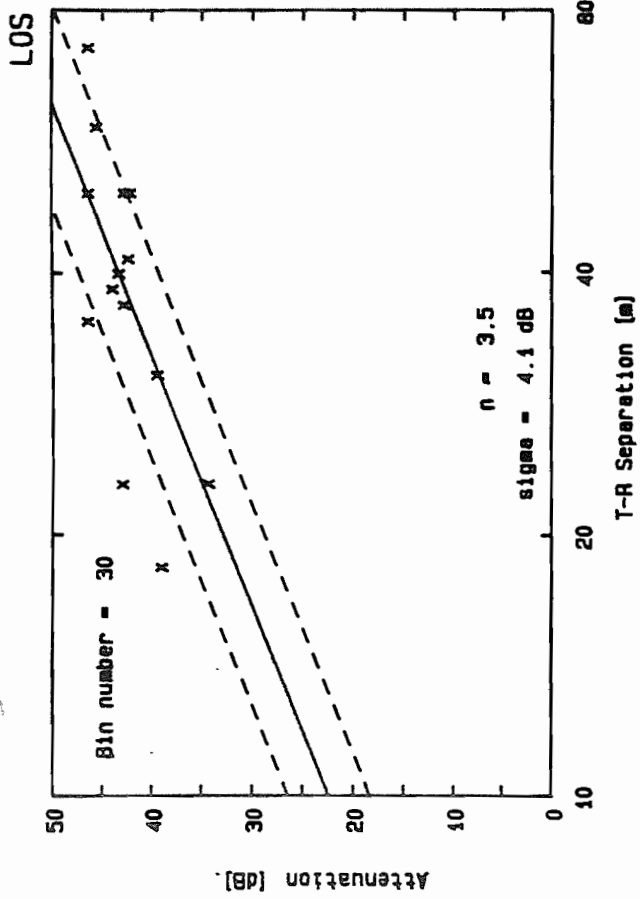


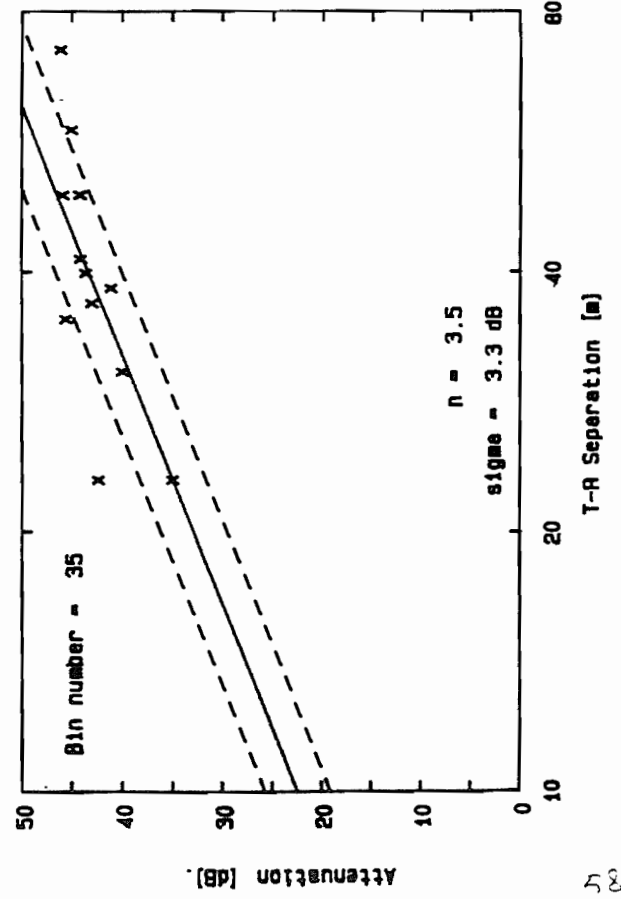
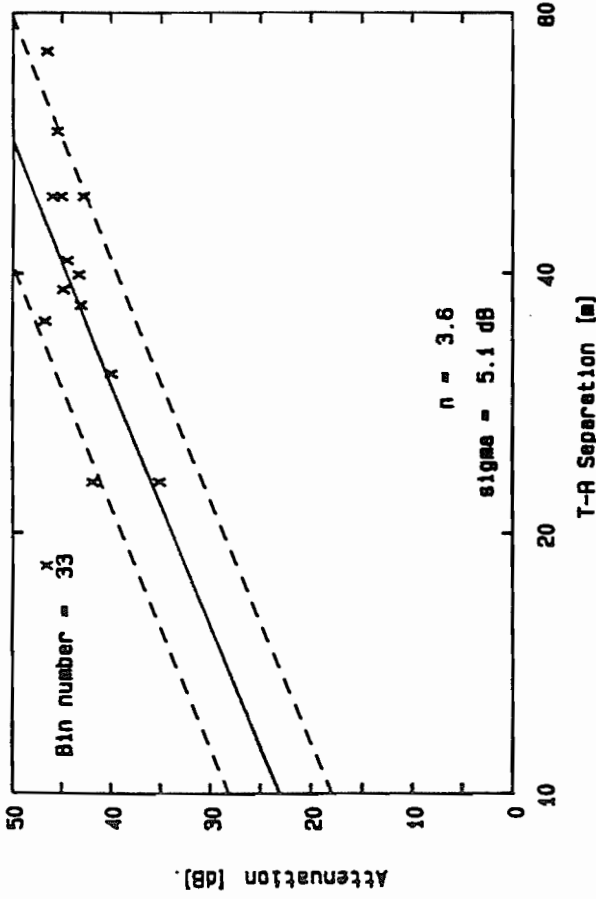
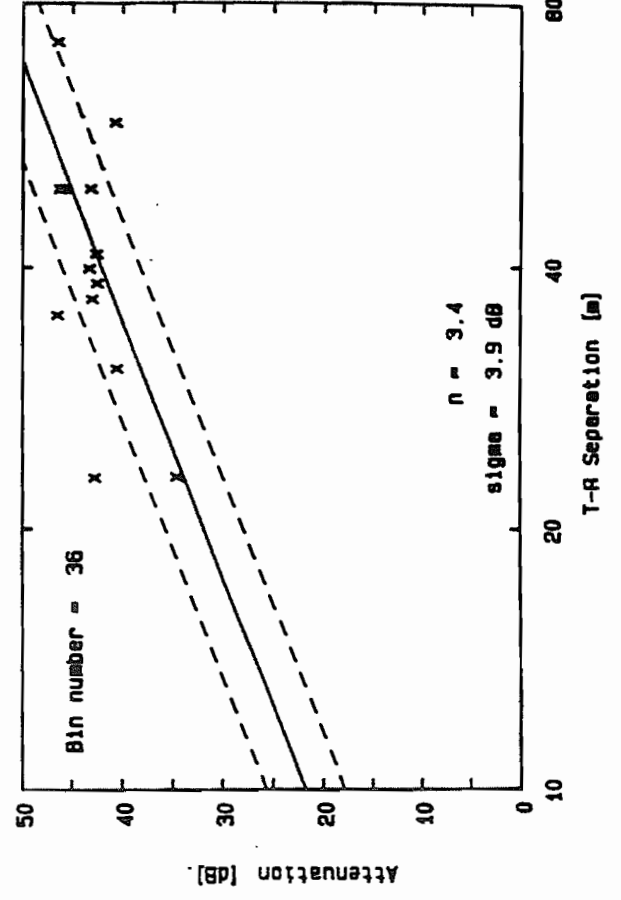
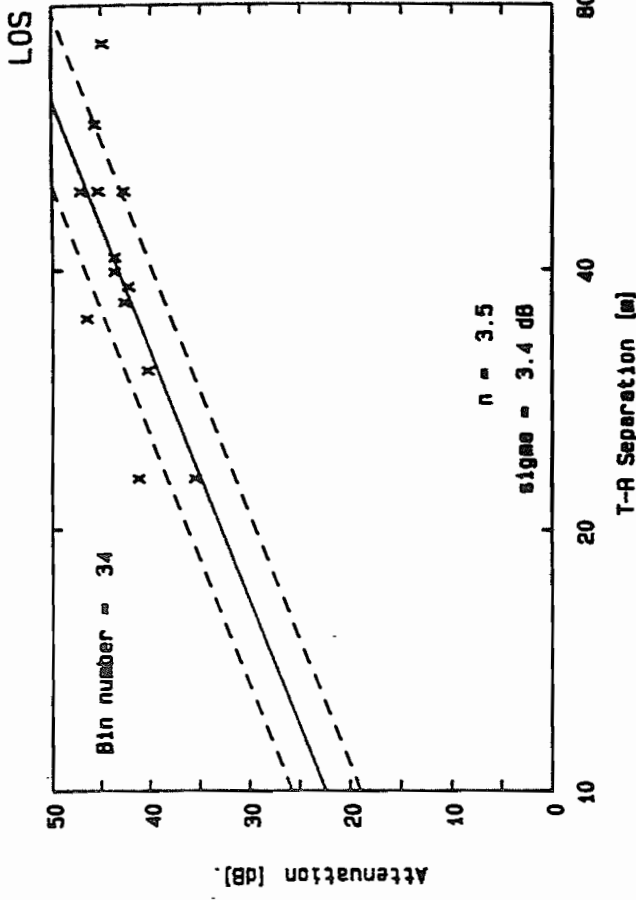




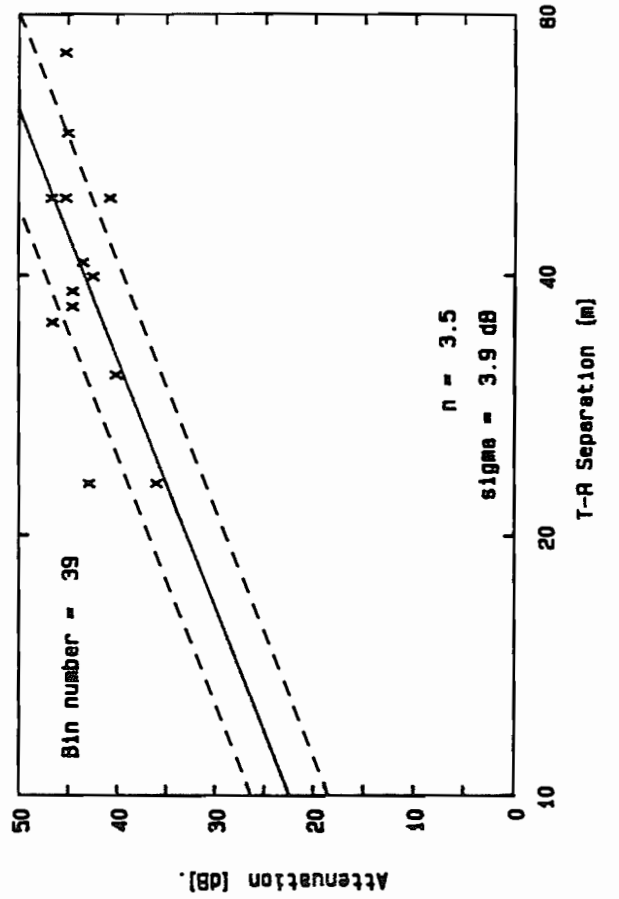
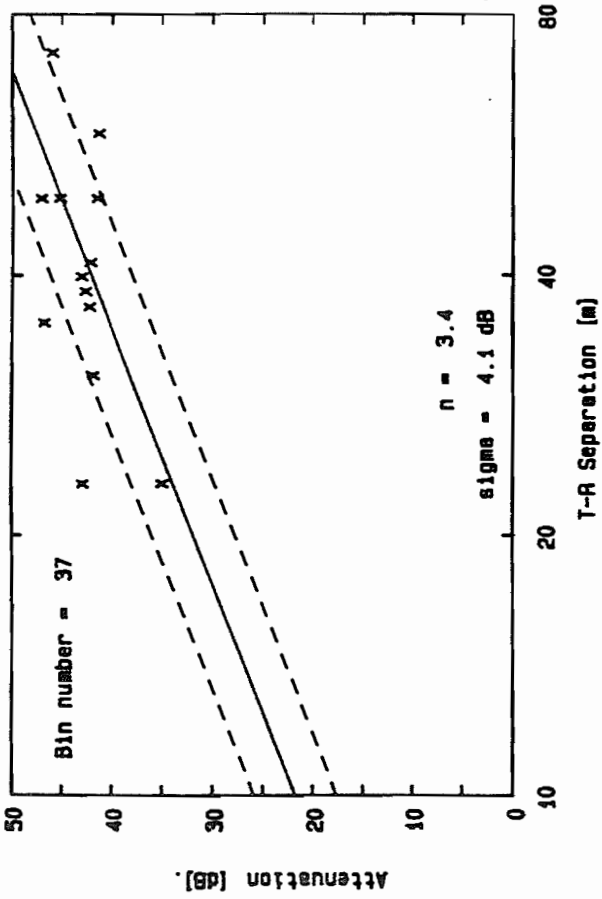
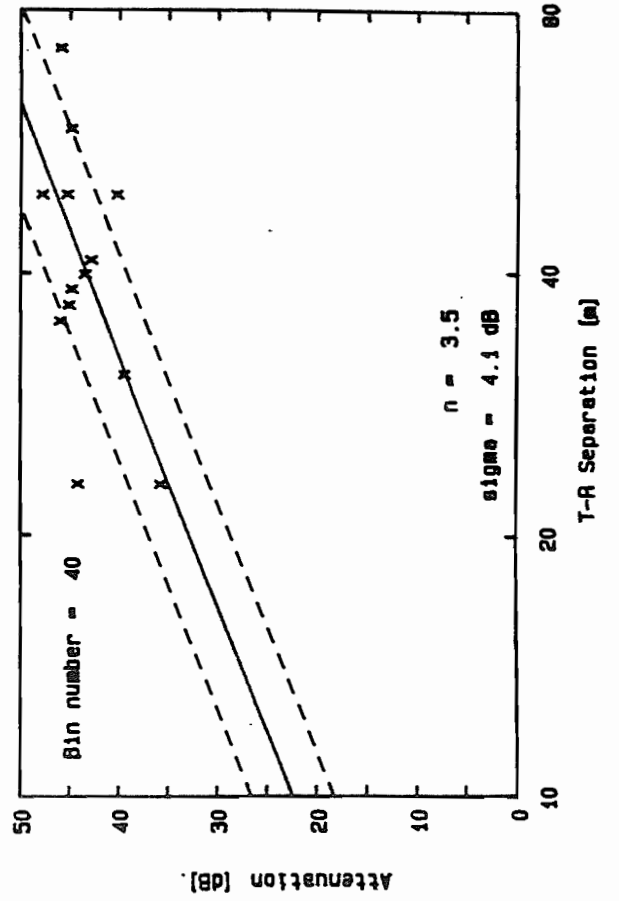
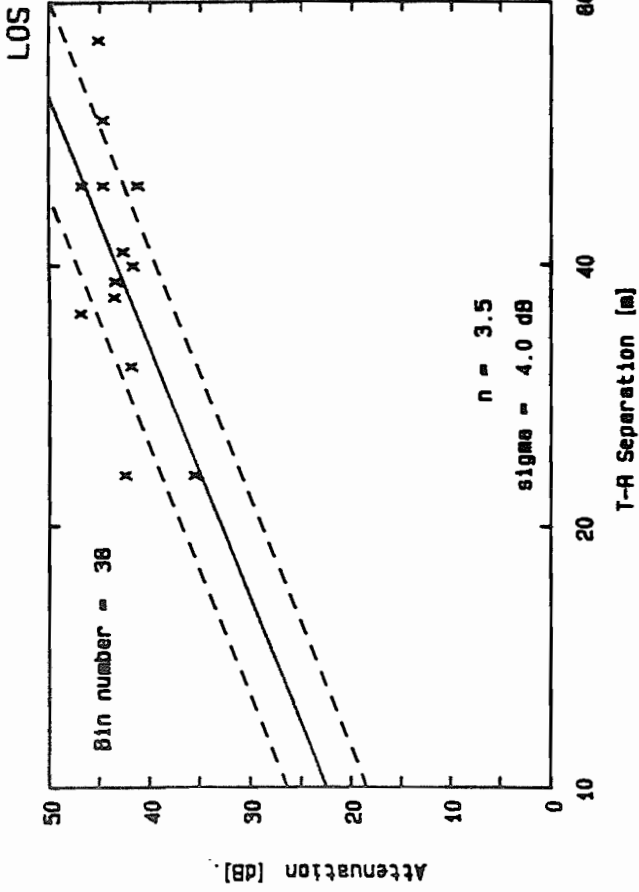


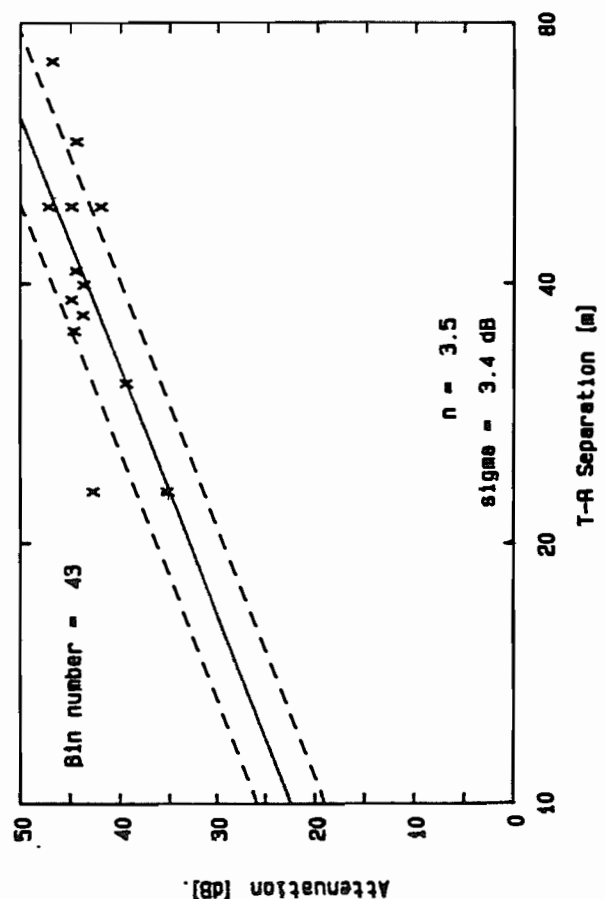
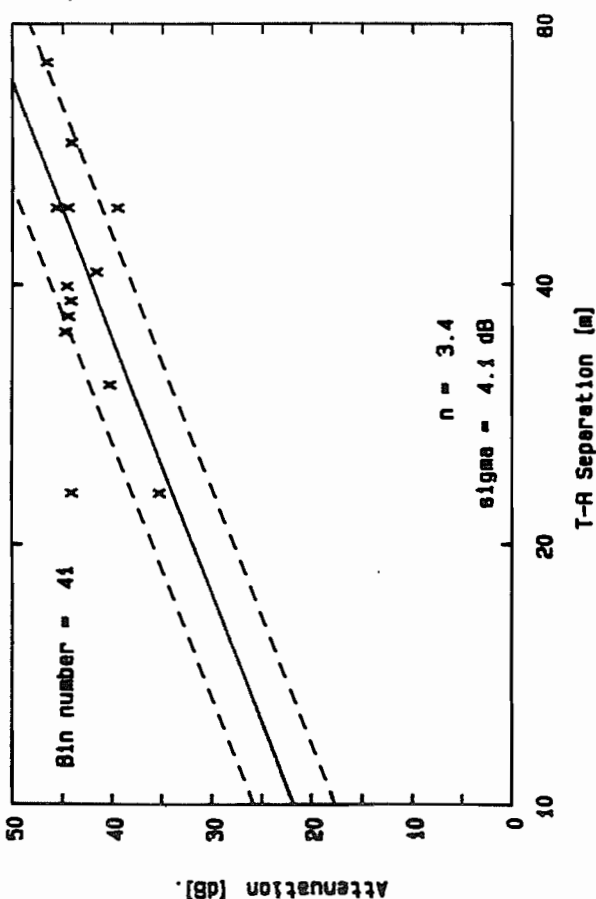
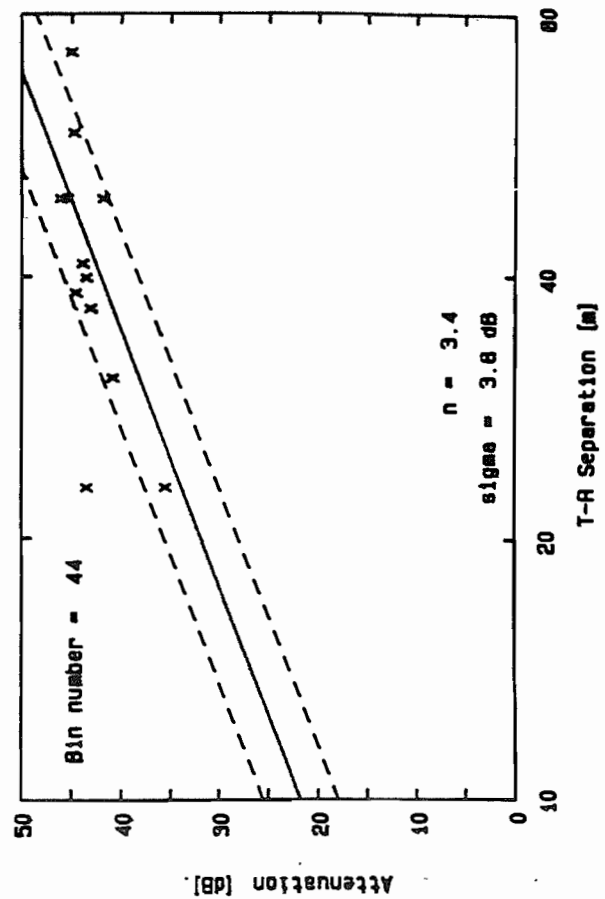
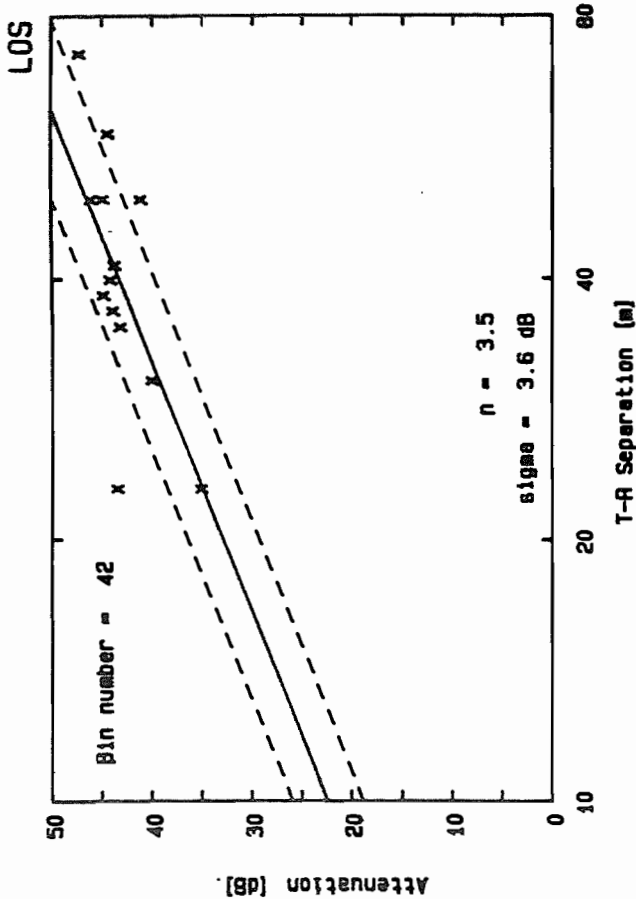


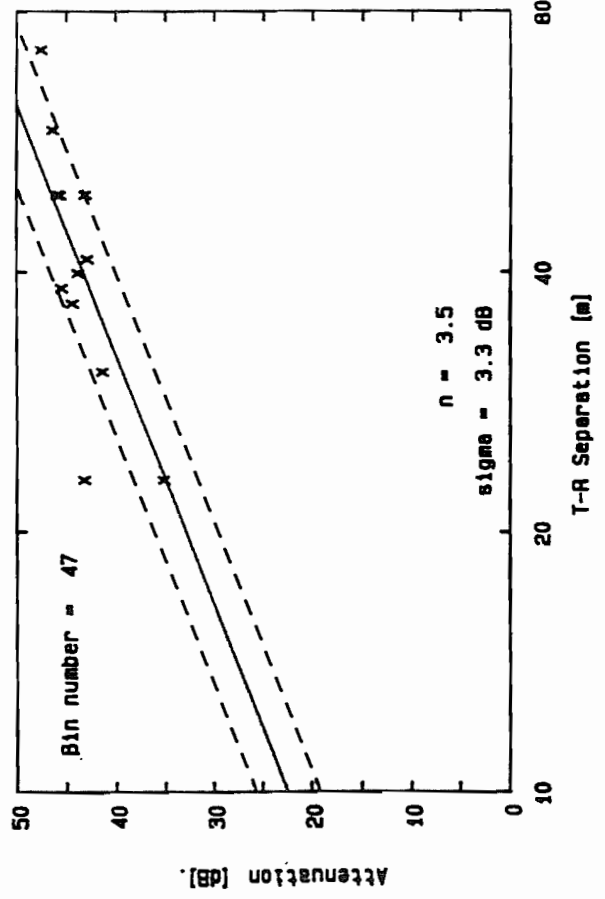
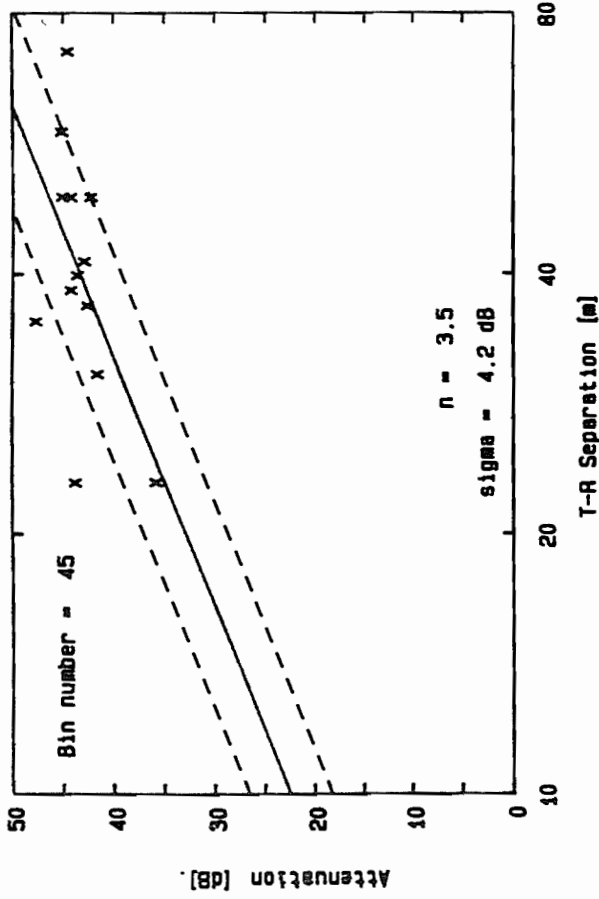
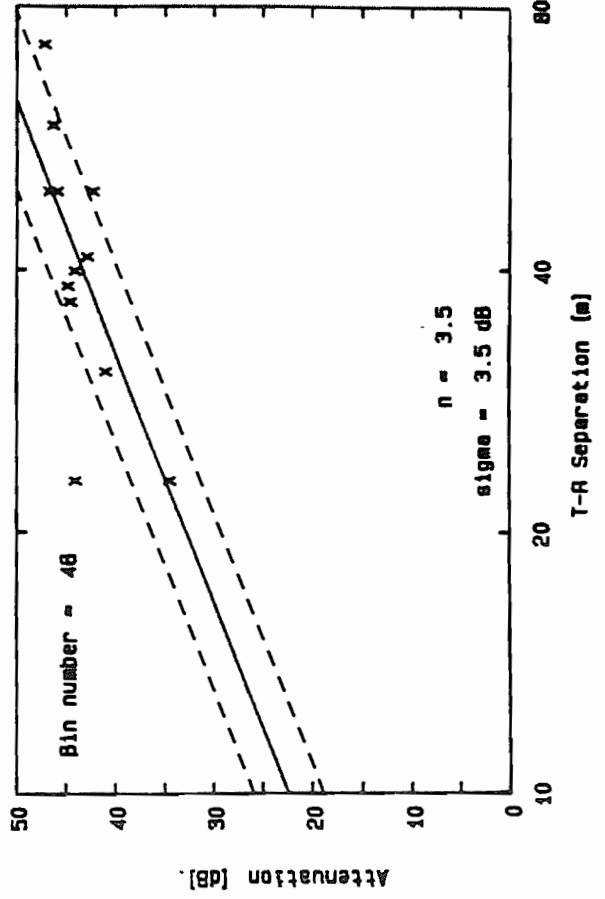
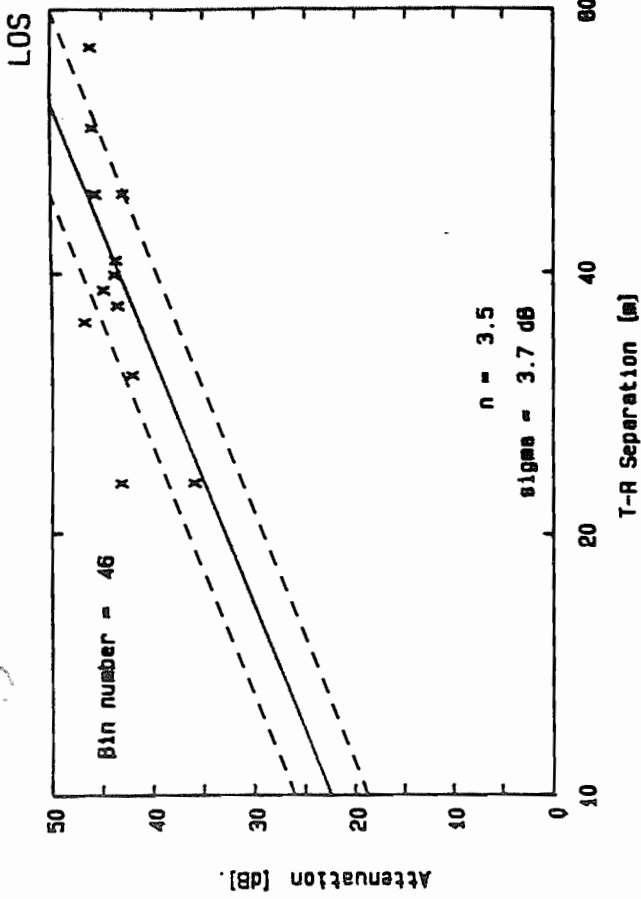


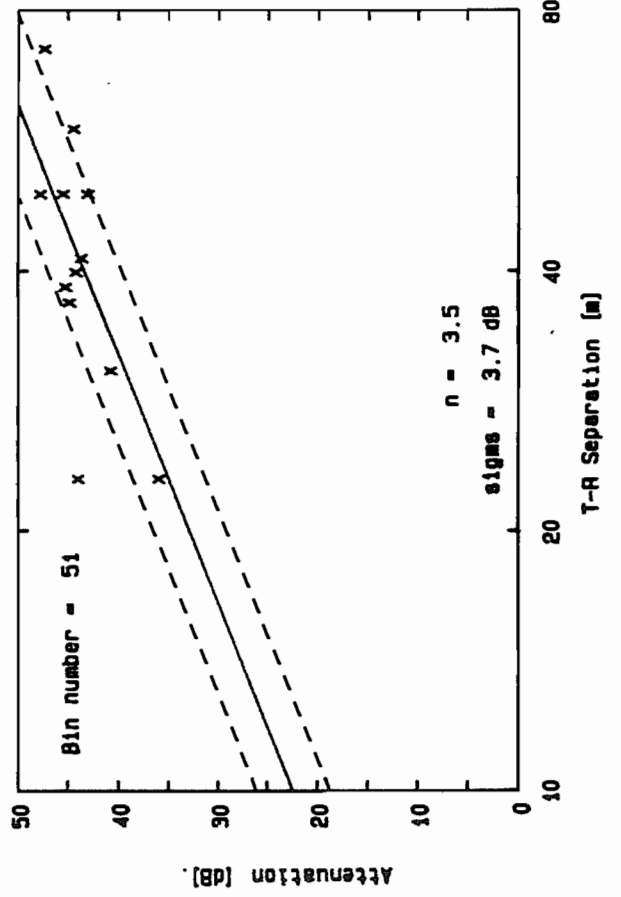
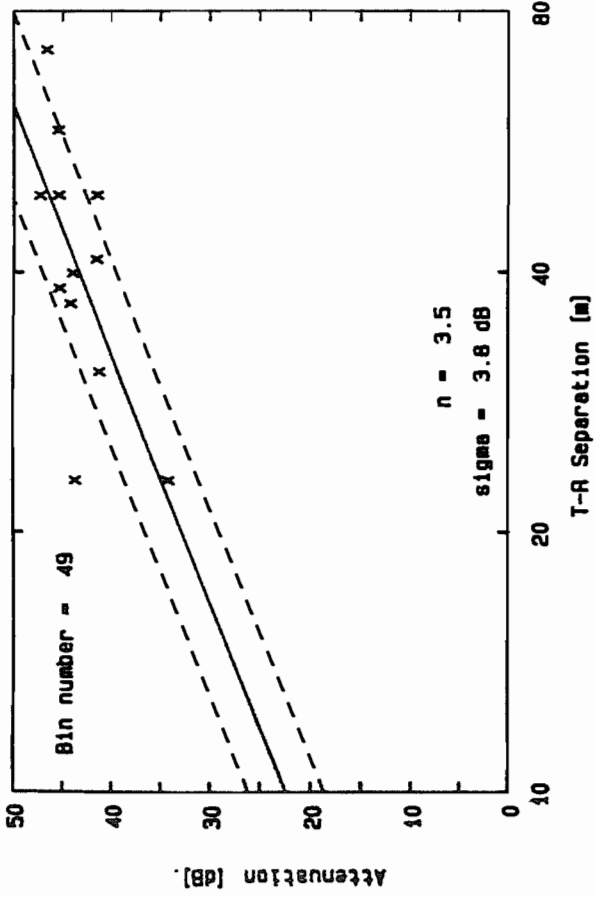
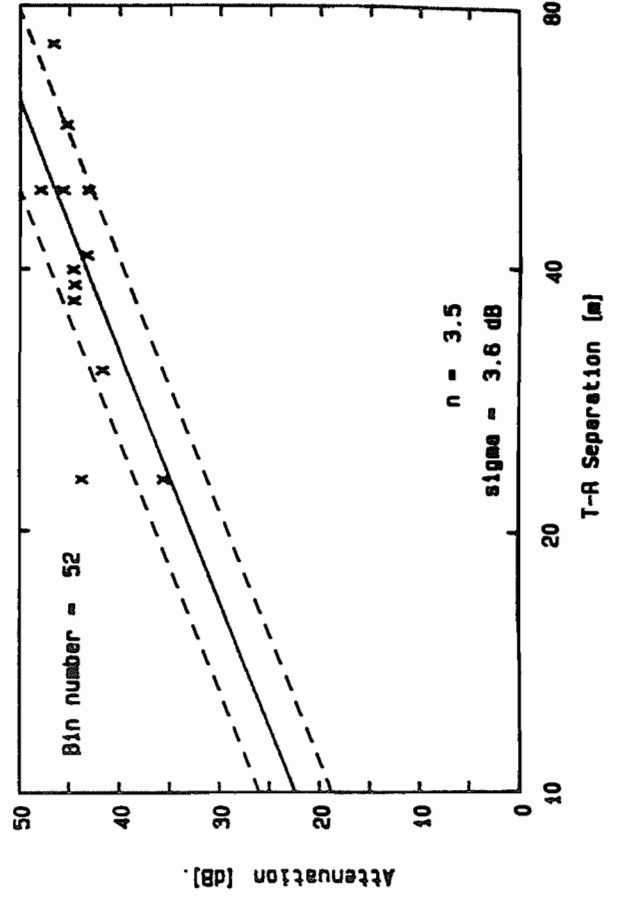
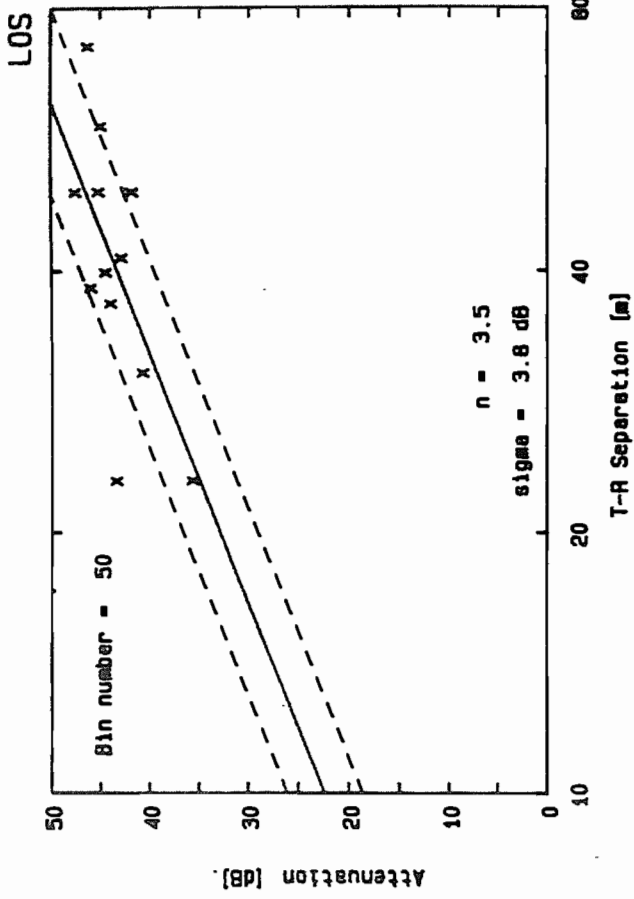


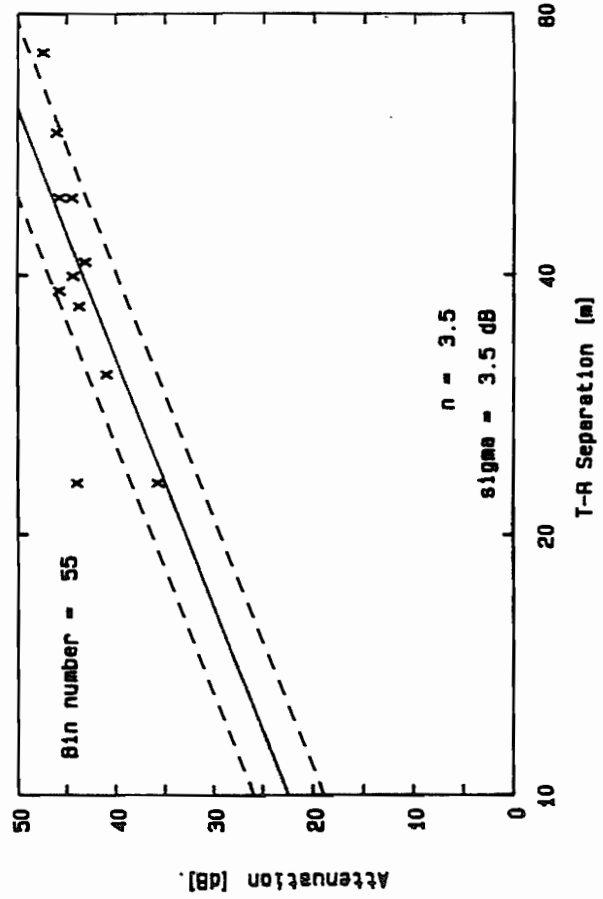
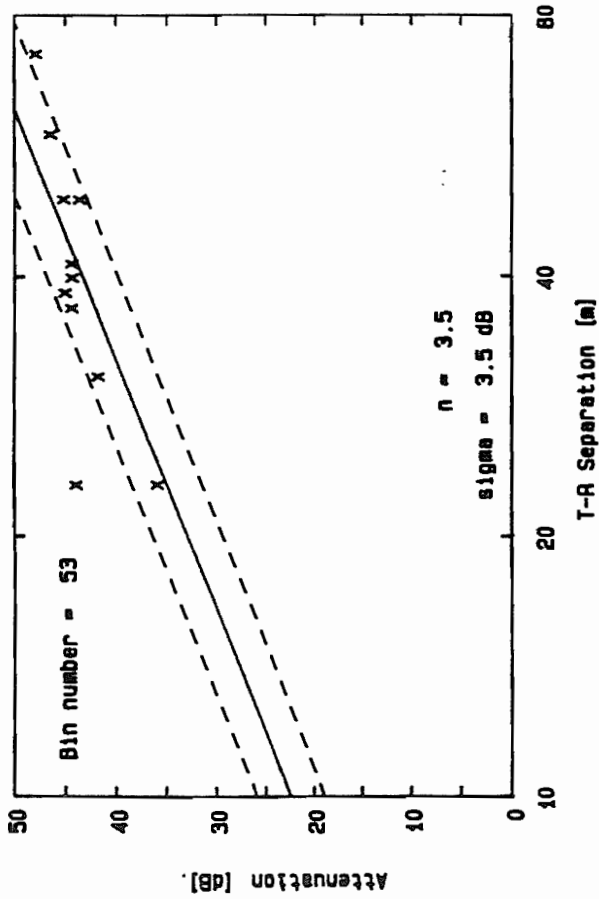
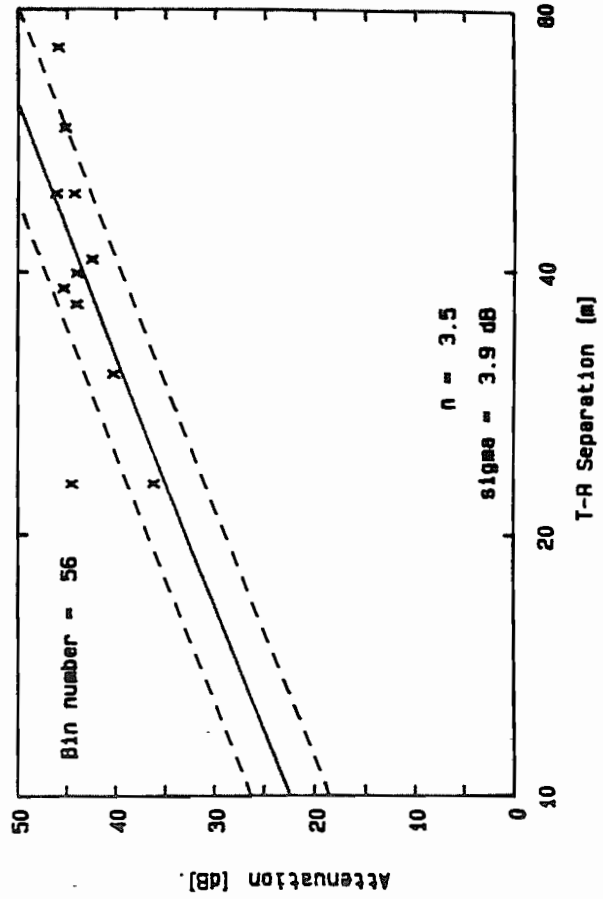
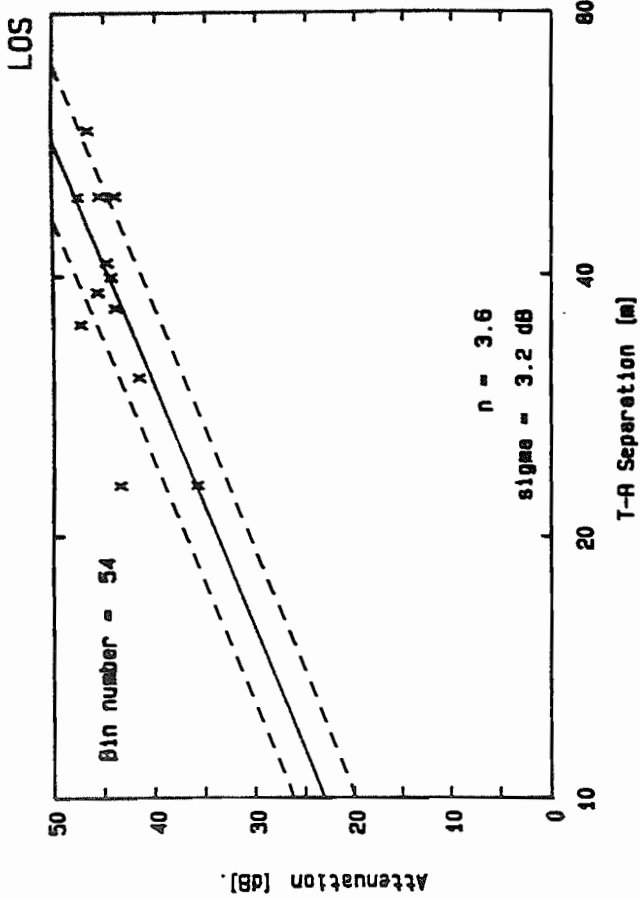


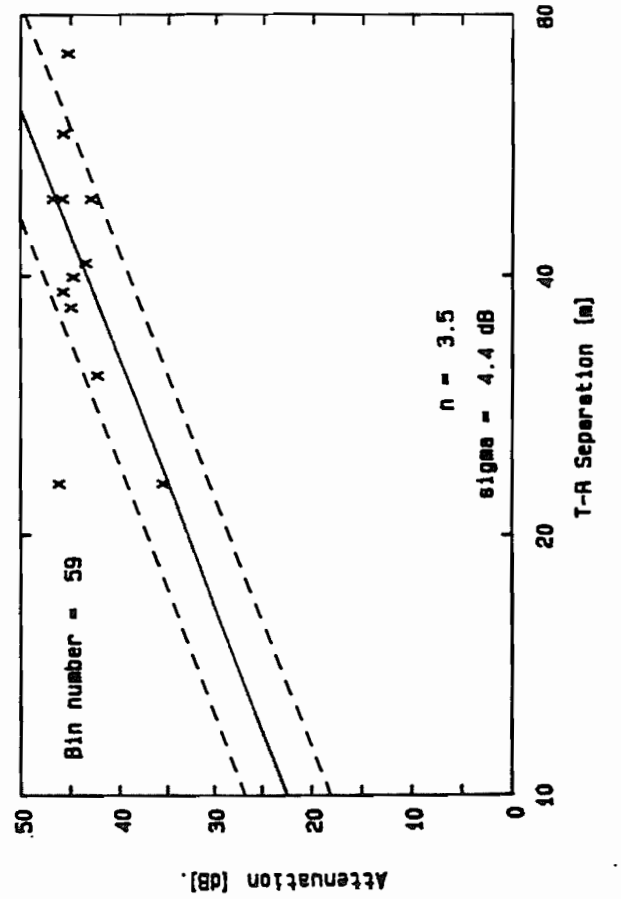
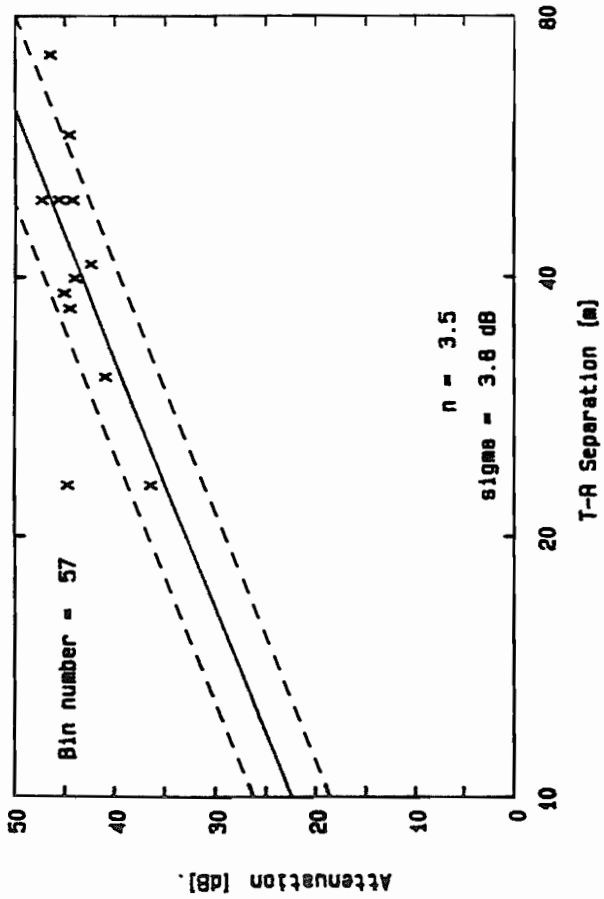
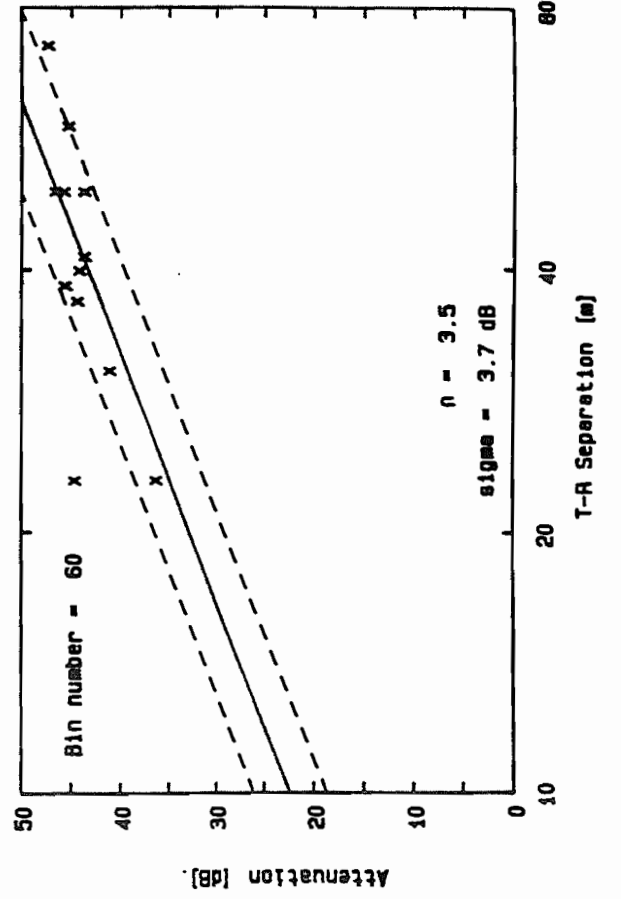
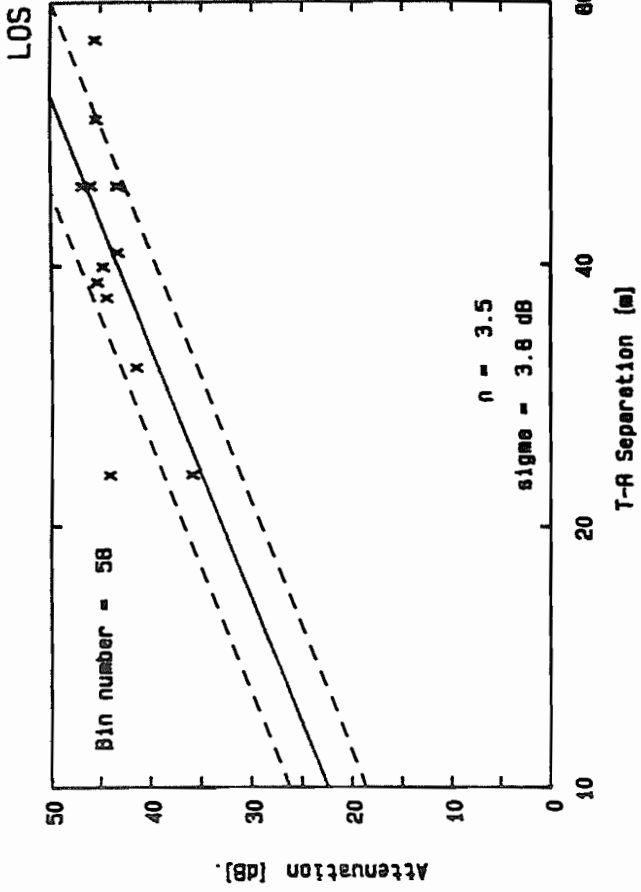


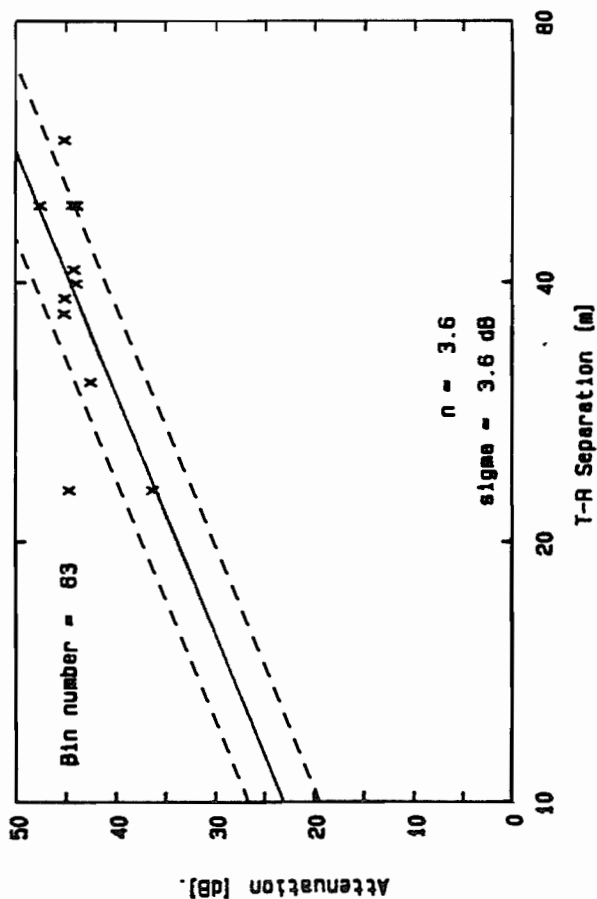
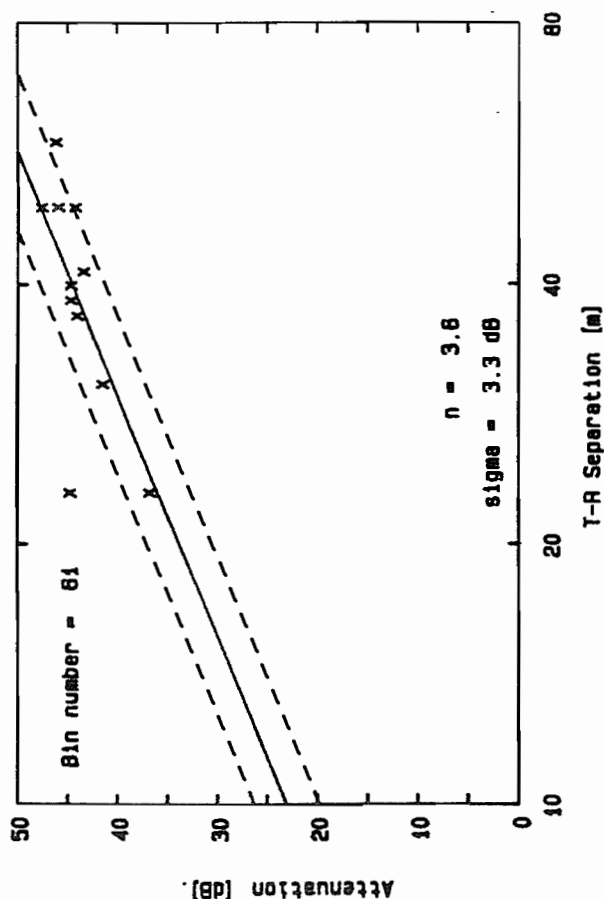
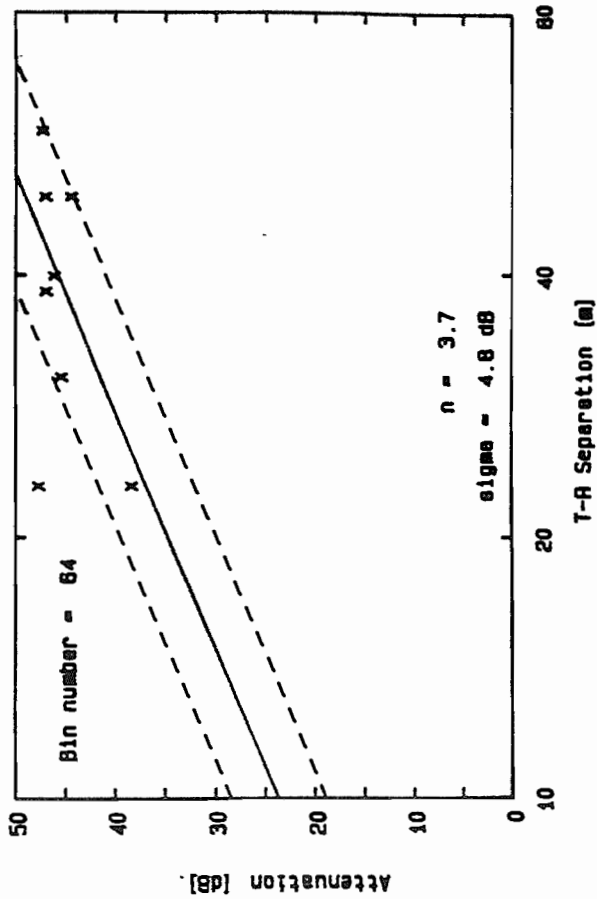
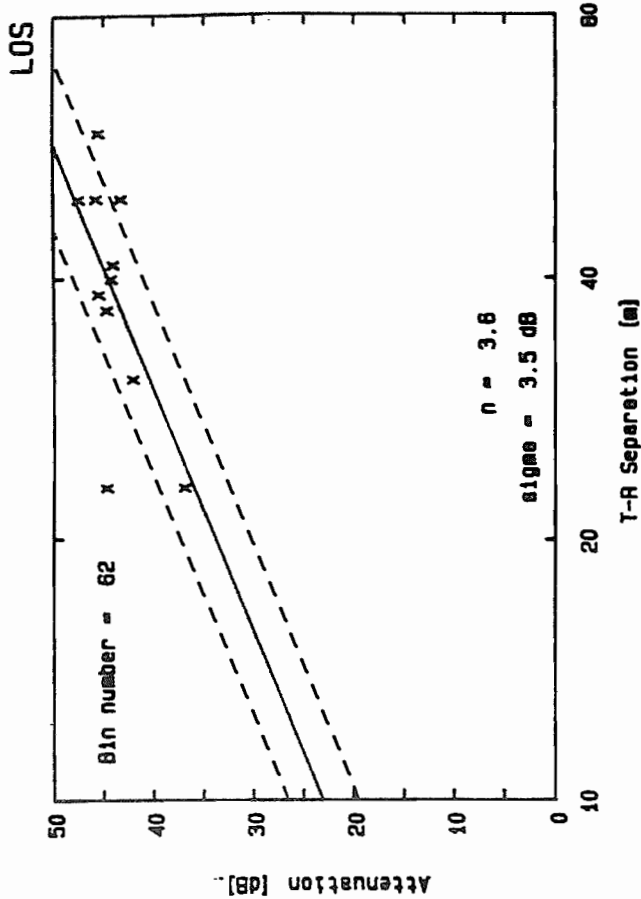


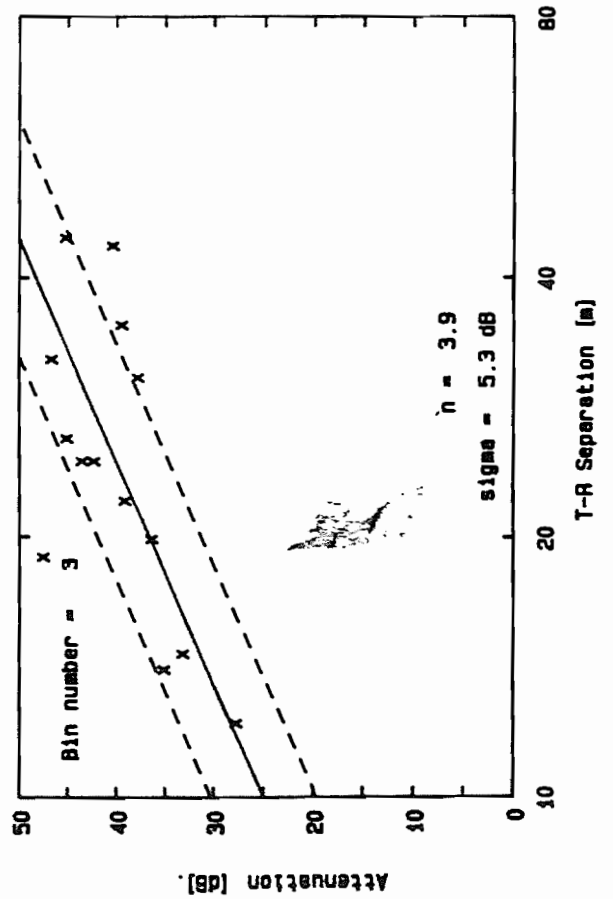
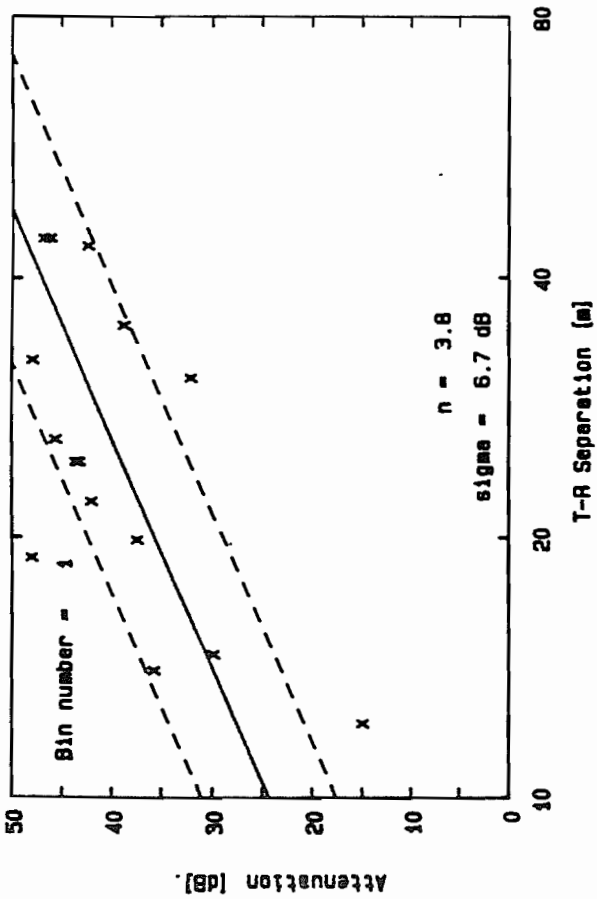
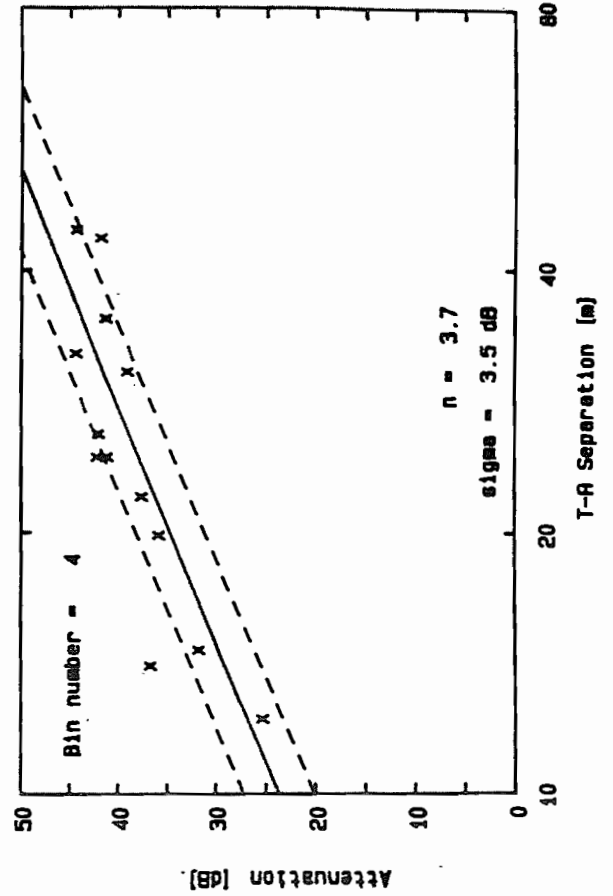
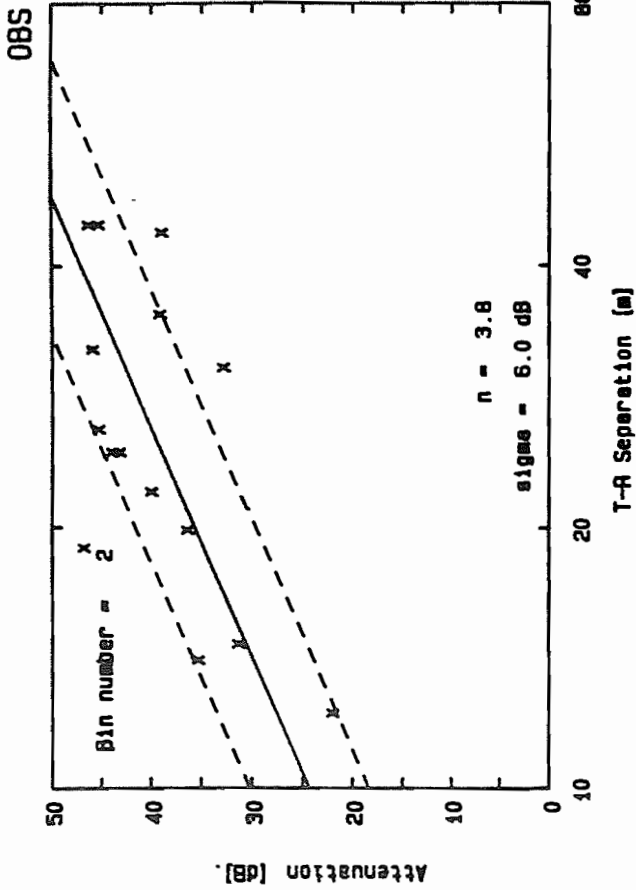




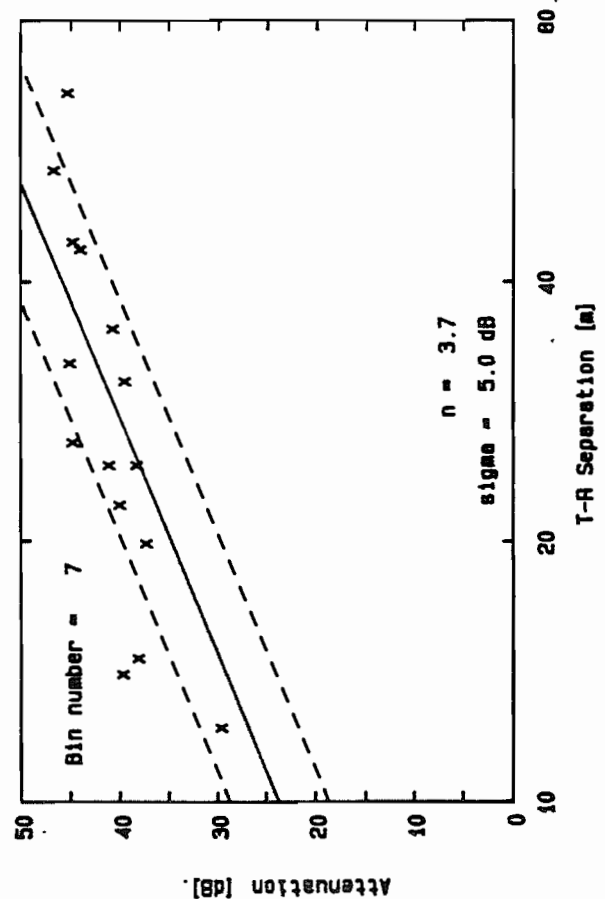
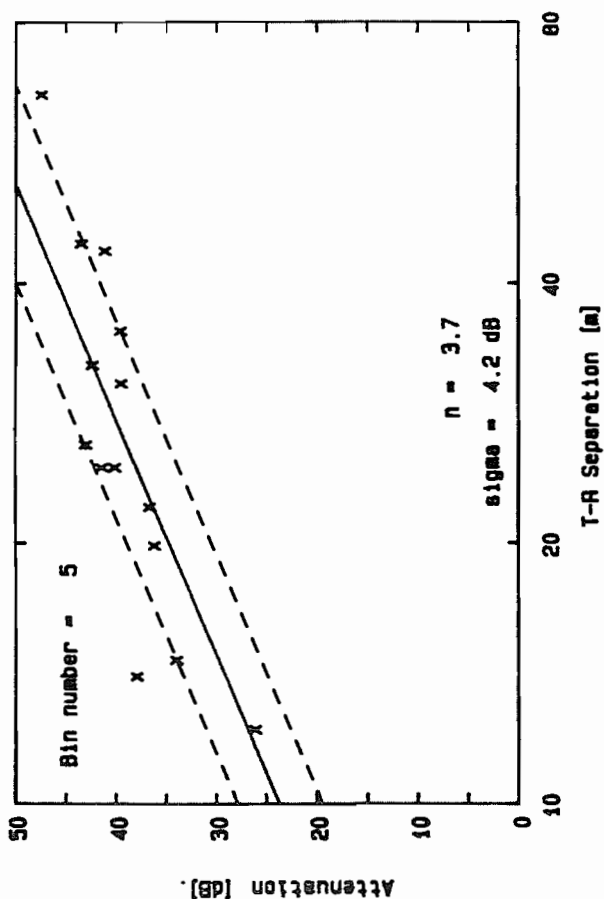
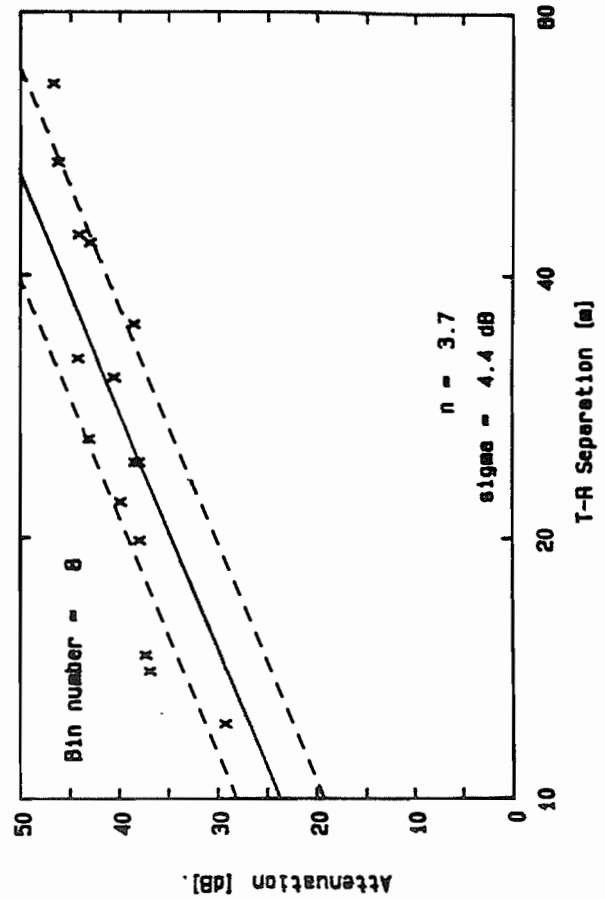
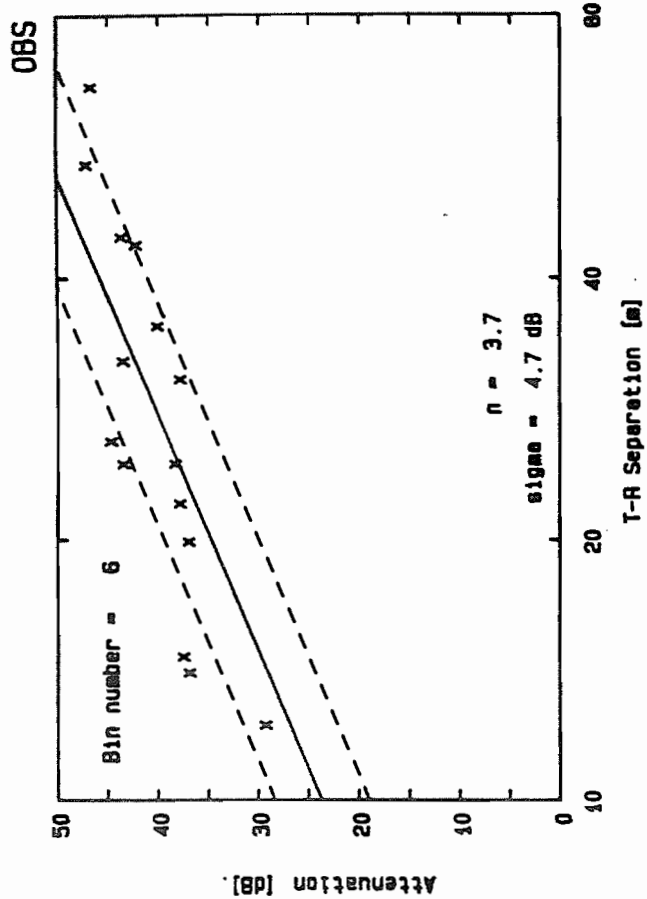




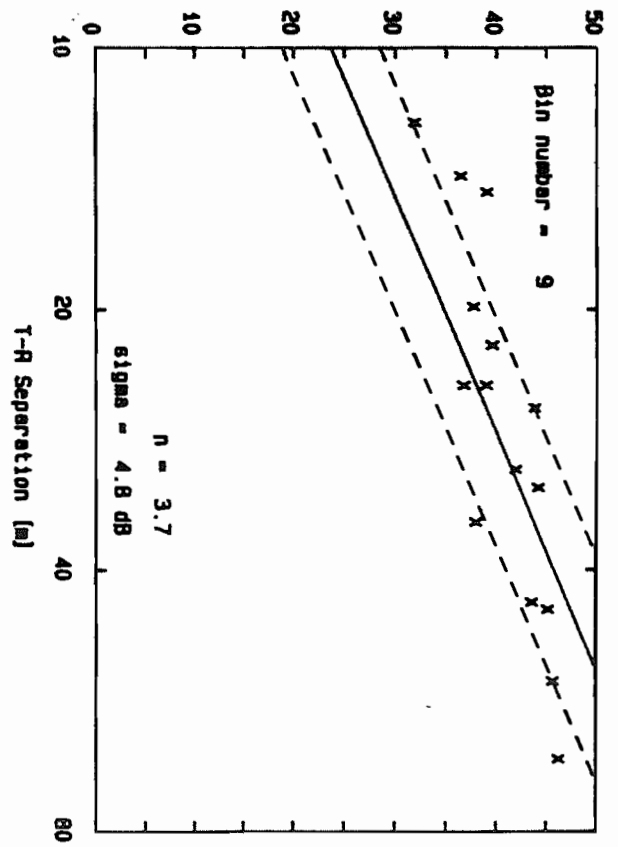




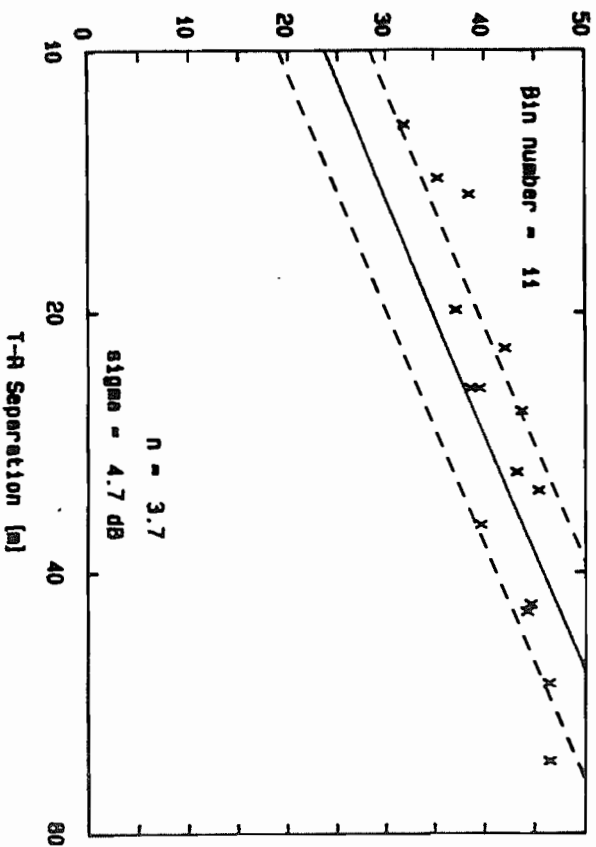




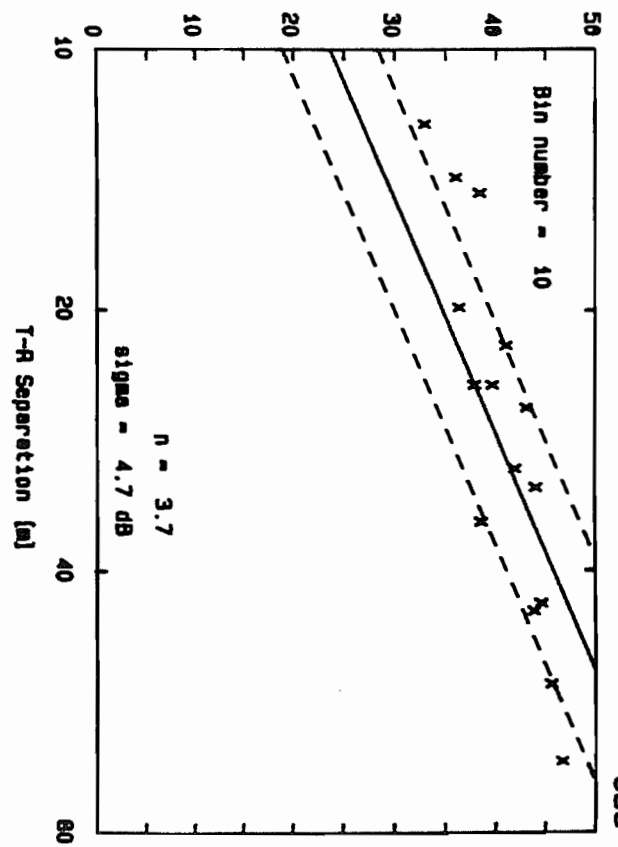
Attenuation [dB].



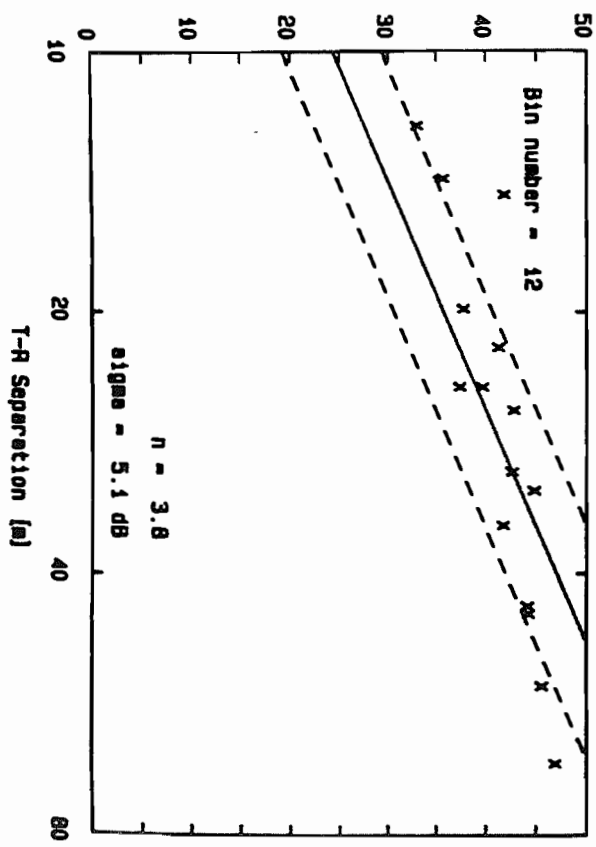
Attenuation [dB].



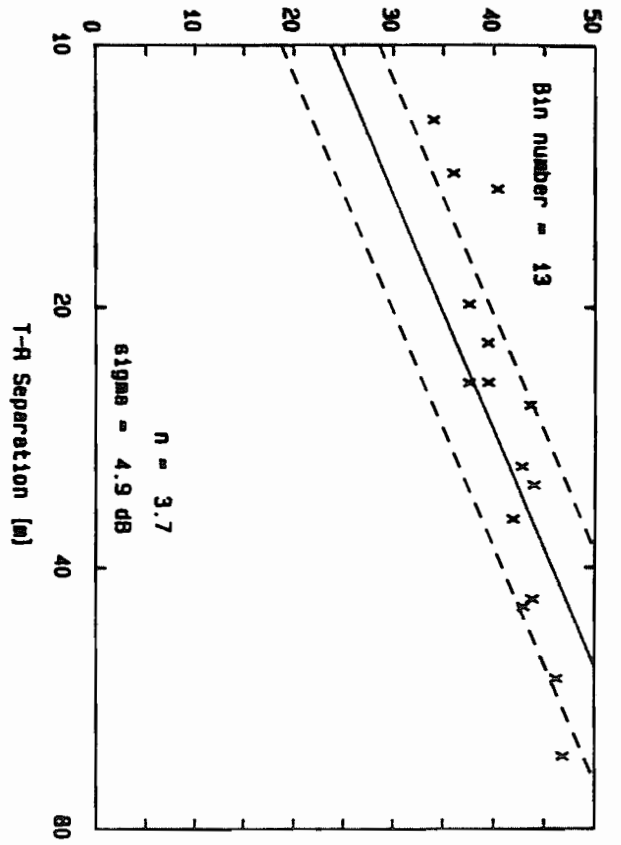
Attenuation [dB].



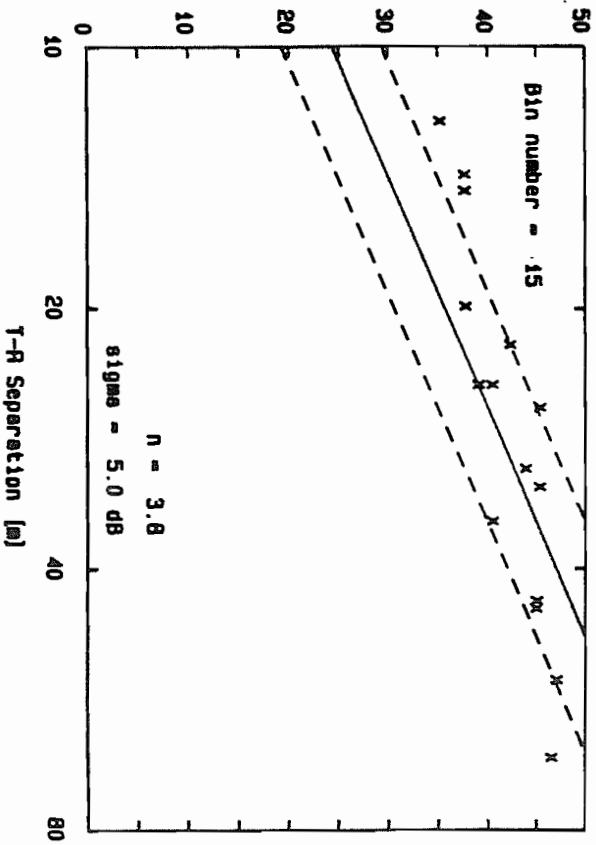
Attenuation [dB].



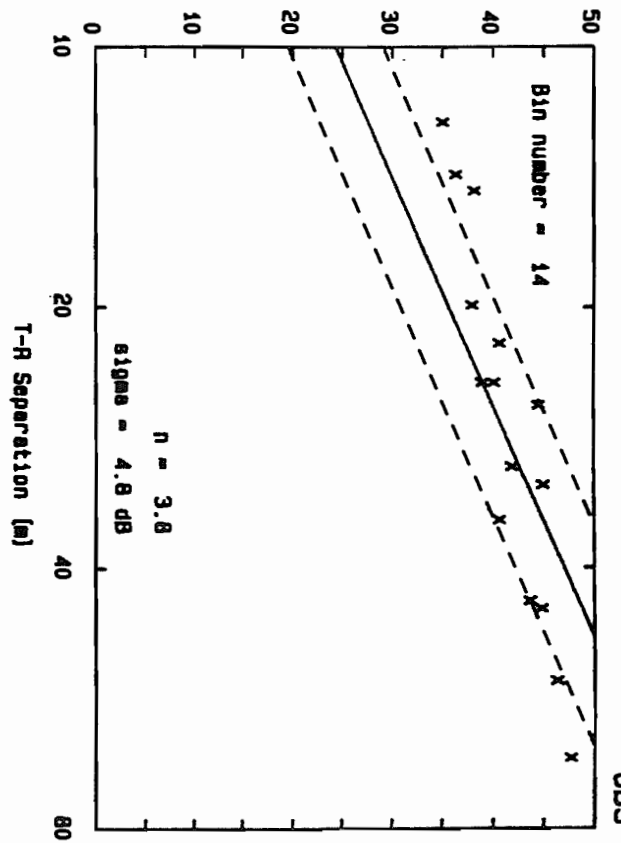
Attenuation [dB].



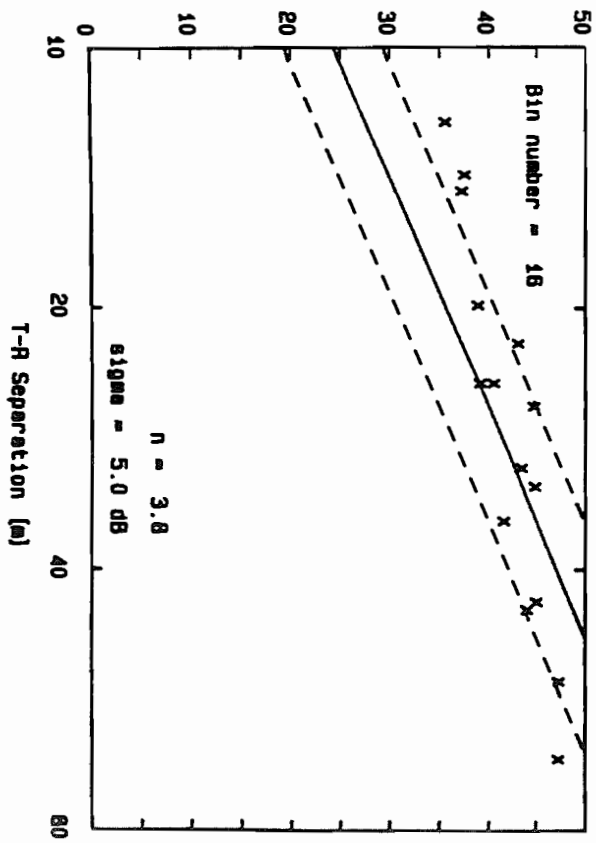
Attenuation [dB].



Attenuation [dB].

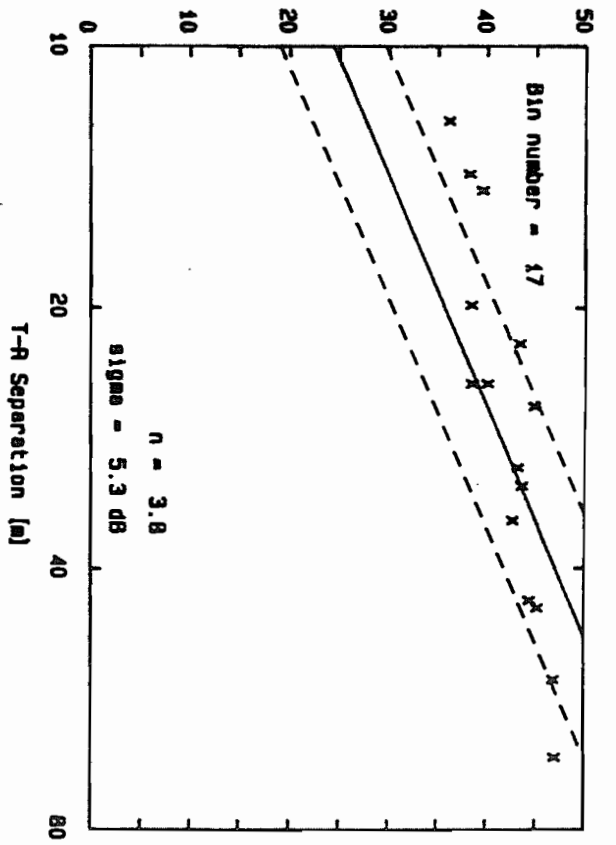


Attenuation [dB].

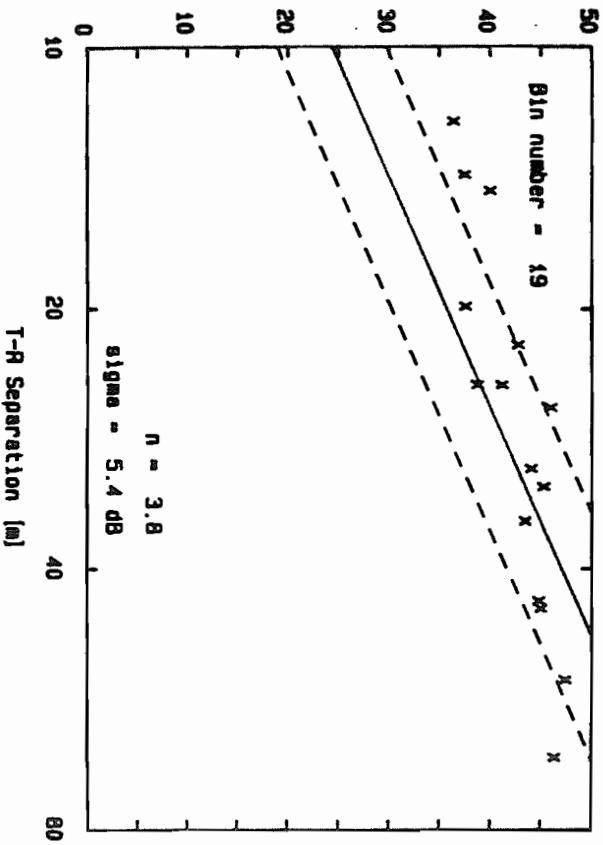


OBS

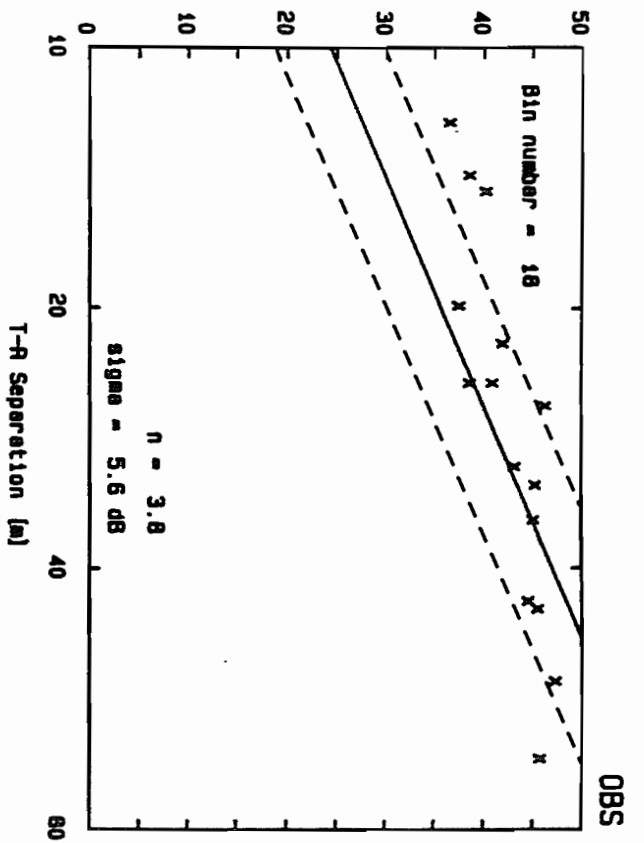
Attenuation [dB].



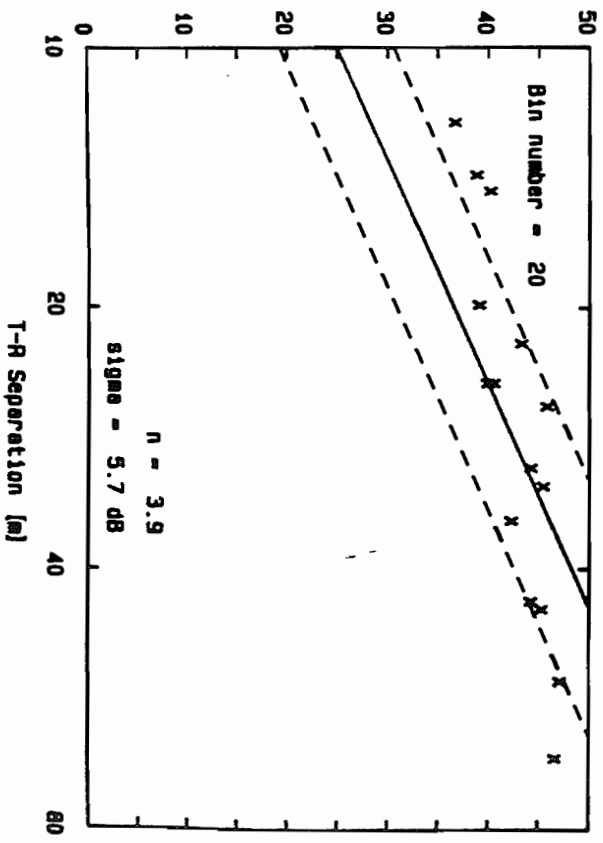
Attenuation [dB].



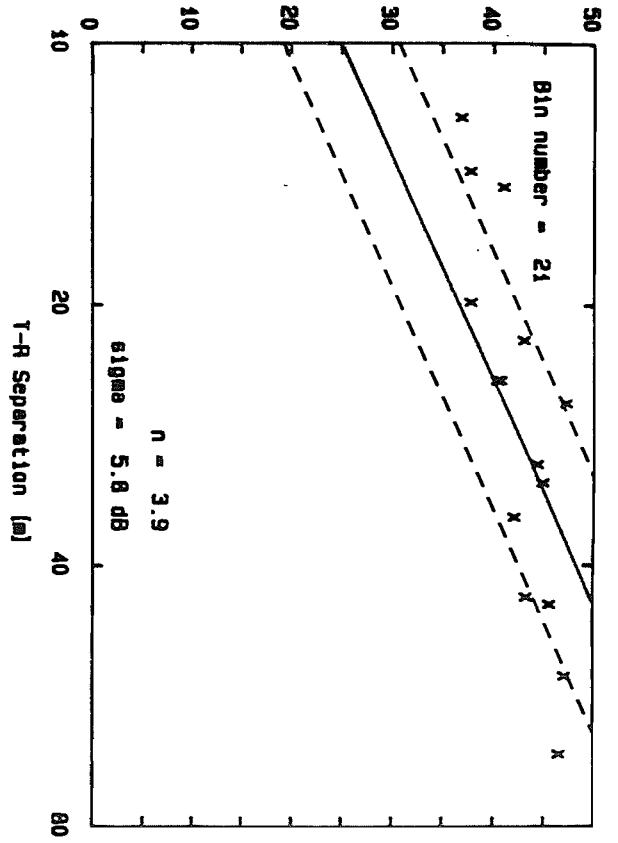
Attenuation [dB].



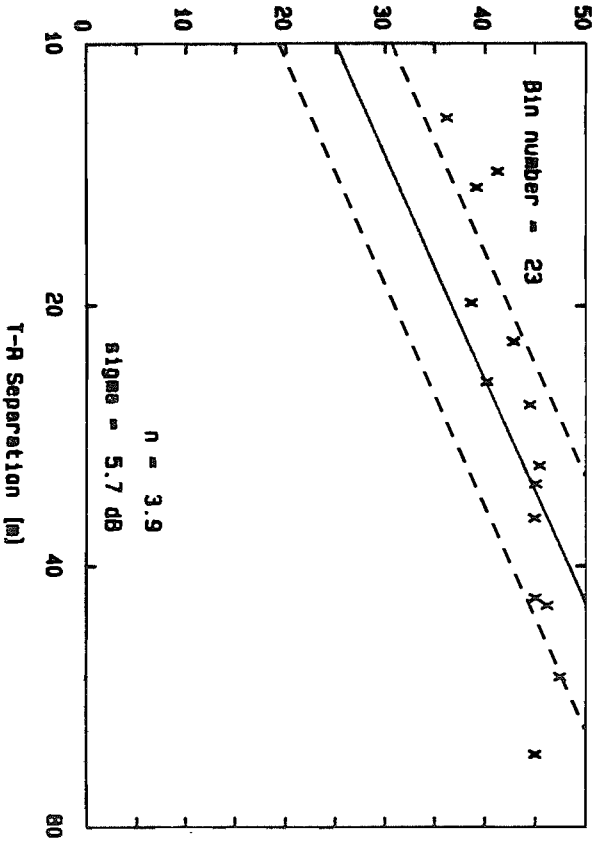
Attenuation [dB].



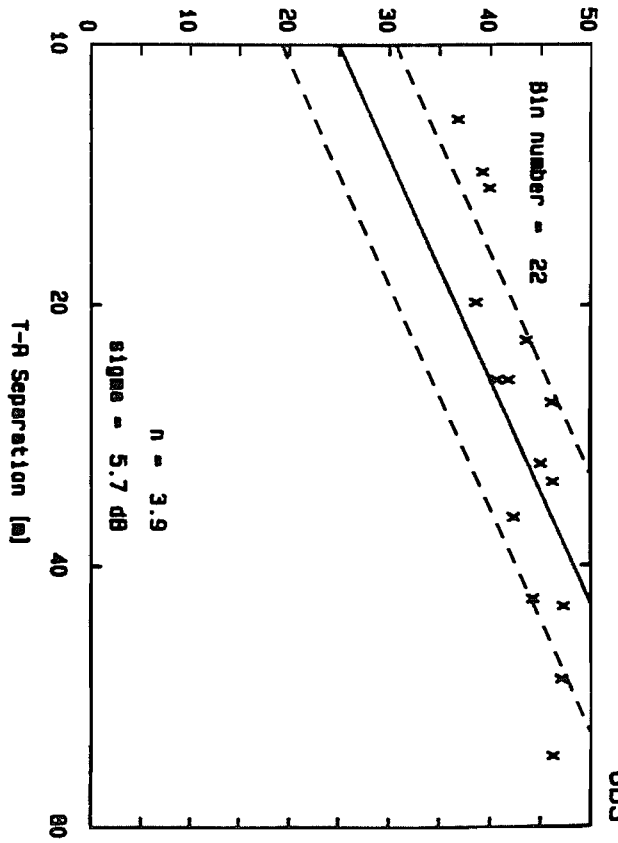
Attenuation [dB].



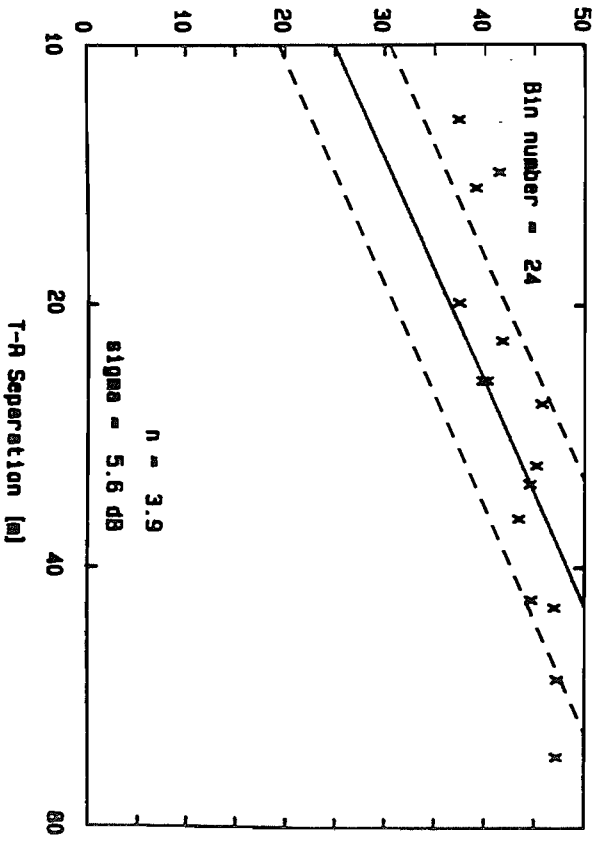
Attenuation [dB].



Attenuation [dB].

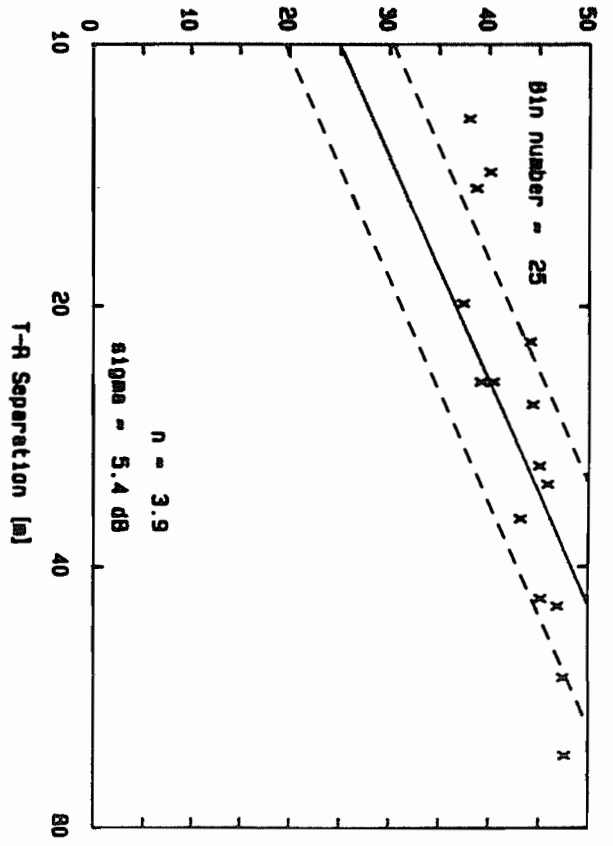


Attenuation [dB].

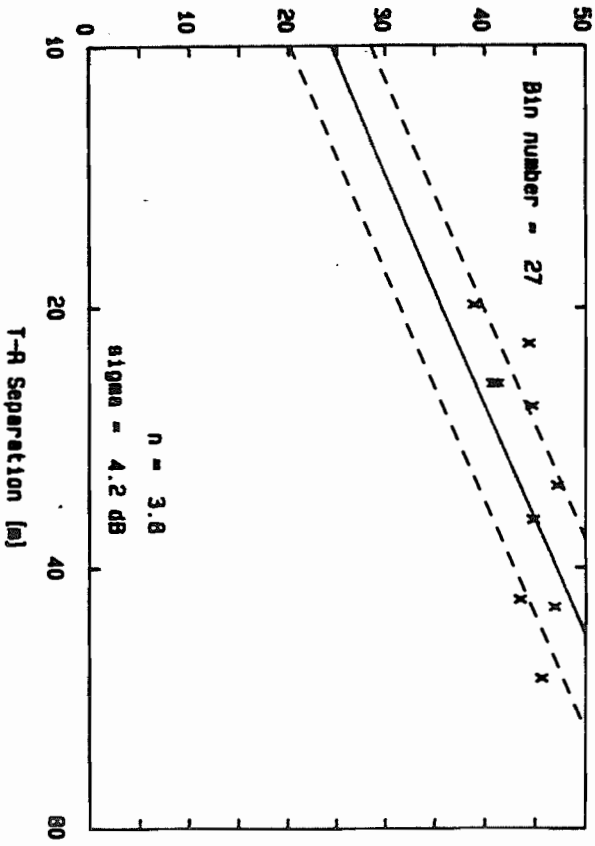


OBS

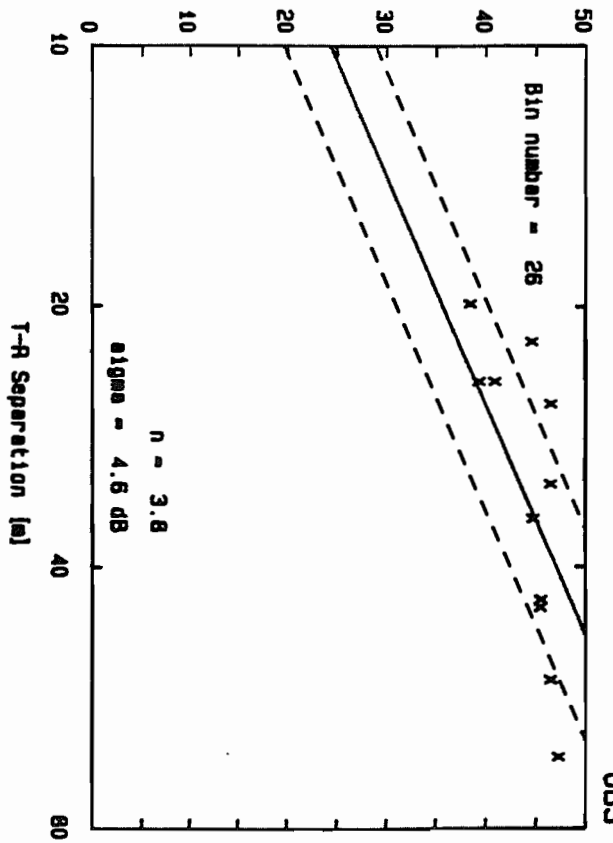
Attenuation [dB].



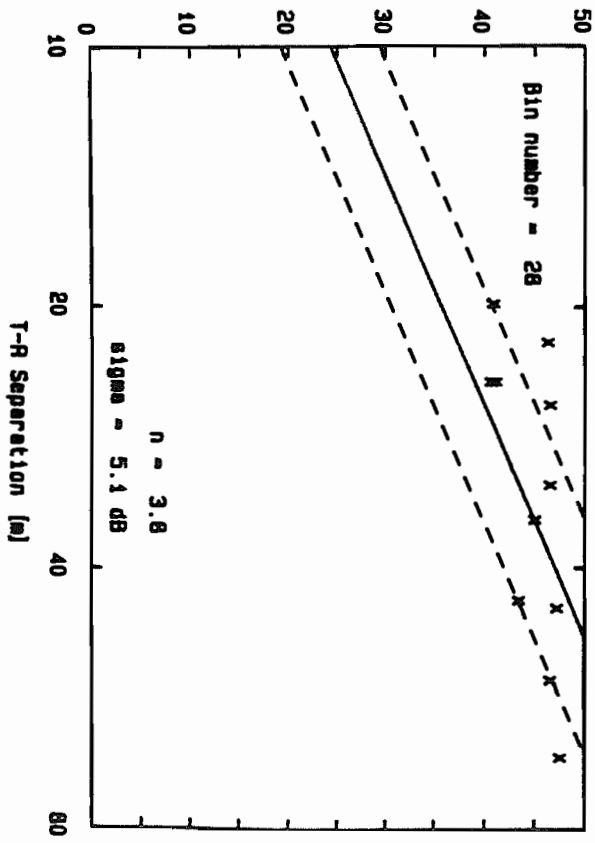
Attenuation [dB].



Attenuation [dB].

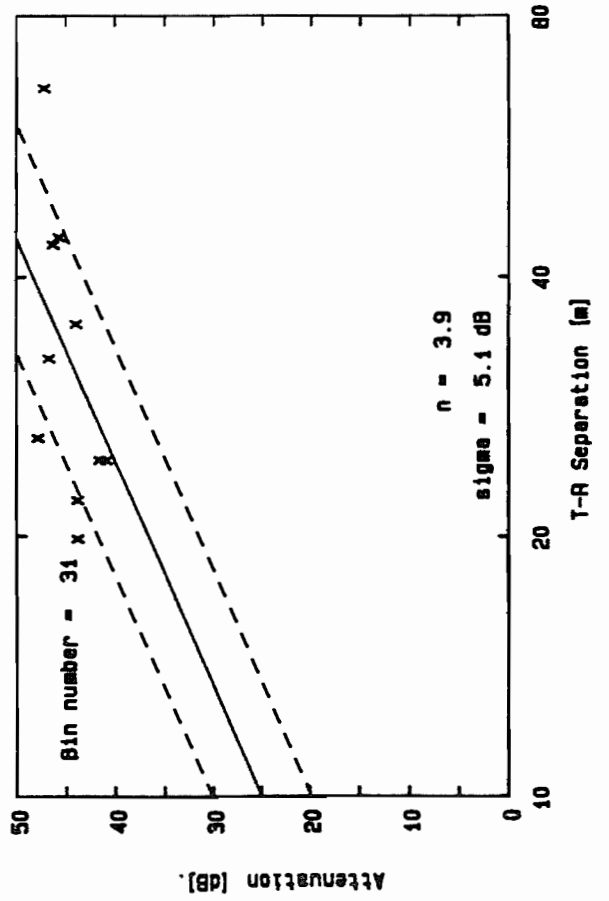
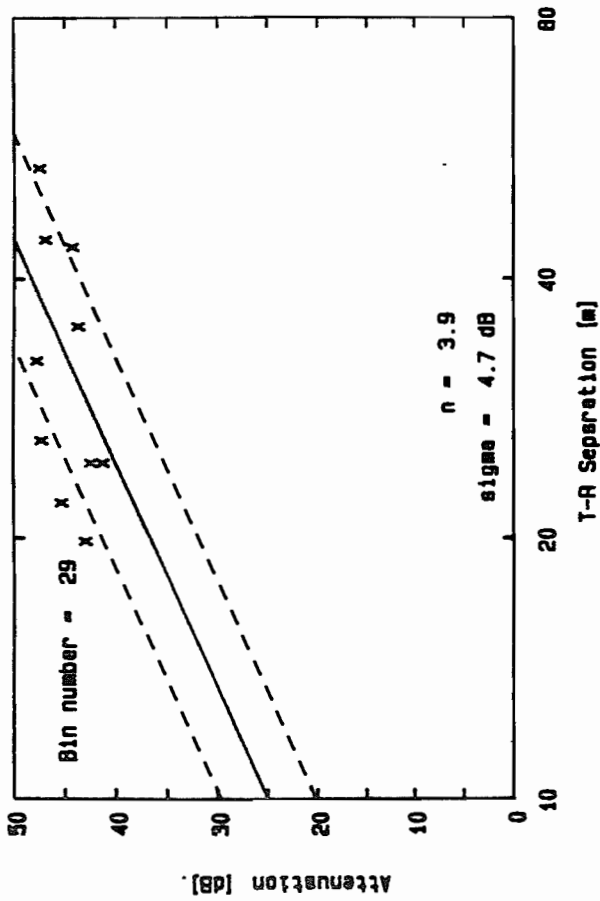
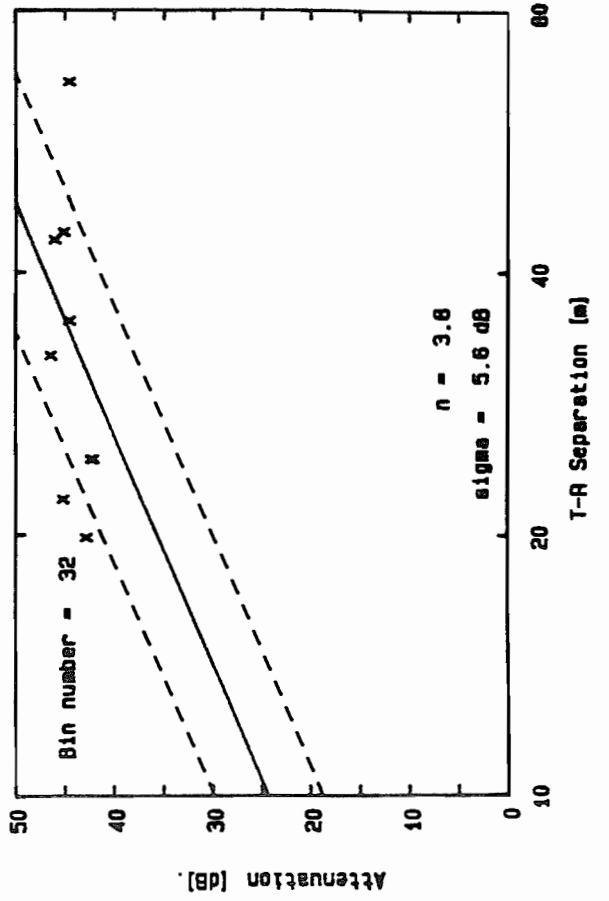
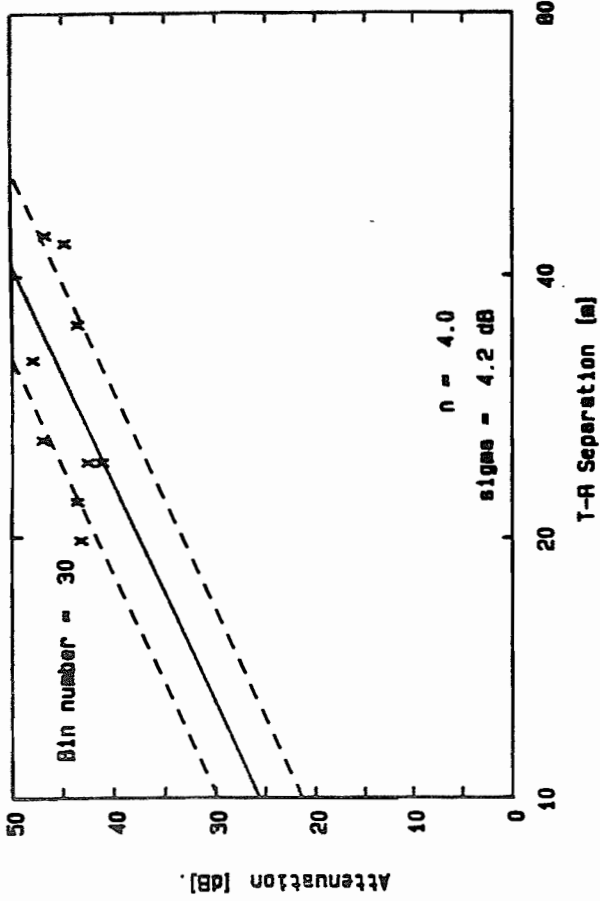


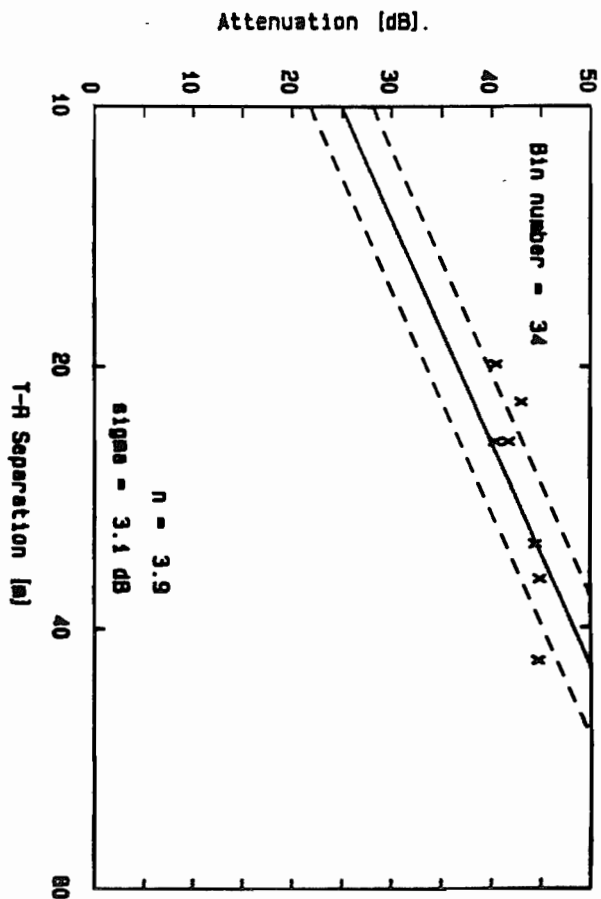
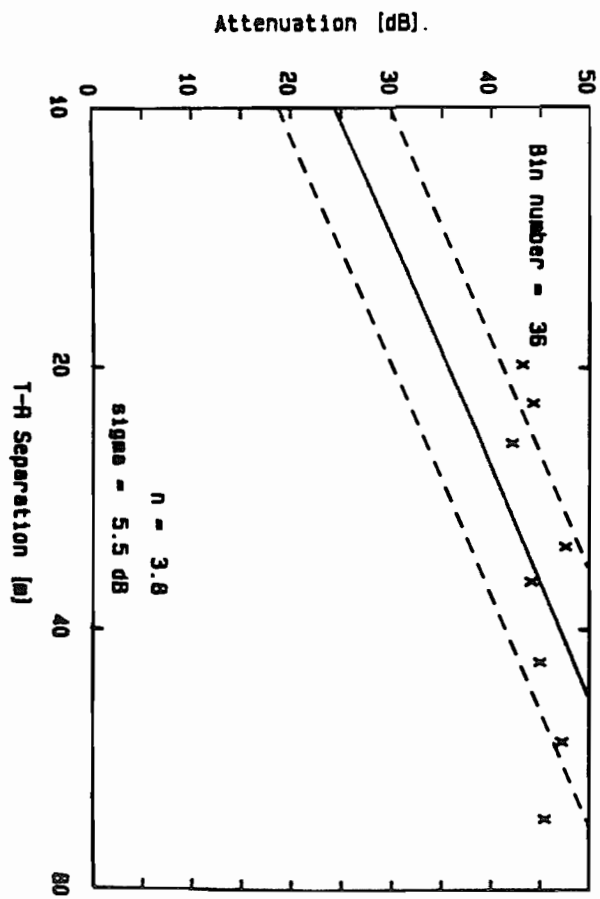
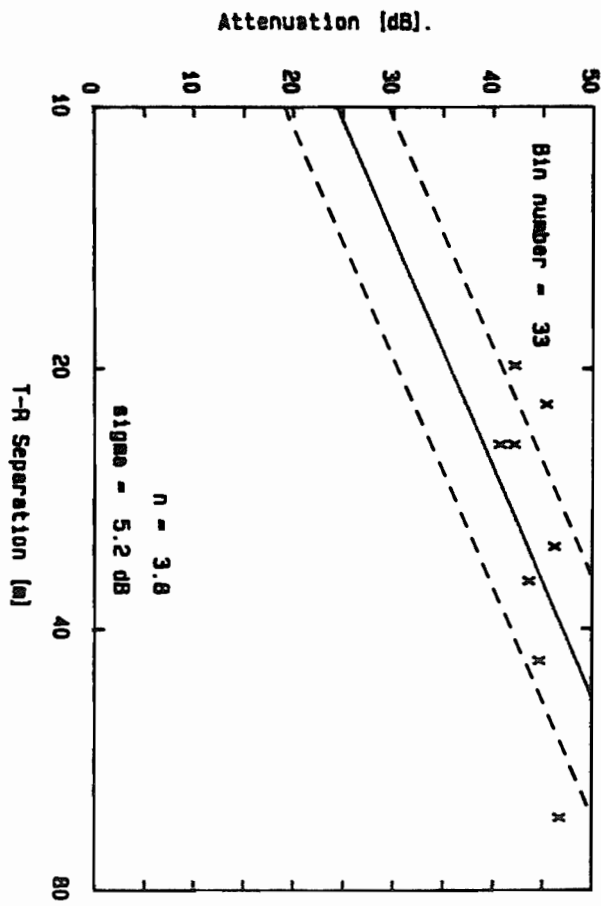
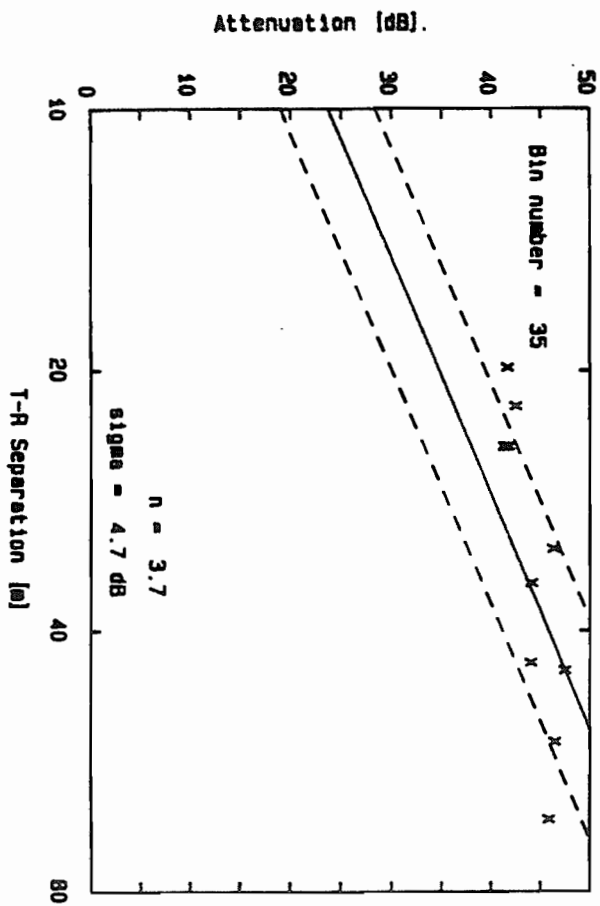
Attenuation [dB].



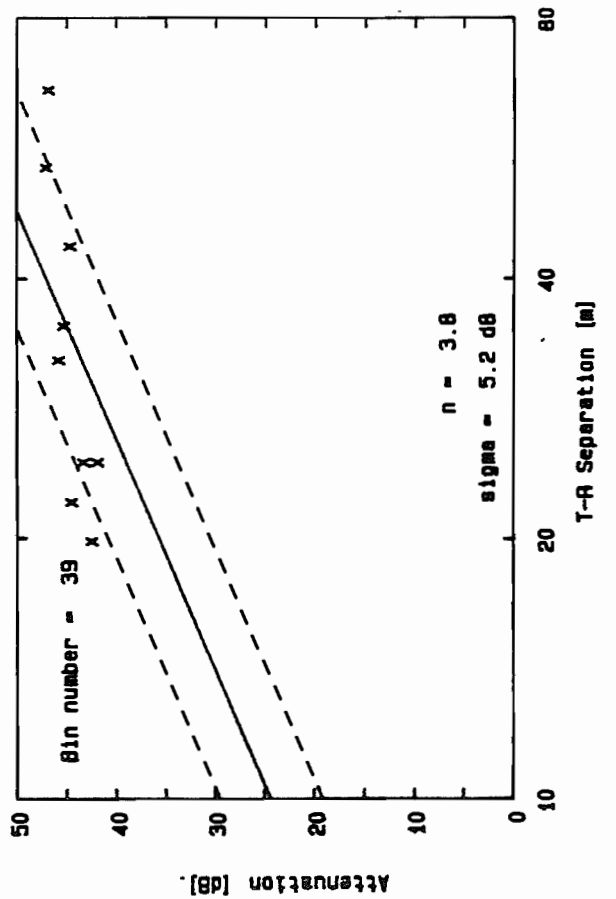
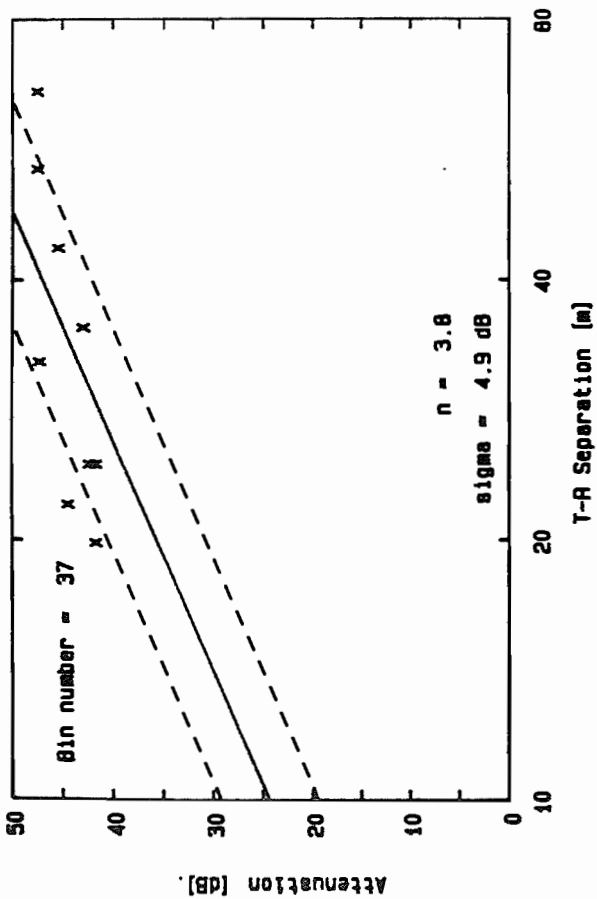
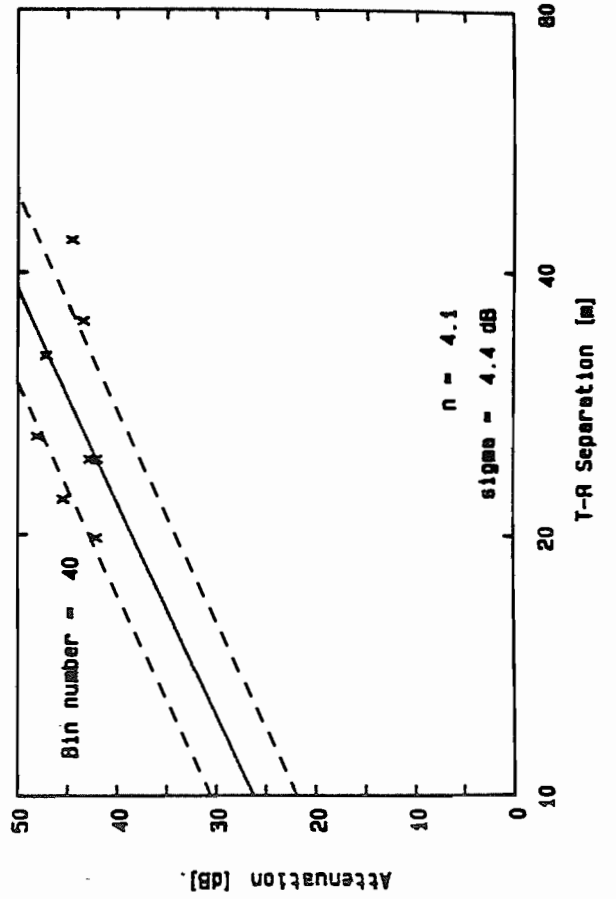
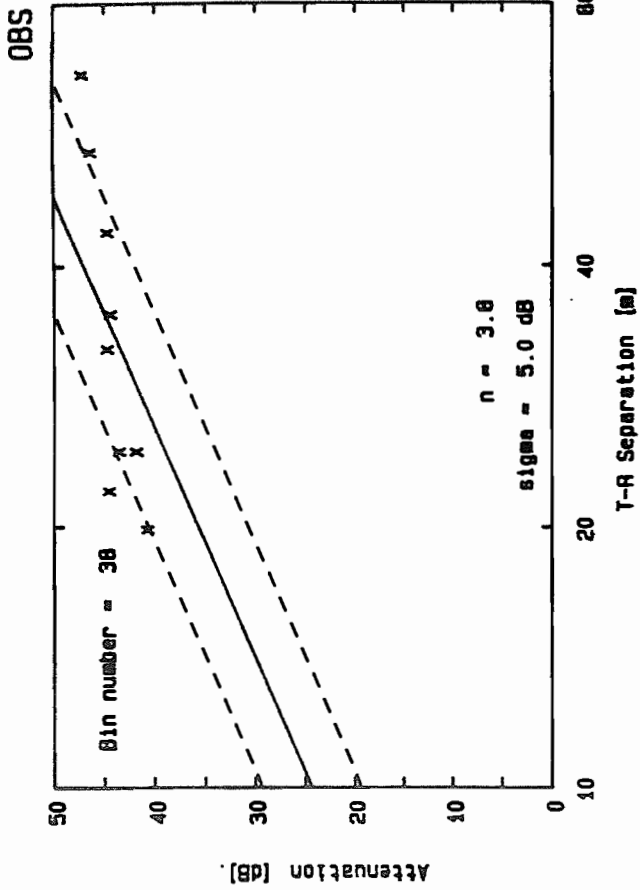
OBS

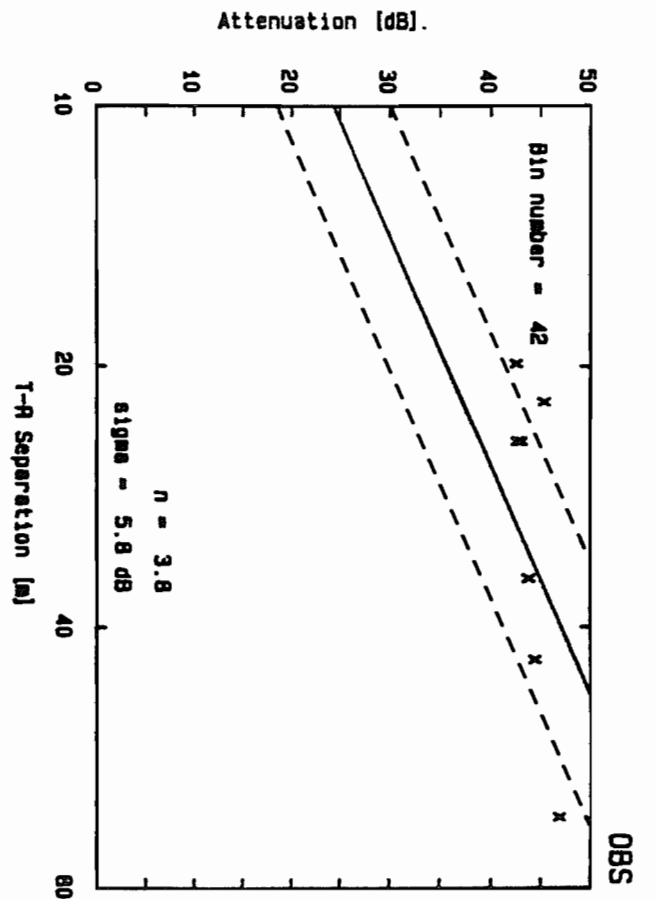
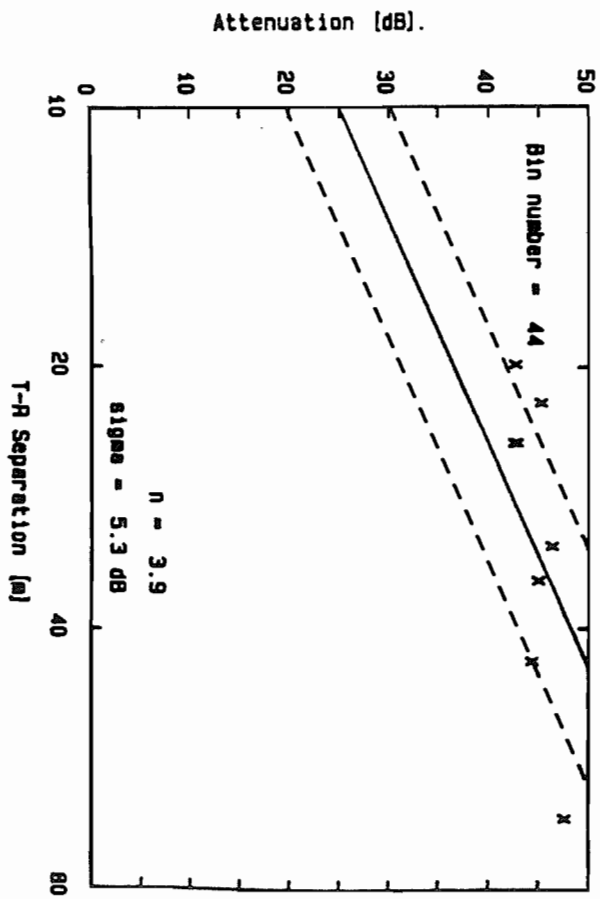
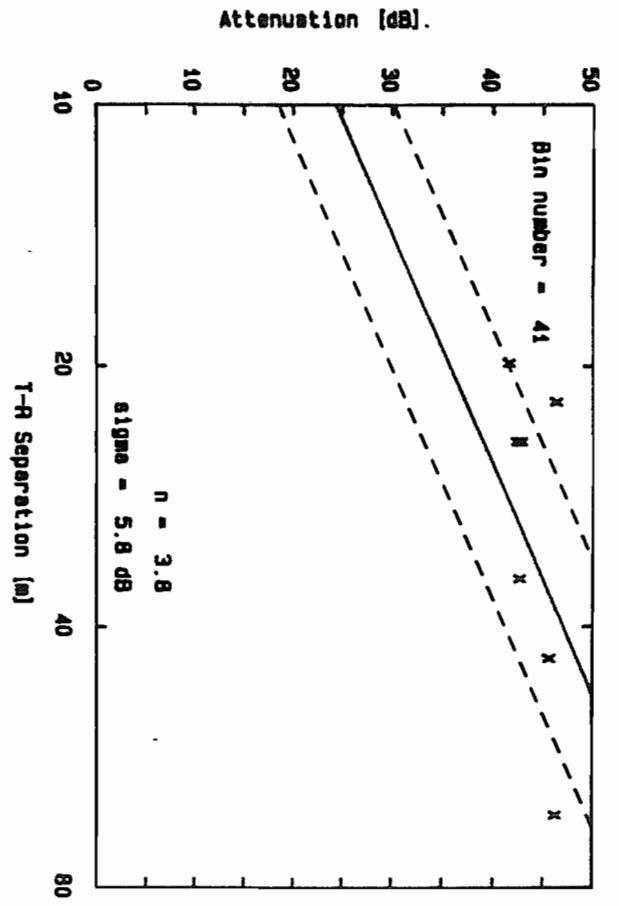
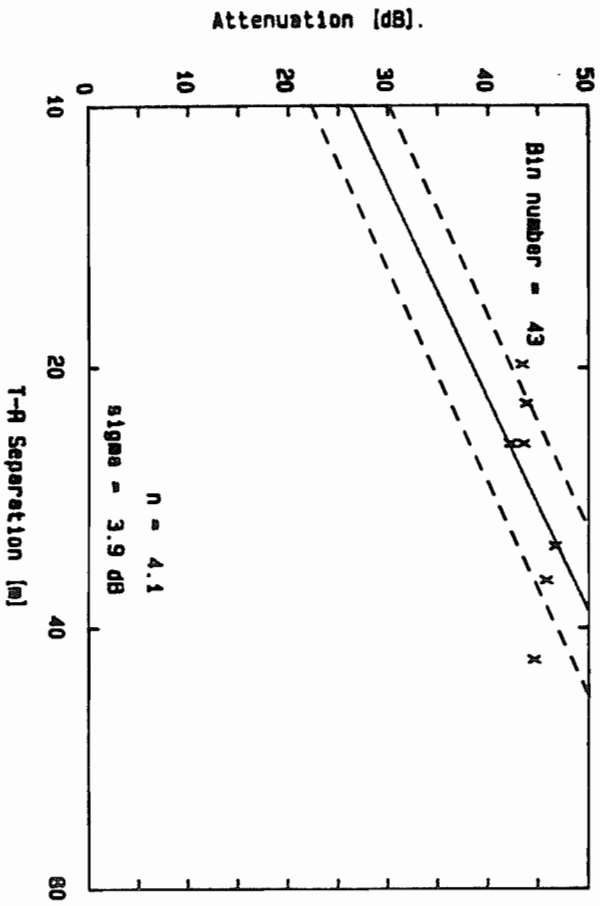
OBS



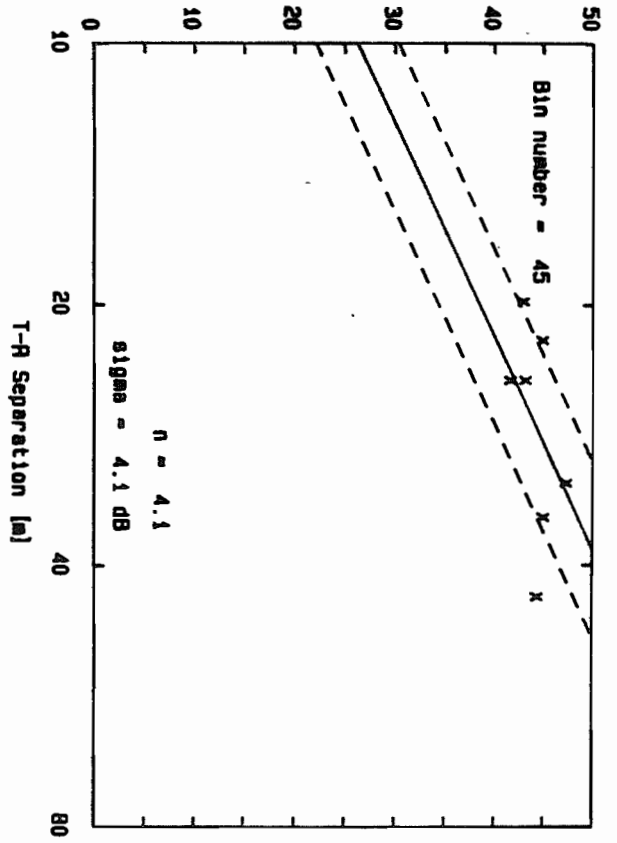




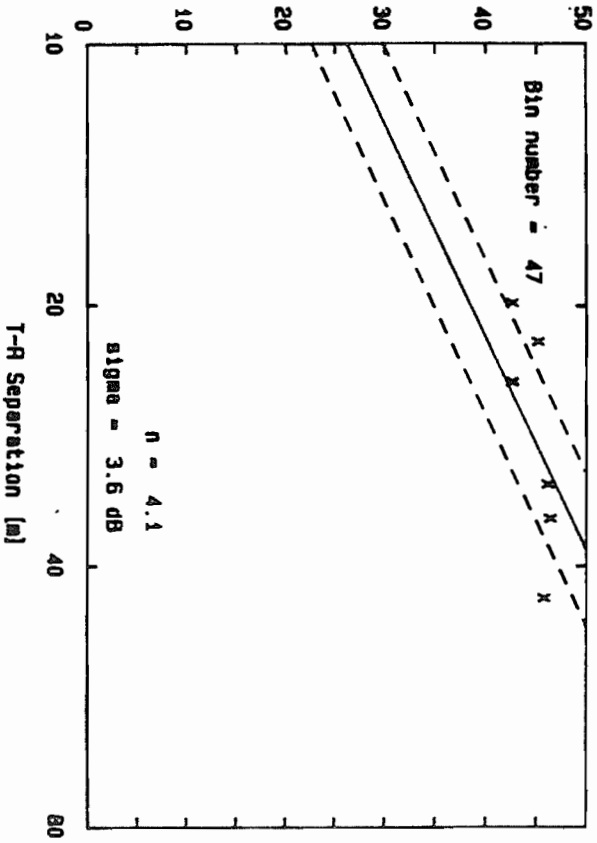




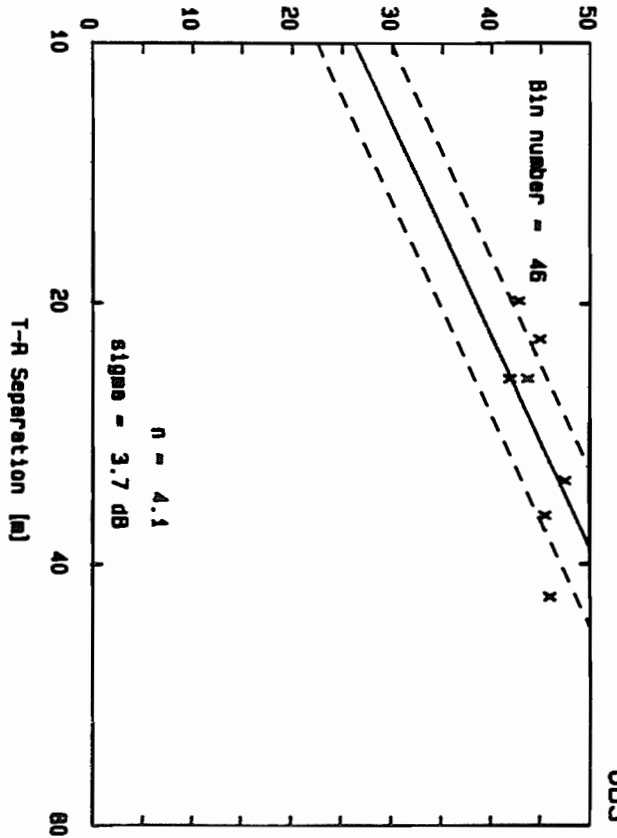
Attenuation [dB].



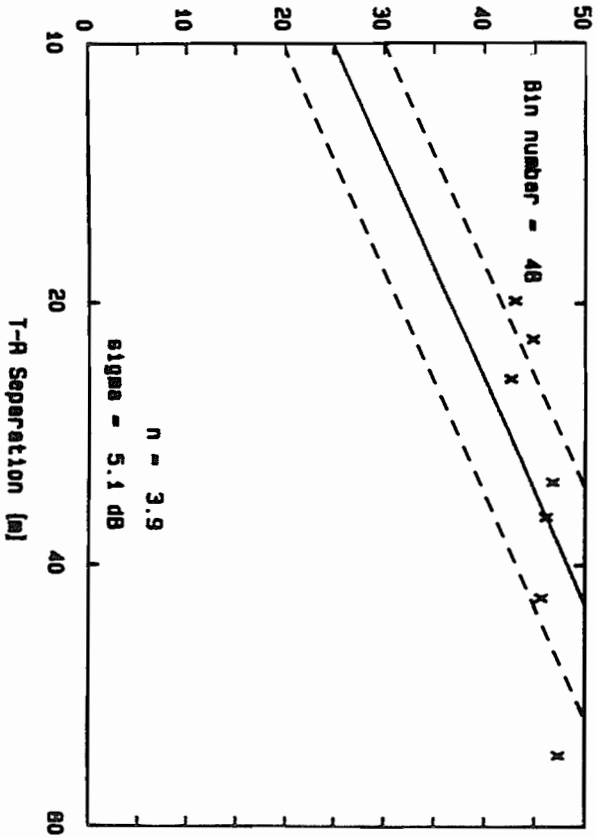
Attenuation [dB].



Attenuation [dB].

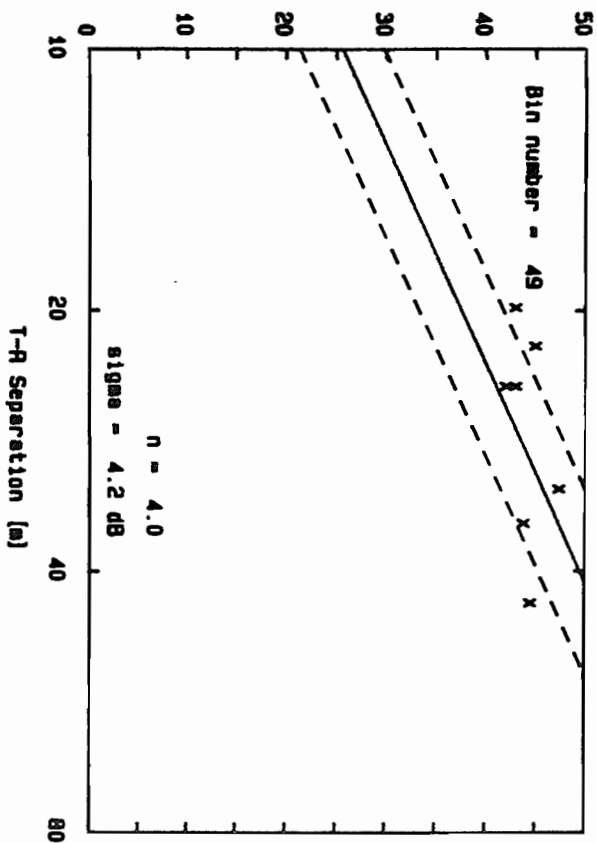


Attenuation [dB].

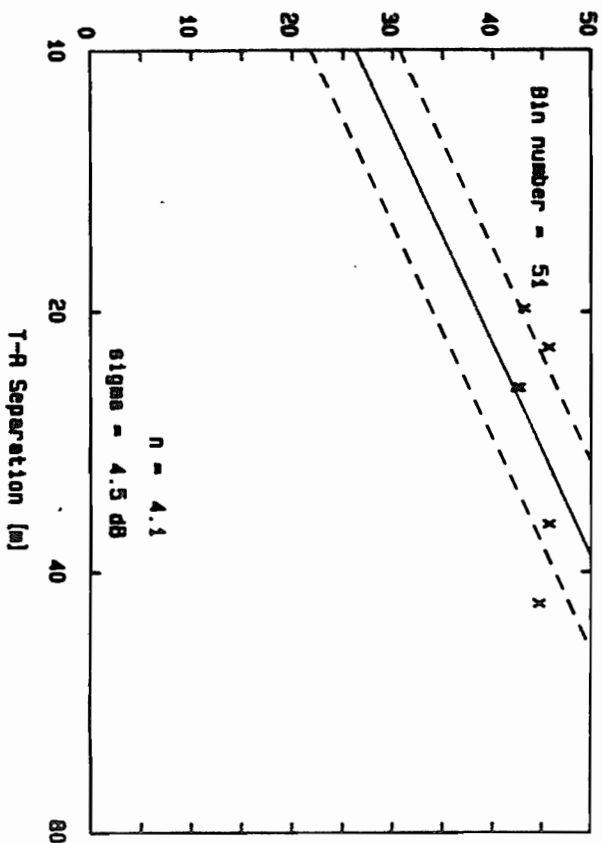


OBS

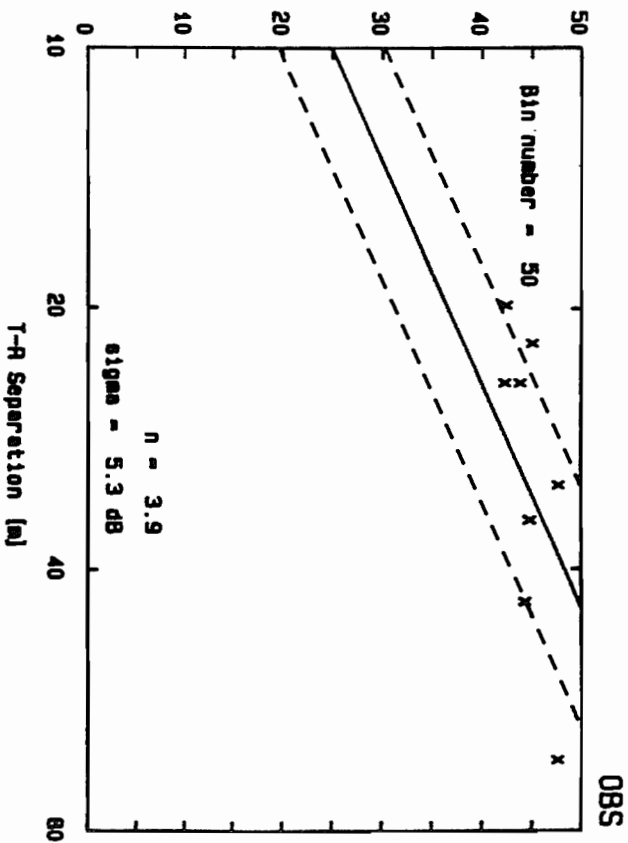
Attenuation [dB].



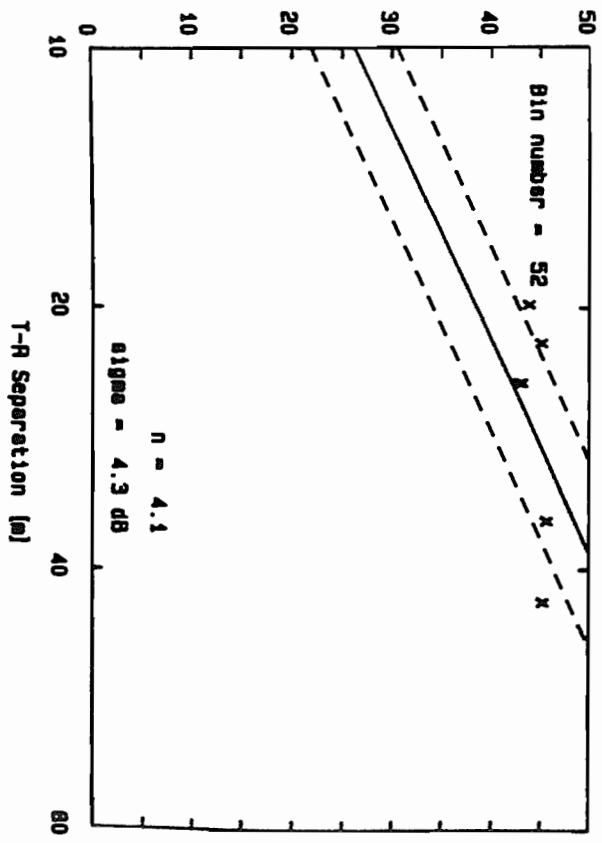
Attenuation [dB].



Attenuation [dB].

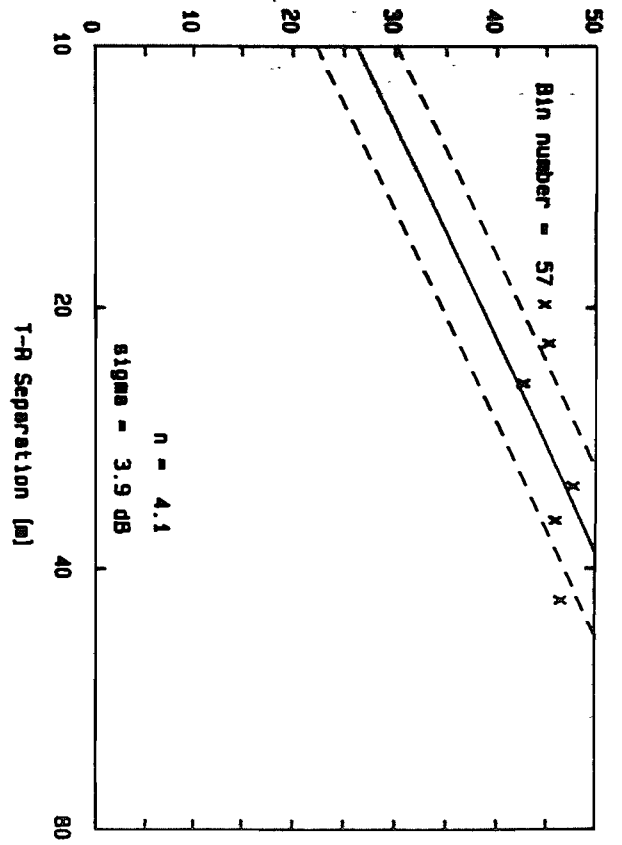


Attenuation [dB].

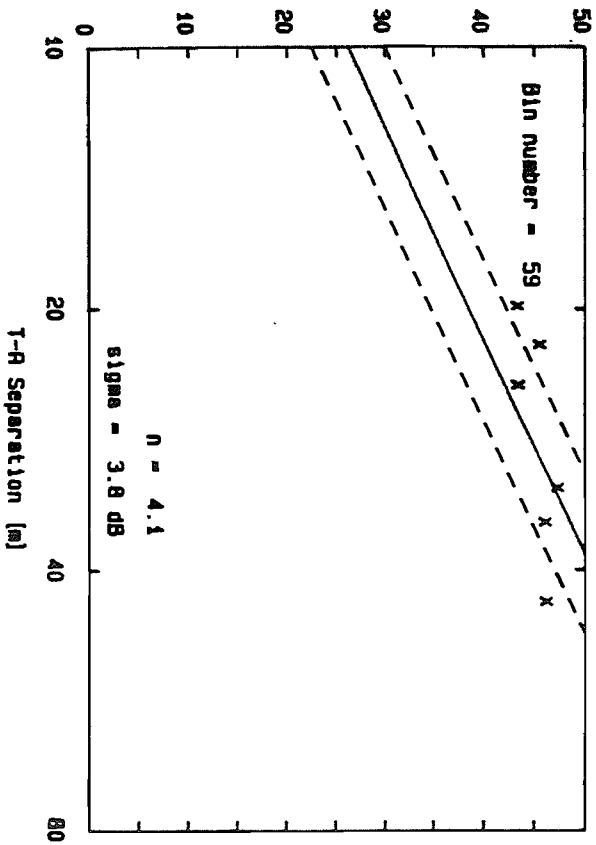




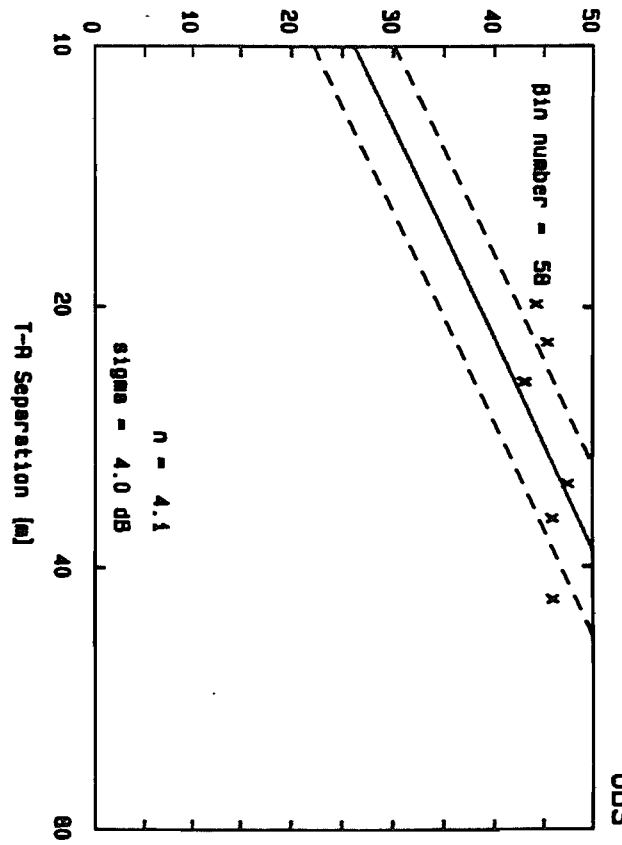
Attenuation [dB].



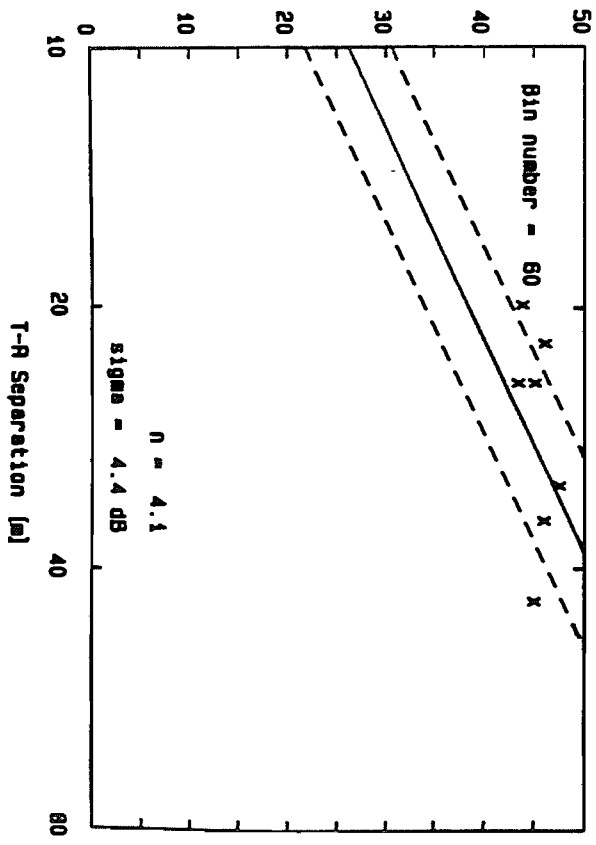
Attenuation [dB].



Attenuation [dB].

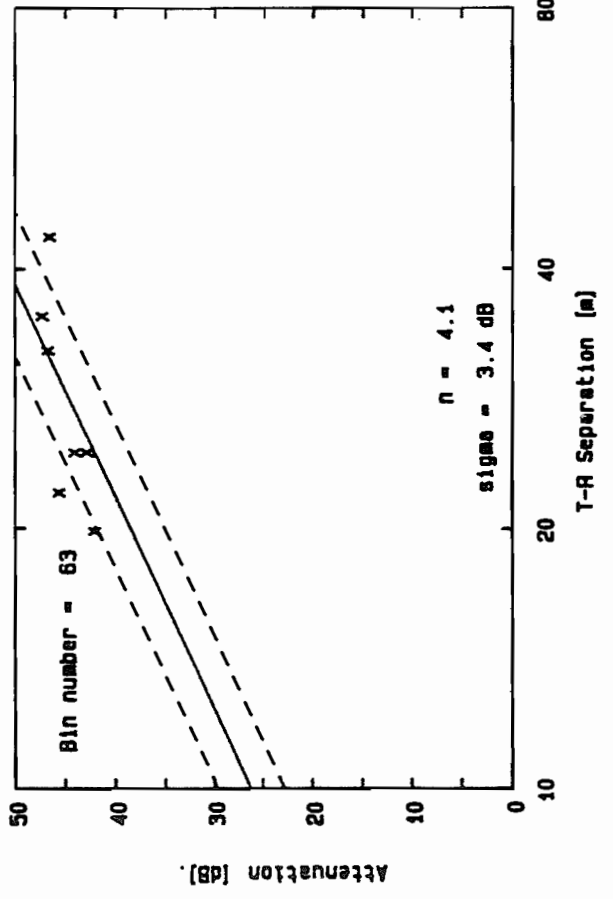
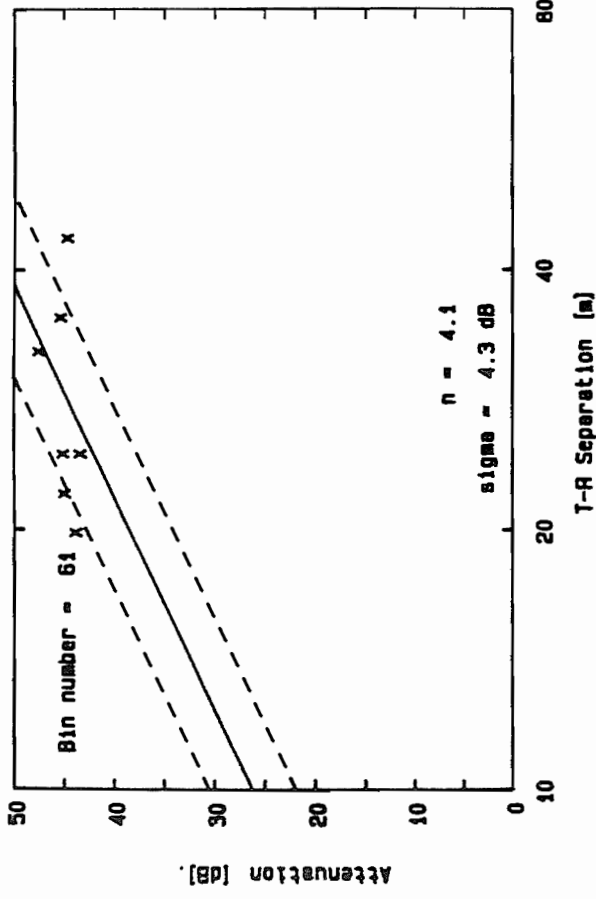
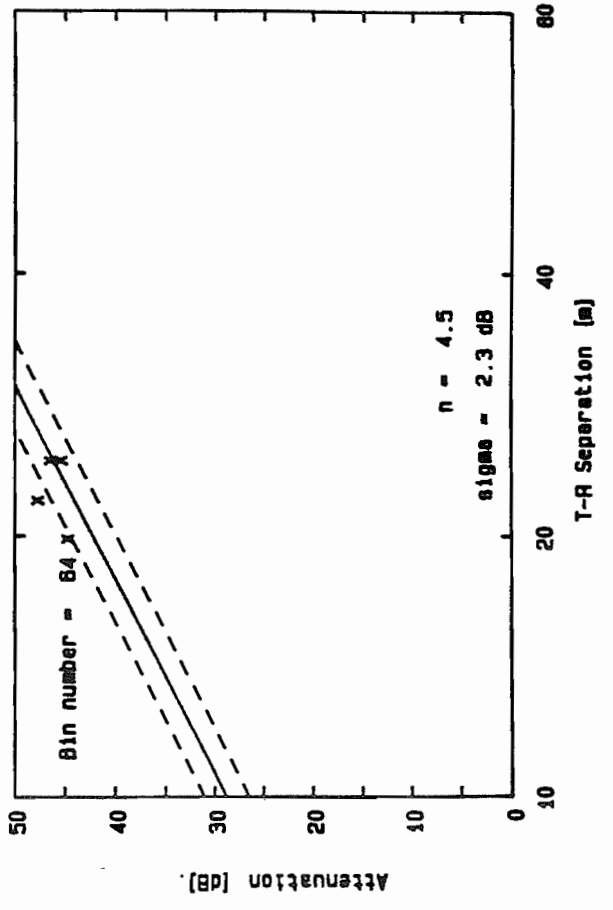
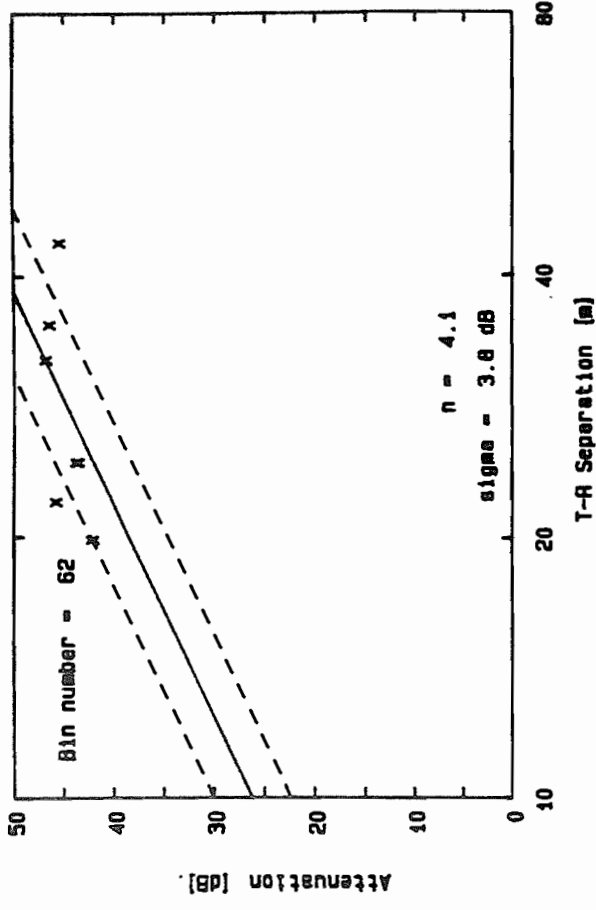


Attenuation [dB].



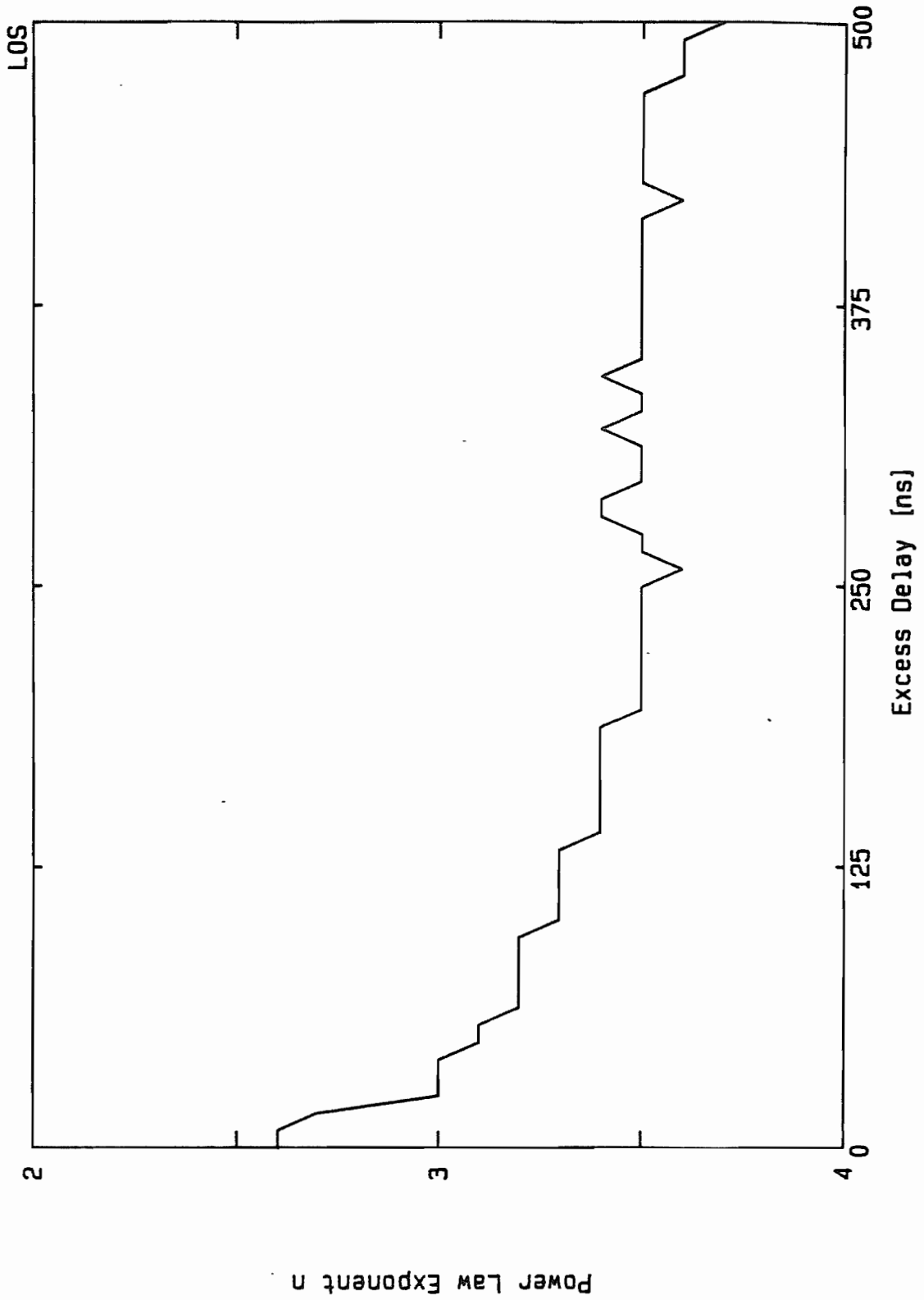
OBS

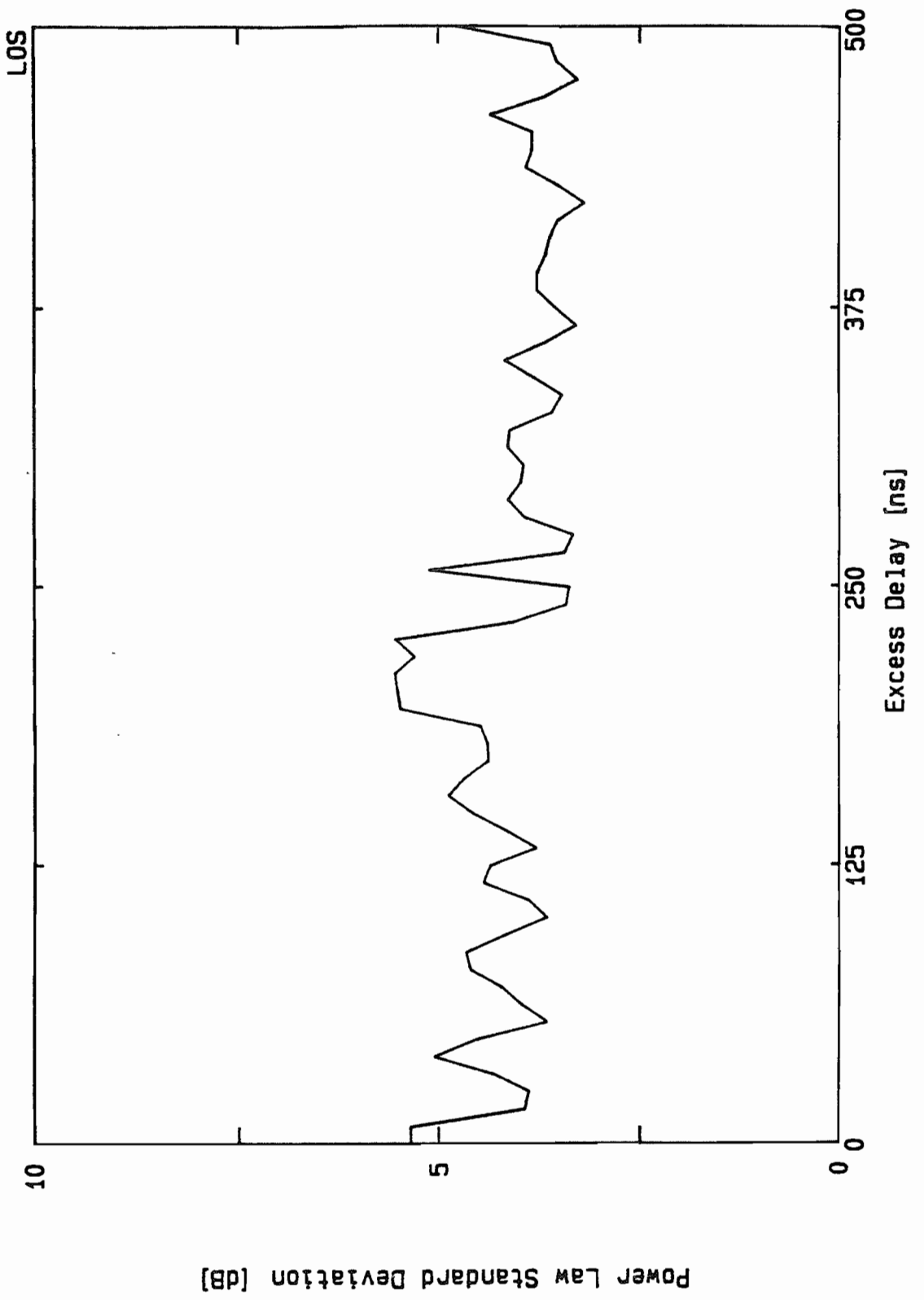
OBS

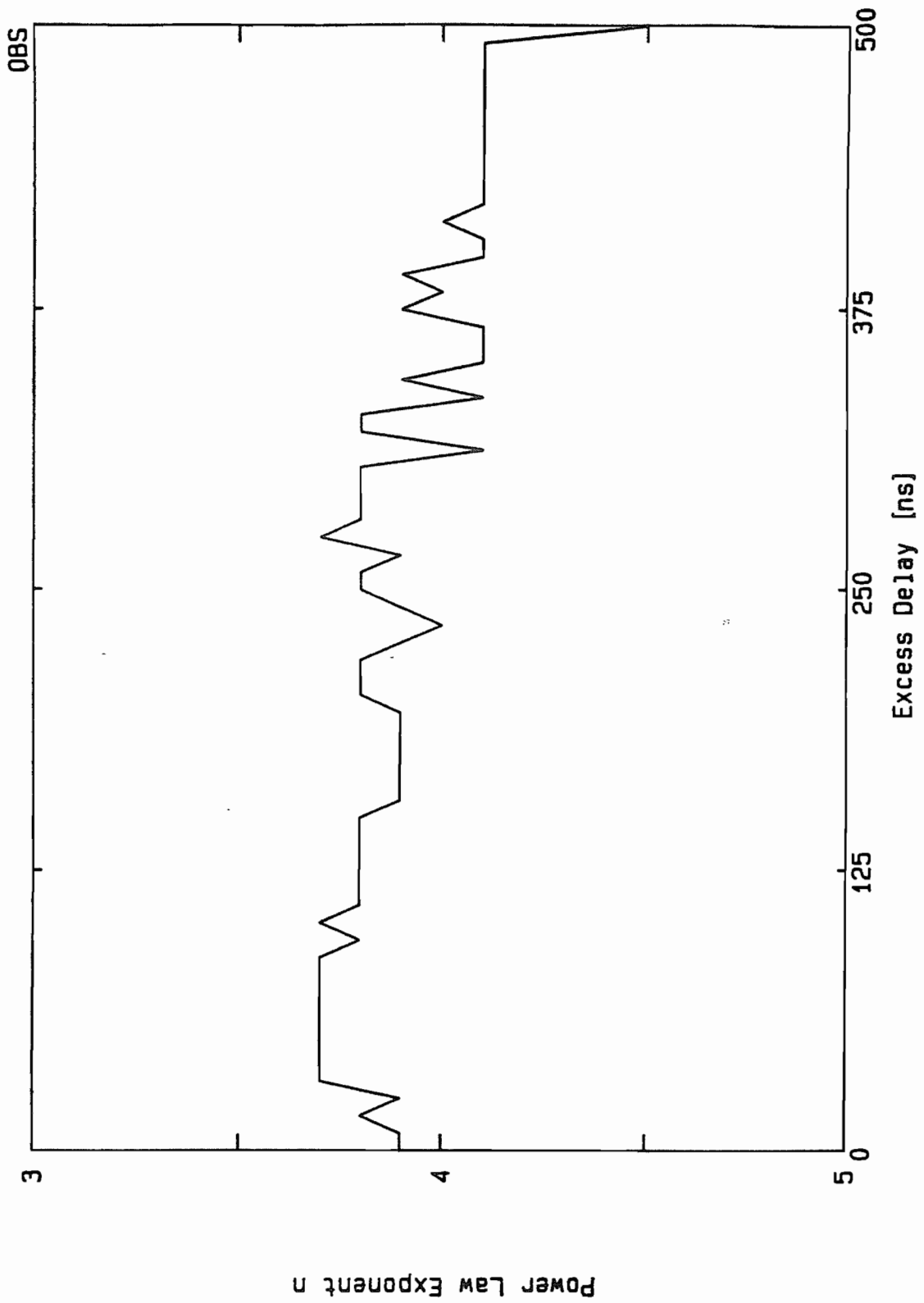


## Appendix C. Power Law Exponent and Standard Deviation

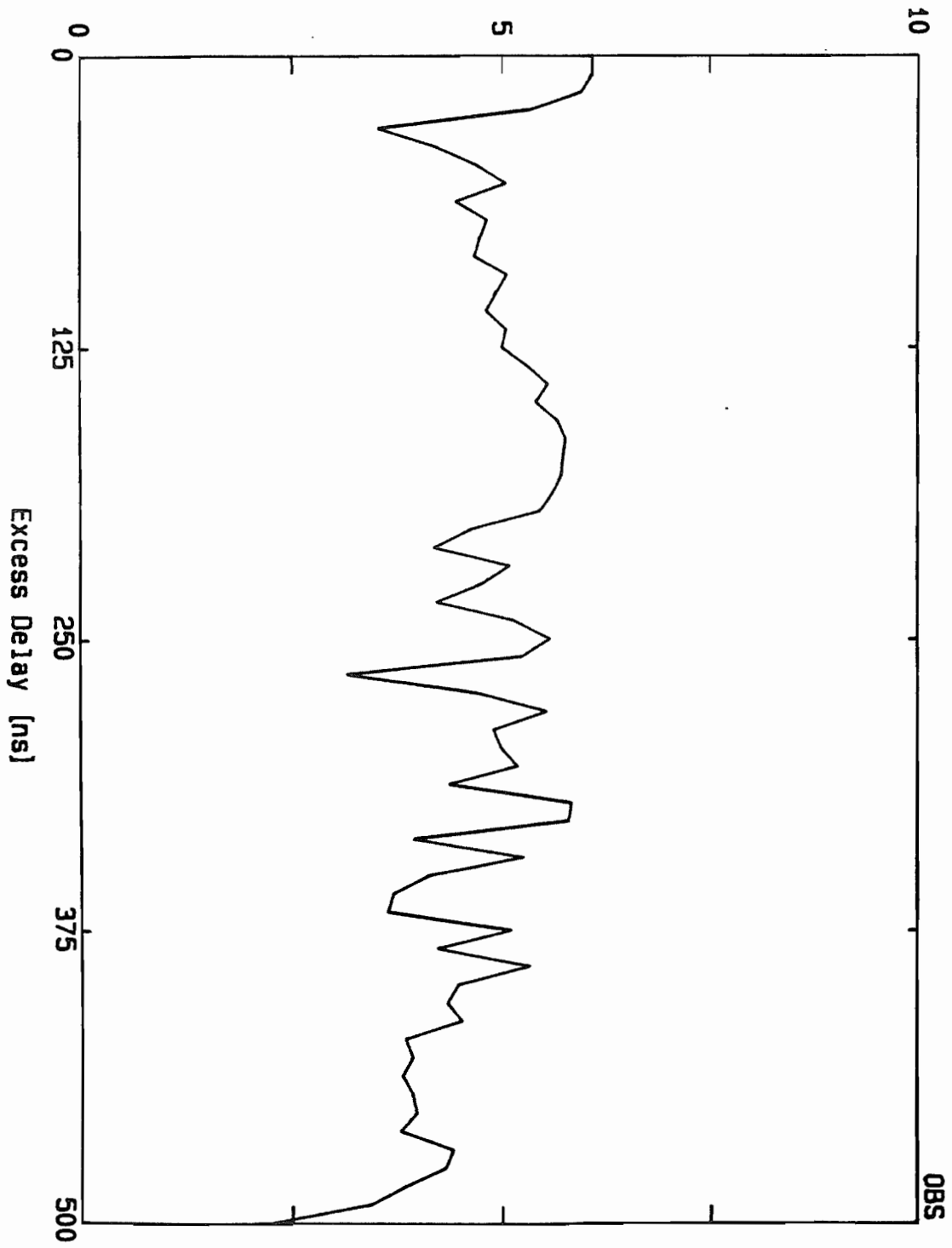




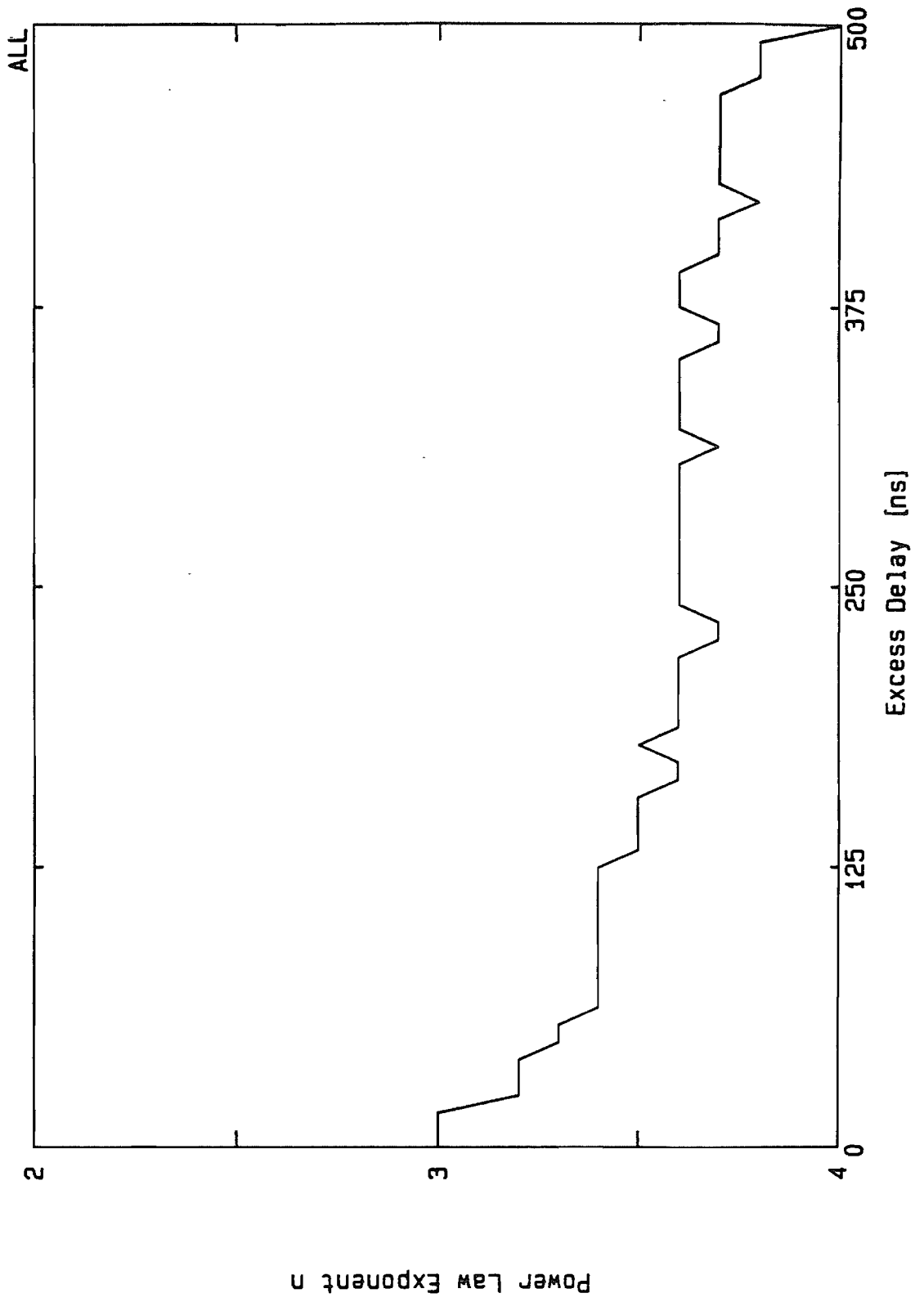




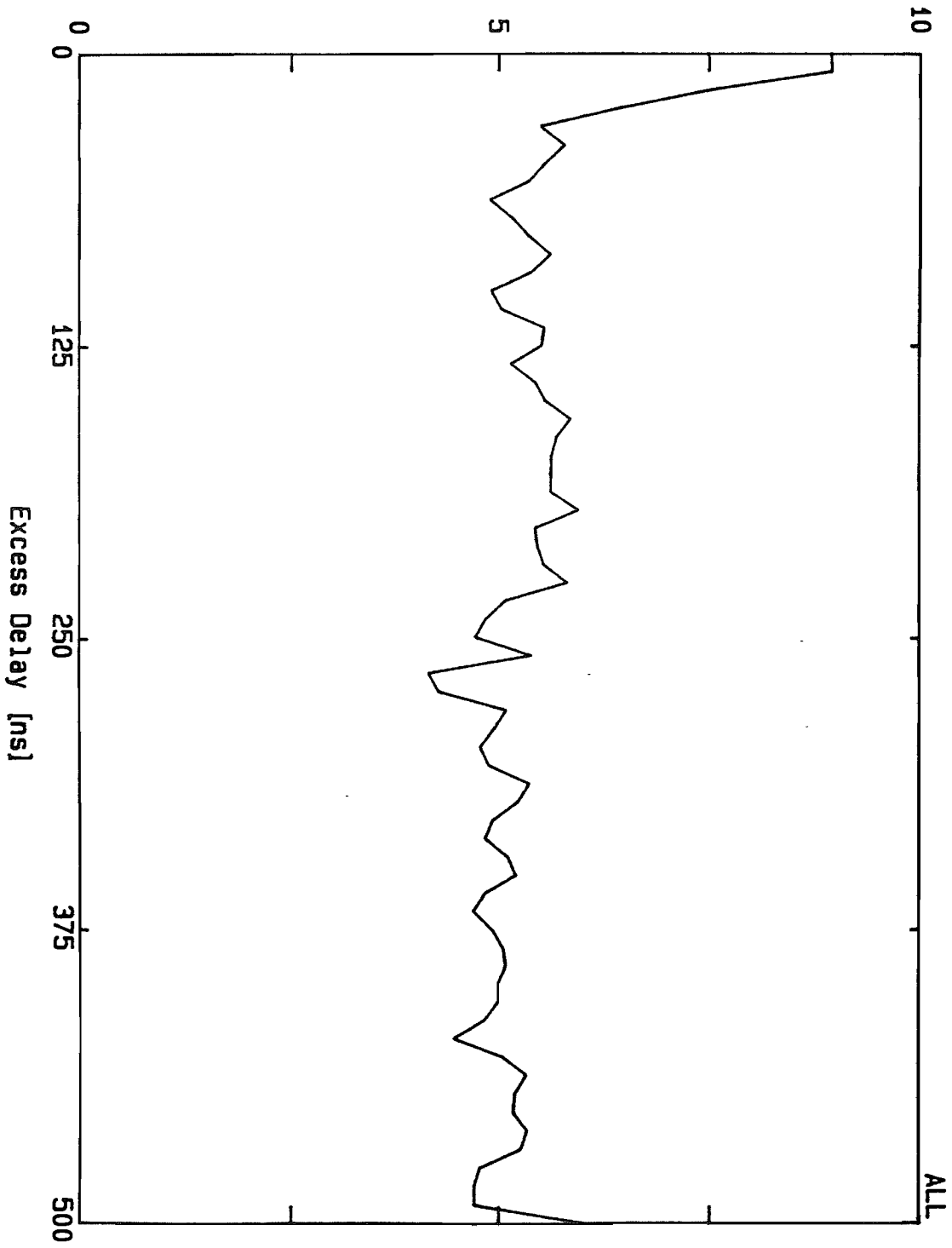
Power Law Standard Deviation [dB]



OBS



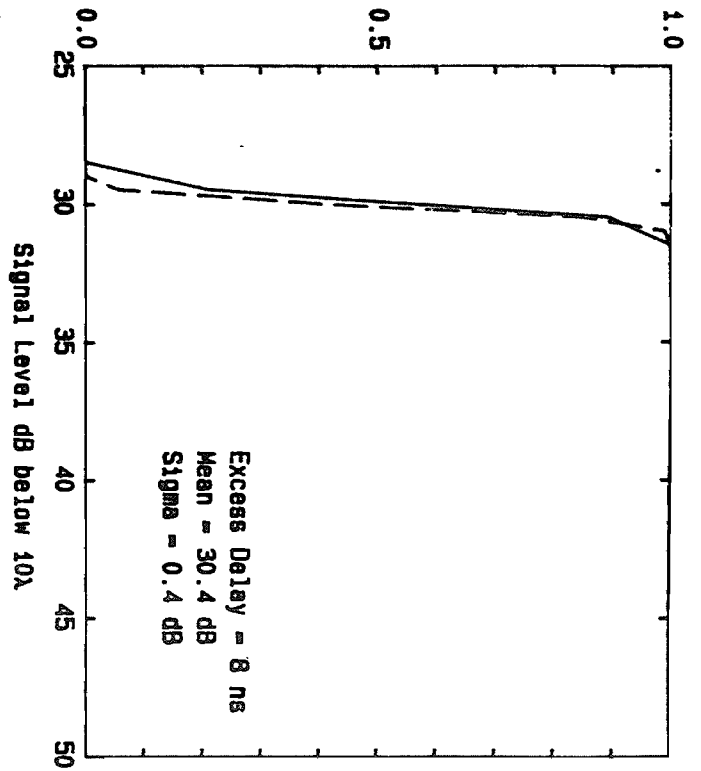
Power Law Standard Deviation [dB]



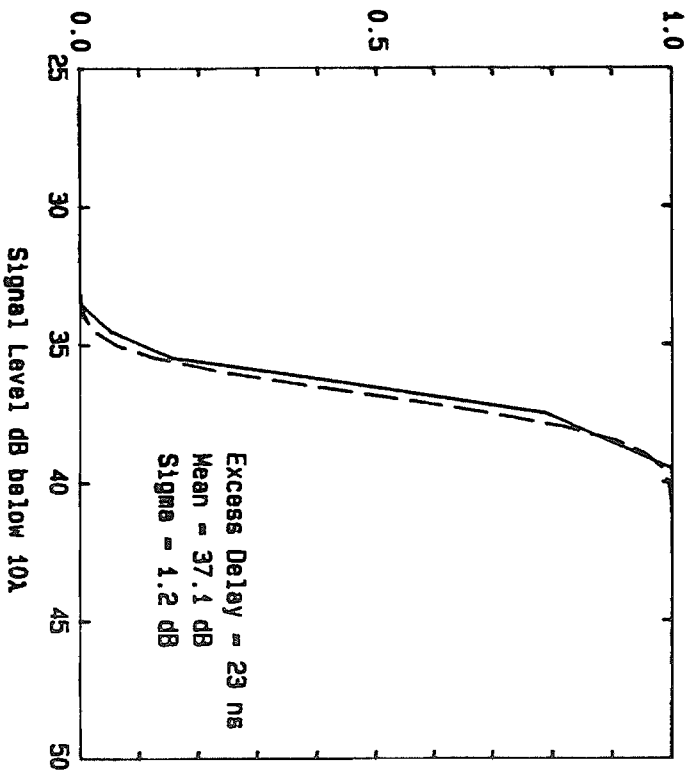
ALL

**Appendix D. CDF of Received Power over Local Areas**

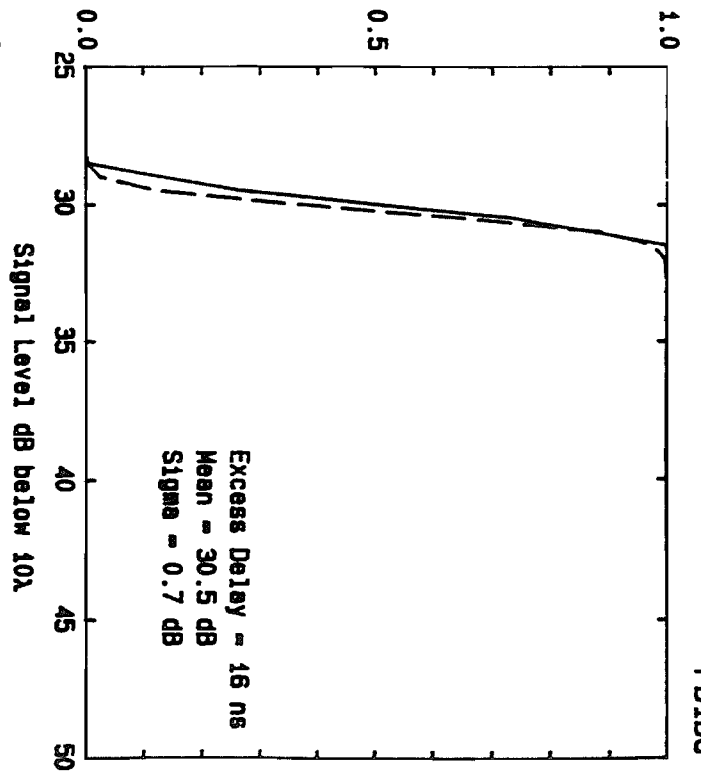
Probability of Signal Level > Abscissa



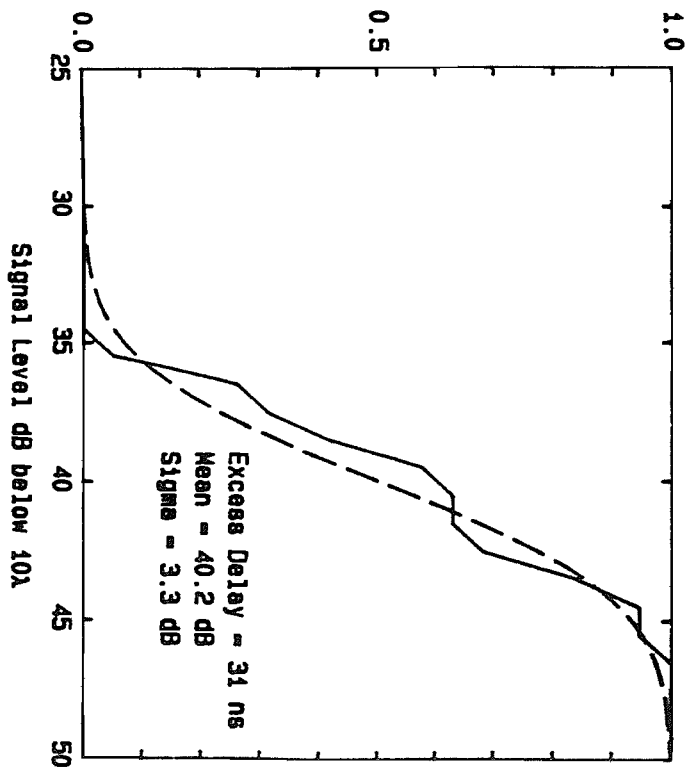
Probability of Signal Level > Abscissa



Probability of Signal Level > Abscissa

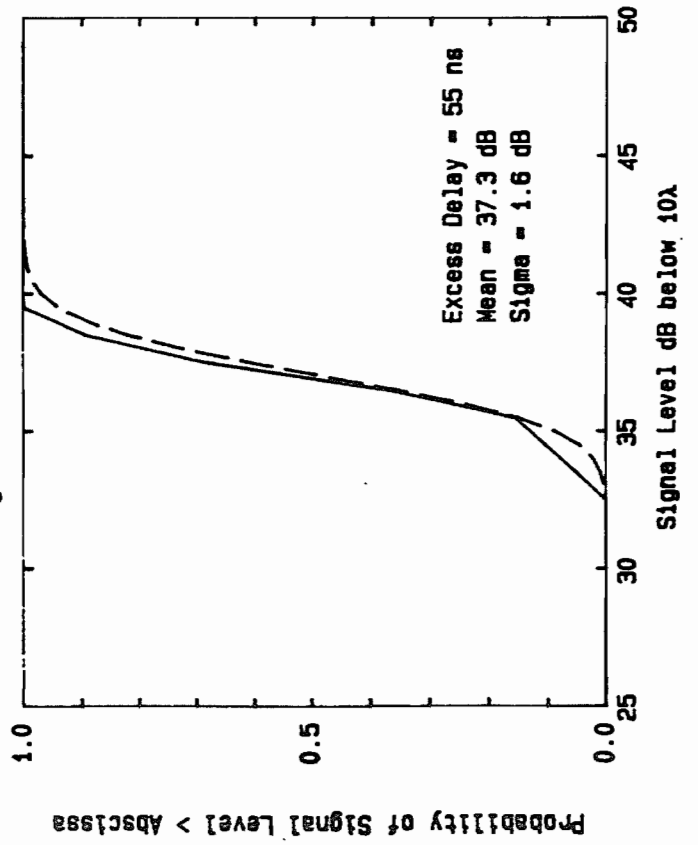
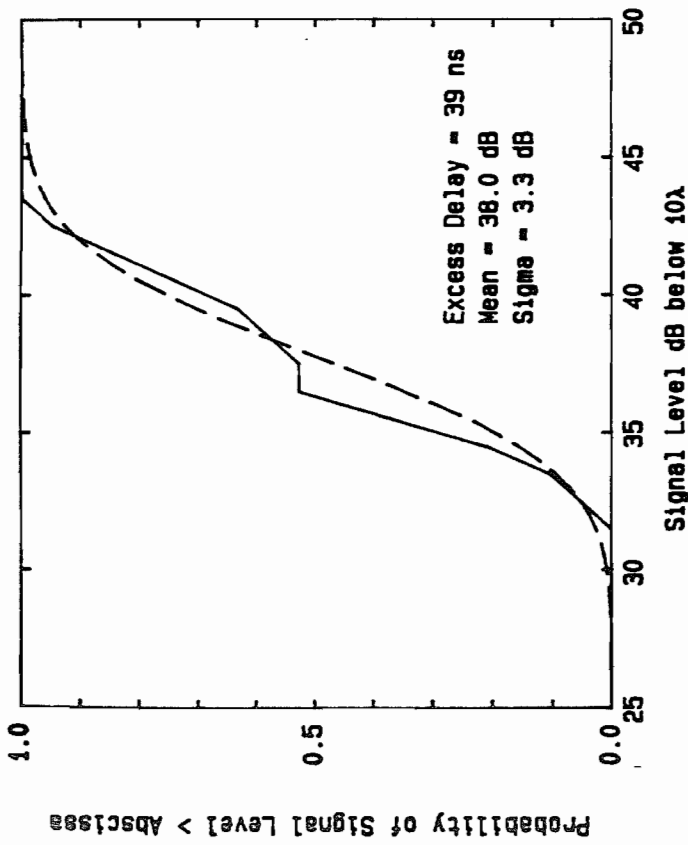
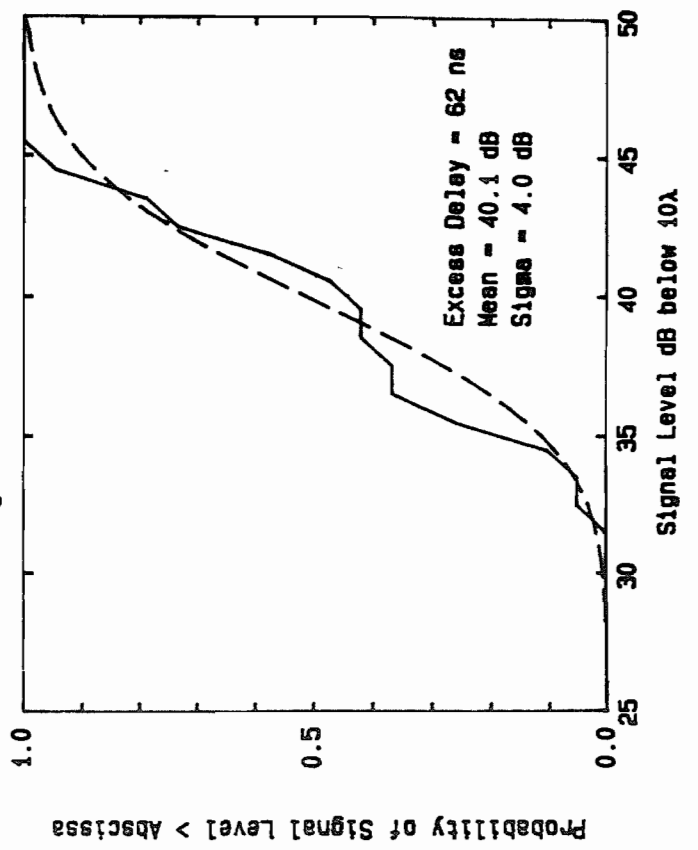
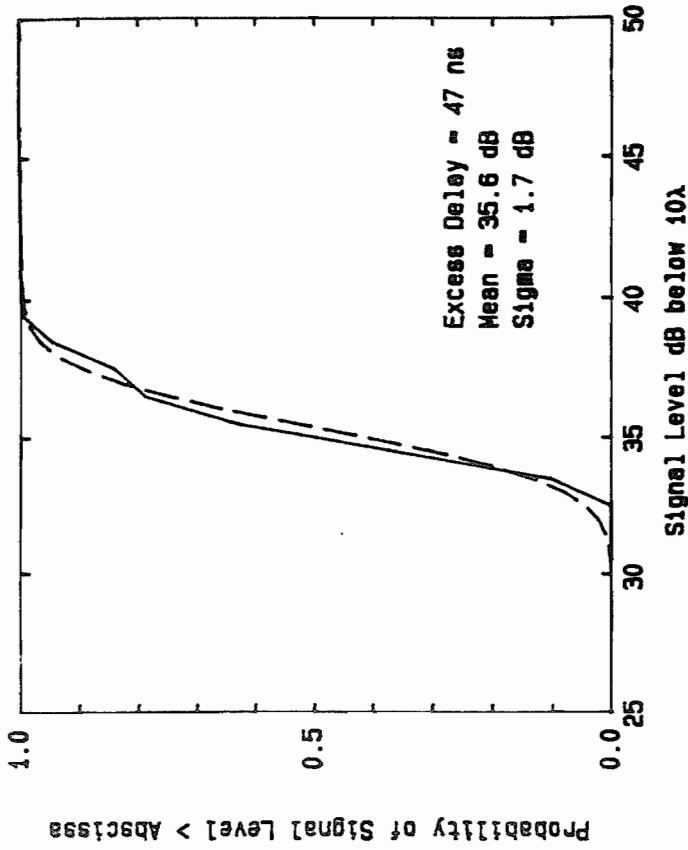


Probability of Signal Level > Abscissa

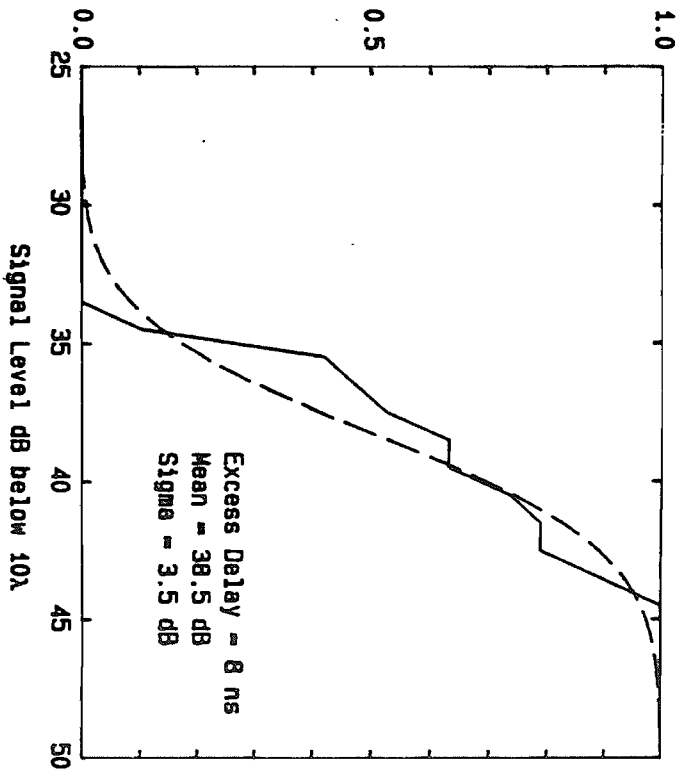




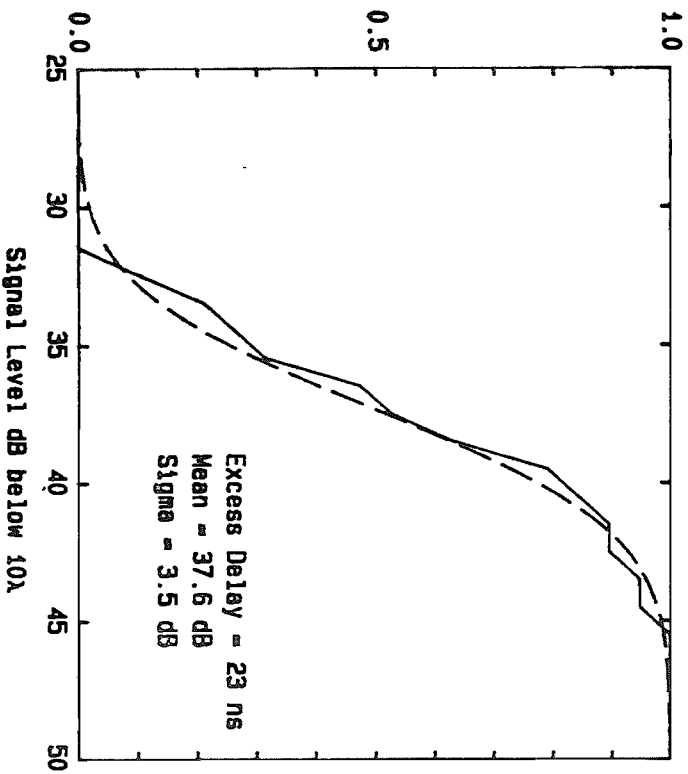
PB1BC



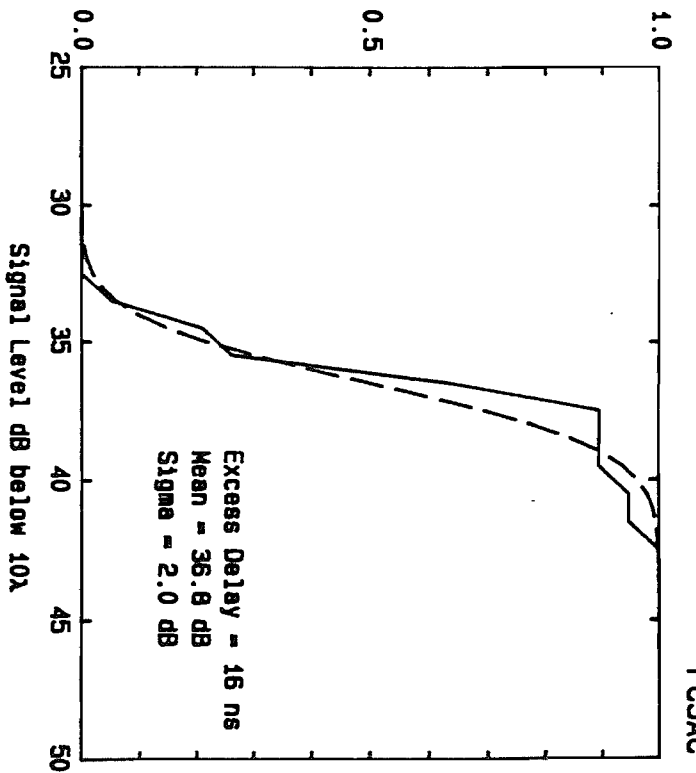
Probability of Signal Level > Abscissa



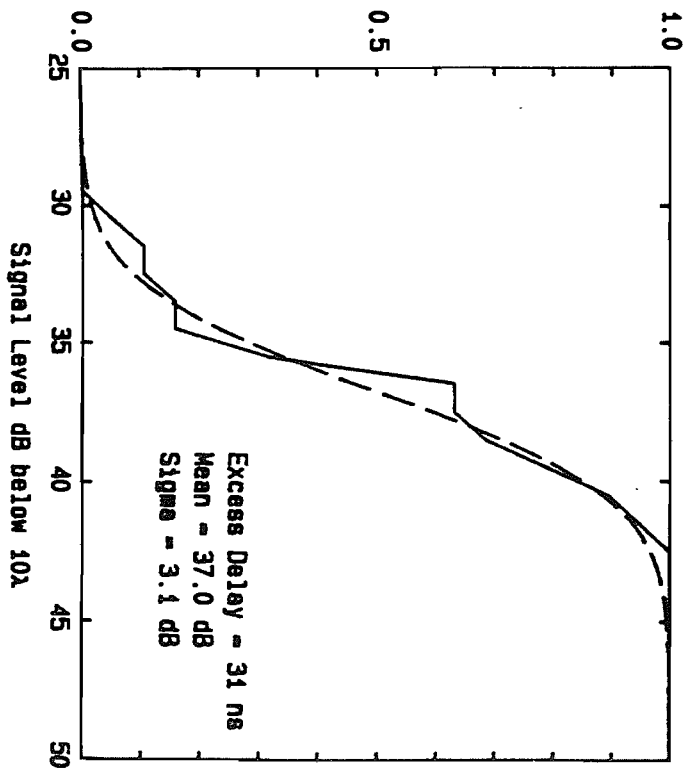
Probability of Signal Level > Abscissa



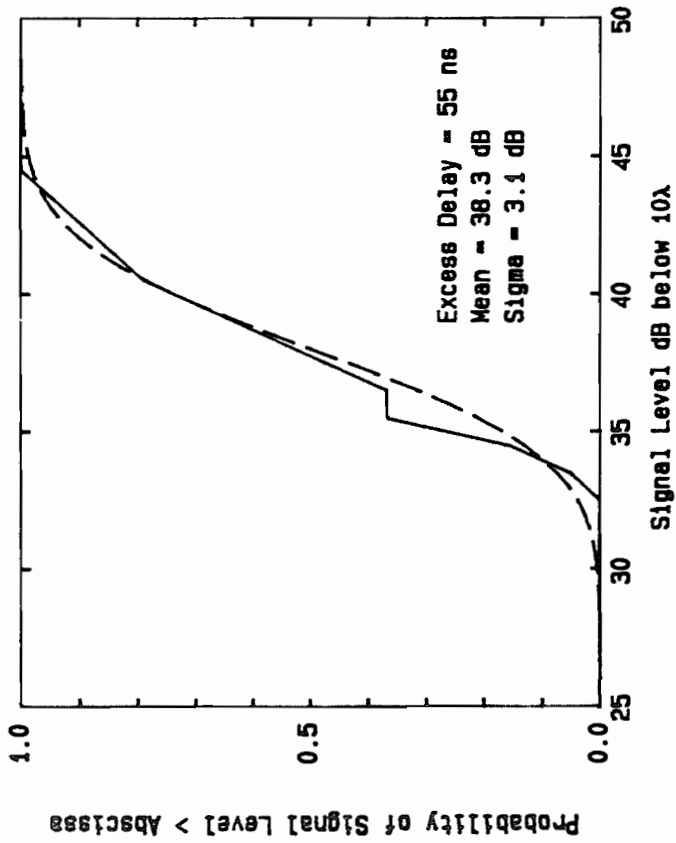
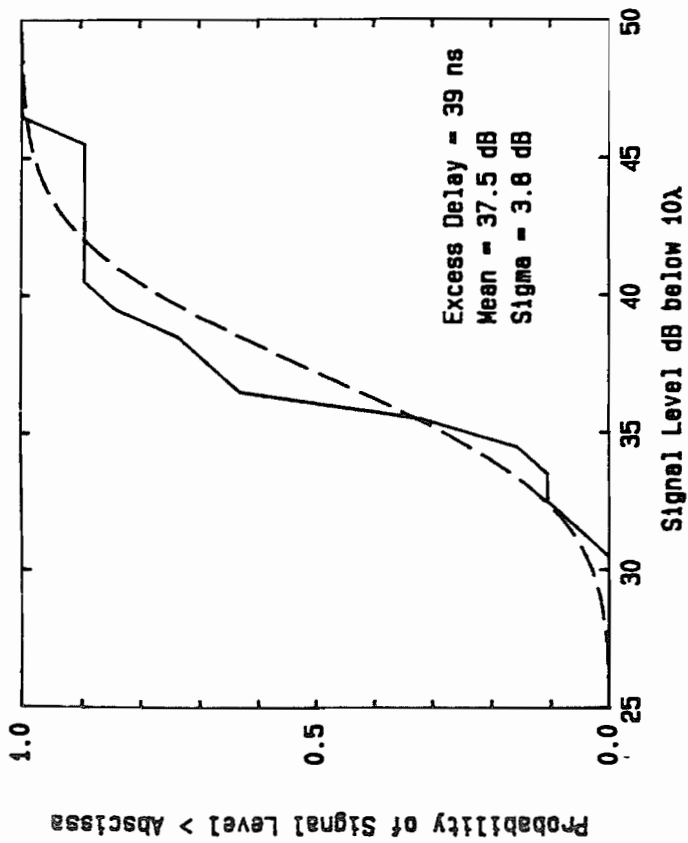
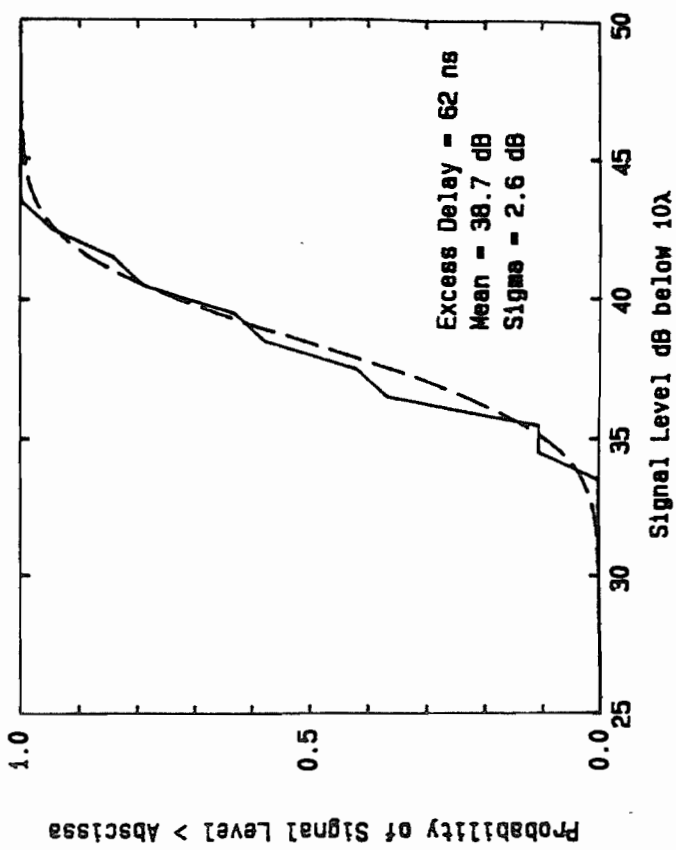
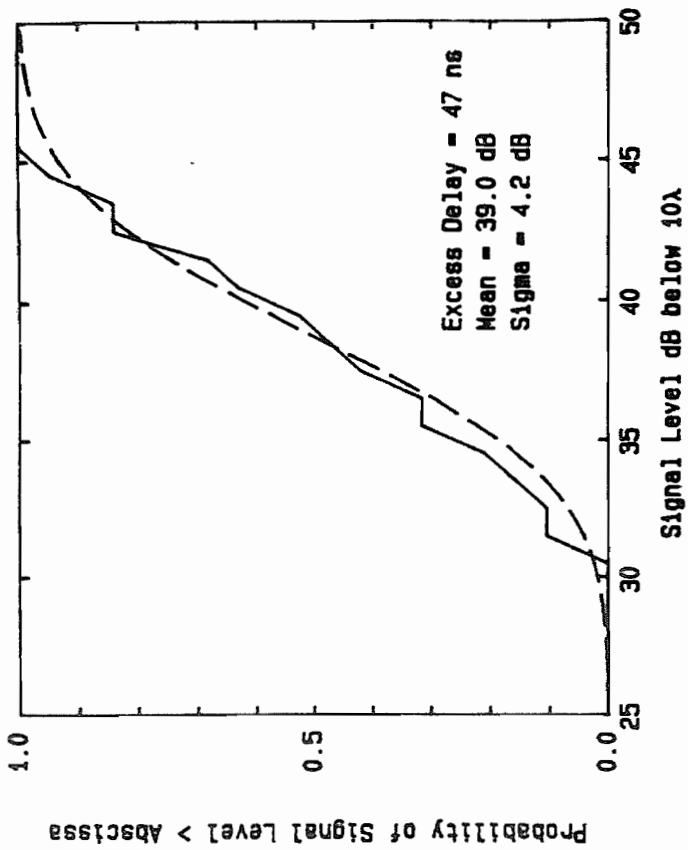
Probability of Signal Level > Abscissa



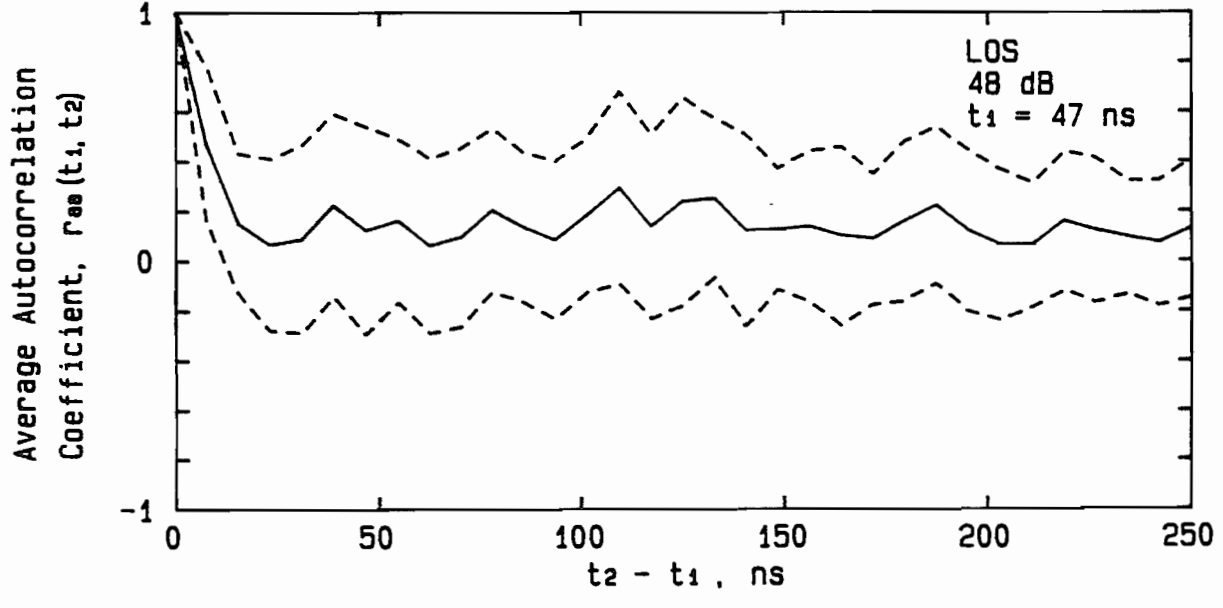
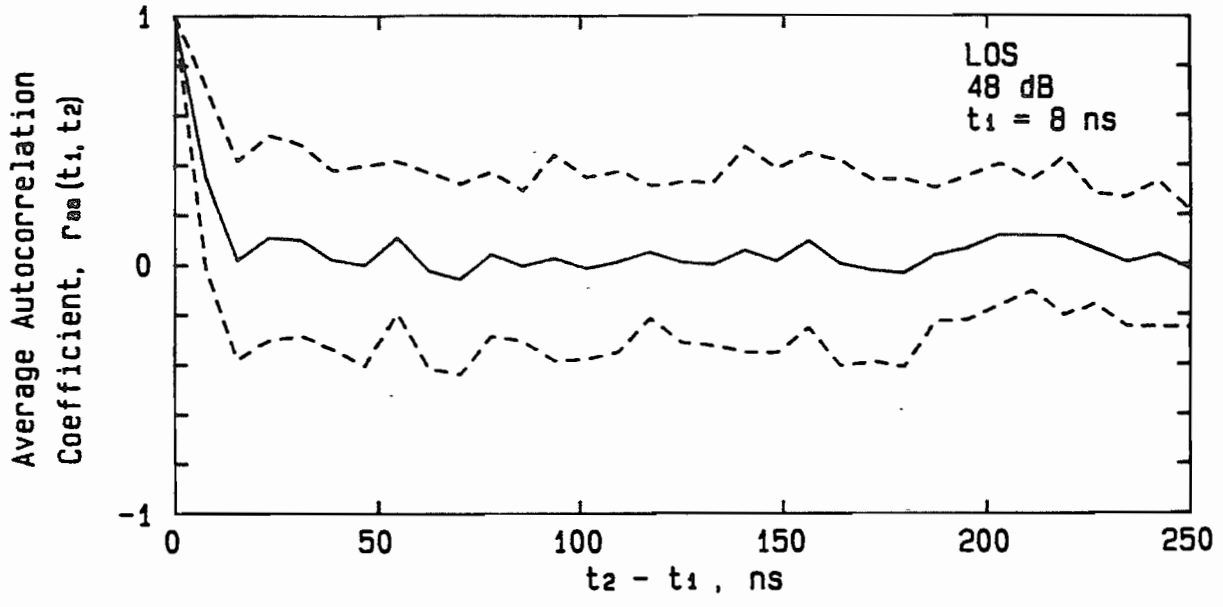
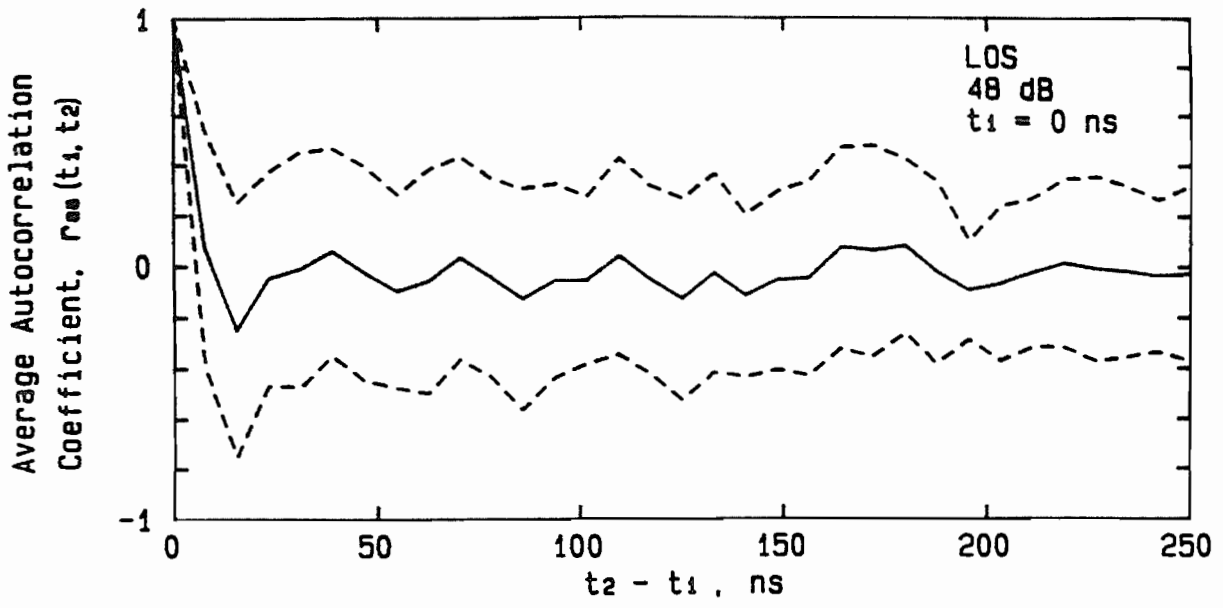
Probability of Signal Level > Abscissa

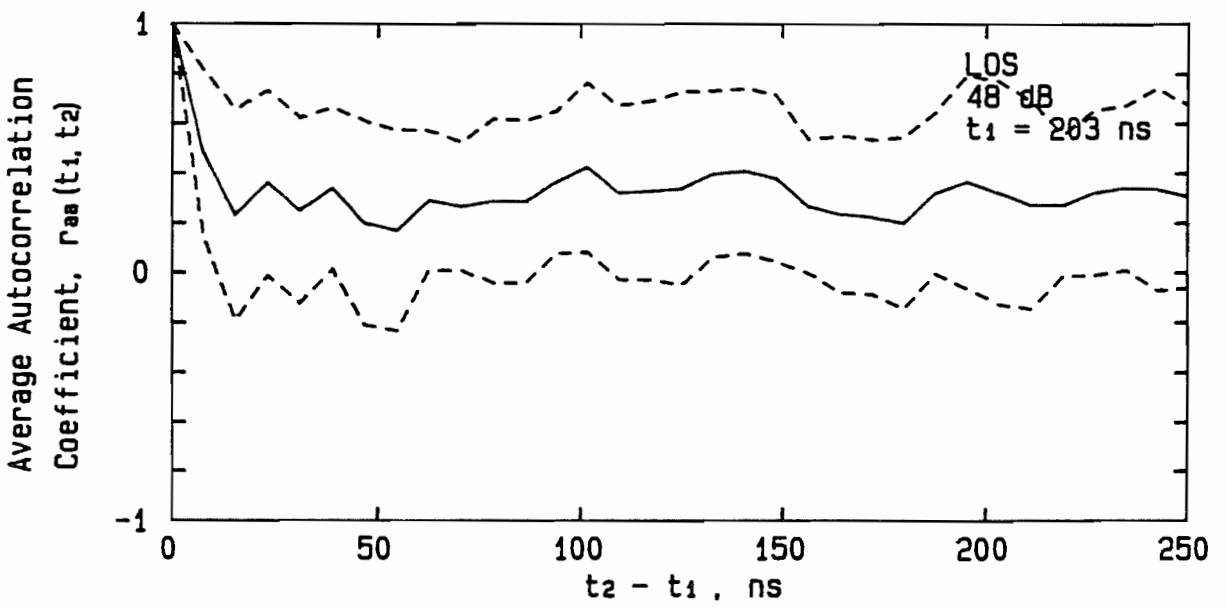
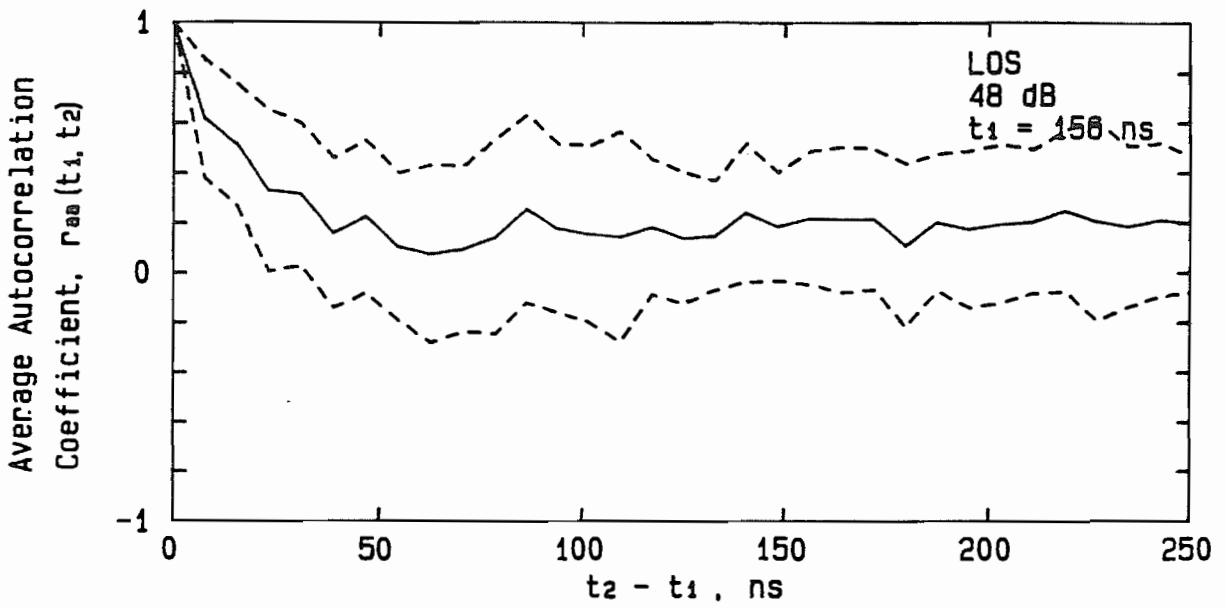
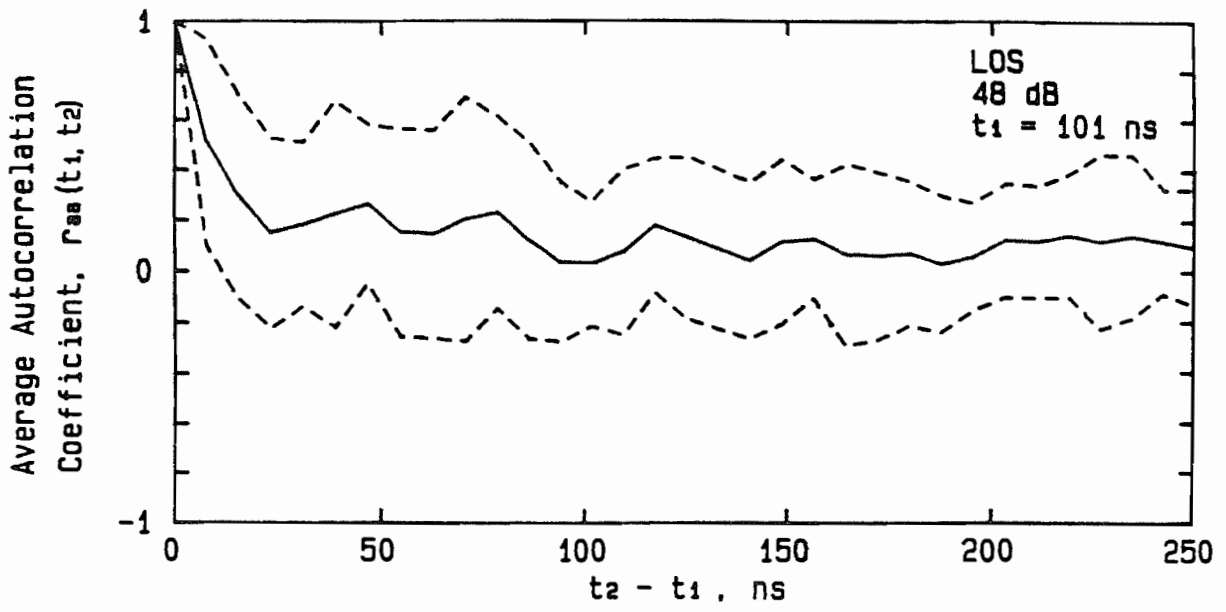


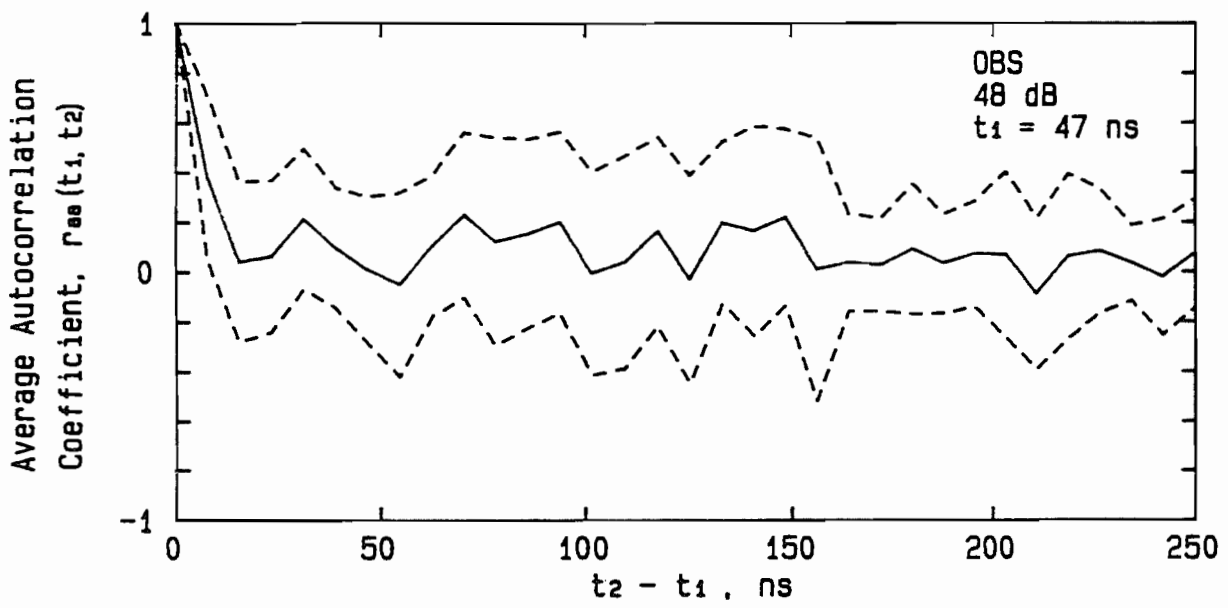
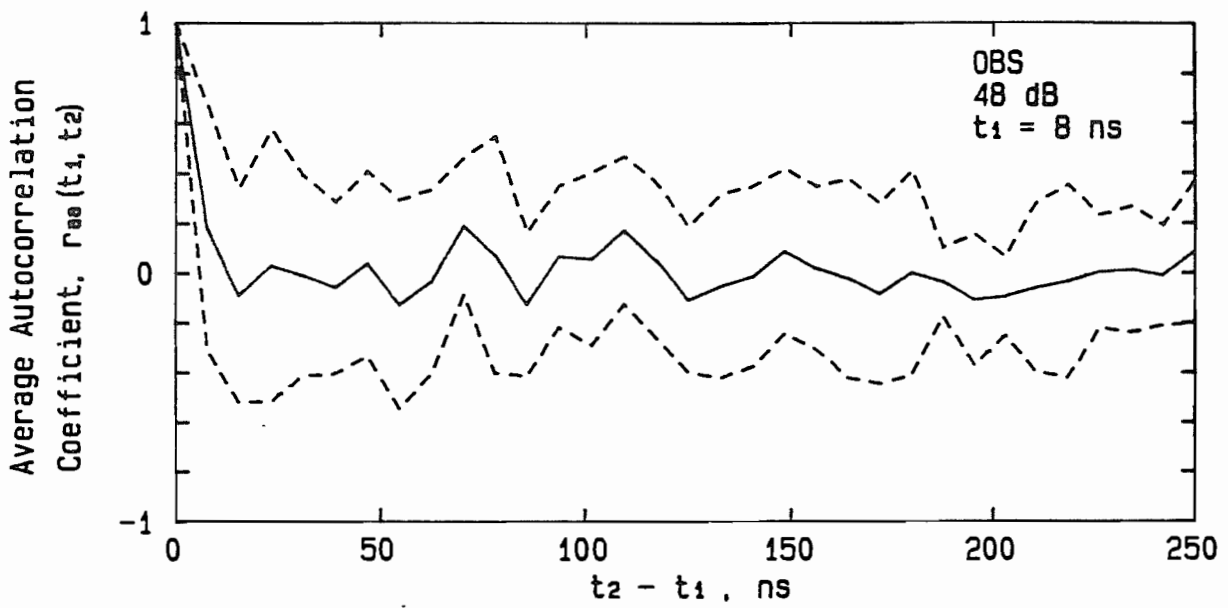
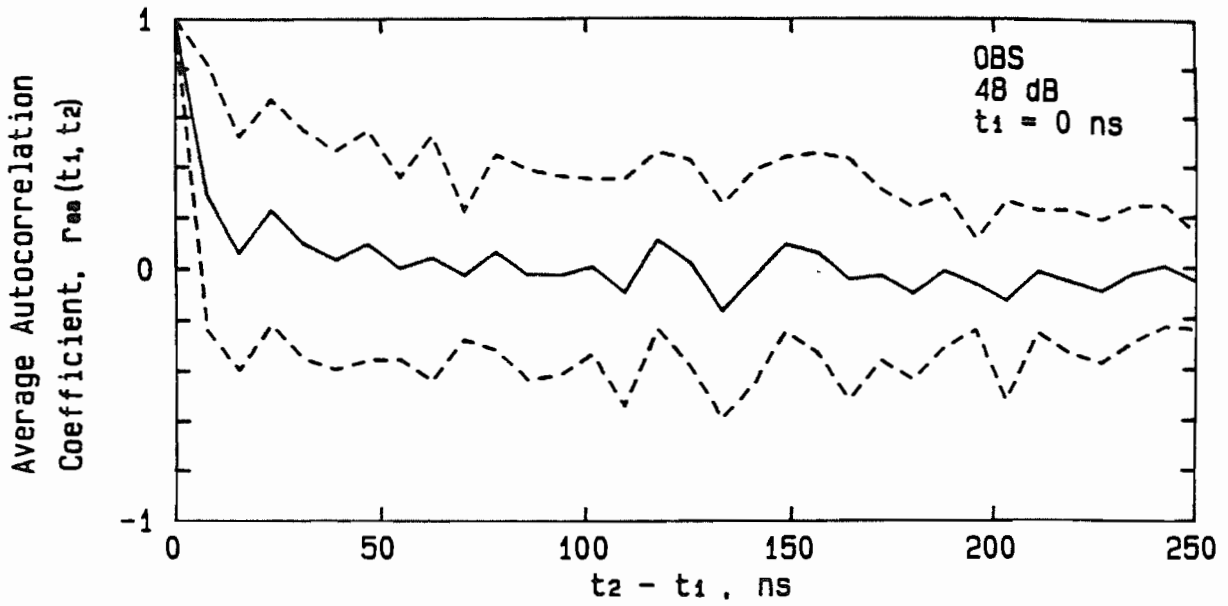
PC5AC

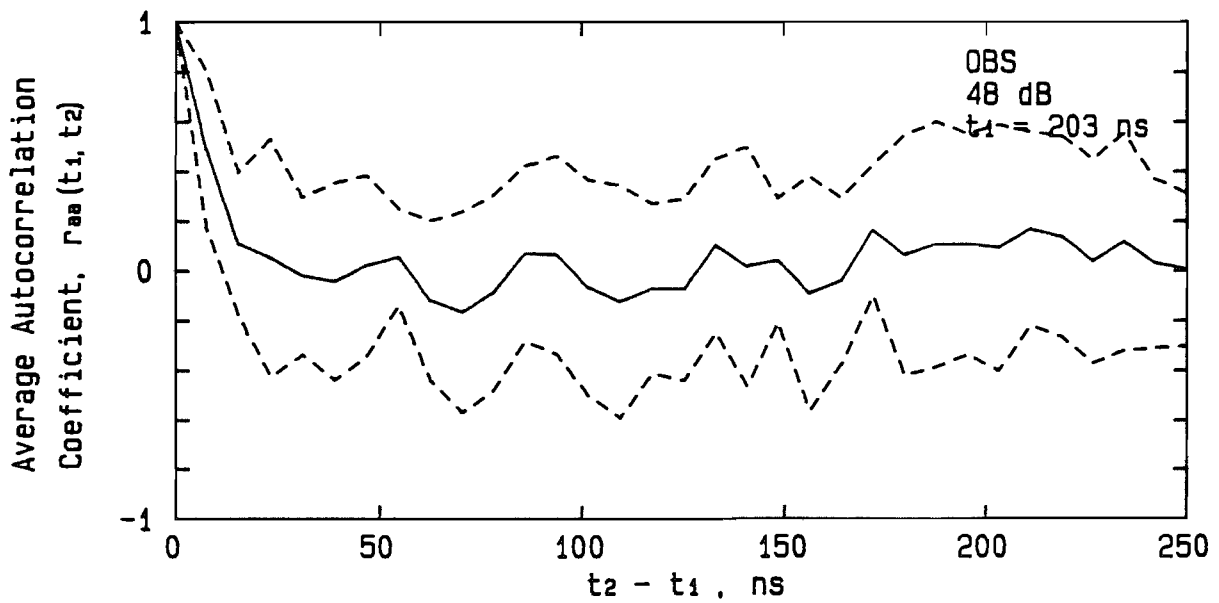
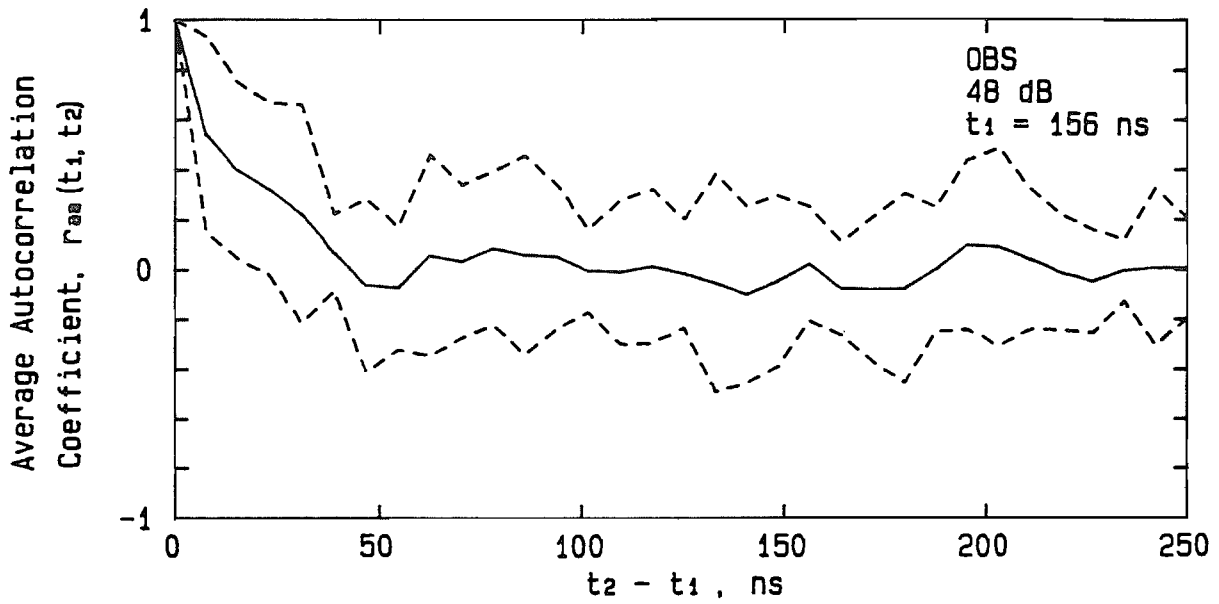
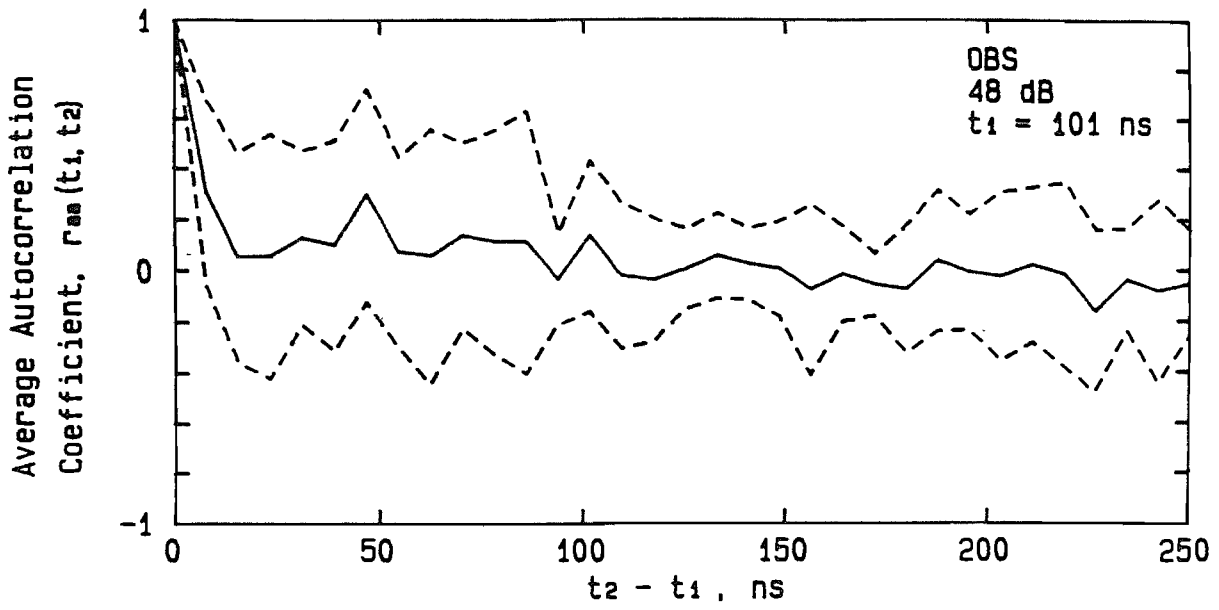


## Appendix E. Temporal Autocorrelation Coefficient Functions

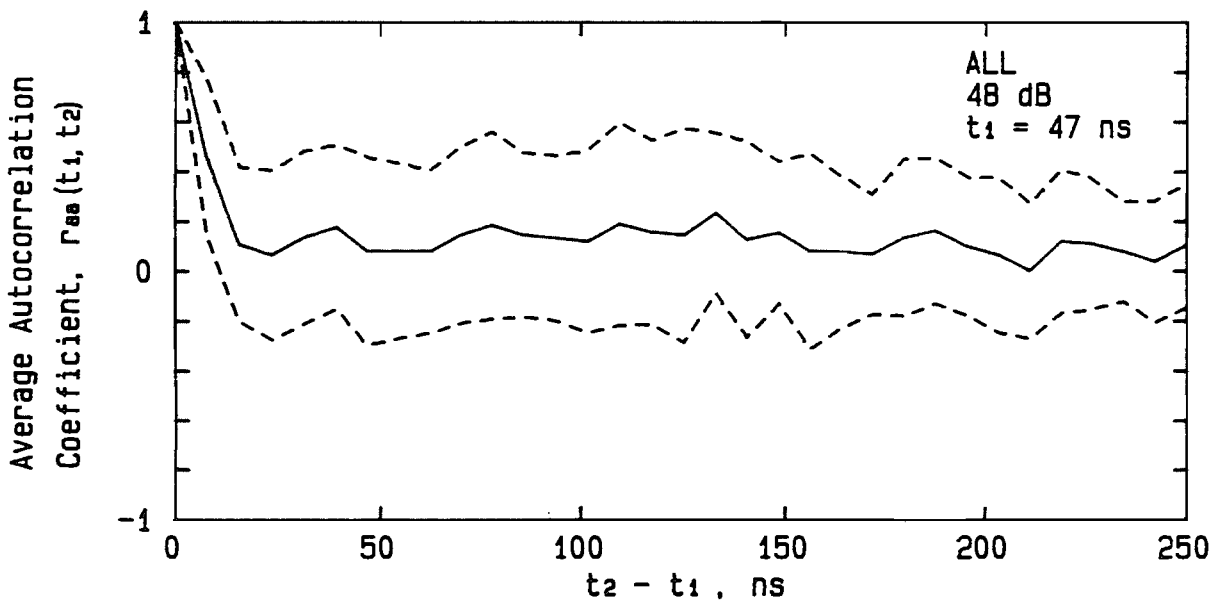
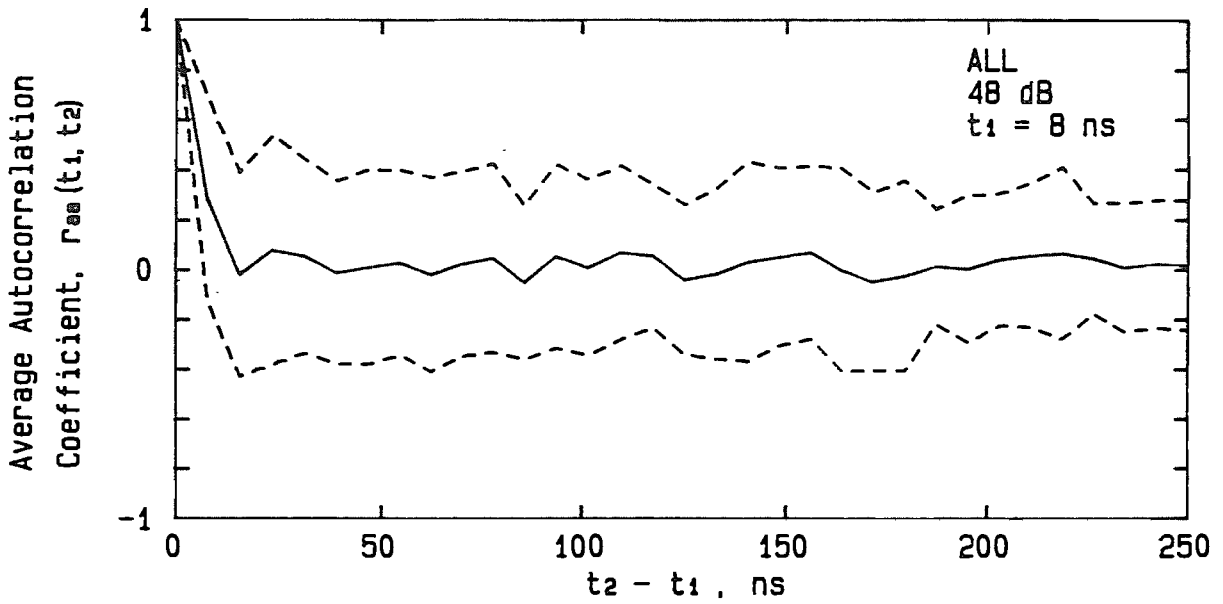
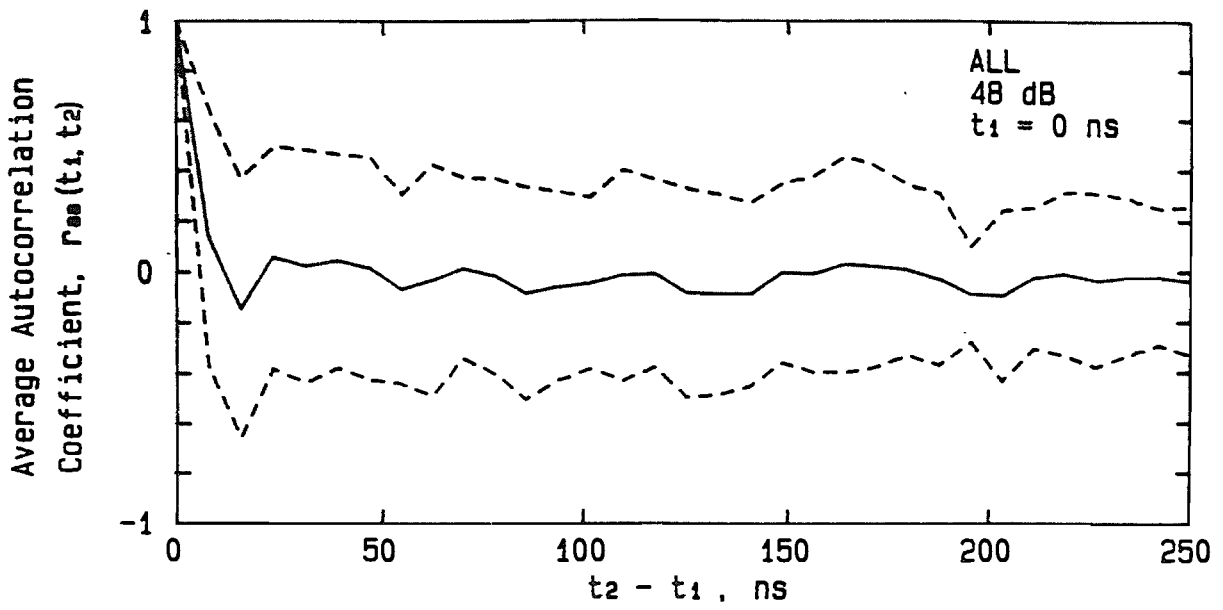


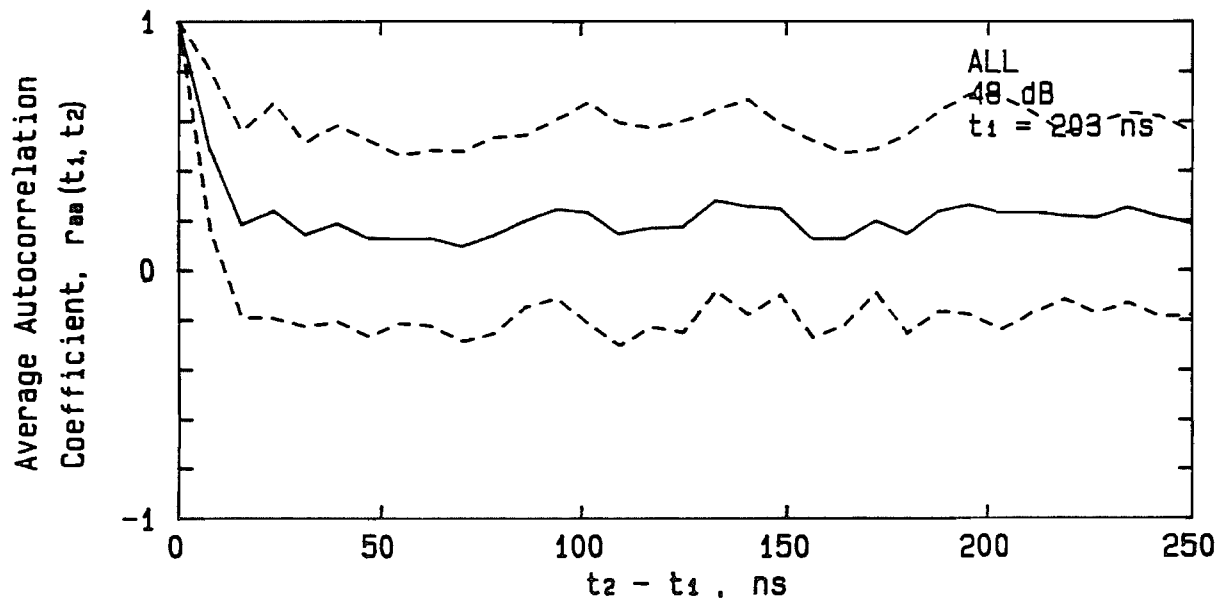
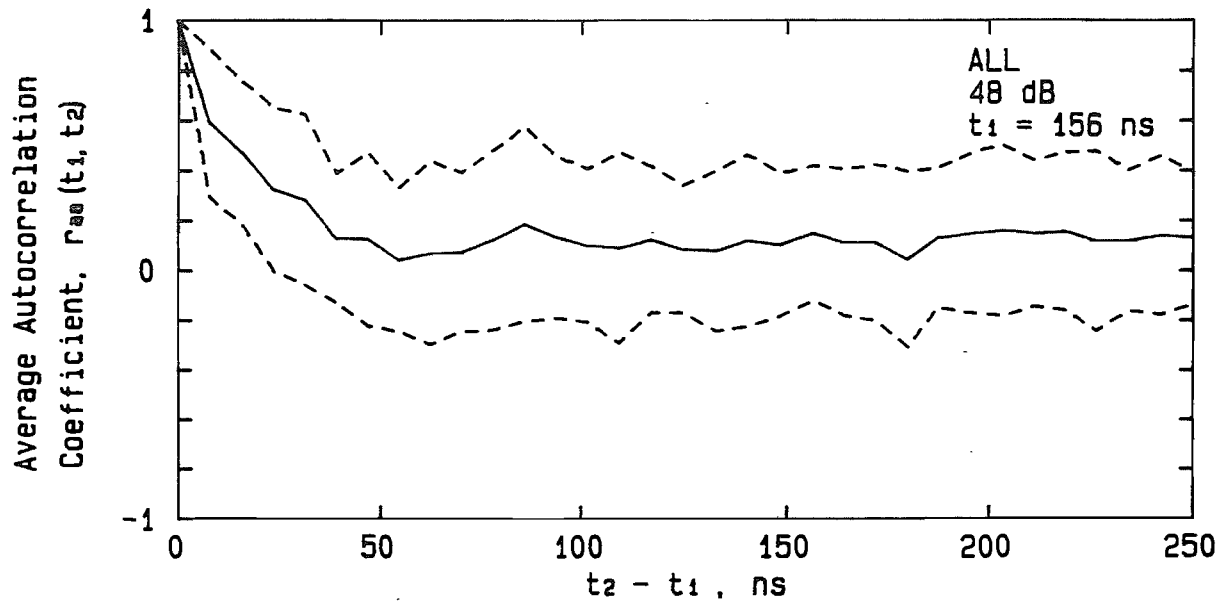
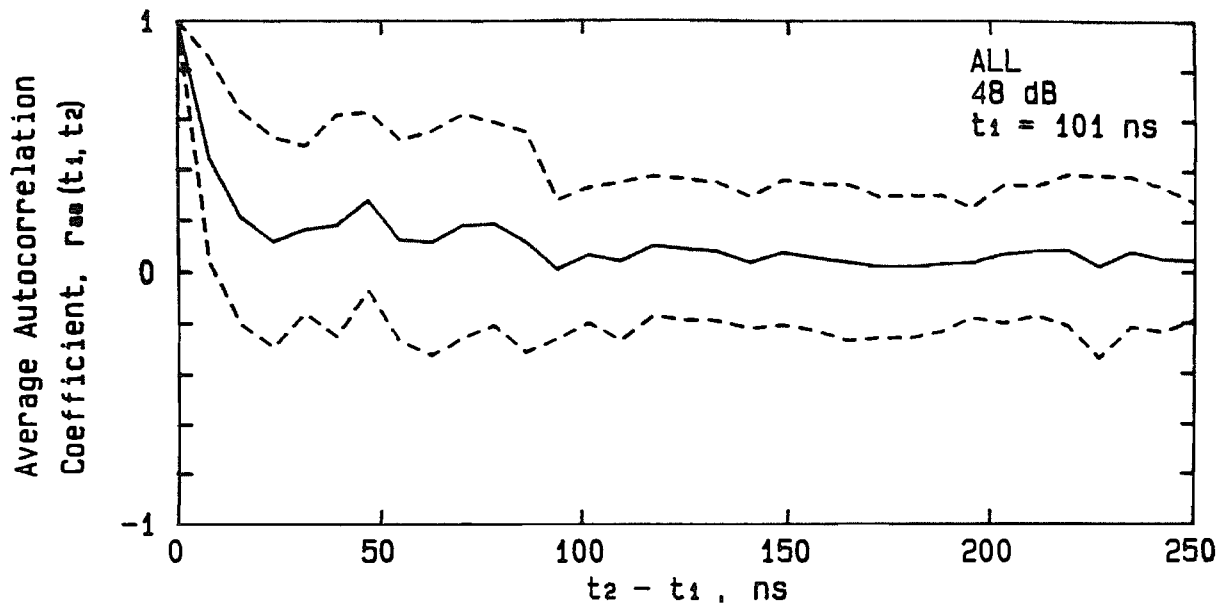


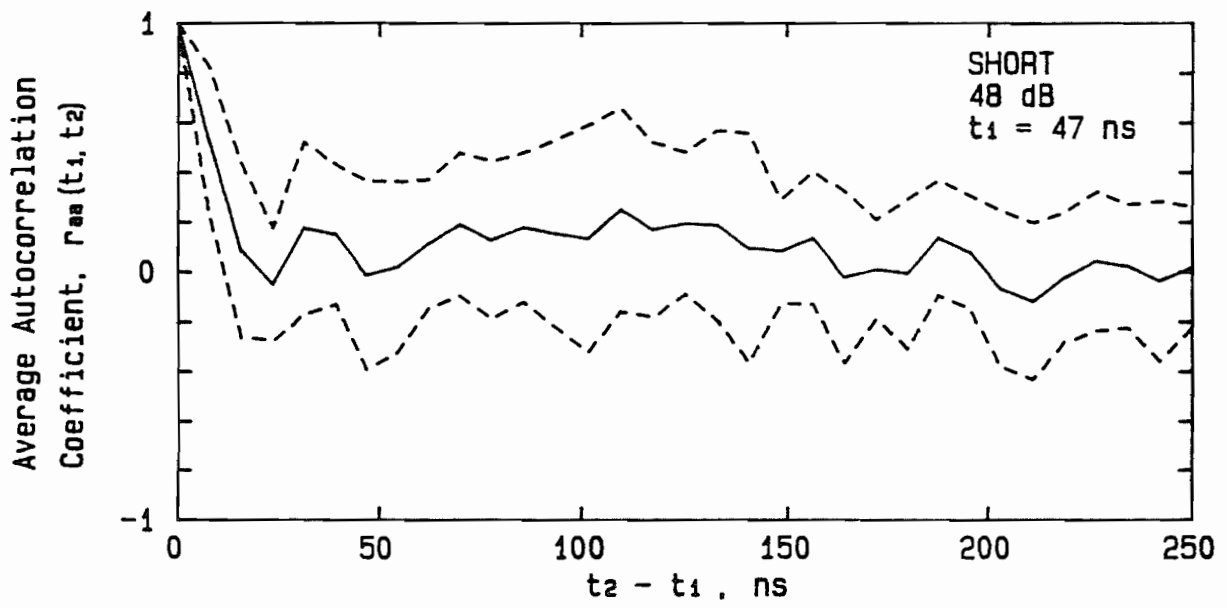
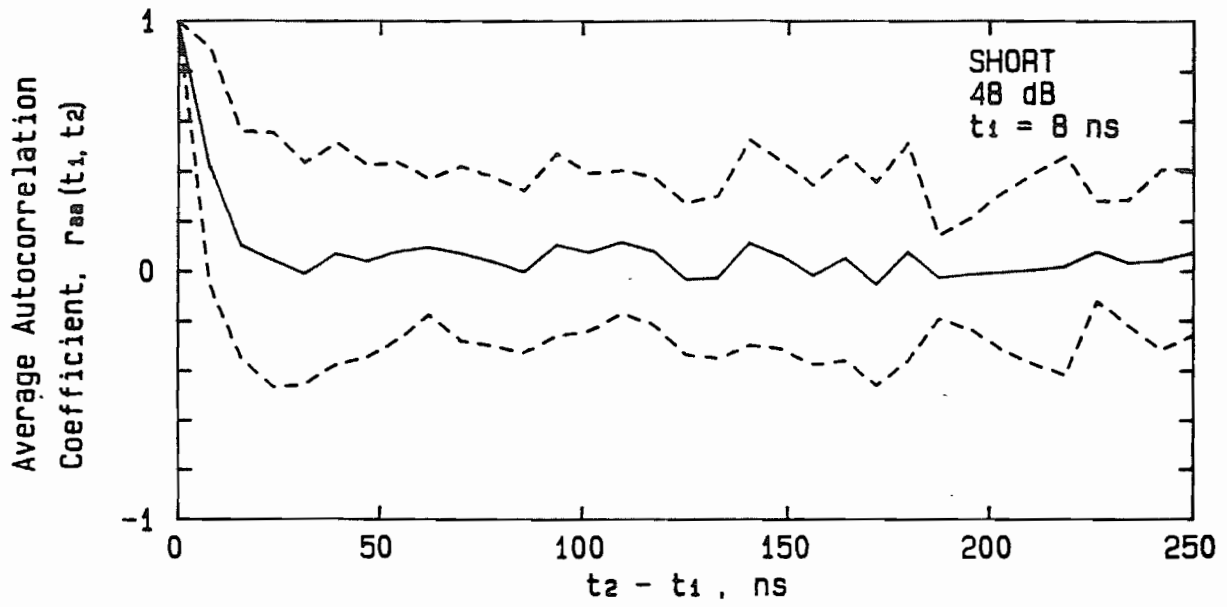
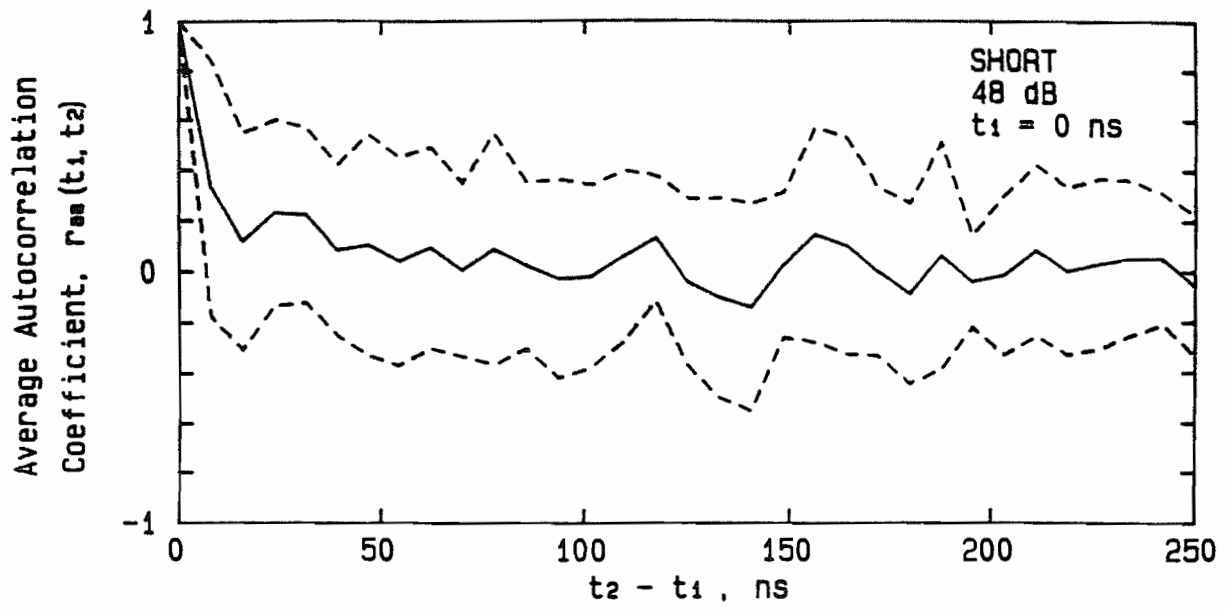


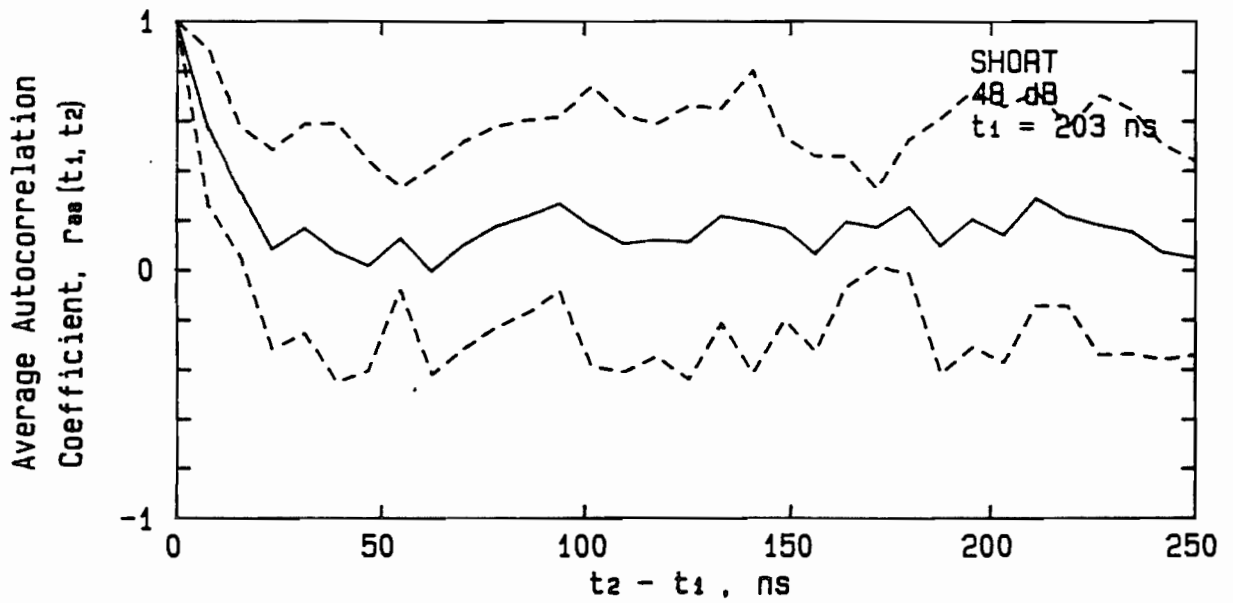
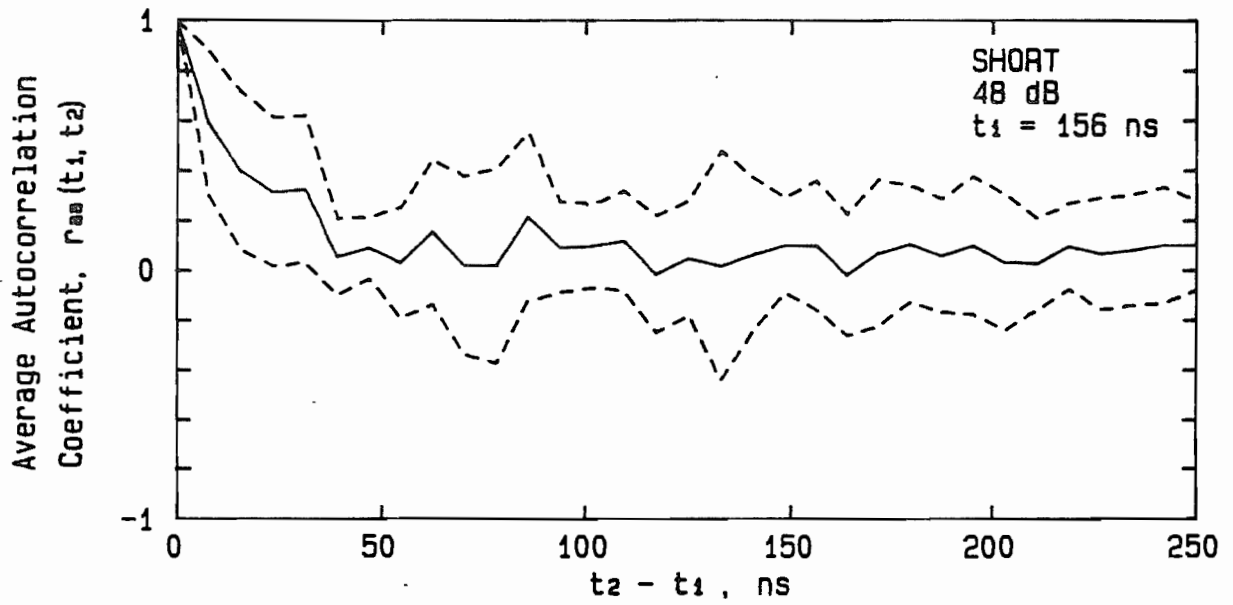
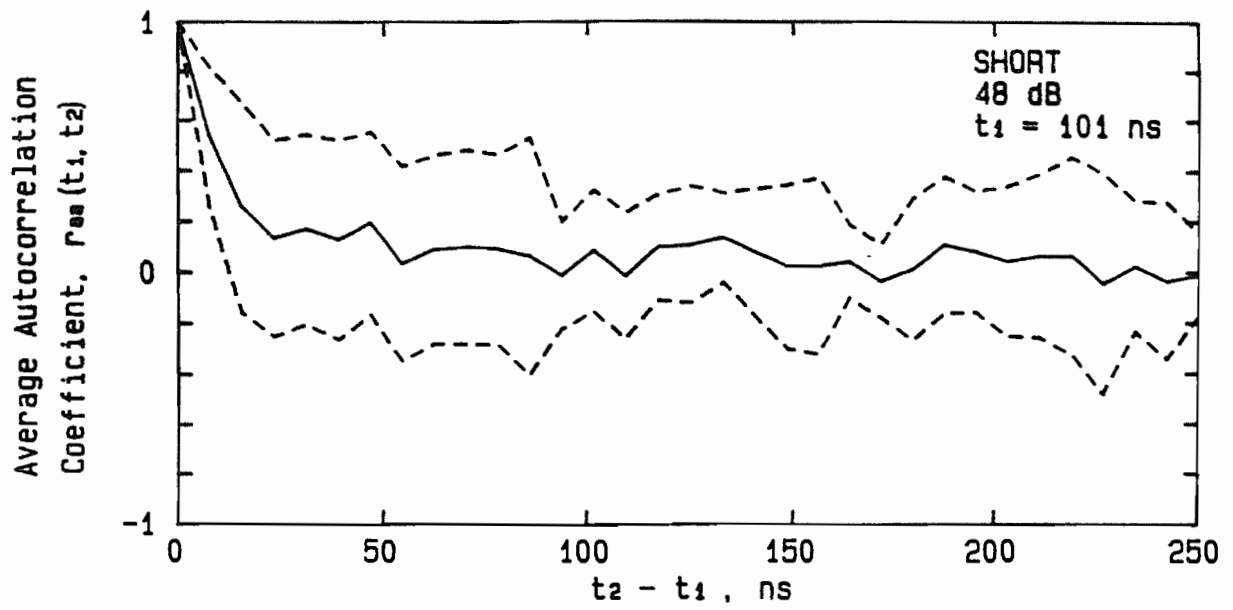


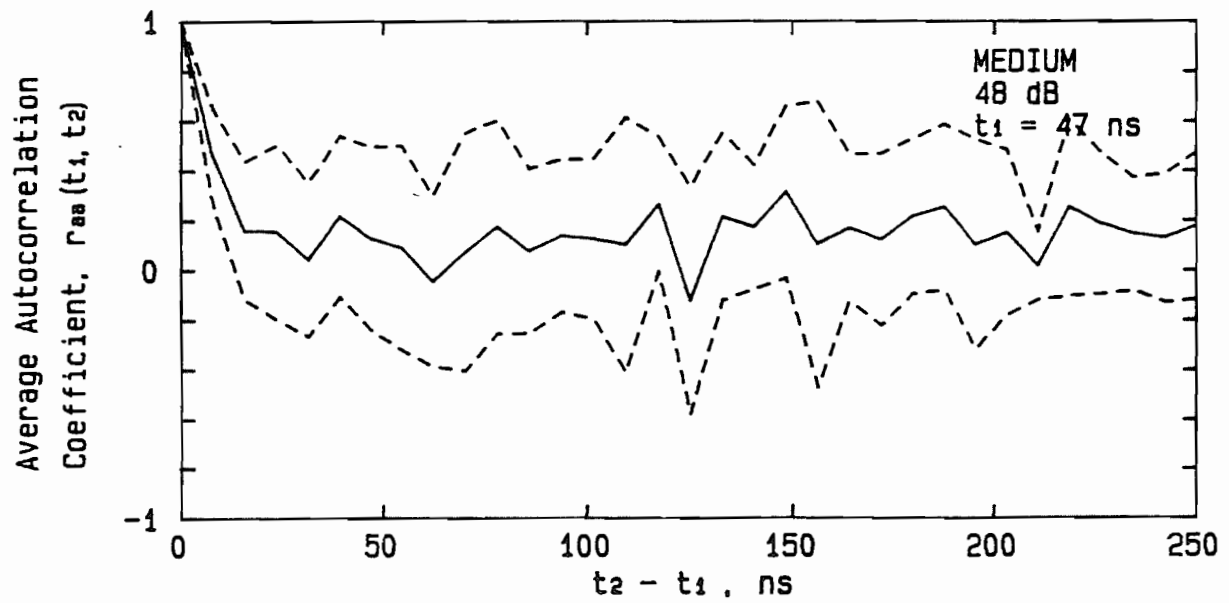
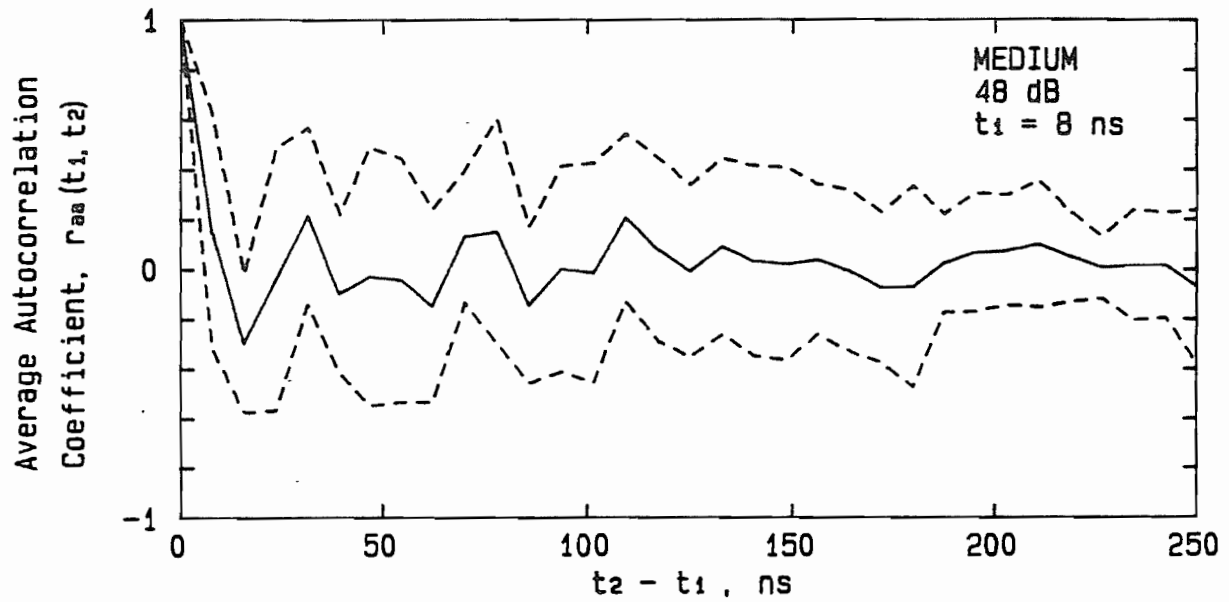
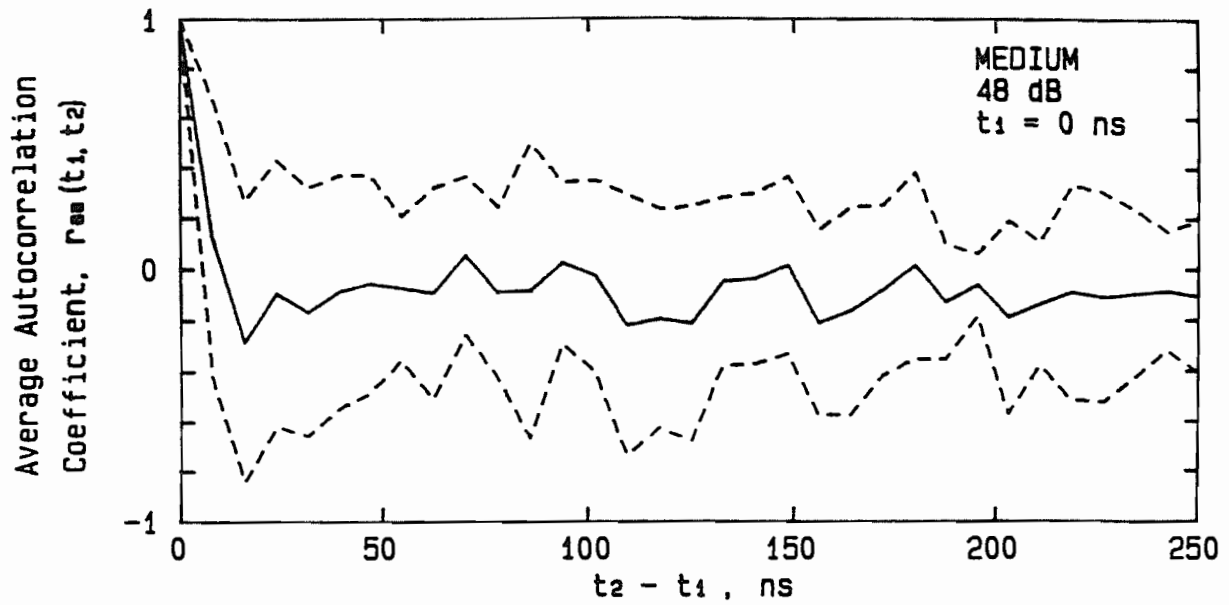


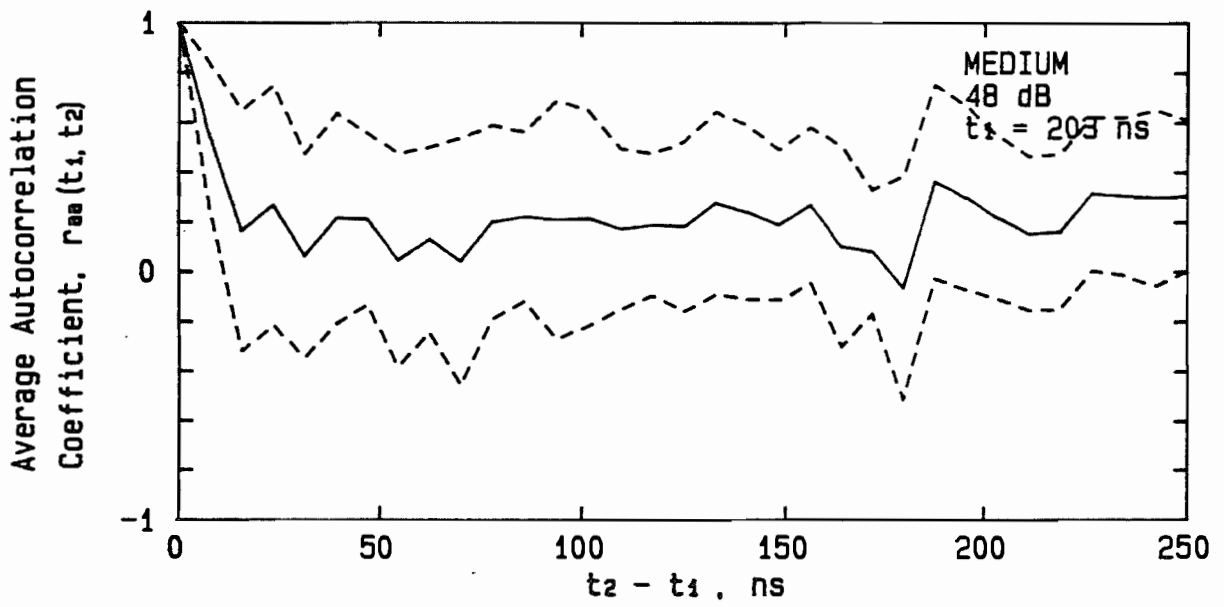
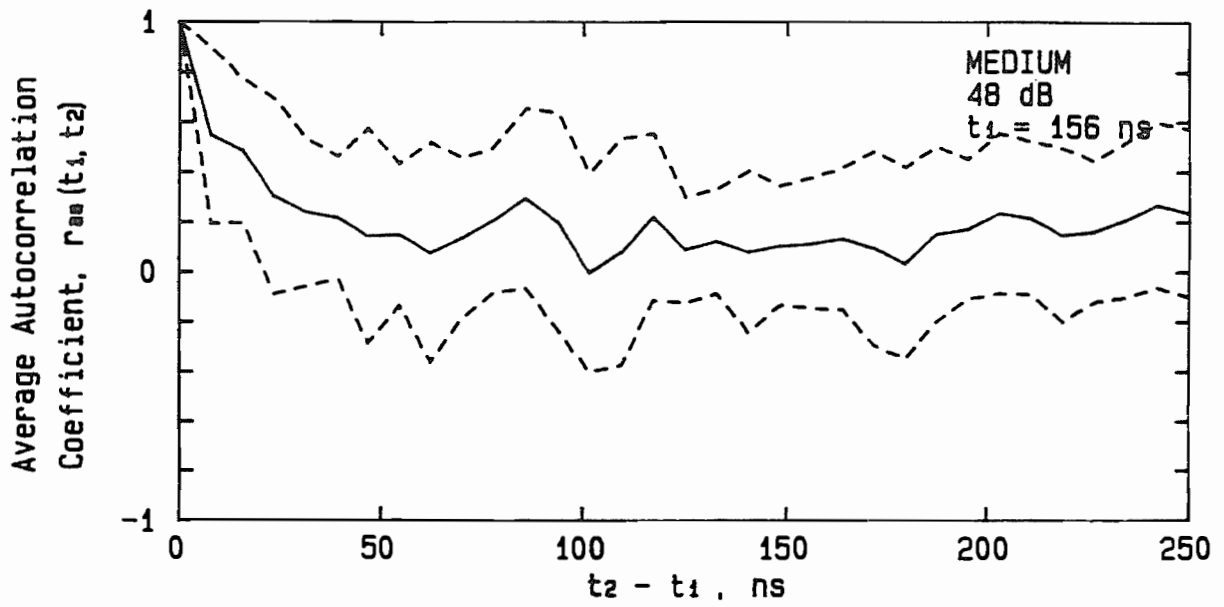
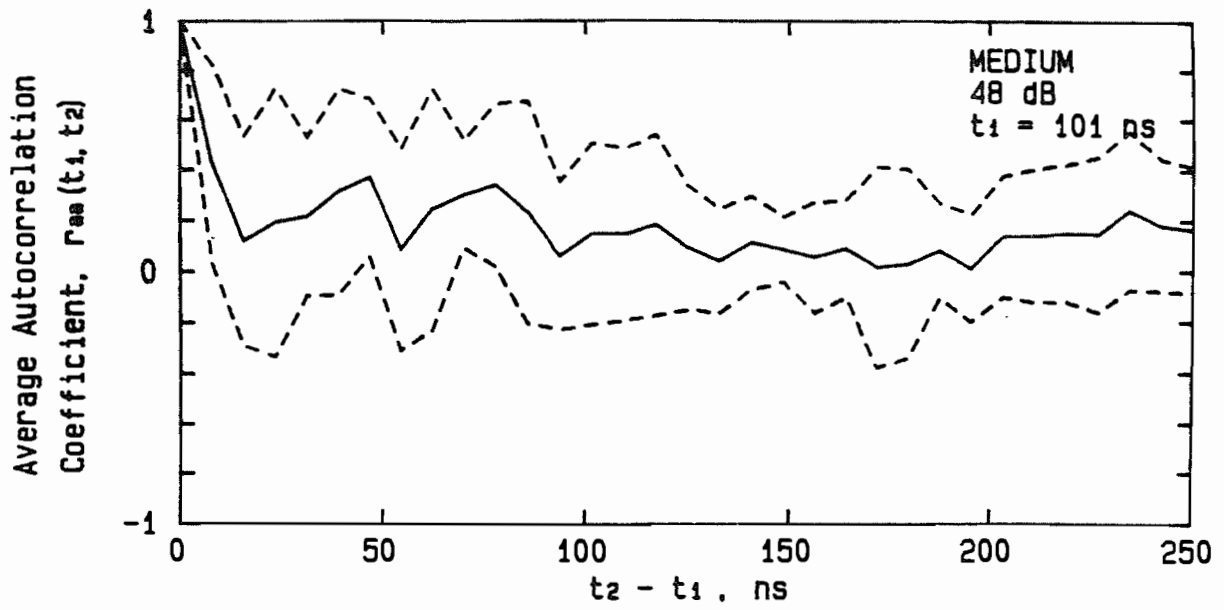


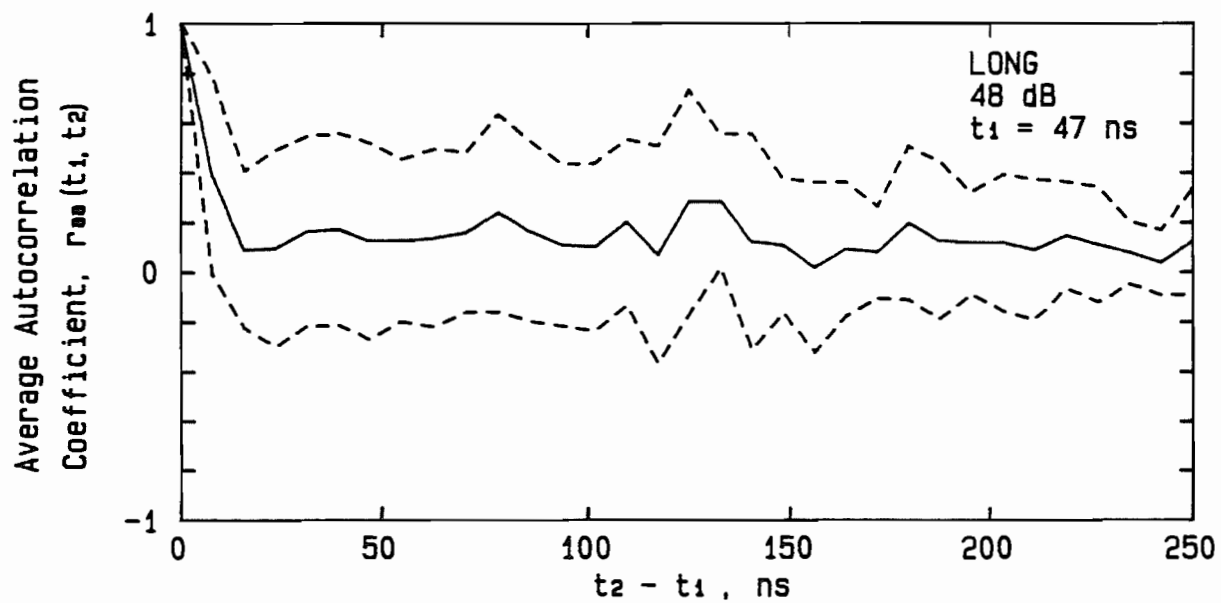
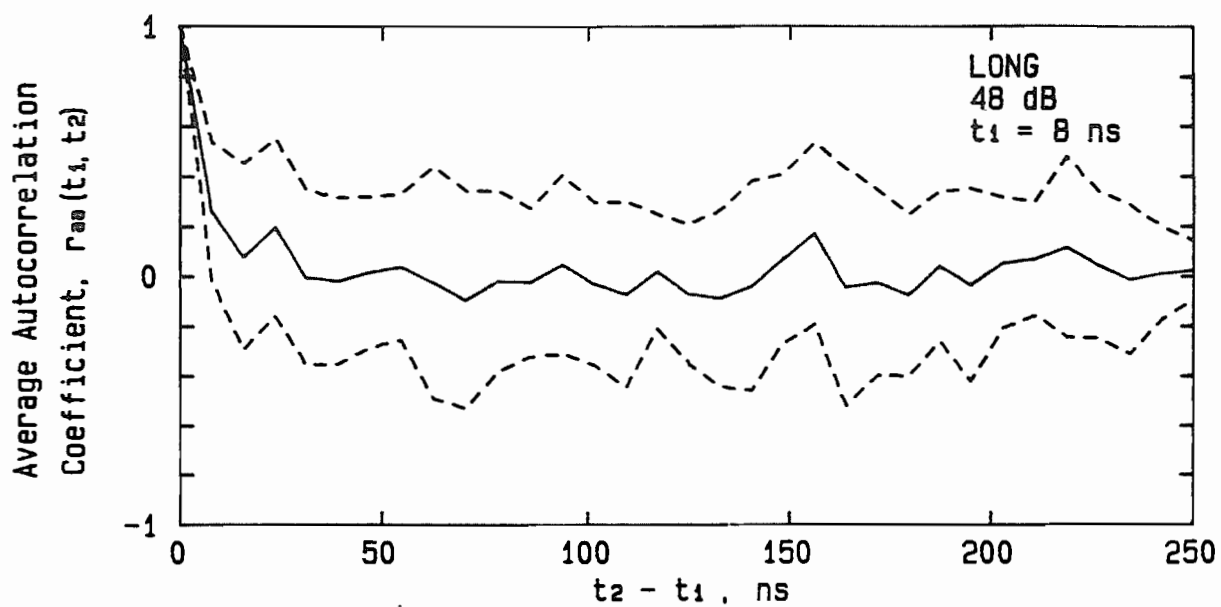
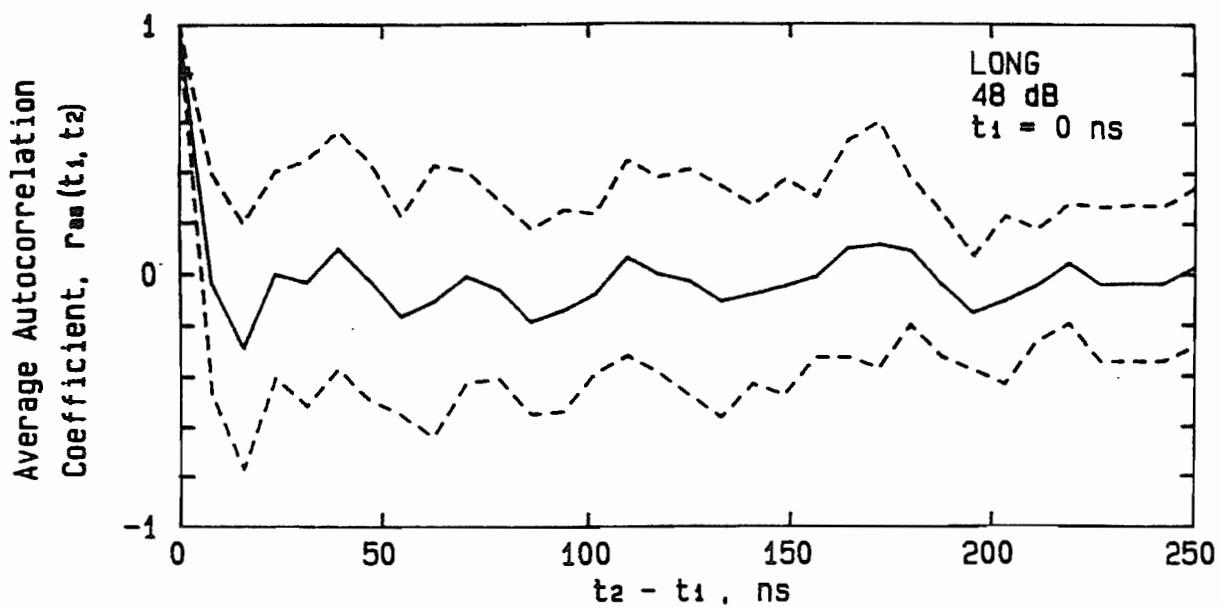


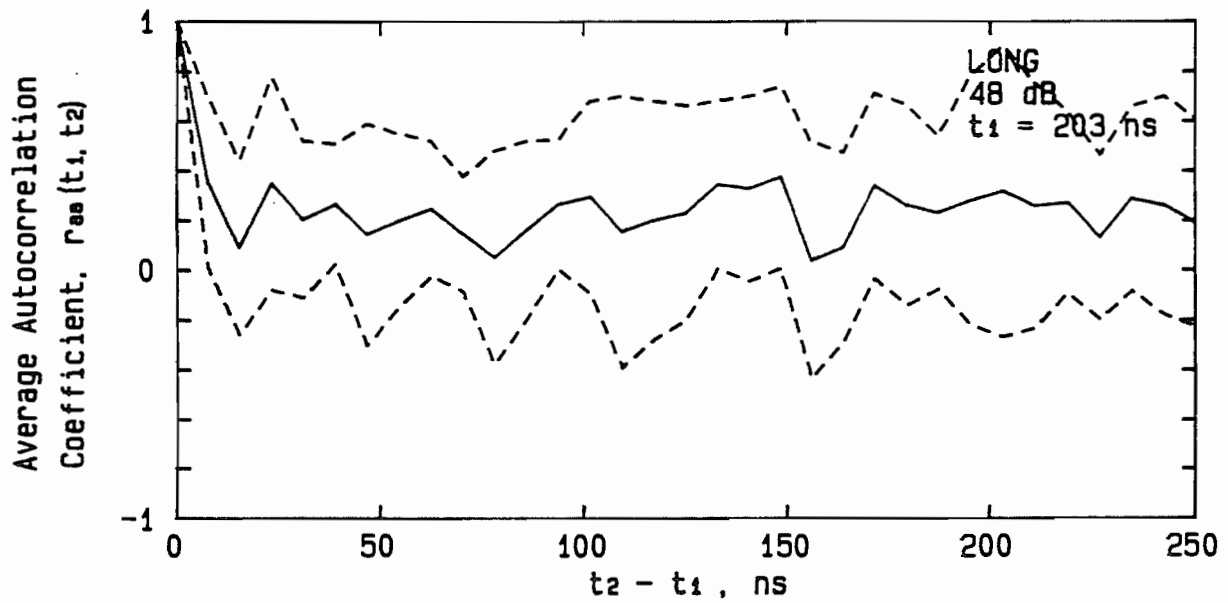
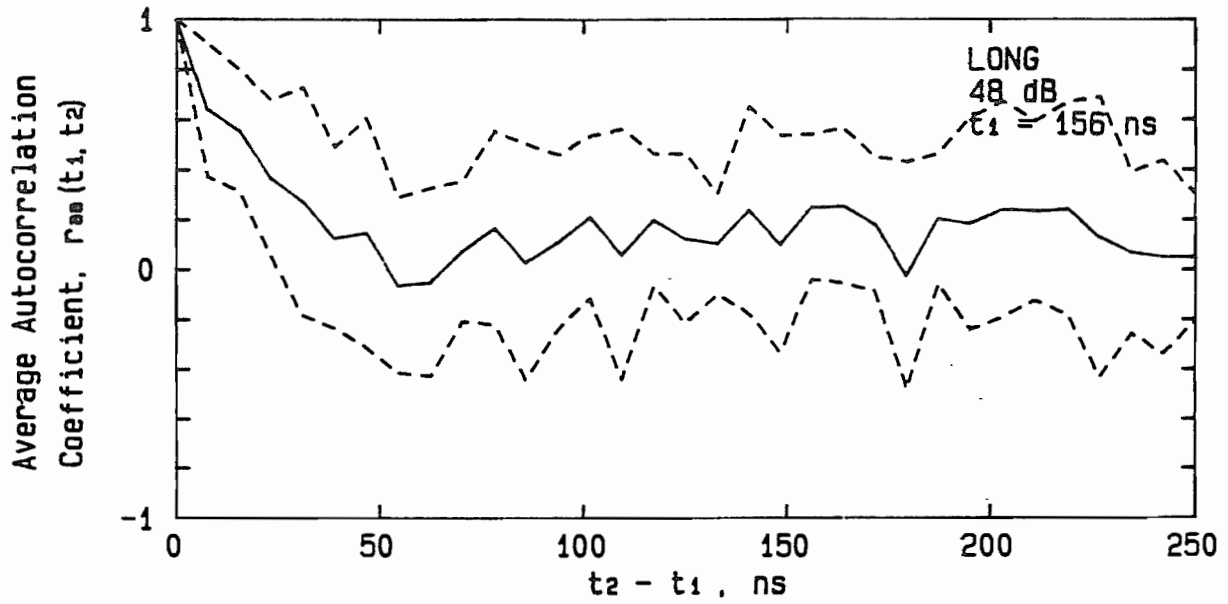
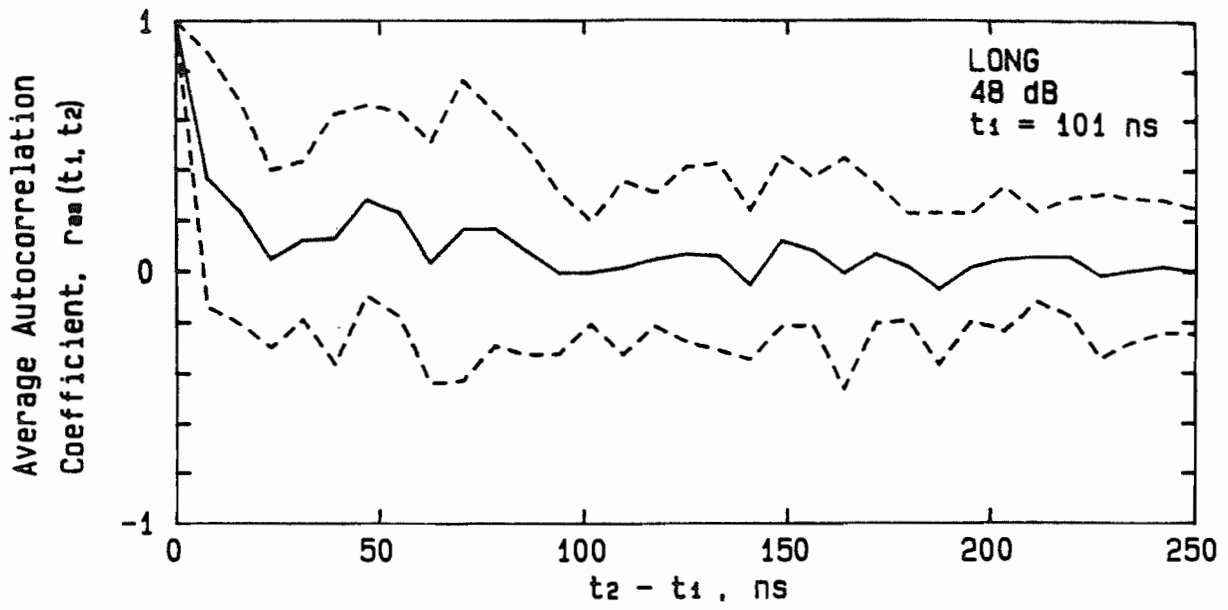






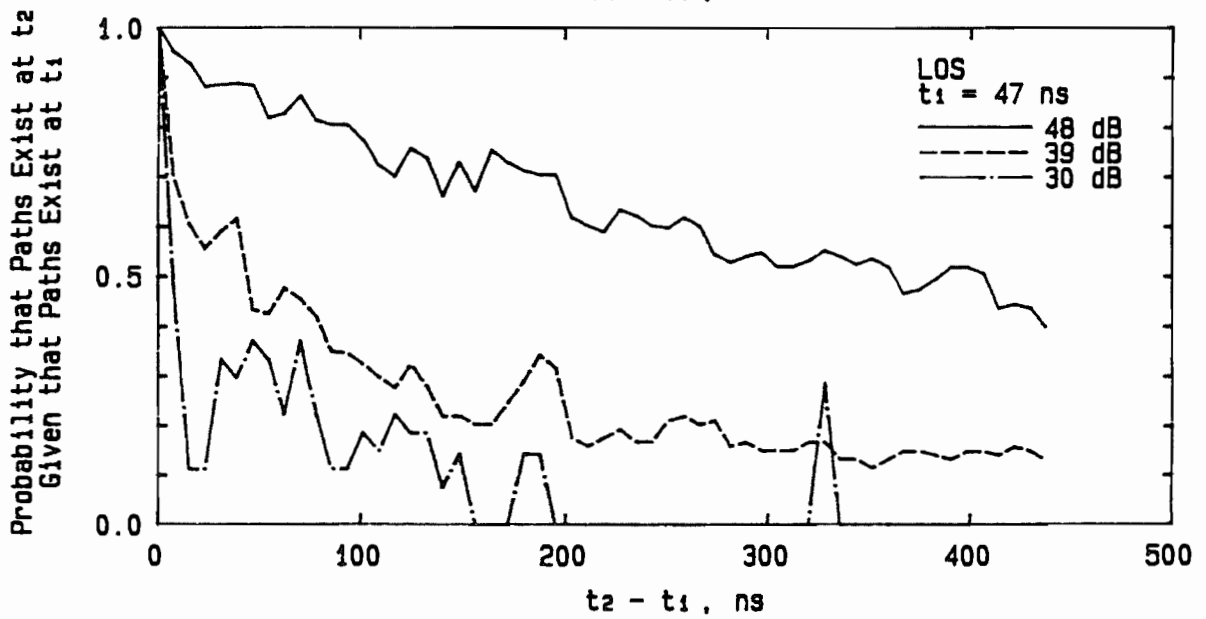
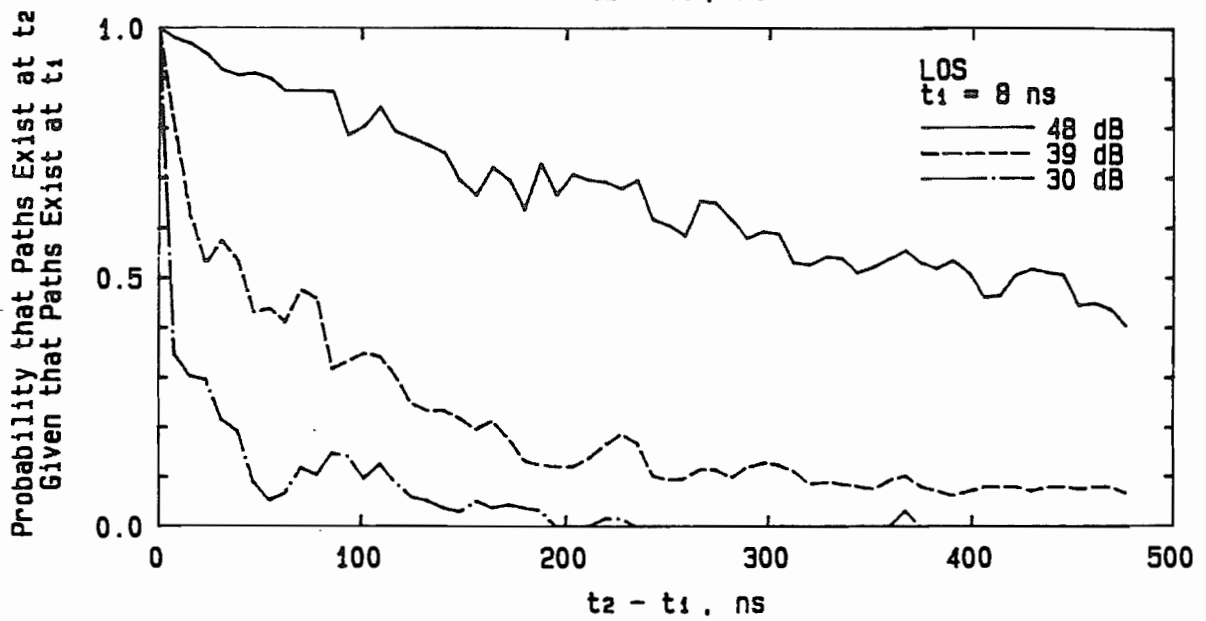
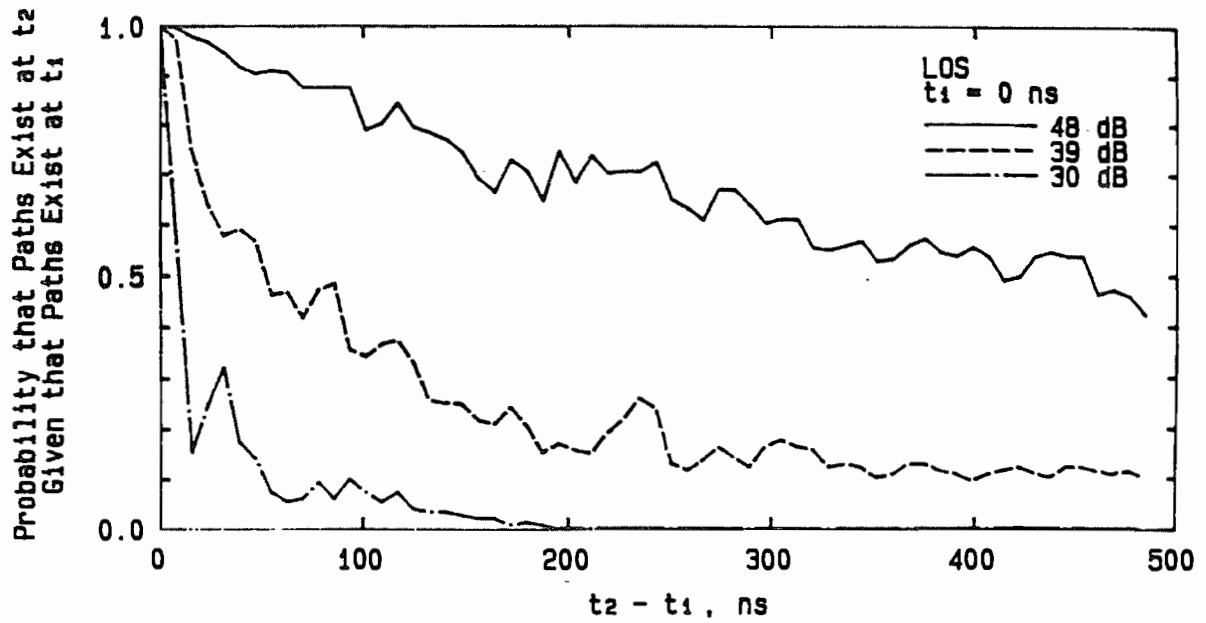


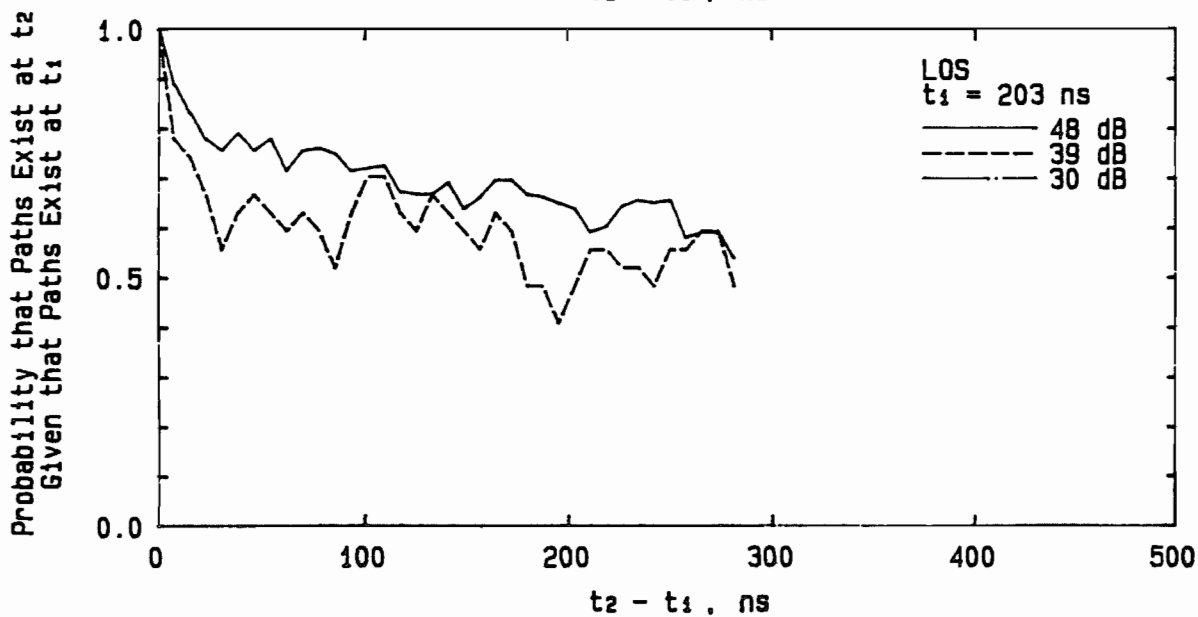
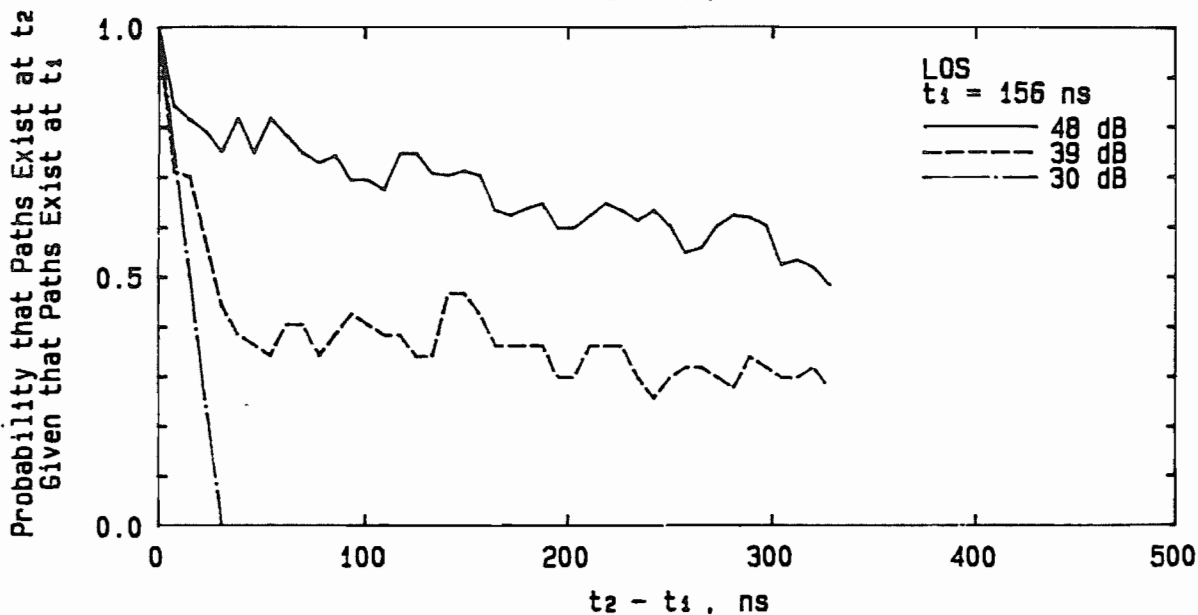
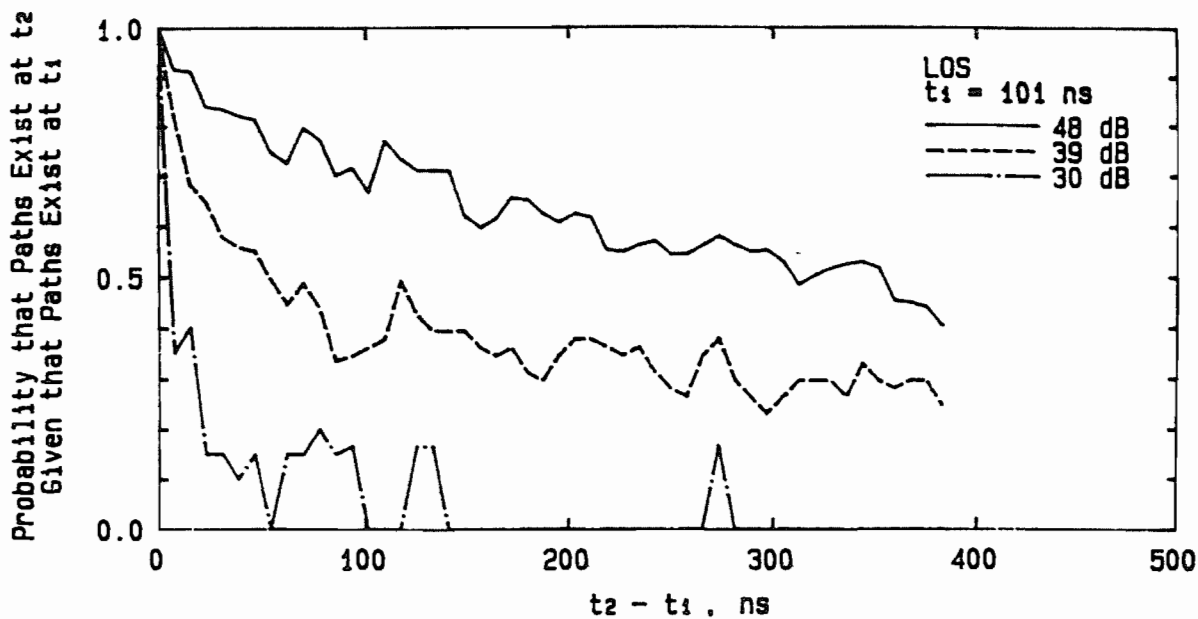


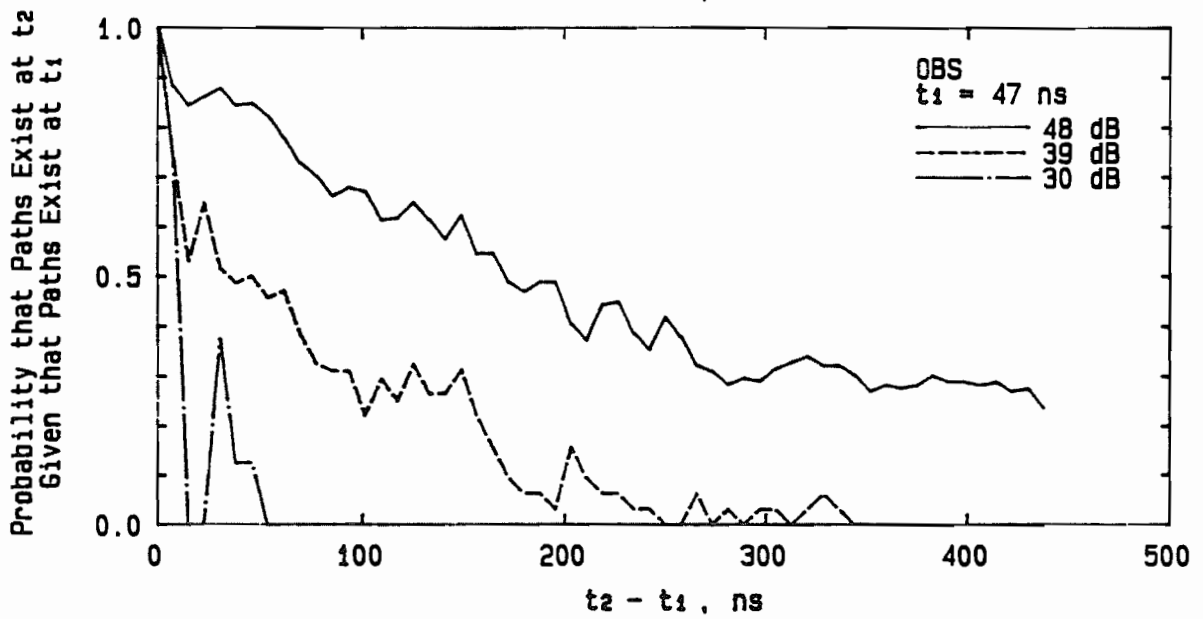
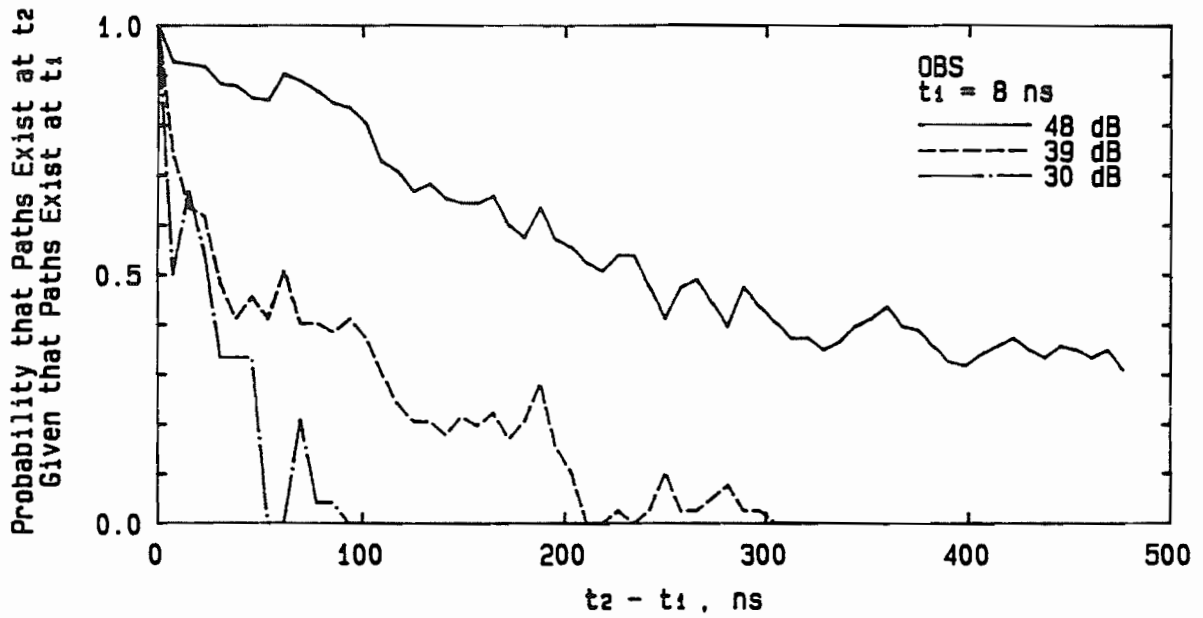
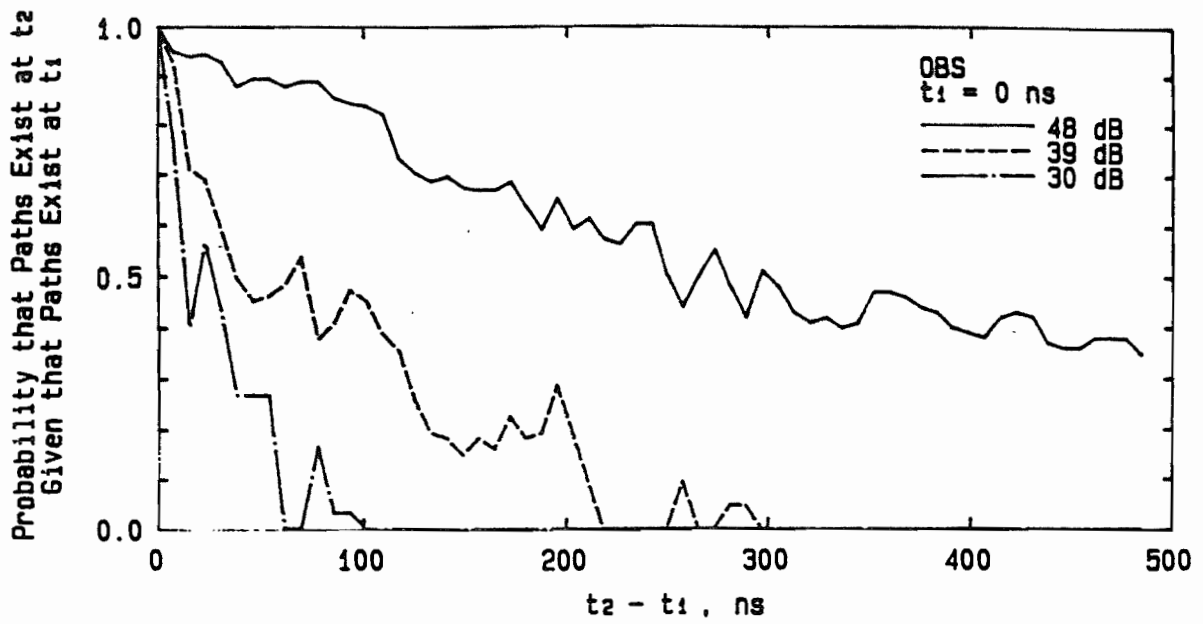


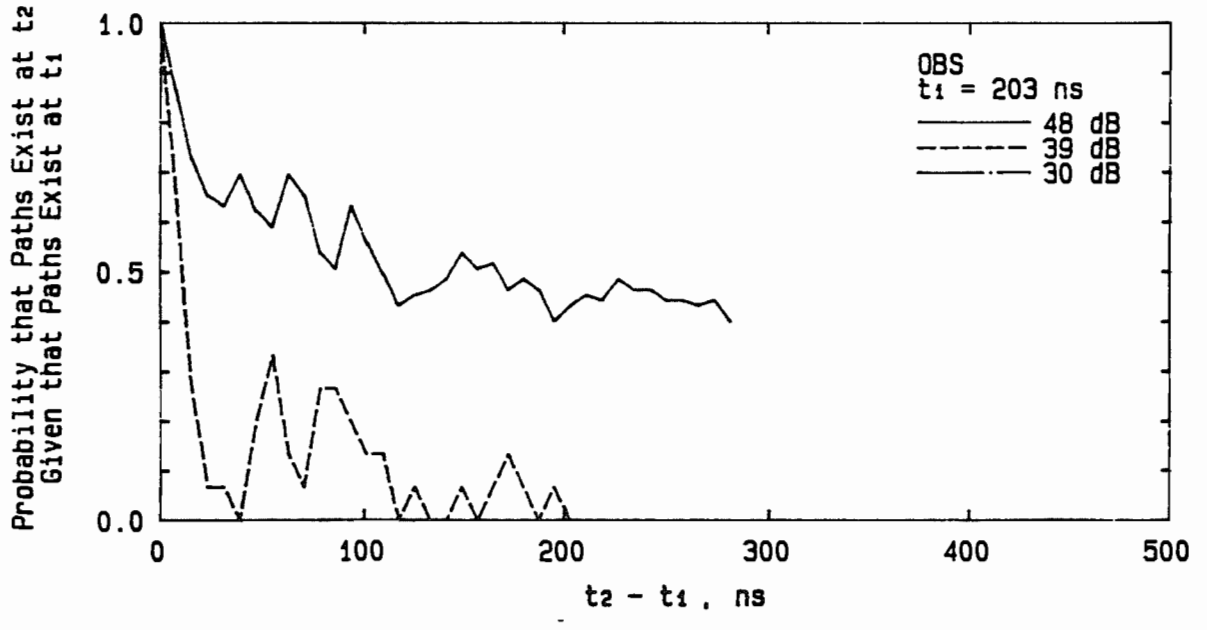
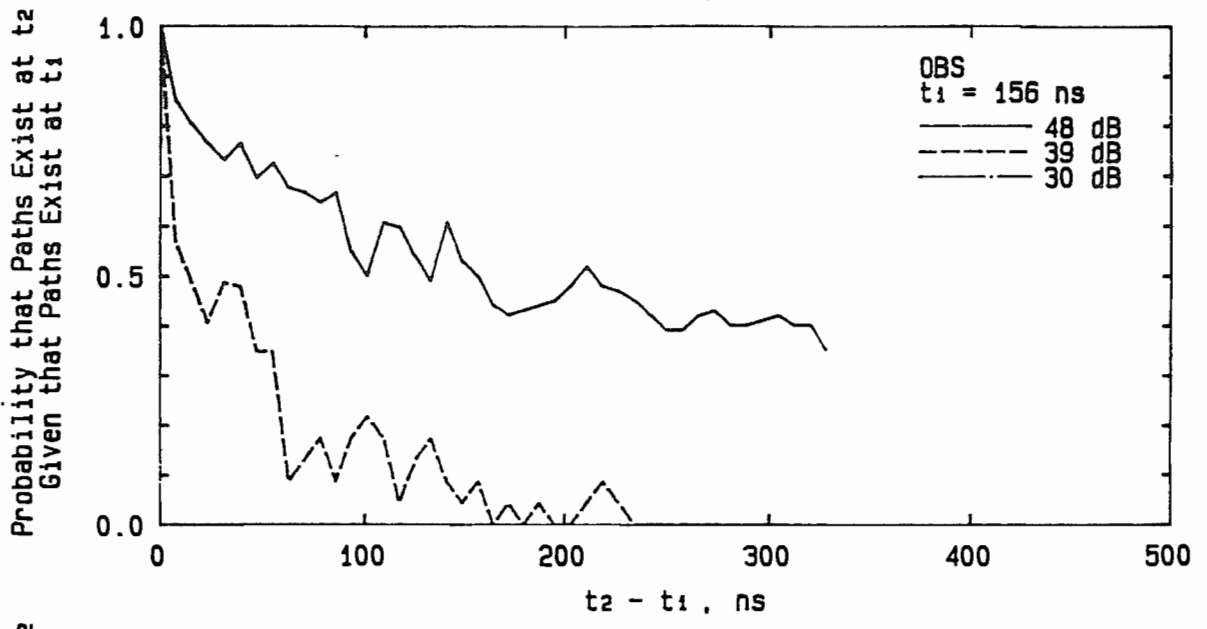
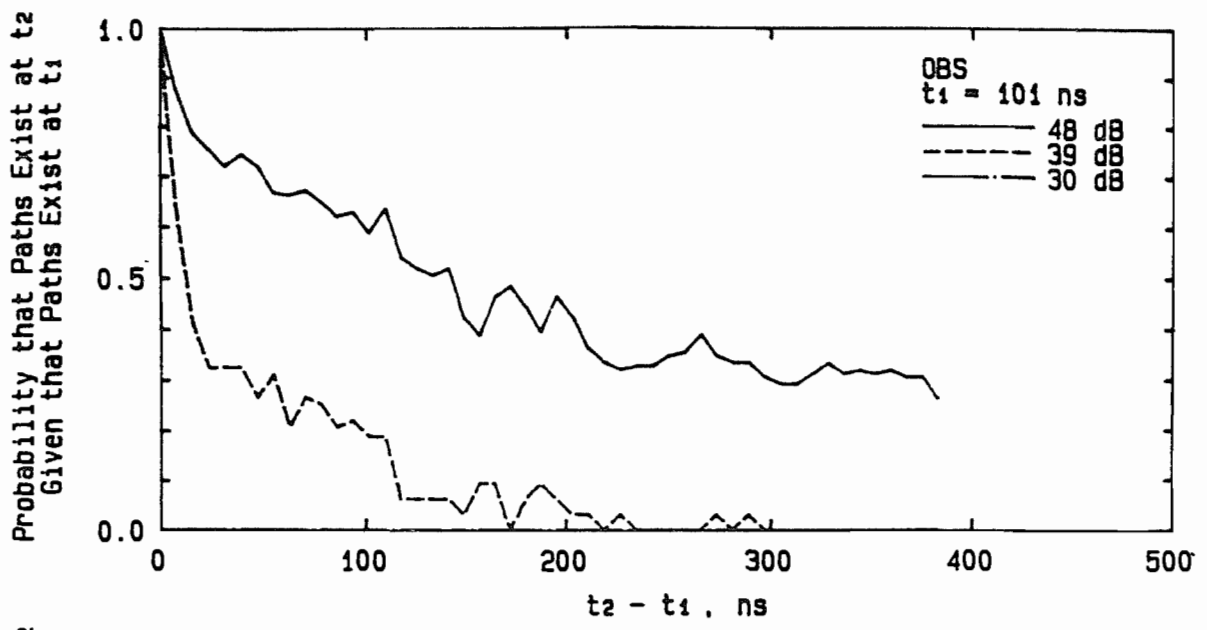


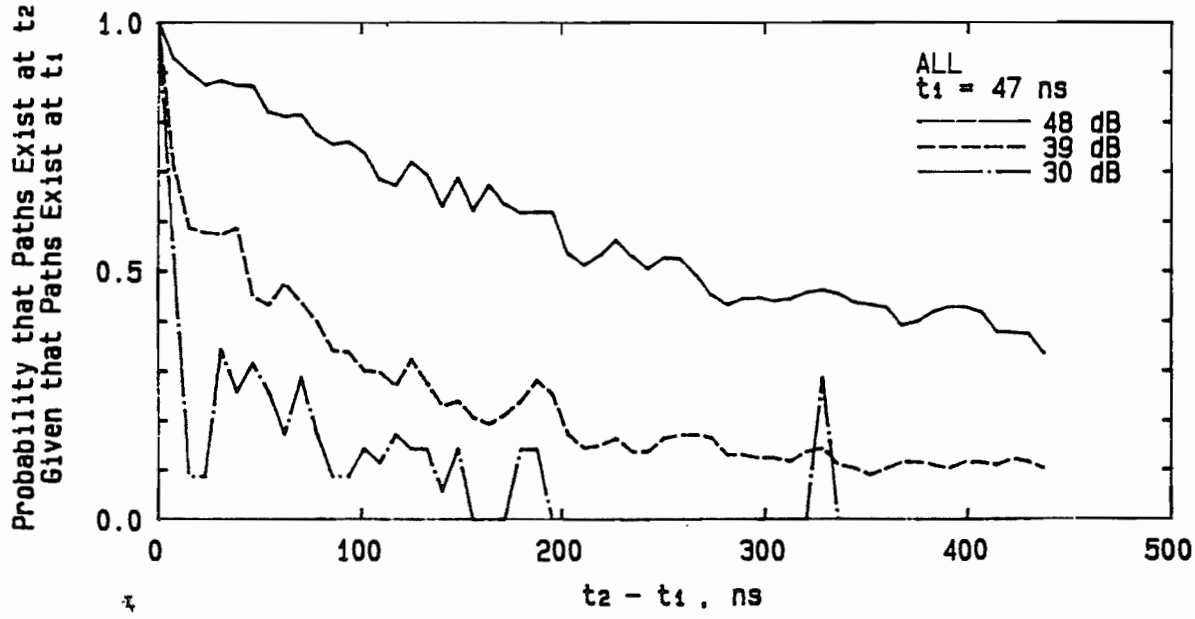
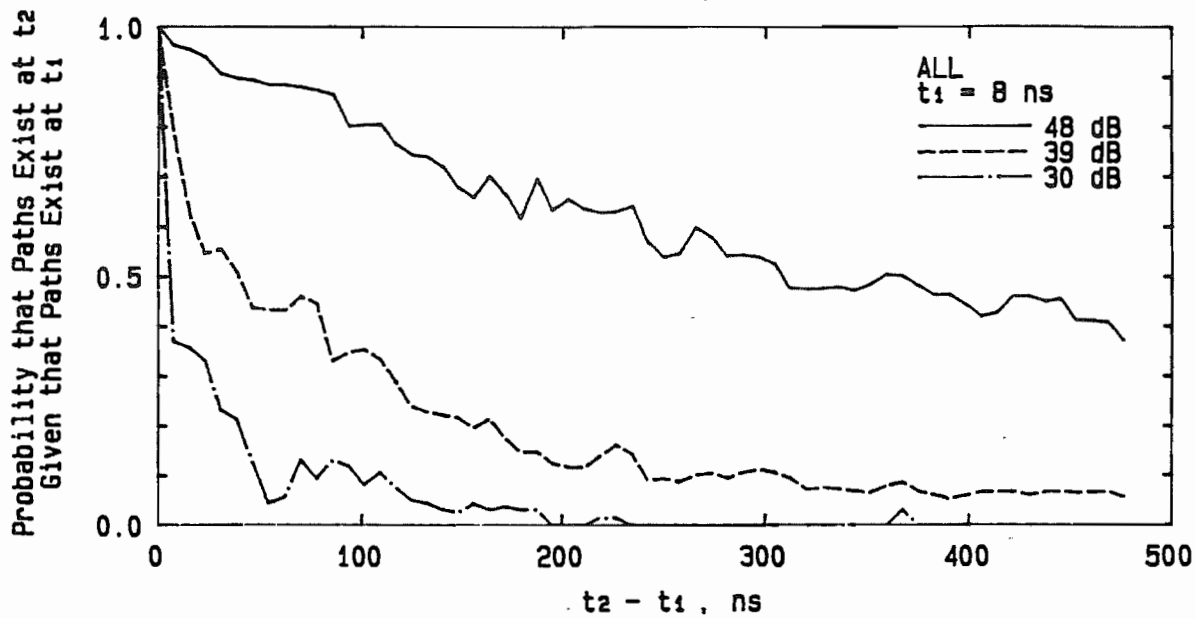
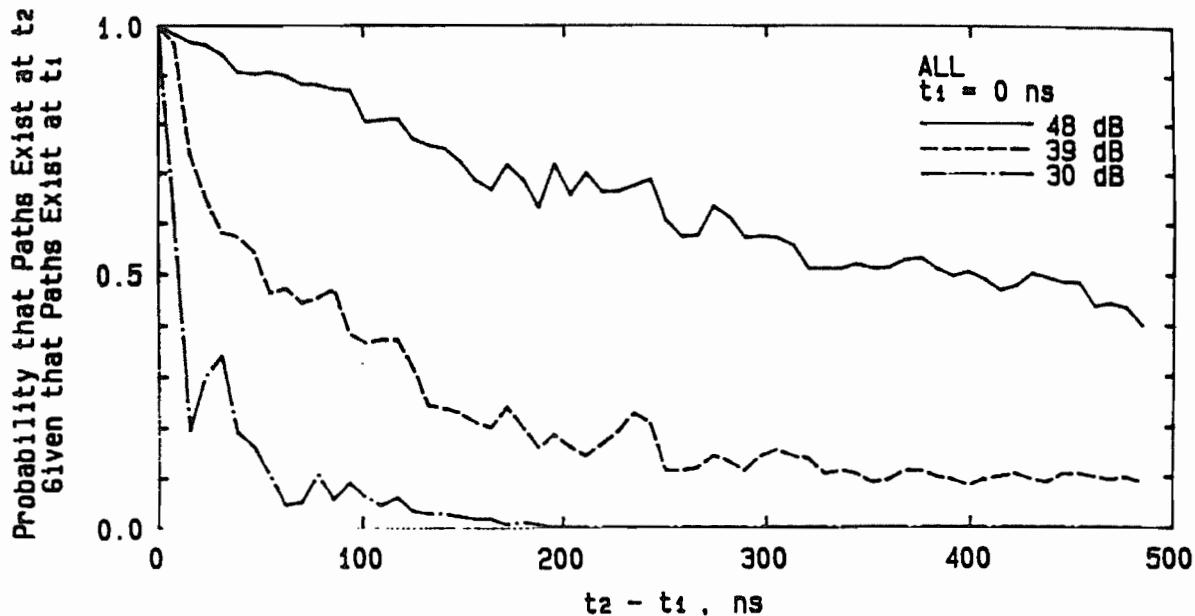
## Appendix F. Conditional Probability of Path Occupancy

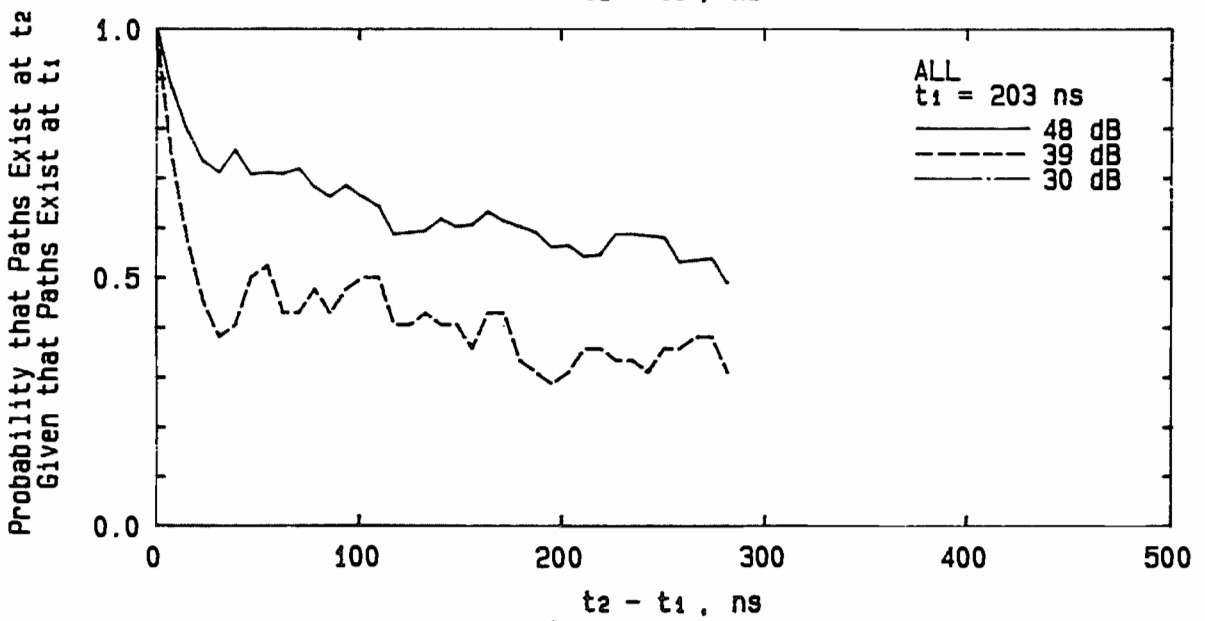
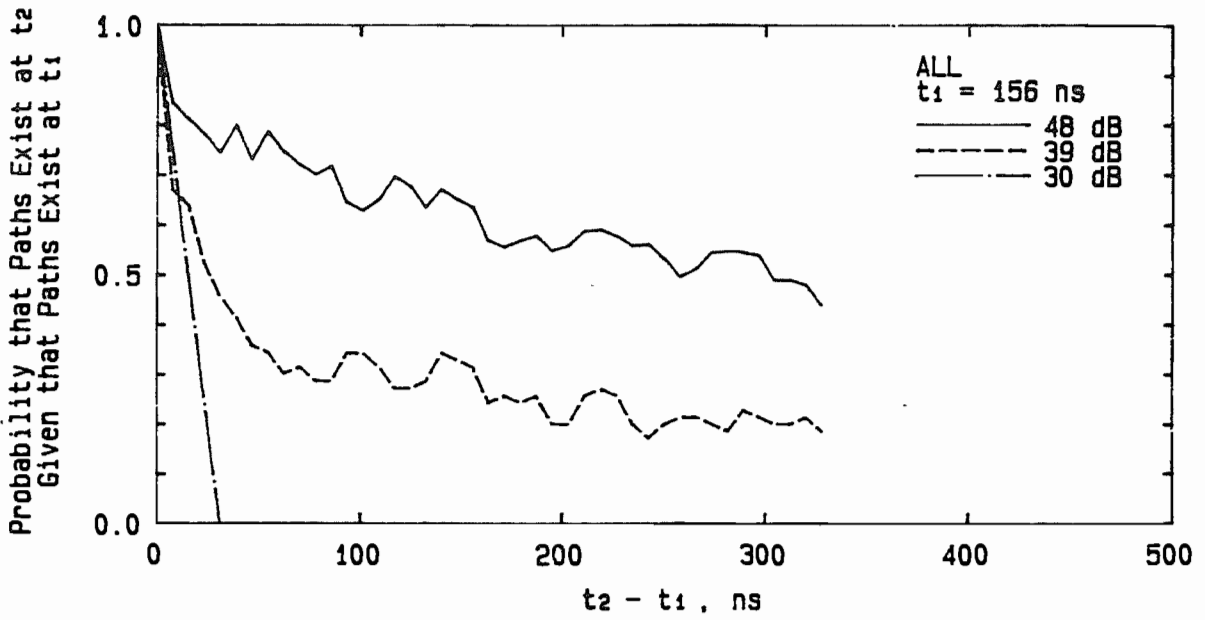
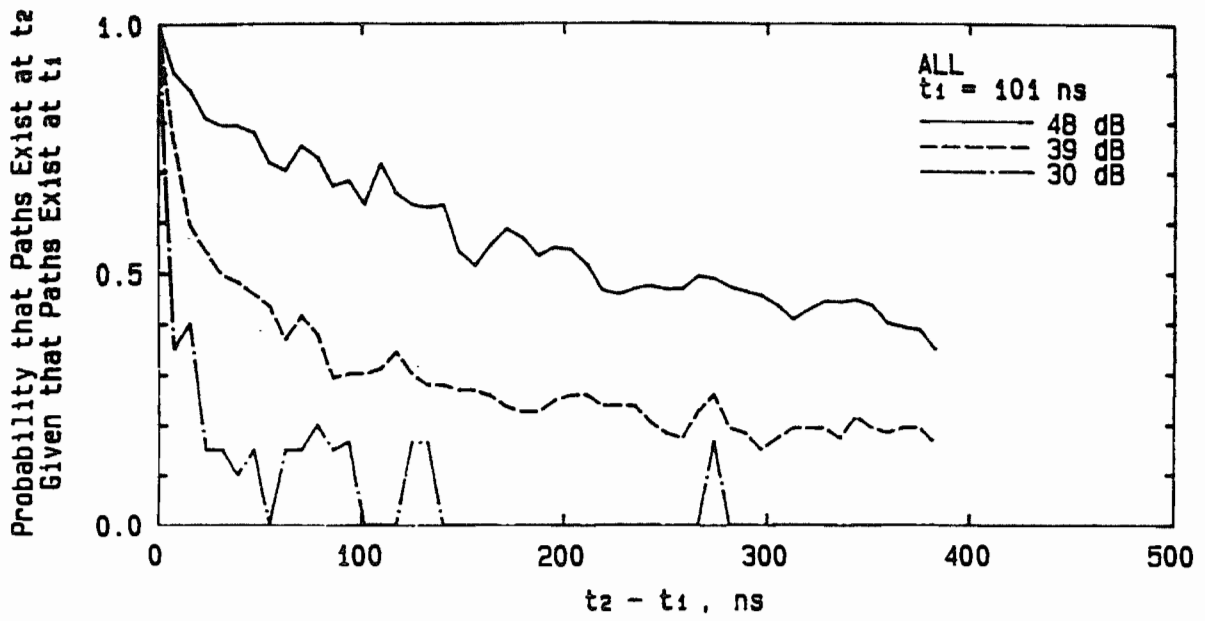




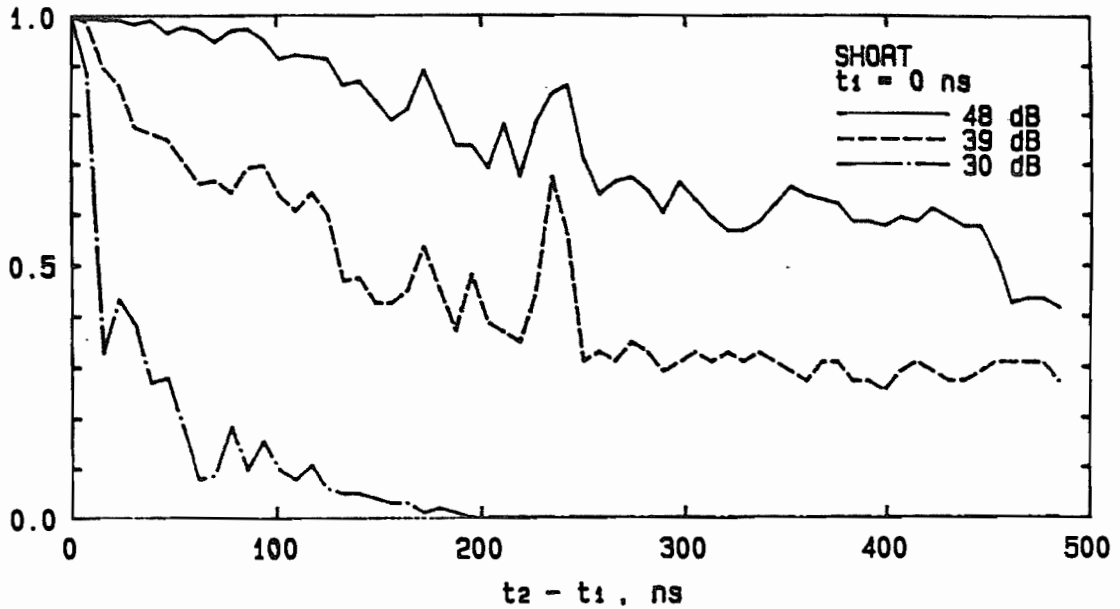




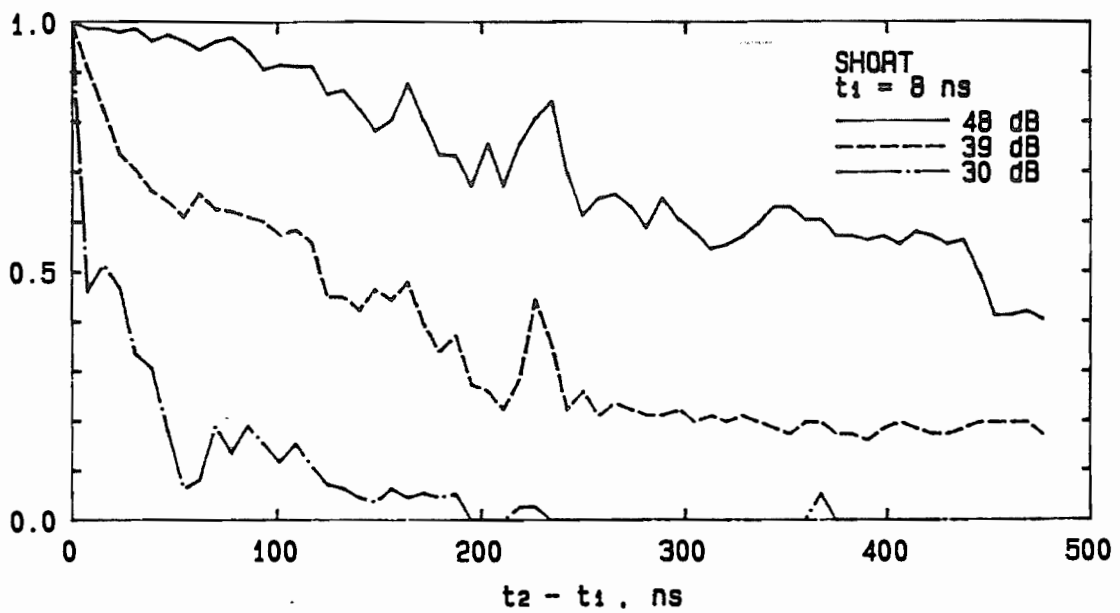




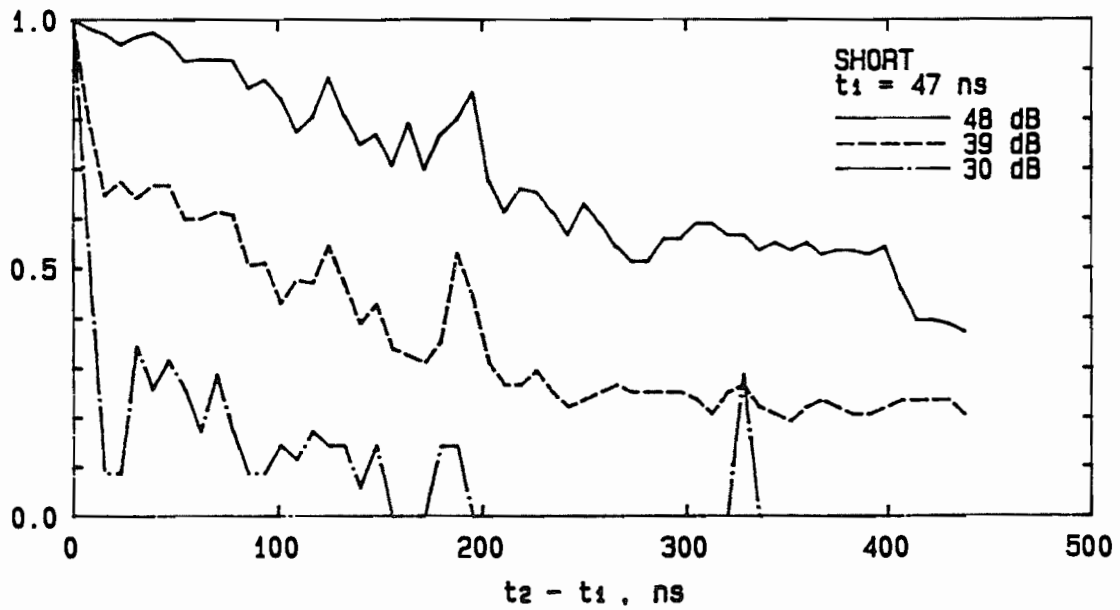
Probability that Paths Exist at  $t_2$   
Given that Paths Exist at  $t_1$



Probability that Paths Exist at  $t_2$   
Given that Paths Exist at  $t_1$

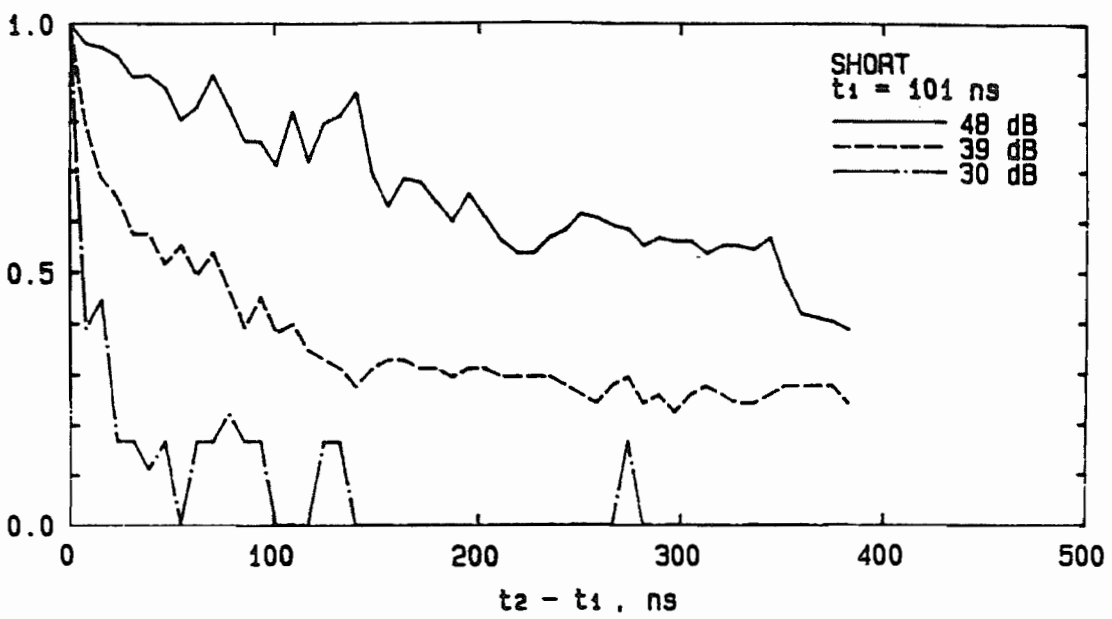


Probability that Paths Exist at  $t_2$   
Given that Paths Exist at  $t_1$

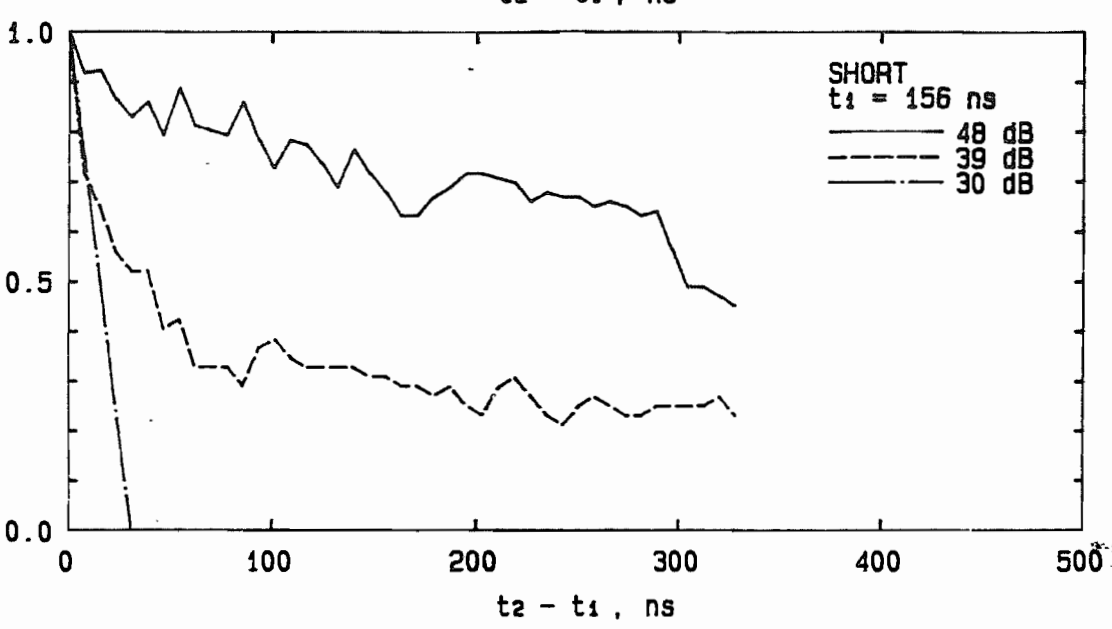




Probability that Paths Exist at  $t_2$   
Given that Paths Exist at  $t_1$



Probability that Paths Exist at  $t_2$   
Given that Paths Exist at  $t_1$



Probability that Paths Exist at  $t_2$   
Given that Paths Exist at  $t_1$

